

Technologies to study protein oxidation in ageing
Investigating the effect of protein
oxidation on protein function

Stuart Richard Gilbert Calimport

Doctor of Philosophy

ASTON UNIVERSITY

September 2015

©Stuart Richard Gilbert Calimport, 2015

Stuart Richard Gilbert Calimport asserts his moral right to be identified as the author
of this thesis

This copy of the thesis has been supplied on condition that anyone who consults it is
understood to recognise that its copyright rests with its author and that no quotation
from the thesis and no information derived from it may be published without proper
acknowledgement.

ASTON UNIVERSITY
Technologies to Study Protein Oxidation in Ageing
Investigating the Effects of Protein Oxidation on Protein Function
Stuart Richard Gilbert Calimport
Doctor of Philosophy
2016

Thesis Summary

Protein oxidation can cause aggregation, fragmentation, and affect enzymatic activity and binding partner interactions. Protein oxidation is implicated in a range of age-related pathologies including neurodegeneration and cancer. The VHR and PTEN phosphatases studied are sensitive to oxidation and regulated by protein-protein interactions. PTEN acts by dephosphorylating phosphatidylinositol (3,4,5)-triphosphate, negatively regulating the Akt pathway as part of a signalling control network that can protect against apoptosis, and is involved in the regulation of cell fate regulation and cancer. VHR is involved in neural development and cancer. A technology workflow for detecting protein oxidation and to correlate oxidative modifications to enzymatic activity and protein-protein interaction was developed; which may contribute towards the advancement of fundamental science as well as potential therapeutic and biomarker target identification in proteins. The technology platform consists of the mass spectrometric technique MS² to detect, validate, map and quantify oxidative modifications. The technology workflow consists of enzymatic activity assays to correlate modification with changes in activity, targeted MS² and statistical analysis. The fundamental and distinct contribution to knowledge in this thesis is a systematic mapping of protein oxidative modifications over a range of oxidants and concentrations of hypochlorous acid (HOCl), 3-morpholino-sydnominine (sin-1) and tetranitromethane for VHR (vaccinia H1 related) and PTEN (phosphatase and tensin homolog on chromosome 10), including modification identification including active site residues and putative binding domain, mapping the relative abundances of those modification and statistically correlating them to changes in enzymatic activity. Additional contributions to knowledge have been i) the non-specificity and complexity of oxidation profiles and oxidant damage of nitrating agents, that have largely been proposed to be specific without substantial oxidative capacity and ii) expanding the known interactome of VHR (vaccinia H1 related) through array and co-immunoprecipitation.

Keywords: Omics, mass spectrometry, nitration, VHR, PTEN

I acknowledge with precedence my supervisors Professor Andrew Pitt and Doctor Corinne Spickett for the opportunity they have given me of which I am eternally thankful for. I am appreciative of their leadership and mentoring skills as well as their scientific expertise.

I acknowledge Aston University and Imperial College London and those that created the environment and infrastructure that made my personal and professional development and successes possible. In particular I would like to acknowledge the members of Professor Andrew Pitt's and Doctor Corinne Spickett's laboratory and members of the Proxomics Project.

I acknowledge the funding sources for my work including the EPSRC, the CDRL grant, and Aston University for the studentship.

Declaration of authorship:

All work presented was performed wholly by Stuart R. G. Calimport unless otherwise declared.

Declaration of collaborations:

Industry collaboration and knowledge and technology transfer from Dynamic Bioarray, Doctor Ekaterina McKenna. This included the following:

- Modified ProtoArray® Human Protein Microarray protocol.
- On site training on sciFLEXARRAYER S3.
- Collaboration using Dynamic Bioarray silicon dioxide hydrophilic microfluidic chip device and associated technology for array probing and incubation.

Academic collaboration within the PROXOMICS multidisciplinary research programme:

Knowledge and technology transfer from Imperial College London, Institute of Chemical Biology, Doctor Rudiger Woscholski and Doctor Lok Hang Mak. This included the following:

- Technology transfer of Glutathione-S-Transferase tagged Phosphatase and tensin homolog (PTEN) and vaccinia H-1 (VHR) related phosphatase samples.
- Technology transfer of PTEN and VHR containing pGEX plasmid vectors.
- Knowledge transfer of protocol for transformation, expression and purification of PTEN and VHR with glutathione column.

- Knowledge transfer of 3-*O*-methylfluorescein phosphatase assay including laboratory visit.
- Gift of *E.coli* DH5™ (alpha) cells.

Technology transfer from the Imperial College London, Molecular Dynamics Group, Professor David Klug:

- HCT-116 cell line derivative (C. Lee, Kim, & Waldman, 2004)

Academic collaboration with Doctor Alexis Boukouvalas from Aston University Engineering & Applied Sciences.

- Statistical modelling for analysis of oxidative modifications and phosphatase activity

List of Contents

Title page	1
Thesis summary	2
Acknowledgements	3
Declaration of authorships and collaborations	4
List of Contents	6
List of Tables	14
List of Figures	15
List of Appendices	18
Abbreviations	20
CHAPTER 1. INTRODUCTION	24
1.1. Damage, error, ageing and disease	25
1.1.1. The state of the patient	31
1.1.1.1. Omics: Markers and targets	31
1.1.1.1.1. Proteomics	37
1.1.1.1.1.1. Protein Post-Translational Modifications	42
1.1.1.1.1.1.1. Protein Oxidative Post-Translational Modifications	44
1.1.1.1.1.2. Cys-X ₅ -Arg phosphatases	52
1.1.1.1.1.2.1. Phosphatase and tensin homolog deleted on chromosome ten (PTEN)	54
1.1.1.1.1.2.2. Dual specificity phosphatase Vaccinia H1-related phosphatase (VHR/DUSP3)	61
1.1.3. Technology Development	65
1.1.3.1 Mass Spectrometry	65

1.1.3.2 Biochips, biosensors and bioprinting	71
1.2 Aims	75
CHAPTER 2: MATERIALS & METHODS	77
2.1. Methods Summary	78
2.2. Methods	79
2.2.1. Plasmid constructs	79
2.2.2. Minipreps and Maxipreps	80
2.2.3. Transformation of PTEN and VHR	81
2.2.3.1. Generating competency in <i>E.coli</i> cells	81
2.2.3.2. Transformation	82
2.2.4. Expression of PTEN and VHR	83
2.2.5. Bradford assay determination of protein concentration	84
2.2.6. Purification of PTEN and VHR	85
2.2.7. SDS-PAGE gel electrophoresis and Coomassie staining	88
2.2.7.1. SDS-PAGE	88
2.2.7.2. Coomassie staining	89
2.2.8. Filtration	90
2.2.9. Oxidation	90
2.2.9.1. Hypochlorous acid (HOCl) oxidation	91
2.2.9.2. 3-Morpholinopyrrolidinone (SIN-1) oxidation	92
2.2.9.3. Tetranitromethane (TNM) oxidation	92
2.2.10. Digestion protocols	92
2.2.10.1. In-gel digestion	93
2.2.10.2. Double digestion	95
2.2.11. OMFP assay of phosphatase activity	95
2.2.12. Liquid chromatography coupled mass spectrometry	97

2.2.12.1. TOF MS/MS	97
2.2.12.2. Targeted ion scan	99
2.2.12.3. <i>In silico</i> identification of modified peptide	100
2.2.12.3.1. Mascot <i>in silico</i> identification	100
2.2.12.3.2. Progenesis <i>in silico</i> identification	103
2.2.12.3.3. Analysis of raw MS data	104
2.2.12.3.3.1. Extracted ion chromatography	104
2.2.12.3.3.2. <i>De novo</i> sequencing	105
2.2.12.3.4. Computational modeling	106
2.2.12.3.4. Mediator modeling	106
2.2.13. Protein-protein interactions	107
2.2.13.1. Arraying protein and antibody spots onto substrate using sciFLEXARRAYER SE	107
2.2.13.2. Protoarray probing for antibody-protein, protein-protein and protein-peptide arrays using Dynamic Bioarray biochip and lifterslip technologies	111
2.2.13.3. Array Scanning	113
2.2.13.4. Array data acquisition and analysis	113
2.2.14. Molecular Biology	114
2.2.14.1. Sub-cloning tagged VHR for mammalian expression system and immunoprecipitation experiments	114
2.2.14.2 Digestion	114
2.2.14.3 Ligation	115
2.2.14.4. Transformation	115
2.2.14.5 Cell culture	115
2.2.14.5.1. Culturing HCT 116 cells for transfection and co-immunoprecipitation	115
2.2.14.5.2. Cell passaging	116
2.2.14.5.3. Adherent cell transfection	116

2.2.14.5.4. Cell harvesting	117
2.2.15. Co-immunoprecipitation	117
2.2.16. Western Blotting	119
2.2.17. Informatics analysis	120
2.2.17.1. ExPASy ProtParam	120
2.2.17.2. NCBI BLAST local alignment search tool	120
2.2.17.3. Protein-protein interaction databases	121
2.2.17.4. Molecular viewers	122
2.2.17.4.1. Chimera	122
Preface	123
CHAPTER 3: OXIDATION OF CX₅R PHOSPHATASES	126
3.1. Introduction	127
3.1.1. Investigation of the effects of hypochlorous acid, sin-1 and tetranitromethane	127
3.2. Results	129
3.2.1. Transformation, expression and purification of PTEN-GST and VHR-GST	129
3.3. Assaying phosphatase activity of CX ₅ R phosphatases	133
3.3.1. Assessment of gel filtration and retainment of PTEN-GST and VHR-GST activity	133
3.3.2. Tests to assess the effect of different methods for buffer exchange on enzymatic activity as assayed by the OMFP activity assay	136
3.3.2.1. Column filtration	136
3.4. Oxidation of PTEN-GST and VHR-GST	138
3.4.1. Oxidation of PTEN-GST with HOCl and sin-1 generated peroxy nitrite	138
3.4.2. Tandem mass spectrometry of PTEN	140

3.4.3. Mascot search of PTEN modification	143
3.4.4. Extracted Ion Chromatography (XIC) of PTEN modifications induced by SIN-1 and HOCl oxidation	149
3.4.5. Oxidation of VHR-GST with HOCl, sin-1 generated peroxynitrite and tetranitromethane	154
3.4.5.1. SDS-PAGE and Coomassie staining of oxidised VHR	154
3.4.5.2. Tandem mass spectrometry of VHR	157
3.4.5.2.1. Correlation of VHR activity and oxidative modifications via mediation modeling method	164
3.4.5.2.2. Search for modified and unmodified VHR active site nucleophilic residue and peptides	167
3.5. Discussion	176
3.5.1. Discussion of purification and expression of PTEN-GST and VHR-GST	176
3.5.2. Discussion of assaying enzymatic activity of PTEN-GST and VHR-GST before and after filtration	177
3.5.3. Discussion of SDS-PAGE and Coomassie staining of oxidised PTEN-GST and VHR-GST	179
3.5.4. Discussion of oxidative treatment of PTEN	180
3.5.4.1. Discussion of the combinatorial bottom-up mass-spectrometric analysis and phosphatase assays of oxidised PTEN	180
3.5.4.2. Discussion of domain regions of PTEN oxidised and nitrated by sin-1, HOCl and tetranitromethane	186
3.5.4.3. Discussion of oxidative and nitrative modifications in the context of crystal structure information for PTEN	187
3.5.5. Discussion of oxidative treatment of VHR	190

3.5.5.1. Discussion of the combinatorial bottom-up mass-spectrometric analysis and phosphatase assays of oxidised VHR	190
3.5.5.2. Discussion of domain regions of VHR oxidised and nitrated by sin-1, HOCl and tetranitromethane	207
3.5.5.3. Discussion of oxidative and nitrative modifications in the context of crystal structure information for VHR	208
3.6. Conclusions on the novel discovery, workflow and process for functional proteomics of PTEN and VHR	211
CHAPTER 4: CX5R PHOSPHATASE ARRAYING AND ARRAY INTERACTIONS	213
4.1. Introduction	214
4.1.1. Development of high resolution, low sample size antibody and protein pair arrays for protein interaction and oxidation studies	214
4.1.2. Library array optimisation and screening for PTEN and VHR	215
4.2. Results	216
4.2.1. Dynamic Bioarray chip versus Lifterslip library screenings	216
4.2.2. Optimisation of PTEN and VHR antibody and solution conditions for protein-protein interaction arraying and probing using Dynamic Bioarray chip	217
4.2.3. Protein library array screening of VHR using Dynamic Bioarray chip	221
4.3. Discussion	230
4.3.1. Discussion of technology selection and protocol optimisation for VHR arraying and probing	230
4.3.2. Discussion of the protein-protein array VHR interactome screening	231

4.4. Conclusions for optimisation and development of arraying technologies for the investigation of oxidised protein-protein interactions and protein-protein library screenings of VHR	234
CHAPTER 5: VHR IMMUNOPRECIPITATION WITH MASS SPECTROMETRIC ANALYSIS	235
5.1. Introduction	236
5.1.1. Comparative analysis, discovery and validation of protein-protein interactors of VHR	236
5.2. Results	238
5.2.1. Transfection of HCT116 cells with VHR-Flag	238
5.2.2. Immunoprecipitation of VHR interactors	240
5.2.2.1. Mass spectrometric and <i>in silico</i> analysis of VHR interactors	240
5.3. Discussion	245
5.3.1. Discussion of transfection of HCT116 cells with VHR-Flag	245
5.3.2. Discussion of immunoprecipitation of VHR interactors	246
5.4. Conclusion of immunoprecipitation and mass spectrometric VHR interactome discovery and protein-protein array comparative analysis	248
CHAPTER 6: DISCUSSION	251
6.1. Summary of Oxidation of VHR and PTEN results	252
6.2. Summary of nitration, chlorination and oxidation reagent results	253
6.3. Summary of interactome results	253
6.4. Justification of methods	254
6.4.1 Treatments	254
6.4.1.1. Advantages of treatments	254
6.4.1.2. Limitations of treatments	255
6.4.1.2. Quality of treatments in thesis	257

6.4.2. Mass spectrometry	258
6.4.2.1. Advantages of mass spectrometry for functional proteomics of oxidative modifications	258
6.4.2.2. Limitations of mass spectrometry for functional proteomics of oxidative modifications	259
6.4.2.3. Quality of mass spectrometry in thesis	261
6.4.3. Protein arrays	263
6.4.3.1. Advantages of protein arrays	263
6.4.3.2. Limitations of protein arrays	263
6.4.3.3. Quality of protein arrays in thesis	264
6.4.4. Immunoprecipitation	265
6.4.4.1. Advantages of immunoprecipitation	265
6.4.4.2. Limitations of immunoprecipitation	265
6.4.4.3. Quality of immunoprecipitation in thesis	266
6.4.5. Modeling	266
6.4.6. Justification of methods: Conclusions	266
6.5. What are the valuable factors in systematic functional proteomics of oxidation in protein tyrosine phosphatases?	267
6.6. Clinical potential for PTEN and VHR oxidative proteomics	269
6.7. Future paths	272
List of References	276
Appendices	319

List of Tables

Table 1. Plasmid constructs	79
Table 2. Exemplar specific activities of expressed and purified protein in non-reducing buffer	135
Table 3. Exemplar sequence coverage versus treatment for PTEN	144
Table 4. Summary of unique residue modifications predicted by Mascot for sin-1 oxidation found in 1:75 and 1:150 sin-1 oxidation at 37 ⁰ C for 1 hour	147
Table 5. Summary table of unique residue modifications predicted by Mascot for HOCl oxidations found in 1:30 and 1:300 molar concentration HOCl oxidation at room temperature for 1 hour	148
Table 6. Relative modification levels for non-nucleophilic active site regulatory cysteine Cys71 modifications from oxidation by sin-1 and HOCl	154
Table 7. Sequence coverage versus treatment for VHR	159
Table 8. Multivariate mediation modelling for modified amino acids in VHR on phosphatase activity upon sin-1 treatment displaying inhibitory effects on activity	166
Table 9. In silico digest, tryptic digest and GluC/AspN digest VHR peptides	169
Table 10. Target scan method ion selection for search for VHR active site peptides	175
Table 11. Summary of residues identified as modified and number of types of modifications identified in PTEN and VHR	212
Table 12. Selected putative interactors from VHR-GST Protoarray protein-protein library array screening	227
Table 13. Putative interactors from VHR-Flag Dynabead-anti-VHR antibody co-immunoprecipitation from HCT116 cell screening using LC-MS and Progenesis analysis	245

List of Figures

Figure 1. Methionine residue oxidations	46
Figure 2. Cysteine residue oxidations	47
Figure 3. Tyrosine residue modifications	50
Figure 4. PTEN regulation of the AKT signalling pathway	56
Figure 5. PTEN structure	57
Figure 6. VHR regulation of the ERK signalling pathway	62
Figure 7. VHR 3D structure	63
Figure 8. Fragmentation pattern and nomenclature	71
Figure 9. pGEX-4T1 vector map	80
Figure 10. Array spotting layout schematic	108
Figure 11. Dynamic Bioarray chip configurations	109
Figure 12. SDS-PAGE and Coomassie staining analysis of PTEN-GST expression and purification protocol and purified fractions	131
Figure 13. SDS-PAGE and Coomassie staining analysis of VHR-GST expression and purification protocol and purified fractions	132
Figure 14. Representative OMF calibration curve	134
Figure 15. OMFP assay for phosphatase activity of expressed and purified PTEN-GST in reducing conditions	134
Figure 16. OMFP assay for phosphatase activity of expressed and purified VHR-GST in reducing conditions	135
Figure 17. OMFP assay for phosphatase activity of VHR-GST after NAP-5 column filtration	137
Figure 18. OMFP assay for phosphatase activity of PTEN-GST after NAP-5 column filtration	137

Figure 19. SDS-PAGE and Coomassie staining of PTEN-GST oxidised using 75:1 and 150:1 molar ratio sin-1 and 30:1 and 300:1 molar ratio HOCl	139
Figure 20. Representative Total Ion Chromatogram of PTEN-GST	142
Figure 21. Representative sequence coverage analysis of PTEN after trypsin in-gel digestion	143
Figure 22. Representative Mascot output for Cys71 modification in sin-1 treated PTEN-GST	146
Figure 23. Representative extracted ion chromatograms and spectra of peptides containing trioxidised versus unmodified Cys71 in 1:150 molar concentration SIN-1 treated PTEN	152
Figure 24. Representative extracted ion chromatograms and spectra of peptides containing nitrated versus unmodified Tyr336 in 1:150 molar concentration SIN-1 treated PTEN	153
Figure 25. OMFP activity assay of phosphatase activity, densitometric analysis of SDS-PAGE and Coomassie stained SDS-PAGE of VHR upon treatment with sin-1	155
Figure 26. OMFP activity assay of phosphatase activity, densitometric analysis of SDS-PAGE and Coomassie stained SDS-PAGE of VHR upon treatment with tetranitromethane	156
Figure 27. Mass spectrometric analysis of VHR to calculate peptide relative abundances.	160
Figure 28. Functional proteomics of VHR upon oxidative treatment with sin-1 and tetranitromethane and phosphatase assay and in-gel digest of the major band corresponding to the molecular weight of the intact and active protein	161
Figure 29. Functional proteomics of VHR upon oxidative insult of HOCl and phosphatase assay and in-gel digest of the major band corresponding to the molecular weight of the intact and active protein	162

Figure 30. Select residues from functional proteomics of VHR upon oxidative treatment with sin-1 and in-gel digest of the major band corresponding to the molecular weight of the intact and active protein	163
Figure 31. Mediation modeling for modified amino acids in VHR on phosphatase activity upon sin-1 treatment displaying inhibitory effects on activity.	165
Figure 32. Representative Mascot output from identification of VHR active site Cys124 peptides	171
Figure 33. Extracted ion chromatography and spectra for identification of Cys124 unmodified, uncarbamidomethylated peptide in Peakview	172
Figure 34. De novo sequencing for identification of Cys124 unmodified, uncarbamidomethylated peptide in Peakview	173
Figure 35. Mapping of all residue modifications predicted by Mascot search from oxidation of PTEN by sin-1 and HOCl oxidation and nitration	187
Figure 36. Tyrosine modifications found in sin-1 oxidation of PTEN mapped onto PTEN crystal structure model	189
Figure 37. Cysteine modifications found in sin-1 oxidation of PTEN mapped onto PTEN crystal structure model	189
Figure 38. Modifications found in sin-1 treatment of VHR mapped onto VHR crystal structure mode	209
Figure 39. Modifications found in HOCl treatment of VHR via automated analysis with Mascot and Progenesis mapped onto VHR crystal structure mode	210
Figure 40. Anti-PTEN primary antibody and Alexafluor 647 conjugated secondary antibody probing 5uM PTEN-GST arrayed spots with Lifterslip™ and Dynamic Bioarray chip	217
Figure 41. Arraying range of PTEN-GST concentrations on Path substrate slide array with sciFLEXARRAYER, probing with PTEN-GST and antibodies	219

Figure 42. Anti-GST sandwich array probed with range of VHR-GST concentrations, anti-VHR primary antibody and Alexafluor 647 conjugated secondary antibodies	220
Figure 43. Anti-GST and anti-VHR sandwich array probed with VHR-GST, anti-VHR and anti-GST primary antibodies and Alexafluor 647 conjugated secondary antibodies	221
Figure 44. Protoarray protein-protein library screening of VHR-GST	224
Figure 45. Protein analysis through evolutionary relationships of VHR-GST protein-protein Protoarray library screening of selected putative interactors	229
Figure 46. Coomassie staining of HCT116 cells transfected with range of quantity of pcDNA3.1-VHR-Flag	239
Figure 47. Western blot of transfection of HCT116 cells with pcDNA3.1-VHR-Flag	240
List of Appendices	319
Appendix 1. PTEN protein-protein interactors	322
Appendix 2. VHR protein-protein	322
Appendix 3. pGEX-4T-1-PTEN plasmid construct.	324
Appendix 4. pGEX-4T-1-VHR plasmid construct.	325
Appendix 5. PTEN amino acid sequence	325
Appendix 6. GST affinity tag amino acid sequence	325
Appendix 7. Analyst MS chromatography method	325
Appendix 8. Oxidative modifications observed in tryptic peptides of PTEN by MS/MS with collisionally-induced decomposition after validatory sequencing of b and y series ions from 75:1 and 150:1 SIN-1 oxidation and incubation at 37 ⁰ C	332
Appendix 9. Oxidative modifications observed in tryptic peptides of PTEN by MS/MS with collisionally-induced decomposition after validatory sequencing of b and y series	

ions from 1:30 and 1:300 molar ratio HOCl oxidation and incubation at room temperature for 1 hour	333
Appendices 10. Oxidative modifications observed in tryptic peptides of VHR by MS/MS with collisionally-induced decomposition after validating sequencing of b and y series ions from 10:1, 75:1, 150:1 and 300:1 molar ratio sin-1 oxidation and incubation at 37°C for 1 hour	342
Appendices 11. Oxidative modifications observed in tryptic peptides of VHR by MS/MS with collisionally-induced decomposition after validating sequencing of b and y series ions from 30:1, 150:1 and 300:1 molar ratio HOCl oxidation and incubation at room temperature for 1 hour	345
Appendices 12. Oxidative modifications observed in tryptic peptides of VHR by MS/MS with collisionally-induced decomposition after validating sequencing of b and y series ions from 10:1, 75:1, 150:1, 300:1 and 1000:1 molar ratio tetranitromethane oxidation and incubation at 37°C temperature for 1 hour	356
Appendices 13. Excision of protein from SDS PAGE post Coomassie staining from HOCl treated VHR	356
Appendices 14. Western blot tests of anti-GST, anti-PTPMT1 and anti-VHR primary and secondary antibodies conjugated to horseradish peroxidase vs. PTPMT1-GST and VHR-GST purified samples	357
Appendices 15. Excision of protein from SDS PAGE post Coomassie staining from HCT116 cells transfected with pcDNA3.1-VHR-Flag for LC-MS, Mascot and Progenesis analysis	357

Abbreviations

3D	3-Dimensional
4-HNE	4-hydroxynonenal
Aβ	β –amyloid
ATM	Ataxia-telangiectasia mutated
BLAST	Basic Local Alignment Search Tool
BSA	Bovine Serum Albumin
CNS	Central Nervous System
CSF	Cerebrospinal Fluid
C-terminus Carboxy-terminus	
CX₅R	Cys-X₅-Arg
Cys	Cysteine
DNPH	2,4-dinitrophenylhydrazine
DMEM	Dulbecco's Modified Eagle's Medium
DTT	Dithiothreitol
DUSP	Dual specificity protein phosphatase
<i>E.coli</i>	<i>Escherichia coli</i>
EGFR	Epithelial growth factor receptor
emPAI	Exponentially modified Protein Abundance Index
ERK	Extracellular signalling related kinases
ESI	Electrospray ionisation
FASTA	FAST ALL
FBS/FCS	Foetal Bovine Serum/Foetal Calf Serum
FDR	False-discovery rate
FPR	False-positive rate
GST	Glutathione S-transferase
HIF	Hypoxia Inducible Factor

HR	Heart Rate
HRV	Heart Rate Variability
<i>H. sapiens Homo sapiens sapiens</i>	
IDA	Independent Data Acquisition
IEX	Ion Exchange Chromatography
IPTG	Isopropyl β-D-1-thiogalactopyranoside
JAK-STAT	Janus kinase-signal transducer and activator of transcription
JNK	c-Jun N-terminal kinase
LAMTOR2	Late endosomal/lysosomal adaptor and mitogen-activated protein kinase and mammalian target of rapamycin activator/regulator complex adaptor molecule 2
LB	Luria Broth
LC-MS	Liquid Chromatography Coupled Mass Spectrometry
Lys	Lysine
MAPK	Mitogen activated protein kinase
MEG	Magnetoencephalography
MCC	Mutant cancer protein
MOPS	3-(N-morpholino)propanesulfonic acid
MRI	Magnetic Resonance Imaging
MS	Mass Spectrometry
MS/MS (MS2)	Tandem mass spectrometry
mTOR	Mammalian target of rapamycin
NanoLC	Nano Liquid Chromatography
NBPF21	Neuroblastoma breakpoint family 21
NCBI	National Center for Biotechnology Information
NEUROD1	Neurogenic differentiation 1
OD	Optical Density

ON	Over Night
OMF	3-O-methylfluorescein
OMFP	3-O-methylfluorescein phosphate
ORF	Open reading frame
PBS	Phosphate buffered saline
PBST	Phosphate buffered saline with Tween-20
PDGFR	Platelet derived growth factor receptor
PET	Positron Emission Tomography
pGEX	pGEX GST fusion plasmid system
pGEX-4T1	pGEX GST fusion plasmid system 4T1
PIP2	Phosphatidylinositol-4,5-bisphosphate
PIP3	Phosphatidylinositol-3,4,5-triphosphate
PPARA	Peroxisome proliferator activated receptor alpha
PPI	Protein-protein interaction
PMT	Photomultiplier times
PTEN	Phosphatase and tensin homolog deleted on chromosome ten
PTEN-GST	Phosphatase and tensin homolog deleted on chromosome ten with glutathione S-transferase fusion construct
PTP	Protein Tyrosine Phosphatase
PTM	Post-translational modification
Qx	Quadrupole x
ROS	Radical oxygen species
RPC	Reverse phase chromatography
RNS	Radical nitrogen species
RT	Room temperature
S100A9	S100 calcium binding protein A9
SERCA	Sarcoplasmic reticulum Ca²⁺-ATPase

SDS	Sodium dodecyl sulphate
SDS-PAGE	Sodium dodecyl sulfate polyacrylamide gel electrophoresis
Sin-1	3-morpholinopyrrolidine
Ser	Serine
TEMED	Tetramethylethylenediamine
TIC	Total ion chromatogram
Thr	Threonine
TNM	Tetranitromethane
TOF	Time of flight
TRIP6	Thyroid hormone receptor interactor 6
TRIS	Tris(hydroxymethyl)aminomethane
UV/VIS	Ultraviolet/visible light
VHR	Vaccinia H1-related phosphatase, Dual specificity protein phosphatase VHR (DUSP3).
VHR-GST	Vaccinia H1-related phosphatase, Dual specificity protein phosphatase VHR (DUSP3)-glutathione S-transferase fusion construct
ZAP70	Zeta-chain associated protein kinase

Chapter 1

Introduction

1. Introduction

1.1. Damage, error, ageing and disease

Health may be defined as a state associated with a particular type of functioning, and absence of disease, damage and error. Health may be increased by 1) Restoral of health to that greater than no intervention yet lower than any previous state of health 2) Restoral of previous state of health directly prior to damage/error 3) Restoral of previous state of health to a prior timepoint before damage/error 4) Increase in health superior to any prior timepoint.

There is a role of the environment and a sub-optimal environment can affect health and longevity, including environmentally induced errors and damage contributing to ageing and disease processes. One potential role of the environment on ageing is through contribution to inflammatory-linked ageing through lifelong exposure to environmental antigens. Chronic antigenic stress resulting from exposure to multiple antigens, including allergens from the environment, may lead over time to an accumulation of memory and effector T cells, a reduction of naïve T cells and shrinkage of the T cell repertoire. This may be important as many diseases have an inflammatory pathogenesis, including neurodegeneration, atherosclerosis, diabetes, osteoporosis and sarcopenia (reviewed by De Martinis et al, 2005).

Behaviour has also been demonstrated to lead to organ regeneration, whereby sexual experience has been demonstrated to stimulate neurogenesis (Leuner et al, 2010), thus suggesting a role of modification to behaviours on ageing and disease.

Physiological homeostasis and homeostatic capacity has been demonstrated to be involved in age-related diseases, such as the association between physiological homeostasis and early recovery from stroke via medical interventions with molecules, including antipyretics, antibiotics, oxygen and insulin, and regulation of physiologic

variables such as serum osmolarity, temperature, arterial oxygen saturation and blood glucose (Langhorne et al, 2000).

Organ and tissue structure loss, such as pineal gland degeneration and calcification, occur progressively with age. This pineal gland calcification has been correlated with an exacerbated effect on decreased functioning and organ and tissue structure loss (Turgut et al, 2008). The pineal gland produced neuropeptide epithalamin has been demonstrated to normalise basic functioning in *H. sapiens* such as cardiovascular, immune and nervous systems, homeostasis and metabolism, with associated reduced incidence of acute respiratory disease, hypertension, deforming osteoarthritis, and osteoporosis (Khavinson & Morozov, 2003). Turgut *et al* (2008) state that the relationship between organ structure of the pineal gland is associated with a loss in secretory activity. Khavinson & Morozov (2003) demonstrate the potential of specific organ systems, organs, tissues and molecules to effect systemic alterations as part of their function or during dysfunction from accumulation of damage and error. This is demonstrated through the therapeutic application of pineal neuropeptides, that are reduced with age-related pineal gland calcification. Loss of homeostasis in the brain includes damage to the blood brain barrier (BBB) of epithelial cell tight junctions, where impaired BBB permeability may lead to the error of impaired clearance of moieties including the β –amyloid (A β) peptide which may contribute to brain deposits of A β peptide, a process implicated in neurodegeneration (Weiss et al, 2009).

Moving down from the organ and tissue level to the cellular level - Cells also have a cellular homeostasis, where differentiated and undifferentiated cells may undergo stress accumulate errors and have replicative limitations due to chromosomal telomere length which when shortened during cellular replication to a point of loss of chromosomal integrity (Corey et al, 2009, review), lead to a loss of cellular homeostasis. There are multiple cellular outcomes that can come from interaction

with stressors, with defined end points that result in maladaptive cellular functioning, limiting their function or leading to cell death, these are proliferation, quiescence, apoptosis, necrosis and cellular senescence (Hayflick, 1961).

Cellular senescence represents, for that cell, a potential replicative endpoint due to an inability to perform cell division, usually as a result of telomere shortening and the triggering of a DNA damage response. Although it is possible for the regenerative capacity of an organism to compensate for this as demonstrated by *Hydra vulgaris* (Martinez, 1998; Vaupel, 2004) which has multiple features including a high proportion of stem cells, constant and rapid cell turnover, few cell types, a simple body plan and an absence of the germ line being separated from the soma. Hence, there may be the potential to negate both senescence and cell proliferation by cellular, tissue and organ removal and replacement strategies in *H. sapiens*.

Cellular senescence has a trade off against another homeostatic dysregulation, that of uncontrolled cell proliferation, an attribute of cancerous cells (Campisi, 2001; Collado et al., 2005; Wagner et al., 2008; Rodier and Campisi, 2011). Cellular senescence is associated with the diseases of ageing through inflammation leading to cancer, and organismal ageing, and in preventing proliferation of potential cancer cells, and also has a role in promoting tissue repair (Sharpless and Depinho, 2004; Rodier and Campisi, 2011).

Damage and errors can also occur at the molecular level, intracellularly or extracellularly. Molecule loss and molecular structural damage and errors, and molecular interaction errors may occur intracellularly and extracellularly, which may contribute towards a loss of tissue and cell homeostasis. Damaged or dysfunctional proteins that are not cleared by the cell or organism may form intracellular aggregates or extracellular plaques, which are either unstructured aggregates or structured into amyloid insoluble fibrils (Knowles et al, 2015, Sin and Nollen, 2015, review). Protein misfolding, aggregation, accumulation and plaques have been suggested to be

involved in disease pathology across tissues and organs including the pancreas with aggregates of the islet amyloid polypeptide (Mukherjee et al, 2015), and the brain in Alzheimer's disease pathology (Haass and Selkoe, 2007).

Proteasomes are protein complexes which degrade unneeded, damaged or misfolded proteins down to peptides of seven or eight amino acids in length. The proteasome is essential to the cell cycle and also to apoptosis (Orlowski, 1999), so is involved in organismal homeostasis in addition to cellular homeostasis. The proteasome is also involved in the regulation of gene expression and responses to stress, including involvement in the ubiquitin post-translational modification of p53, where the p53 tumour suppressor pathway is a frequently altered in *H. sapiens* cancers (Devine and Dai, 2013). Alteration of the proteasome-ubiquitin pathway demonstrates the role of protein damage, protein homeostasis and stress for ageing and cellular homeostasis, and is an example of a pathway involved in cellular and organismal homeostasis.

In addition to the role of proteins in molecular damage and error, reactive oxygen species and cellular energy metabolism in the mitochondria are linked to cellular biochemical homeostasis, damage and error. This has been demonstrated by mouse knockouts of hypoxia-inducible factors (HIFs), where the HIF knockout mice displayed multiple organ pathology. Biochemical assays of HIF knockout mice samples showed enhanced generation of reactive oxygen species, reduced expression of anti-oxidant enzymes, studies showing lactic acidosis, altered Krebs cycle function, and dysregulated the molecular and reaction dynamics of fatty acid oxidation (Scortegagna et al., 2003). Reactive oxygen species are also implicated in the process of carcinogenesis including the formation of protein adducts (Bensaad and Vousden, 2005; Ziech et al, 2010, review).

Stressors such as inflammation (Kaur and Halliwell, 1994) and dietary fat (Djuric et al, 2001) can cause an increase reactive molecules, dysregulate the mechanisms

of redox homeostasis, or lead to an inability of the mechanisms of redox homeostasis to handle an increase in stressors, at the intracellular and molecular level; these collectively are classified as oxidative stress. Kaur and Halliwell (1994) demonstrate 3-nitrotyrosine to be present in the inflamed joint from patients with rheumatoid arthritis; 3-nitrotyrosine is a product of the reaction of nitric oxide with the superoxide radical, which generates peroxynitrite which then can decompose to products that nitrate aromatic amino acids such as tyrosine. Djuric et al (2001) found oxidative damage to DNA, 5-hydroxymethyluracil, to be 3X higher in a non-intervention group than low-fat diet group.

Short term controlled oxidative stress can be important in preventing oxidative damage, as long as homeostasis is maintained (Harris et al., 1998). This is known as hormesis, where hormesis describes a dose-response relationship where treatments at a lower level are beneficial but harmful at a higher level (Gems and Partridge, 2008).

Oxidative stress is thought to be involved in the development of a range of clinical conditions. Infections are thought to induce oxidative stress (Dey et al., 2009; Pacher et al., 2007), an example of which is the activation of the mitochondrial apoptotic pathway, which has been implicated in hepatocyte apoptosis during malaria. Fluorescence imaging has been used to monitor intramitochondrial superoxide anion generation during malaria, and inactivates mitochondrial aconitase (Dey et al., 2009). Oxidative stress has been implicated in carcinogenesis through the activation of transcription factors and subsequent expression of growth factors, inflammatory cytokines, chemokines, cell regulatory molecules and anti-inflammatory molecules. During the initiation stage of cancer, reactive oxygen species may produce DNA damage introducing gene mutations and structural alterations of DNA. In the promotion stage of carcinogenesis, reactive oxygen species may contribute to abnormal gene expression, block cell-to-cell communication and modify second

messenger systems. In the progression stage of carcinogenesis, reactive oxygen species may contribute to both genetic and epigenetic mechanisms (Klaunig et al., 1998). Reuter et al (2010, review) suggest that oxidative stress and inflammatory pathways contribute to cancer through chronic inflammation, recruitment of inflammatory cells to generate reactive oxygen species, involvement in cancer stem cell and tumour cell survival, cell proliferation, cell invasion and angiogenesis, detailing a signalling role in pathogenesis through errant signalling in addition to a role of damage causation. Oxidative stress may also be implicated in neurodegenerative disorder pathogenesis (Smith et al., 2000; Perry et al., 2002; Grune et al., 2004; Gella and Durany, 2009, Pacher et al., 2007,). Perry *et al* (2002, review) state that oxidative stress precedes protein aggregation, fibril and plaque formation in age-related neurodegeneration and involves oxygen radical damage including advanced glycation end products, nitration, lipid peroxidation adduction products, carbonyl-modified neurofilament protein and free carbonyls.

The utility of understanding types of ageing damage includes identifying markers for health, longevity and disease, drug target identification and drug development and therapy and medical device development and intervention. Given that ageing is a multifaceted process, there is a resource allocation risk of exploring and developing 1) Biomarkers and drugs that target mechanisms, molecules and processes that are correlated with ageing but do not have the capacity to restore homeostatic function, regenerate tissue and/or slow damage and error processes 2) Drugs that have side effects that progress other ageing pathways and damages, or 3) Biomarkers and drugs that have no correlation or causation for ageing or diseases of ageing in a way that is clinically relevant to maximise gains in health and longevity with efficient time and resources. Resource allocation risks may also come from assessing clinical targets and biomarkers at an inappropriate level of biological hierarchy or complexity.

Understanding enough physiology and biology to systematically repair, regenerate and replace physiological systems at the appropriate system level, and at the right time has the potential to deliver maximal health and longevity gains to a patient. In order to deliver maximal health and longevity gains to the patient, the development of techniques, understanding of biological processes, discovery of therapeutic targets, developing therapeutics and discovering effective biomarkers is required, and these require high quality, appropriate biological datasets and appropriate action following acquisition, handling and analysis.

1.1.1. The state of the patient

1.1.1.1. Omics: Markers and targets

Ome denotes a mass or part of a specified kind and the collection and analysis of that specified mass or kind is defined as *omics*, such as a proteome, and proteomics for a set of proteins and the collection and analysis of a protein set. Omes are sub-sets of samples with cut-offs in space and time, pertaining to one set of molecules, person, population, environment or a combination of these which may be analysed, modified or engineered. Pre-defined omes tend to be separated and classified by the type of molecule they contain or a particular tissue type or state of health or disease that they are associated with. Work that combines these omes together for complimentary analysis and modification is often denoted as panomics (Chen et al., 2012). Omics represents a systems approach to science and omics is a conceptual framework that has been made possible through high-throughput, multiplexed and automated technologies. Omics allows multiple biomolecules and data points to be detected in one sample and multiple samples to be processed.

Markers, predictors and targets for intervention can be environmental, and may correlate with the geographic location an individual lives and thus what molecules and stressors an individual comes into contact with, and the resources available in a particular environment or location, Cheshire (2012) demonstrates differences in life expectancy at birth and child poverty across geographic locations. Markers for assessing exposure to environmental carcinogens may include protein oxidation (Ziech et al., 2010, review).

Markers, predictors and targets of intervention may be social and behavioural. For example, Terracciano *et al* (2008) found general activity, emotional stability and sociability, and conscientiousness to be personal predictors of longevity, by performing a temperament survey as part of a longitudinal studying of ageing. Palmore (Palmore, 1982) also showed health self-rating, work satisfaction and performance intelligence as predictors of longevity and morbidities, within both fixed time windows and longitudinal studies, an example of which is morbidity within a 25-year time follow up.

Markers and predictors may be physiological, such as heart rate (HR) and heart rate variability (HRV) (Poirier, 2014). HR is indicative of the status of the cardiovascular system, cardiac autonomic nervous system and metabolic rate. Exercise can reduce HR and there is an association between functional cardiovascular capacity and mortality, where effect of exercise on cardiovascular capacity can be measured with HR (Myers et al., 2002). Soares-Miranda *et al* (2014) analysed cross-sectional and longitudinal data for physical activity and HRV, and reported that greater total leisure time activity, walking alone, walking pace and walking distance were prospectively associated with favourable HRV indices.

Physiological and organ system markers and predictors such as HRV patterns may indicate which system may fail first, the likelihood of failure, time-to-failure and order of failure given mechanical models, such as the mechanical models for heart

failure (Louridas and Lourida, 2012), whilst to detect some organ failures, organ specific time-to-failures, cancer incidence and relative failure rates between organs additional testing modalities may be required. Mechanical and engineering mathematics may be useful including applying stress testing, time-to-failure, mechanical part longevity and part lifecycles methods to biology and medical devices, not only for preventative, predictive and personalised medicine but in the engineering and maintenance of tissue engineered organs, organ transplants and implanted medical devices. Magnetic resonance imaging (MRI) has also been used to monitor brain ageing at an organ and tissue level, where ventricular enlargement was demonstrated in rodents during ageing, and has been proposed as a structural biomarker (Chen et al., 2011).

Biological markers, or biomarkers, are molecules, signatures or patterns that are indicative of a particular process, capacity, response, phenotype, state of the organism or ome, and predictive, prognostic, diagnostic and utilised to monitor a particular outcome. Biomarker diagnostics can have several characteristics including early detection of state or phenotype formation, ability to be detected in small amounts, ease of detection, time taken to process sample for biomarker, high correlation to state or phenotype and direct role in state or phenotype. Biomarkers infer the existence of a state or phenotype and the utility of biomarkers can come from the ability to rapidly make decisions and take actions based on current data. Accurate diagnostic molecular biomarkers are at the forefront of changes from one state or phenotype to another that may be involved in an out-of-homeostasis occurrence or damage, and so research and utilisation of biomarker-led scanning, screening and diagnostics allow for the detection of states and phenotypes so that these states can be attempted to be modified via a potential intervention. This modification may be in the form of an alteration in clinical therapeutic administration, healthcare, healthcare

recommendations for lifestyle and environment, surgery, or optimisation of regenerative medicine bioreactor variables for growing tissues and organs.

Omics may be used for marker discovery, discovery of therapeutic targets, assessing states of survival and disease, and engineer and select for survival states through personalised, predictive, preventative and therapeutic strategies to select for omes that have associated endpoints or likelihoods for survival. Biomarker omics may be used to assess the real-time, or longitudinally sampled, survival outcomes linked to a particular phenomena (Chen et al., 2012). Chen *et al* (2012) perform a personalised analysis of genomic, transcriptomic, proteomic, metabolomic and auto-antibody profiles of an individual over a 14 month period, and utilised the omic data to identify disease risk. Chen *et al* (2012) performed the auto-antibody profiling using Invitrogen ProtoArray Protein Microarray v5.0 array technology that contained 9,483 unique proteins spotted in duplicate, and patient serum and plasma samples alongside those of healthy controls. They detected antigens with increase reactivity including an insulin receptor binding protein. They also performed proteomic mass spectrometry across healthy and diseased states for the relative levels of 6,280 proteins across 14 timepoints, using isobaric mass tags, liquid chromatography and mass spectrometry of protein peptides (Cox and Mann, 2010; Theodoridis et al., 2011). In addition to personalised medicine approaches, longitudinal studies of ageing populations and populations with age-related disease may have utility for discovery and assessment of markers and targets. Engelfriet *et al* (2013) provide a review of markers of ageing in longitudinal studies in *H. sapiens*.

Biomarker analysis of individuals such as super-centenarians and astronauts may provide useful datasets alongside personalised medicine datasets and population studies of ageing and age-related disease, as super-centenarians and astronauts represent exemplar populations and datapoints relating to exceptional fitness, training, and longevity. Thus these patient cohorts may be able to provide

unique data to improve the health of other patients, and potentially providing quality of care and biometric benchmarks, alongside healthy controls and young control for the wider application of preventative, personalised and regenerative medicine. The impact of space travel on astronaut physiology and the potential for oxidative stress represents a usage for biomarkers and personalised and preventative medicine (Schmidt and Goodwin 2013). Schmidt and Goodwin (2013) describe an assessment of pre-mission status of conjugation agents that bind therapeutic agents to be administered therapeutically to the astronauts. This is so an assessment may be made regarding the depletion of molecules such as glutathione, which determine drug metabolism and cellular redox balance and prevent damage to cellular components from reactive oxygen species. Schmidt and Goodwin (2013) state that the purpose of personalised medicine for astronauts, and the biological capacity of the individual, is not to exclude individuals from spaceflight but to mitigate and limit the damage from metabolic processes on a personalised basis.

Omics can be used to discover biomarkers associated with longevity, biomarker differences in long-lived individuals. An example of this being analysis of Japanese centenarian plasma by proteomic peptide mass fingerprinting (Miura et al., 2011). Miura *et al* (2011) found the proteins paraoxonase 1, and apolipoprotein E were decreased in abundance whilst haptoglobin and α_1 -microglobulin were increased in abundance in their super-centenarian cohort. These proteins are involved in oxidative stress response and systemic redox regulation, and it Miura *et al* (2011) suggest that serum paraoxonase 1 may be protective against the development of atherosclerosis via a prevention of oxidation for particular super-centenarians (Ng, 2005; Miura et al., 2011).

Molecular targets may include intracellular moieties such as proteins. Intracellularly targeted therapeutics may affect the binding affinity of a protein to other proteins and moieties in a signalling pathway. 2-Phenylethanesulfonamide is an

example of this, which reduces the binding affinity of p53 to B-cell lymphoma 2 and B-cell lymphoma xL (Wang and Sun, 2010, review).

Molecular targets may include extracellular proteins, such as the Tau protein, where there is an indication that extracellular Tau protein may induce protein aggregation in neighbouring cells. The approaches of blocking protein uptake and interaction with cells, and clearing extracellular Tau protein are suggested by Holmes and Diamond (2014). The Tau protein is an example of a target that is also a biomarker utilised for diagnostic and predictive purposes (Schraen-Maschke et al., 2008).

Molecular targets may include protein post-translational modifications, such as the modification of histone proteins, which are involved in the packaging of DNA and regulation of access to DNA by transcription machinery, and regulators of DNA. Histone modification therapy of cancer may include therapeutics that interfere with the activity of enzymes involved in modifying histones (Biancotto et al., 2010).

Scenarios when there is a requirement for technology development for omics and informatics analysis and for biomarker, target and therapeutic discovery include 1) If and when there is a need to find additional biomarkers, predictors and targets 2) If known markers, known predictors and medical interventions are not the most effective solution or 3) There is a need to analyse large throughputs of patient samples or multiple biomarkers at speed or in multiplex

Method and technology development is a driver of performance in biomarker and therapeutic target discovery and analytics. Reliability, reproducibility, expertise, point-of-care, sensitivity, false positive and false negative rates, health risks, development cost, development time, technology cost and cost per test and test time are factors that need to be considered along the value chain and in biomarker technology development. In research and development of biomarkers and therapeutic targets – for a particular physiology one must consider what the criteria are for the

state that is being measured and which markers and targets as well as which technologies and methods meet criteria. Tandem mass spectrometry is an example of a sensitive technology, which allows large-scale quantitative analysis of peptides and specific modifications to amino acids (Larsen et al., 2006), which may enable markers and therapeutic targets to be discovered and developed.

1.1.1.1.1. Proteomics

Proteins have the properties of markers and therapeutic targets, which may be exploited. This may include being a marker indicative of or target involved in the functioning and state of a given biological intracellular or extracellular system including signalling receptors and cellular signalling, gene expression, catalysing metabolic reactions, and homeostatic and structural roles.

Proteomics, the study of sub-sets of proteins and their states has an important role in the clinic and at the pre-clinical work primarily in marker, predictor and target identification. Dalle-Donne *et al* (2006) detail diseases associated with increased oxidative stress on the basis of potential biomarkers of oxidative damage, which includes damage to proteins. Mayr *et al* (2006) review proteomics-based development of markers in cardiovascular disease and the role of proteomic-based biomarkers for therapeutic development. Mayr *et al* (2006) describe how the usage of 2D electrophoresis of proteins followed by mass spectrometry, to analyse phospholamban genetic knockouts in rodents showed alterations in myofibril proteins, calcium-handling proteins and post-translational modification of proteins (Chu et al., 2004). These proteins may be involved in enhanced cardiac function in the genetically altered rodents, and this approach could potentially yield therapeutic targets through understanding the mechanisms of the sarcoplasmic reticulum and calcium cycling

sub-proteome related to the knockout gene and dysregulated proteins (Mayr et al., 2006).

Proteomics techniques include mass spectrometric techniques deriving from liquid chromatography and tandem mass spectrometry (Larsen et al., 2006; Mann, 2010; Theodoridis et al., 2011) or 2D gel electrophoretic protein separation and mass spectrometry (Chu et al., 2006), immunohistochemical techniques including two-dimensional Western blotting (Zhan and Desiderio, 2004) and microarray techniques (Chen et al. 2012) as well as assays for protein function but can include any technique, with labelling or label free, that detects proteins, the activity of a protein or the function of a protein, including its interactions.

Technologies for protein marker and therapeutic target discovery offer specific criteria, benefits and limitations. Chemical assays usually assess a specific target or more limited set of biomarkers absolutely and comparatively to mass spectrometric and arraying technologies. Chemical assays can offer specificity, chemical as oppose to computational readouts and signal amplification. Mass spectrometric methods may include signal amplification via mass tags, a demonstration of this would be the use of boronic acid isolation of proteins that contain oligosaccarchide chains covalently bonded to polypeptide side-chains, referred to as glycoproteins, followed by tagging of glycoproteins with gold nanoparticles (Liu et al., 2013).

Assays rely on the specificity of the chemical interaction or reaction, where the number of molecules that can generate false-positives and negatives is limited. To decrease the likelihood of false-negatives or positives a complementary method can be used. A demonstration of proteomic assay confirm or compliment mass spectrometry is the usage of Western blotting to detect nitrotyrosine in *H. sapiens* pituitary proteome, alongside the usage of tandem mass spectrometry to confirm the protein sequence (Zhan and Desiderio, 2004).

Protein assays may be qualitative, relative, semi-quantitative or quantitative and can be used to measure enzyme activity levels, such as anti-oxidant capacity, where enzyme kinetics may be measured spectrophotometrically over time or by measuring the substrate or a metabolite, as demonstrated by Paglia and Valentine (1967) for the quantitative direct measurement of glutathione peroxidase by linking the peroxidase reaction to glutathione reductase. Biochemical screening can include screening of blood serum markers using an array of colorimetric tests that detect shifts in absorption maximum and the reflection density of chromophores or complexes present or formed. Staruchova *et al* (2008) demonstrate this in screening aminotransaminase, alanine aminotransferase, γ -glutamyltransferase, alkaline phosphatase, amylase, urea, creatinine, albumin proteins and total protein alongside non-protein metabolites in serum samples from *H. sapiens* to assess the effect of mineral wool exposure using a Vitros 250 analyser.

Chemical assays may have limitations regarding correlation to physiological and higher-order functions and structures than the specific molecular targets of the assay. Samples may not be practical to take, sample collection may be invasive, there may be low resolution if multiple target molecules or signals are required, or if an assay cannot distinguish between different molecules. Chemical assays may be used in combination with each other or with different techniques to identify markers or targets, which may include measurements taken alongside such as non-biochemical markers from an organism and physiologic level, including continuous monitoring of a patient across environments and from personal, cohort, group and longitudinal data maximise the utility of chemical assays for the purposes of elucidating markers and targets of health, disease, organismal states and therapeutic targets. To assess the full utility of chemical markers and targets, having more markers may be of utility, as may the acquisition of corresponding functional data and correlational data – such as

combining the enzymatic activity measurements of proteins via chemical assays with mass spectrometry of proteins.

Mass spectrometry offers qualitative, relative, semi-quantitative or quantitative methods for identifying and measuring protein markers and targets from their mass.

Mass spectrometry proteomics may be utilised for non-invasive samples as demonstrated by Zimmerli *et al* (2008) who use electrospray time-of-flight mass spectrometry to develop coronary artery disease from urinary samples from patients.

High throughput technologies such as mass spectrometry and protein microarrays have allowed for algorithmic models to be created that are predictive to clinically appropriate and approved levels of sensitivity to diagnose between patients at risk and healthy controls, including different types of growths including between and benign versus malignant growths, and cardiovascular disease, allowing appropriate treatment, stratified medicine and assign risk groupings and the use of multiple protein biomarkers developed from high throughput proteomics can improve clinical sensitivity of tests (Zimmerli *et al*, 2008; Moore *et al.*, 2010; Yurkovetsky *et al.*, 2010). Zimmerli *et al* (2008) demonstrate the development of a biomarkers set that is a signature for coronary artery disease and is predictive, showing a 98% sensitivity and 95% specificity, and demonstrate that a change in biomarkers in patients given therapy and those who make behavioural changes. The biomarker panel consisted of 15 polypeptides with identifier, masses and migration time.

Microarray technology proteomics includes forward and reverse phase protein arrays. Forward-phase arrays have the capture agent immobilised on the array and are probed with samples, and reverse-phase arrays have the samples immobilised and are probed with to detect the presence of a specific moiety.

Microarrays contain a miniaturised dot-blot, where antibodies or proteins bound to a surface are probed with a solution that contains moieties that bind the desired arrayed surface molecule, which is followed by the further probing with of the array

with solutions of detection molecules such as antibodies with conjugated fluorophores, followed by scanning with a fluorescence reader to associate fluorescent signal with protein-protein binding to assess molecule interaction function. Array technology can be used for quantifying the relative, semi-quantitative or quantitative abundances of proteins and protein modifications.

A demonstration of the use of protein microarrays for analysing disease samples is analysing ovarian metastasis in epithelial ovarian cancer, which has the worst prognosis of all gynaecological cancers and late stage presentation (Sheehan *et al.*, 2005). Sheehan *et al* (2005) demonstrates the analysing of cell signalling network deregulation, hyperactivity and modifications that occur with metastatic cancer with the outcome of finding metastatic signatures from primary tumours via protein array assessment of protein interactions and their modifications. Sheehan *et al* (2005) utilised laser capture microdissected frozen tumour sections as samples to create a reverse-phased array on nitrocellulose slides and the arrays were probed with phosphospecific antibodies to proteins involved in mitogenesis to assess their phosphorylation post-translational modification status.

Protein arrays may have utility for the full potential of biomarkers to add functionality meta-data to biomarker databases to develop metrics and identify the most predictive markers present in a clinical sample. Akbani *et al* (2014) state that reagents of appropriate quality, centralised data repositories, flexible shared standards and best practices, and development of best practices for sample handling have the potential to make protein array technology appropriate for clinical practice, alongside other limitations that may be protein, protein post-translational modification or sample specific.

1.1.1.1.1. Protein Post-Translational Modifications

Protein post-translational modifications (PTMs) indicate a particular state that a protein is in and have a significant effect on protein and cellular function by modifying stability, interaction, conformation, sub-cellular localisation, activity and binding (Spickett et al., 2006; Spickett & Pitt, 2010). PTM occurs after the translational step in protein production. PTMs are caused via interaction with other proteins and moieties and are, enzymatically or non-enzymatically, chemically or biologically induced. PTMs effect protein function and may include gain of activity or function, and thus have a role in regulating signal transduction pathways that control cell states, survival and function. PTMs represent both markers for a state, and also targets for therapeutic intervention. Protein phosphorylation PTM involves a substantial set of the proteome (Cohen, 1998), this modification occurs when a phosphate group from adenosine triphosphate is transferred to serine, threonine or tyrosine protein residues enzymatically via protein kinases, a reaction which is reversible enzymatically via protein phosphatases. The regulation of kinase and phosphatase enzymes that modify proteins with phosphorylation PTMs are themselves regulated and dysregulated. For proteins involved in transcriptional regulation and cell signalling, sub-stoichiometric quantities of protein PTM may be required to alter signalling dynamics and competing signalling pathway strengths. p53 is a example of a protein that is modified at Serine 315 by kinase activity with stoichiometric levels of phosphorylation PMT, which is associated with changes in protein interaction and transactivation (Loughery et al., 2014).

As the PTM state of a protein may directly affect its function, any PTM that occurs that increases the protein, cell or organism's likelihood of survival may give that protein, cell or organism a selective advantage that can increase its own survival and/or its mutual survival along with other cells and tissues. PTMs may also decrease

the survival likelihood of a protein, cell or organism, and thus may favour the survival of a particular process, state, molecule or cell to the health detriment of the organism.

There are many types of PTM and PTM-status events, and phosphorylation and de-phosphorylation of cellular signalling proteins have been widely studied in cellular biology and biology of cell proliferation and cancer. Cellular signalling transduction pathways control cell states and gene transcription involve a series of protein kinases and regulatory phosphatases, including 90 protein tyrosine kinases and 107 protein tyrosine phosphatases in *H. sapiens* (Alonso et al., 2004). Alonso *et al* (2004) state that whilst the genes are known, alternative spliced products, PTMs and protein-interactions for kinases and phosphatases are required in a comprehensive, detailed and quantitative manner.

Signal transduction pathways have a role in the control of cell fate, survival and function, and involve enabling protein activities, crosstalk and sub-cellular localisation. Signalling proteins exist as multiprotein micromachines complexes, that contain control, execution and feedback mechanisms. Signalling protein complexes exist transiently, with binding strengths and kinetics of such interactions having the potential to be regulated by PTMs. A demonstrated example of this is the SH2 and PTB domains, where phosphorylated tyrosine residues are the docking sites within a sequence that confers specificity to specific docking proteins (Pawson, 2004). Tyrosine kinase receptors, such as epidermal growth factor receptor, are a class of protein which use ligand-binding triggered auto-phosphorylation to generate phosphotyrosine docking sites for subsequent recruitment of SH2 and PTB domain contain proteins that have specificity and are in a particular sub-cellular localisation, which leads to activation of a particular receptor-activated signalling pathway and competing signalling pathway strength (Schulze et al, 2005).

Another instance of PTM are oxidised proteomes, or proxomes, which are sub-omes that includes a unique sub-set of proteins undergoing redox reactions and the

organism's proteome. Previous proxomics has been used to map proxomes for fundamental biological knowledge (Thamsen & Jakob., 2011). Thamsen & Jakob (2011) show how mass spectrometry with specific probes and gel separation can be used for particular thiol modifications, and that this has been used to map reversible cysteine thiol oxidation status across cellular redox networks. Proxomics has been utilised to map proxomes in Alzheimer's disease, including protein nitrotyrosine and carbonyls in proteins (Sultana et al., 2006). Dalle-Donne *et al* (2005) review how the proxome relates to oxidative stress and disease, which is a step in the workflow for screening for potential biomarkers and therapeutic targets, subsequent biomarker and therapeutic development and diagnostics and understanding similarities and shared processes involving protein oxidation between disease, cell and tissue types.

Protein oxidative PTM is additionally important as oxidation arising from oxidative stress plays a role in many diseases and processes that advance ageing such as inflammation and also is involved in the interaction and correlation between inflammation, cancer and ageing (Reuter et al, 2010).

1.1.1.1.1.1. Protein Oxidative Post-Translational Modifications

Proteins can become oxidised including nitrations and chlorinations, due to the presence of oxidising agents, *in vivo* this occurs via oxidants and free radicals that enter the body, or are produced in the body including intracellularly via enzymatic reactions or as part of energy metabolism or signal transduction and redox signalling. Oxidants that modify proteins include reactive oxygen species (ROS) such as H₂O₂, superoxide and HOCl, reactive nitrogen species (RNS) such as peroxynitrite and metal ions Fe (III) and Cu (II) (Stadtman, 1991) and molecular products of other primary oxidation reactions (Spickett et al., 2006). Oxidants are also generated enzymatically (Sauer et al, 2001) through electron leakage from the mitochondrial

electron transport chain, cytochrome P450 and redox-cycling enzymes, oxidase enzymes such as NADPH oxidase, dual oxidases, xanthine oxidase and phagocyte oxidases.

Protein oxidation consists of an attack by an oxidising agent that modifies the protein leading to protein backbone cleavage, protein adducts or protein side chain oxidative PTM (Stadtman, 2001). Protein oxidation can be damaging to proteins causing or leading to degradation or sub-optimally affecting protein function by side-chain modification. Protein oxidation can also be damaging to cells and organisms if redox signalling is dysregulated. The interplay between protein oxidations that are involved in cell signal transduction and protein regulation, and protein oxidations that sub-optimally affect function and lead to disease may be an important class of biomarkers and targets if additional markers and targets are needed.

Oxidation can lead to protein aggregation, cross-linking, fragmentation and loss or gain of enzymatic and functional properties, including interactions (Capeillere-Blandin et al, 1991). This has been demonstrated by the exposure of β_2 -microglobulin to radical oxidation leading to aggregation and the formation of dityrosines. Protein aggregates caused by protein oxidation may have a role in disease via aggregates contributing to the formation of plaques in amyloidosis (van Ypersele de Strihou et al, 1991; Koch 1992).

Methionine oxidation (Figure 1.) has biological relevance in homeostasis and ageing including, oxidant scavenging, redox cycling and protection systems such as Methionine sulphoxide reductase A (MsrA) (Wu et al., 2012) exist in the mitochondria. Methionine sulfoxide (Figure 1.b) is chemically and biologically reversible, via chemical reduction or sulfoxide reductase enzymes. Methionine sulphone (Figure 2.c) has been proposed to be chemically and biologically irreversible, aside from via protein degradation and protein synthesis, which effectively replaces modified proteins with unmodified versions. Methionine residues in proteins have been

proposed to functionally act as a scavenger and protect other more critical residues from oxidation and thus have an anti-oxidant role (Levine et al., 1996). Ghesquiere *et al* (2011) perform an experiment *in vivo* using *H. sapiens* Jurkat cells stressed with H₂O₂, stable isotope labelled methionine, diagonal chromatography and tandem mass spectrometry to assess the cellular proteome of protein-bound methionine oxidation.

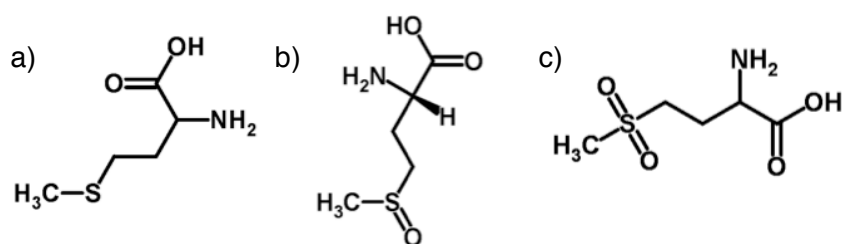


Figure 1. Methionine residue oxidations

a) Methionine b) methionine sulfoxide c) methionine sulfone

Experimentally, methionine oxidation analysis is non-trivial as methionine residues are readily and continually oxidised, including by air, by protein separation on sodium dodecyl sulphate polyacrylamide gel electrophoresis (SDS-PAGE) and by electrospray ionisation before mass spectrometric analysis.

The most readily oxidised protein residues are cysteine and methionine. This biochemical feature is due to the sulphur on the amino acid side chains of cysteine and methionine.

Cysteine oxidation is important (Figure 2.), as biological evolution has taken advantage of the oxidisibility of the cysteine residue by utilising it in protein active sites, including redox-based molecular switch regulatory mechanisms, such as in the active site of the CX₅R phosphatase and tensin homologue deleted on chromosome ten (PTEN) protein (Leslie et al., 2003), and also in maintaining secondary and tertiary protein structure due to cysteine disulphide bridge formation. The thiol of

cysteine and its oxidation to a disulphide (Figure 2.b) is biologically reversible, as is the singly oxidised sulfenic acid and the doubly oxidised sulfinic acid (Figure 2.c) (Jeong et al., 2006) with the sulfonic acid (Figure 2.d) described as biologically irreversible. S-nitrosothiols are another class of cysteine oxidation *in vivo* (Forman et al., 2004; Hess et al., 2005). Cysteine specificity for redox signalling can also come from accessibility to the residue, whereby active site clefts may alter accessibility to oxidants and anti-oxidants such as glutathione, as well as spatial location of the protein to the oxidant source, such as PTEN localisation to the cell membrane. Enzymatic reversibility of cysteine oxidation is possible with protein disulphide oxidoreductase activity via enzymes such as glutaredoxin, thioredoxin, thioredoxin reductase and thioredoxin peroxidases and protein disulphide isomerases (Holmgren, 1989). The reversible reactions can function as molecular redox switches, and are thusly considered a regulatory mechanism, although the possibility of dysregulated reversible signalling has the possibility to be a class of damage depending on the state the switch should be in and the downstream outcomes of the reversible but sub-optimal state of the molecular logic gate.

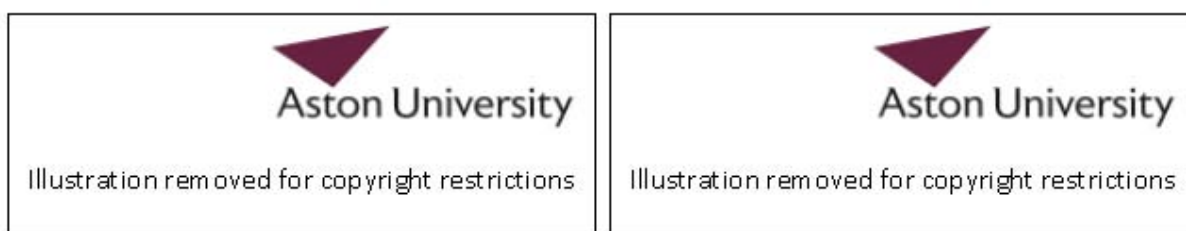


Figure 2. Cysteine residue oxidations

a) Cysteine b) cysteine disulphide c) cysteine sulphinic acid d) cysteine sulphonic acid

Non-sulphur residue oxidations include tyrosine modifications (Figure 3.), including 3-chlorotyrosine, 3-nitrotyrosine and 3-hydroxytyrosine, but also include modifications such as 5-hydroxyproline. Studies have indicated that tyrosine nitration is a highly selective process limited to specific residues on specific proteins (Aulak et al., 2001; Gow et al, 2004; Kanski et al, 2005; Kanski et al 2005a) due to both the charges of neighbouring residues, absence of proximal cysteines (Rubbo et al., 2000) and hydrophobicity of the environment.

Nitrated PTMs are caused by RNS, which are a sub-set of oxidants. *In vivo* nitrations occur due to the formation of nitrating agents such as peroxynitrite. Peroxynitrite is formed from nitric oxide (NO) and the ROS superoxide ($O_2^{\cdot-}$). Peroxynitrite is formed when NO and superoxide are synthesised in close proximity, combining spontaneously via a diffusion limited reaction (Huie & Padmaja, 1993). Peroxynitrite is an oxidising and nitrating agent and has multiple biological targets including protein transition metal centres and cysteine thiol oxidation (Alvarez & Radi, 2003). Peroxynitrite can oxidise the cysteines of enzyme active site residues including those of protein tyrosine phosphatases (Buchczyk et al, 2003; Rubbo et al, 1996) amongst others including glyceraldehyde-3-phosphate dehydrogenase, creatine kinase and mitochondrial respiratory chain complex I, II and III proteins (see Pacher et al. 2007 comprehensive peroxynitrite review).

Determination of the prevalence of peroxynitrite oxidation of enzyme active sites, and the relevance of these to cell signalling, cell states and end fates, and disease states may have utility for therapeutic target development and marker identification.

Peroxynitrite has been shown to nitrate tyrosine (Pacher et al, 2007). Pathological conditions can increase peroxynitrite generation leading to dysfunction of critical processes and signalling and induce cell death (Spickett et al., 2006). Nitrotyrosines are an interesting moiety as it is formed in at least 50 human diseases (Greenacre & Ischiropoulos, 2001) including acute inflammatory lung tissue,

atherosclerosis and rheumatoid arthritis (Shacter, 2000). Nitrotyrosines are also a marker of nitroxidative stress on a cellular, tissue and systemic level and can disrupt nitric oxide signalling (Radi, 2013). Radi (2013) states that nitrotyrosine *in vivo* is generated from peroxynitrite-mediated nitration and other sources including heme peroxidase-catalysed reactions and that yields may be quantified via calculation of the steady-state of nitrating species, secondary radical processes over tyrosyl radicals, superoxide dismutase presence and diffusion of relevant moieties across cellular compartments.

The formation of nitrotyrosine in proteins was demonstrated in 1966 via tetranitromethane treatment (Sokolovsky et al, 1966). Tyrosines are also targets of de-/phosphorylation, and phosphorylation and de-phosphorylation are critical for cellular signalling, cell cycle and cell fate. Nitrotyrosine (Figure 4. b) has been proposed to mimic phosphotyrosine (Mallozzi et al., 2001), which may provide a direction for diagnostics development, biomarker development and drug target development if additional biomarkers and small molecule therapeutics are needed above and beyond what exists rather than developing regenerative and prosthetic medicine, translating current knowledge and implementing diagnostics.

An example of tyrosine oxidations having been used as markers, has been demonstrated by 3-nitrotyrosine, which has been seen in bio-banked samples to be elevated over 6-fold in Fabry disease patients (Shu et al., 2014) measured by liquid chromatography coupled electron spray ionisation mass spectrometry. Shu *et al* (2014) demonstrate that in a mouse model of Fabry disease 3-nitrotyrosine was increased in aortic samples 40 to 120-fold and Shu *et al* (2014) suggest 3-nitrotyrosine is a marker for vascular involvement in Fabry disease – when it may be a biomarker for the vascular pathology that is part of Fabry disease.

Proteins are recycled, repaired and protected by a series of mechanisms including proteolysis, proteostasis, translation, anti-oxidant systems, enzymatic

systems to reverse oxidative modifications, lysosomes, redox sensing systems. Yet, ROS and oxidative stress related damage may still occur in cells, and proteins that are irreversibly oxidised and have gained or lost function are predicted to disrupt protein, cellular and organismal homeostasis and homeostatic capacity.

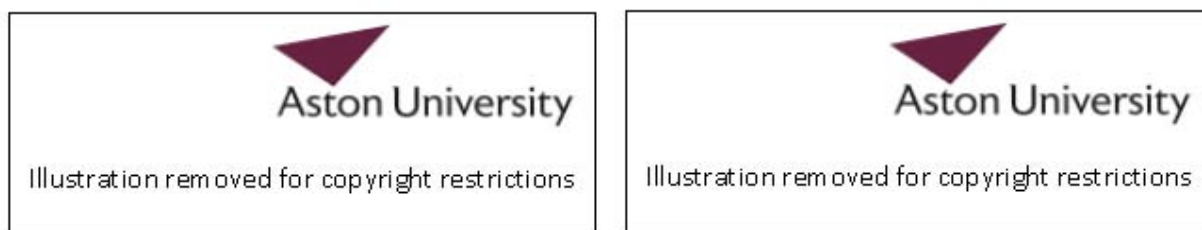


Figure 3. Tyrosine residue modifications

a) Tyrosine b) Nitrotyrosine c) Hydroxytyrosine d) Chlorotyrosine

Some protein oxidations are biologically reversible, others are irreversible such as methionine sulfone, and cysteine sulphonic acid. The reversibility, clearance, amino acid location, abundance, occurrence and function of a protein oxidation will all have an effect on whether a particular instance of a modification affects health sub-optimally.

To measure protein oxidations, the amount of oxidised protein, specific oxidations, specific proteins, specific protein sites, general levels of oxidation, indirect measures of oxidation, oxidised protein aggregates and protein interactions and enzymatic function can be measured.

Carbonylation is a non-enzymatic PTM, where carbonyl stress leads to carbonyl compound formation via the autooxidation of carbohydrates and lipids reacting with protein amino groups, and is used a general marker for ageing. Kalim *et al* (2014) suggests that as protein carbonylation is mechanistically involved in adverse clinical

outcomes for kidney disease. Protein carbonyls have been observed in Alzheimer's disease, arthritis, diabetes, sepsis, chronic renal failure and respiratory distress syndrome (Dalle-Donne, 2003, review). 2,4-dinitrophenylhydrazine (DNPH) can be used to detect carbonyls through spectrophotometric assay, enzyme-linked immunosorbent assay, western blot immunoassay (Dalle-Donne, 2003, review), or laser desorption/ionisation mass spectrometry with enrichment protocols and labelling such as the use of DNPH (Fenaille et al., 2004; Fenaille et al., 2005; Bollineni et al., 2011), biotinylated probes and hydrazines coupled to fluorescent moieties alongside label-free techniques (reviewed by Fedorova et al, 2013).

Wang et al (2007) demonstrated amino acid analysis and quantification of protein-bound homocitrulline and assessment of proportional amounts of lysine on a global level for outcomes for kidney disease. The carbamylation of protein targets has been analysed at specific sites of protein targets (Claxton et al., 2013; Pietrement et al., 2013) and mass spectrometry used to determine the most abundant sites of carbamylation (Kalim et al., 2014; Berg et al., 2014), with carbamylated proteins being strongly predictive regarding mortality risk and urea concentrations in kidney disease (Kalim et al., 2014).

A case of a specific protein being oxidised which is involved in disease and which it is has been suggested has use as a biomarker and therapeutic is the oxidative modification of the dopamine transporter, in bipolar disorder (Kim, 2012). The 4-hydroxynonenal (4-HNE) oxidation product has also been found to be increased in these patients (Wang et al., 2009), which has potential for both detection and mechanism-based therapeutics.

To measure oxidised protein aggregates and advanced protein oxidation products, including cross-linked proteins via tyrosine crosslinks, spectrophotometric methods can be combined with chromatographic methods to develop biomarkers for diseases that accelerate ageing processes such as diabetes (Witko-Sarsat et al.,

1996). Witko-Sarsat et al (1996) demonstrated this using plasma fractionation size-exclusion chromatography, resulting in distinct peaks not present in control plasma and also demonstrated that advanced oxidation protein products correlated, for uremia patients, with advanced glycation end products and di-tyrosine biomarkers of ageing and disease. The top down, non-fragmentative method of polyacrylamide gel electrophoresis was used to visualise protein aggregates as a complimentary method to spectrophotometry. Witko-Sarsat et al (1996) also demonstrate for uremia, that lipid peroxidation markers do not correlate with advanced oxidation protein products, although lipids may enhance the *in vivo* process of advanced oxidation protein product formation.

As a demonstration of a global index of protein oxidation, plasma protein carbonyls and advanced oxidation protein products are stable end products and be significantly increased in diabetic patients versus controls (Pandey et al, 2010). Pandey *et al* (2010) found that protein oxidation products such as carbonyl moieties on lysine, arginine, proline and histidine as well as dinitrotyrosine which have been previously recognised as a measure of protein damage and oxidative stress (Levine et al., 1990; Witko-Sarsat et al., 1996) are markers for type 2 diabetic patients and correlate to the scavenging capacity of blood plasma.

Specific proteins that are already known and used as markers and therapeutic targets can be analysed further to gain higher resolution about the oxidation status for these proteins and what oxidation products they might form in order to have higher resolution or more specific biomarkers, predictors or targets, and assess the relevance of specific oxPTMs in health and disease states.

1.1.1.1.1.2. Cys-X₅-Arg phosphatases

Cys-X₅-Arg motif containing phosphatases are a sub-set of the protein tyrosine phosphatase (PTP) superfamily of phosphatases that contain a characteristic Cys-X₅-Arg sequence motif in the active site region, where the cysteine is in the thiolate form where the sulphur molecule is not bound to a hydrogen (Chiarugi et al., 2005) and can be more readily oxidised. The reaction mechanism of PTPs has, in review, not been fully characterised (Kolmodin and Åqvist, 2001). PTPs are involved in phosphorylation-dependent signaling pathways, although not always the dephosphorylation of tyrosine, the PTP designation refers to a superfamily homology rather than strictly to function or enzymatic substrate. PTPs have a diverse set of biological functions including redox sensing and cellular redox status has a important role in PTP signal transduction (Denu & Tanner., 1998). Oxidants have been shown to cause an increase in tyrosine phosphorylation and thus it has been suggested that this is the result of PTP inhibition (Denu & Tanner., 1998; Hecht & Zick., 1992; Knebel et al., 1996; Sullivan et al., 1994). Denu & Tanner (1998) state that PTPs may be regulated by reversible reduction and oxidation involving cellular oxidants such as H₂O₂ including H₂O₂ transiently generated by growth factor stimulation and that H₂O₂ production is associated with tyrosine phosphorylation. Denu & Tanner (1998) describe that effect of oxidants on PTP function of PTPs utilising chemical modification, pH kinetic assays and mutagenesis experiments. The catalytic cysteine thiolate of PTPs was determined to be oxidised, and formation of a cysteine sulfenic acid intermediate was formed after attack of the catalytic thiolate on H₂O₂; the PTPs assessed were PTP1, leukocyte antigen-related PTP, and vaccinia H1-related (VHR) PTP. PTPs have been suggested as candidate therapeutic targets (Alonso et al., 2004), including PTP1B which may be involved in insulin signalling as a negative regulator (Elchebly et al., 1999). PTP inhibitors are an emerging therapeutic class and multiple small molecule inhibitors for specific PTPs such as PTEN have already been identified (Mak et al., 2010). Although PTPs do not always require post-translational

modification for catalytic activity (Denu et al., 1996), as demonstrated by PTPs expressed using bacterial expression systems showing catalytic activity (Denu et al., 1996; Denu & Tanner., 1998).

1.1.1.1.1.2.1. Phosphatase and tensin homolog deleted on chromosome ten (PTEN)

The roles of PTEN were discovered during the study of genetic mutations and the cancer tumour suppressor role of PTEN (Li, 1997; Steck et al., 1997). The crystal structure of PTEN is known (Figure 5.) (Lee et al., 1999), although high-resolution proteomic, proxomic (omics of protein oxidation), interactomic and intracellular localisation data is scarce as novel technologies and methods are only recently starting to allow this research to take place. PTEN is a protein phosphatase involved in cell signalling and cell survival (Rodriguez & Huynh-Do., 2012). PTEN has a highly conserved active site motif with the arrangement Cys-X₅-Arg (CX₅R), which is homologous to many other proteins in the protein tyrosine phosphatases (PTPs) superfamily. Although unlike other PTPs, PTEN has a non-protein phosphoinositide substrate (Lee et al., 1999; Maehama & Dixon, 1999). PTEN dephosphorylates phosphatidylinositol (3,4,5)-triphosphate. PTEN has been show to be regulated at the transcriptional level, post-transcriptional level, via non-coding RNA, PTM and protein-protein interaction (PPI) levels (Song et al., 2012). This dephosphorylation is a major function of PTEN that is critical to the regulation, specifically the inhibition, of the PI3K/AKT/mammalian target of rapamycin (mTOR) signalling pathway (Figure 5.). The PI3K/AKT/mTOR pathway promotes cell proliferation and inhibits apoptosis and involves the phosphorylation by PI3-kinase (PI3K) of PIP₂ to PIP₃, which acts as a membrane localisation factor for the AKT protein (Figure 5), with rapamycin being a longevity-promoting compound (Harrison et al., 2009). PTEN dephosphorylation,

which has been proposed to be via protein kinase CK2 (Torres & Pulido, 2001), catalyses and regulates the downstream PI3K action on PDK1 and downstream to AKT and all potential downstream AKT signalling endpoints. PTEN action is the opposite of PI3K, and the regulation of kinases and phosphatase action by PTEN is important for cellular and organismal homeostasis with a role in signalling in a major signalling pathway, that is upstream and close to the membrane protein receptors. Thus if PTEN is modified in any way that adversely affects function, this will impact upon the AKT signalling pathway regulation and lead to cell division, cell proliferation, affect cell migration and cell adhesion (Fine et al., 2009; Lin et al., 2004). These features make PTEN genetic mutation a frequent occurrence in a multitude of cancers including prostate cancer (Li, 1997; Lin et al., 2004; Lotan et al., 2011), of which PTEN is a prognostic marker (Lotan et al., 2011), abnormal growths of tissue (Gunaratne et al., 2011) and breast cancer (Li, 1997). PTEN loss in cancer can also be an epigenetic event regulated post-transcriptionally through oncogenic microRNAs, and inhibitory phosphorylation, ubiquitylation and oxidation, and is not exclusively due to genetic mutations in the PTEN gene (Leslie & Foti, 2011).

PTEN has been proposed to be a gatekeeper against cancer of similar import to the tumour suppressor p53 (Yin & Shen, 2008). Partial loss of function of the PTEN gene is important in PTEN disease states (Leslie & Foti, 2011), thus it can be inferred that non-genomic partial loss of PTEN activity may also have a role in cancer risk and disease.

Cell membrane

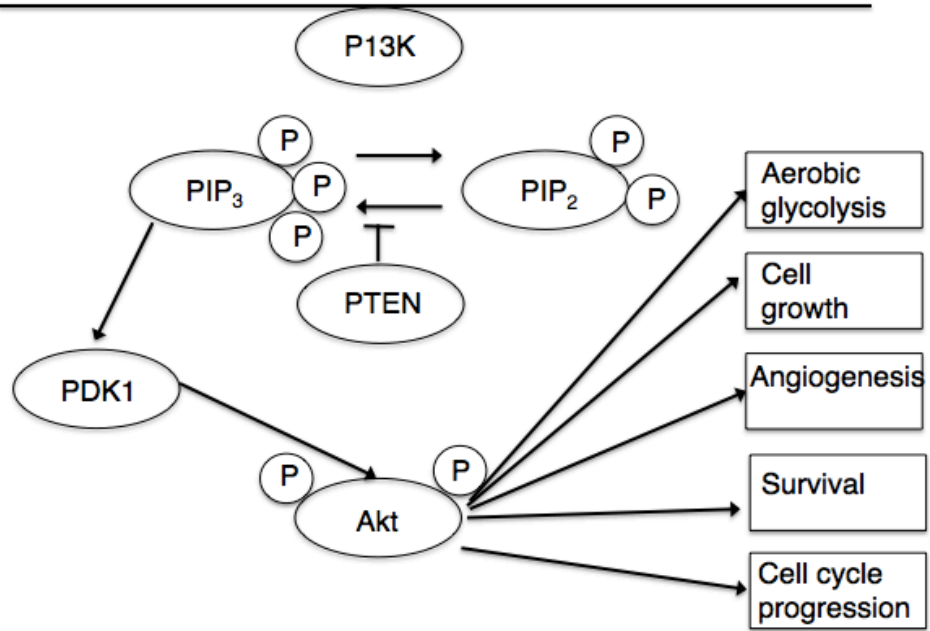


Figure 4. PTEN regulation of the AKT signalling pathway

The AKT signal transduction pathway showing alternate cell fates and PTEN phosphorylation of PIP₃ to PIP₂ at the cell membrane. Figure adapted from Castellino et al (2007). PDK1 = phosphoinositide-dependent kinase 1



Figure 5. PTEN structure

PTEN with active site cysteines Cys71 and Cys124 labelled in yellow. Phosphatase domain, phosphatase active site, C2 domain and Carboxy-terminus (C-terminal) tail labelled with arrows. PTEN structure from Lee et al (2009).

PTEN is involved in a diverse range of pathways and processes in addition to cell fate regulation. PTEN is involved in the regeneration capacity of neurons (Liu et al., 2010). PTEN down-regulation increased regeneration capacity in cortical neurons of adult rodents through compensatory sprouting of uninjured axons past a spinal chord lesion (Liu et al., 2010), which demonstrates PTENs role in growth and repair as well as age-related diseases such as cancer and neurodegeneration which involve cell proliferation and cell loss. PTEN is also involved in the negative regulation of the insulin signalling pathway, where PTEN deletion in the liver leads to insulin resistance, steatosis, inflammation and cancer including through activation of a mammalian target of rapamycin and nuclear factor kappa B complex, (Nakashima et al., 2000; Tang et al., 2005; Vinciguerra et al., 2009; Vinciguerra & Foti, 2008a, 2008b), thus PTEN is important in the ageing of the liver and the age-associated

disease of diabetes, liver steatosis and fatty liver disease (Vinciguerra & Foti, 2008b). Vinciguerra & Foti (2009) describe a potential mechanism of unsaturated fatty acids up-regulating expression of microRNA-21, which binds to PTEN messenger RNA and induces PTEN RNA degradation.

PTEN is an interfacial enzyme that can enter a highly active state when bound transiently to the inner cell membrane containing its substrate and other acid lipids (Leslie et al, 2008). This property of PTEN allows PTEN function to be spatially regulated, and is suggested to explain how PTEN forms PIP3 gradients and sustaining cell polarity needed for motility in neuronal and epithelial tissue development. The function of PTEN in addition to regulation at a spatial and conformational level is also regulated biochemically. Biochemical regulation of PTEN occurs when the nucleophilic and catalytic active site cysteine moiety, whose thiol residue in the active site cleft is involved in a dephosphorylation reaction, forms a cysteine disulphide. Thiols are organosulphur compounds that can undergo s-alkylation, they are acidic, readily oxidised, and can form metal ion complexes. The cysteine disulphide bridge between regulatory Cys71 and nucleophilic Cys124 in PTEN is considered biologically reversible and has been demonstrated to be inducible by oxidants and reversible by reductants. PTEN reversible inactivation has been demonstrated biochemically by Lee *et al* (2002) by disulphide formation with H₂O₂, and after matrix-assisted laser desorption/ionisation mass spectrometric detection of the disulphide bond containing cysteine-cysteine fragment. The inactivation of PTEN through disulphide formation between Cys71 and nucleophilic Cys124 induced by H₂O₂ by oxidation potentiates PIP3 generation and activation of the Akt kinase pathway in experimental *in vivo* overexpression studies Kwon et al suggest that local spatial control of H₂O₂ could have a regulatory function by increasing local PIP3 concentration in order to trigger downstream signalling (Kwon et al., 2004).

Disulphide bonds are weaker than carbon-carbon and carbon-hydrogen bonds, and is susceptible to scission by polar reagents, electrophiles and nucleophiles. Cleavage occurs via reduction, including chemicals in proteomic analysis including mercaptoethanol and dithiothreitol (DTT). Given the role of PTEN in Akt signalling, therapeutic development for PTEN active site has been performed at a pre-clinical stage, with molecular therapeutics based on vanadate scaffolds (Rosivatz et al., 2006), such as VO-OHpic (Mak et al., 2010) and the application of bisperoxovanadium compounds, which are known PTP inhibitors (Schmid et al., 2004). VO-OHpic is a non-competitive inhibitor where the inhibitor can bind the enzyme and enzyme-substrate complex, and is suggested that vanadium compounds deliver vanadium to the active site (Mak et al., 2010).

The PPI interactome of PTEN has been well characterised across species, using multiple experimental techniques, with multiple databases, laboratories and techniques confirming many of the protein-protein interactors (Adey et al., 2000; Diepen et al., 2009; Fan et al., 2009; Giot et al., 2003; Kang-Park, Lee, & Lee, 2003; Leslie et al., 2009; Lin et al., 2004; Maddika et al., 2011; Mori et al., 2008; Pramanik et al., 2009; Salmena et al., 2008; Shen et al., 2007; Shewan et al., 2011; Shu et al., 2008; Song et al., 2011; Stelzl et al., 2005; Takahashi et al., 2006; Valiente et al., 2005; Vazquez et al., 2000; Vogelmann et al., 2005; Wu et al., 2010; Yim et al., 2009). Demonstrated interactions between specific PTEN domains and interactors involve proteins interacting with carboxy-terminus (C-terminus) tail and associated PDZ domain, which interacts with the C-terminus to promote phosphorylation and stability (Okahara et al., 2004) and membrane-associated guanylate kinase inverted 2 and Na⁺ H⁺ exchanger regulatory factor which interact with the PTEN PDZ domain for recruitment of PTEN to the membrane (review, Salmena et al., 2008). The PTEN interactors (Appendix 1.), due to their number are involved in a vast array of biological

processes placing PTEN only a few PPIs away from involvement in most cellular processes, health processes and disease processes.

PTEN has many known PTMs including phosphorylation of the C-terminal tail region including Ser380, Thr382, Thr383, Ser385, Ser370 and Thr366 (Salmena et al., 2008), acetylation of Lys125 and Lys128 and ubiquitinylation of Lys13 and Lys289 (Salmena et al., 2008). It is also established that PTEN Cys124 and Cys71 in the active site form a disulphide bond upon oxidative stress (Lee et al., 2002), PTEN was inactivated via macrophage endogenous ROS or H₂O₂. Salmena *et al* (2008) note that post translational modification of PTEN, particularly oxidative modification may be therapeutically powerful and thus further investigation of the active site cysteines may yield important results.

PTEN oxidation has also been linked to cancer and the development of T-cell acute lymphoblastic leukaemia that have high levels of ROS (Silva et al., 2008). Current findings with regards to PTEN oxidation focus on PTEN redox regulation and reversible modification of active site cysteines (Covey et al., 2007; Lim & Clément, 2007; Pei et al., 2009; Yu et al., 2005).

There are some fundamental features of PTEN that give it the potential to be a biomarker. PTEN is both a highly modifiable signalling protein with many identified sites of modification including at Lys13, Cys71, Cys124, Lys125, Lys128, Ser229, Thr232, Lys289, Thr319, Thr321, Thr366, Ser370, Ser380, Thr382, Thr383, Ser38 (Salmena et al., 2008), in the centre of multiple pathways (Figure 4.) and has many protein-protein interactors (Appendix 1.). PTEN can also take on multiple conformations due to its open and closed conformational states (Leslie et al., 2008) and PTEN exists in multiple states of oxidation with multiple PPI partners in the nucleus (Trotman et al., 2007) in addition to cytoplasmic co-localisation with interaction partners. To conclude, the state of PTEN in cells may be highly predictive of many states, and discovery and diagnosis of those states may give key insights

into the state of a particular cell whether it is a patient sample before or after administration of a therapeutic or to assess or manipulate cellular processes in tissue engineering. PTEN PPI could potentially also be used as a biomarker if samples could be assayed or arrayed. By investigating the PTEN proxome, PTEN interactome and PTEN proxo-interactome this may yield many potential specific biomolecules, that with high-throughput and multiplex technology could be used to categorise healthy and sub-optimal states by their existence and abundance in samples.

1.1.1.1.1.2.2. Dual specificity phosphatase Vaccinia H1-related phosphatase (VHR/DUSP3)

Vaccinia H1-related phosphatase (VHR) is a PTP and dual specificity phosphatase (DUSP). The structure of VHR has been determined by x-ray crystallography (Figure 7.) (Yuvaniyama et al., 1996) DUSPs are structurally related to PTPs and have been implicated in mitogen activated protein kinase (MAPK) regulation (Alonso et al., 2004). DUSPs differ from PTPs in that DUSP active site clefts are shallower which gives reduced biomolecule specificity (Camps et al., 2000; Stewart., 1999; Yuvaniyama et al., 1996). DUSPs are regulated by mitogenic signalling (Grumont et al., 1996; Rohan et al., 1993; Sun et al., 1993; Ward et al., 1994). VHR has been shown to dephosphorylate epithelial growth factor receptor (EGFR) and platelet derived growth factor receptor (PDGFR) *in vitro* (Ishibashi et al., 1992), but *in vivo* studies have failed to support this (Wang et al., 2011). This *in vitro* activity may be due to the shallow active site binding cleft conferring the property of lower substrate specificity on VHR. VHR has also been shown to inactivate c-Jun N-terminal kinases (JNKs) and extracellular signalling related kinases (ERK) (Figure 6.) (Alonso et al., 2001; Denu et al., 1999; Jacob et al., 2002; Todd et al., 2002), although VHRs ability

to suppress MAPK activity is weak compared to other MAPK phosphatases (MKPs) (Alonso et al., 2001).

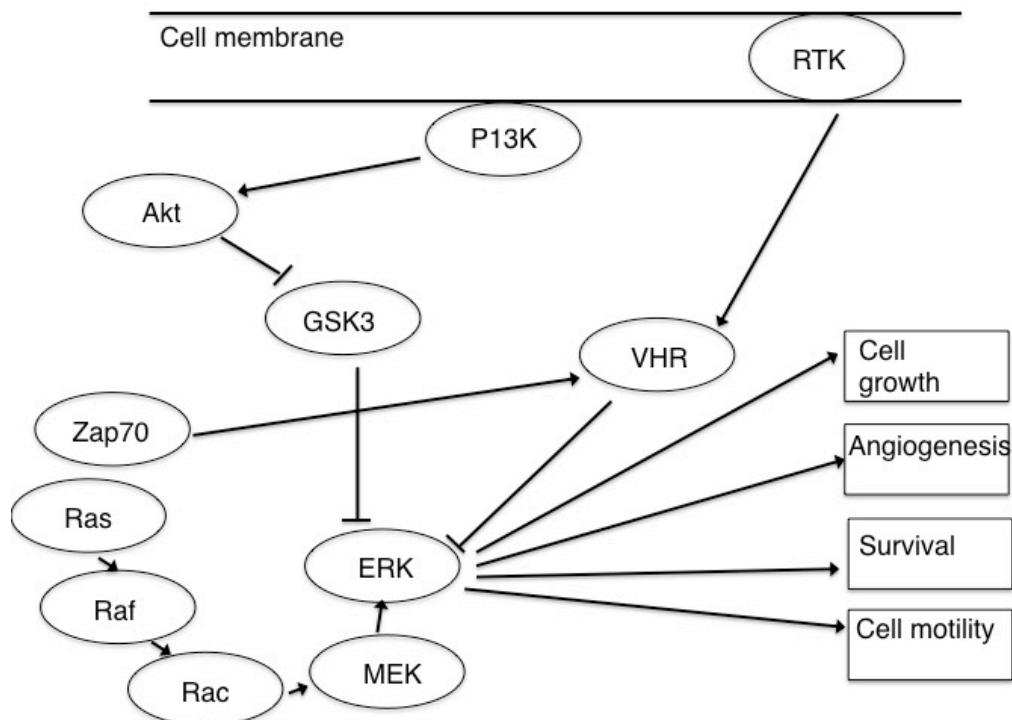


Figure 6. VHR regulation of the ERK signalling pathway

VHR negatively regulates ERK and inhibits ERK pathway, which is connected to the Akt signalling pathway. RTK = Receptor tyrosine kinase. Ras = Rat sarcoma. Raf = Mural leukaemia viral oncogene homolog. Rac = Ras-like protein TC25. MEK = Mitogen activated protein kinase.

The active site of VHR is less complex with regards to cysteine redox regulation (Denu et al., 1998; Yuvaniyama et al., 1996) because it has one active site nucleophilic Cys124 without another local cysteine within 9Å with which to form a cysteine disulphide bridge, making intramolecular disulphide bridges improbable (Denu & Tanner, 1998). This feature is critical for enzymatic regulation of VHR. This does not mean that oxidation and reduction of this active site cysteine cannot occur, only that the reversible disulphide bridge regulatory mechanism is not present. Additionally, cysteine sulphenic, sulphinic and sulphonic acid formation may occur and regulate activity under various cellular states, although cysteine di- and tri-oxidation are not reversible biologically. Thus if non-reversible nucleophile oxidation were to have a regulatory effect, it might conceivably have an effect via a cumulative

build up of oxidation steering cell fate in a particular direction, or regulate cell fate through a balance of oxidation versus protein degradation. Nonetheless irreversible oxidation of VHR, as with PTEN may have a yet-to-be-elucidated functional role in cell fate and disease states and thus be of importance. Denu and Tanner (1998) suggest that a cysteine disulphide bridge formation might be possible in VHR once an initial sulphenic acid has formed.



Figure 7. VHR 3D structure Protein data bank (1VHR). Protein structure discovered by Yuvaniyama *et al* (1996).

Knockdown of VHR expression leads to cell cycle arrest and senescence, (Rahmouni *et al.*, 2006). Evidence from cultured cells, tumour transplants and clinical samples suggests that VHR is involved in cancer, including the pathogenesis of non-small cell lung cancer, through the mechanism of inhibiting phospholipase C γ and protein kinase C (Wang *et al.*, 2011).

VHR is also highly expressed and is localised to the nucleus as well as cytoplasm, which contrasts to its cytoplasmic localisation that is seen in primary keratinocytes (Henkens *et al.*, 2008). VHR upregulation in cancer cell lines has been shown to be due to post-translational stabilisation (Henkens *et al.*, 2008), which is of interest when studying the effects of protein oxidative PTM on function, as oxPTMs

may lead to a gain-in-function modification that promotes growth or carcinogenesis.

Henkens *et al* (2008) suggest increased translation or decreased degradation of VHR in cancer cell lines.

VHR inhibition in cervical cancer cell lines has been shown to halt cell cycle progression and VHR inhibition in cancer, to induce cellular senescence, has been proposed to be an anti-cancer therapy (Henkens *et al.*, 2008). VHR has also been demonstrated to be pro-angiogenic physiologically in a mouse model (Amand *et al.*, 2014).

The VHR protein-protein interactome (Appendices 2.) has been searched experimentally, but the current known interactome remains comparatively small and consists primarily of well characterised signalling pathway protein receptors and kinases (Alonso *et al.*, 2003; Ewing *et al.*, 2007; Ishibashi *et al.*, 1992; Najarro *et al.*, 2001; Rual *et al.*, 2005; Todd *et al.*, 1999). Well characterised signalling protein receptors and kinase interactors include Human leukocyte antigen-B (HLA-B), colorectal mutant cancer protein (MCC), Neurogenic differentiation 1 (NEUROD1), BCL2/adenovirus E1B (BNIP3L) and Zeta-chain associated protein kinase (ZAP70), a T cell surface membrane protein. ZAP70 includes a phosphorylation interaction with Tyr138 of VHR. Thus VHR has specific roles in immune system function, neural development and also a role in cancer with MCC. The well categorised Janus kinase-signal transducer and activator of transcription (JAK-STAT) and MAPK/ERK signalling pathways that VHR interacts with, are known to be critical to cellular cycle regulation including sub-optimal cellular senescence and cell proliferation events associated with ageing, loss of organismal homeostasis and cancer (Aaronson & Horvath, 2002; Sebolt-Leopold, 2008; Zheng *et al.*, 2003). VHR also dimerises, which has been demonstrated to act as a negative regulatory mechanism for catalytic phosphatase activity (Pavik *et al.*, 2014).

VHR can be inactivated by metal ions including Fe^{3+} , Zn^{2+} , Cu^{2+} and Cd^{2+} . The Cu^{2+} ion, which causes VHR inactivation that is over 200-fold as potent as H_2O_2 inactivation (Kim, Cho, Ryu, & Choi, 2000). The addition of dithiothreitol (DTT) can reverse the Cu^{2+} oxidation-based inactivation, and it was inferred from thiol labelling by Kim *et al* (2000) that this reversal was due to inactivation and subsequent reduction and reactivation of the VHR active site cysteine.

1.1.4. Technology Development

1.1.4.1. Mass Spectrometry

Mass spectrometric technology development has utility for biomarker and therapy development and implementation. Mass spectrometry has specific benefits in being high-throughput, accessing protein sequence and modification specific information, allowing semi-quantitative and quantitative experimentation, and high potential and capacity for automation. Mass spectrometry measures the mass-to-charge ratio (m/z) of ions in relation to their motion in an electric or magnetic field. Biomolecules are converted to ions in the gas phase and separated by m/z ratio.

The identification of proteins and protein modifications can be performed combining liquid chromatography and with electrospray ionisation mass spectrometry (LC-ESI-MS). Whether *in vivo* or *in vitro*, the abundance of modified peptide ions can be sub-stoichiometric, with samples containing other biomolecules, whether other proteins, or non-modified peptides, or other modified peptides.

For protein modifications such as protein oxidation, MS/MS is required whereby a peptide is further fragmented so as to be able to predict where the additional mass has been added on the peptide to determine the modification and amino acid.

Sample stability can affect representative detection of protein modifications, as samples and modifications can have limited stability, thus sample preparation as well as sample acquisition are important factors.

Electrophoresis is employed for protein pre-fractionation for high-resolution separation of proteins and peptides prior to LC-MS. Electrophoretic techniques consist of the migration of charged particles in an electric field, where due to the differences in particle size and net charges, migration across the field occurs at variable velocities and thus achieving distinct separation of proteins, peptides, aggregates and fragment biomolecules. Gel matrices are employed as a substrate for the electrophoretic separation of proteins. Polyacrylamide gels are used, which are polymerised from acrylamide monomers using a crosslinking agent. The pore size for migration of proteins is determined by total acrylamide concentration and degree of crosslinking.

Liquid chromatography allows proteins to be separated according to differences in specific properties of charge, size, hydrophobicity and biorecognition. Ion exchange chromatography (IEX) allows separation of molecular species with differences in charged amino acids from their side-chains, carboxyl and amino acid termini, bound ions, and prosthetic groups. The charge on amino acid side-chain is dependent on the pH of the solution and the pK_a of the specific side-chain, and the microenvironment of the side-chain. IEX columns consist of a matrix of spherical particles with ionic groups that are negatively or positively charged in a column packed bed that is equilibrated with a buffer. For IEX, following column equilibration, sample application of oppositely charged peptides bind to ionic groups with uncharged peptides and peptides with the same charge as the IEX medium, eluting. Next, a series of elutions are applied with increasing ionic strength to displace biomolecules, resulting finally in removal of ionically bound biomolecules. Resolution, the degree of separation between peaks, is important for resolution and this is dependent upon the type and

number of functional groups on the column matrix, and experimental conditions such as pH, ionic strength and elution conditions.

Reverse phase chromatography (RPC) separation and pre-fractionation is also used for proteomic analysis. RPC consists of a separation with a column matrix with a hydrophobic surface. The separation is due to differential separation that is predicted to be driven by an entropic phenomenon where more hydrophobic samples elute at a retarded rate in comparison to less hydrophobic samples upon increasing the percentage of organic component in solution. The initial, primarily aqueous, mobile phase leads to a high degree of organised water structure around both the immobilised ligand matrix and the solute, where it is advantageous, as the solute binds the hydrophobic ligand, for the hydrophobic moieties to associate. RPC is an adsorptive process where solute molecules partition between the mobile and stationary phase, where the partition distribution depending on binding properties, hydrophobicity of the solute and the composition of the mobile phase. Initial LC run phases are designed for solute peptide adsorption from the mobile to stationary phase, with later run phases designed to favour desorption of the peptides with gradient elution. Polarity of the mobile phase is controlled by water-miscible organic solvent such as acetonitrile utilitised alongside ion-pairing agents (trifluoroacetic acid, formic acid). Nano Liquid Chromatography (NanoLC) systems are used to attain resolution, sensitive and selectivity for proteomics applications. NanoLC involves columns with internal diameters $\sim <75\mu\text{m}$ and low flow rates ($\sim 300\text{nL}/\text{min}$) for high sensitivity down to sub-femtomole detection, and selectivity to increase peptide identification reliability, which has utility for identification in samples with a large ome, deep omes with a wide dynamic range of molecules, small sample sizes, rare samples, unique samples and expensive samples. A limiting factor of the MS technique is ion intensity. Ion intensity can be modified by taking larger samples, sample enrichment, increasing detection ability, although in a clinical context there

are patent limitations for taking sample size and the abundance of a biomolecule in relation to the health of the patient and stage of therapy or disease process as absolute limitations; where additional limitations exist up to the capacity of the column used for chromatography where concentration is of import. For each run, the duty cycle of the mass spectrometer, that is the time taken to acquire the MS and MS/MS for a given run, dictates how many precursor ions can be selected for MS/MS – when this is combined with complex digests and/or non-abundant ions, less modified ions will be selected. Modification may also affect effective ionisation of peptides.

Following chromatographic separation, peptides are ionised for mass spectrometry, the ionisation and ionisation source is the first stage mass spectrometry, before separation in the analyser and detection by the detector. The ion source is the region of a mass spectrometer whereby peptides are converted to gas phase ions. Fenn *et al* (1989) demonstrated electrospray ionisation (ESI) for biomolecules with high sensitivity. ESI ions are produced when the sample dissolved in a solvent is applied through a narrow capillary tube at atmospheric pressure under the influence of an electrical field, thus creating a potential difference between the capillary and the MS inlet, generating a force extending the liquid, creating a liquid cone formation on the tip of the capillary which then creates a fine mist (Taylor 1964). The cone, formed from repulsive forces between like charges forms droplets, whilst maintaining droplet charge. Droplets form smaller droplets until nano-meter droplets are formed. Charges are distributed over the potential charge sites, leading to multiply charged biomolecules, and an effectively reduced mass for the biomolecule of interest.

Ions are separated using analysers. In Time-of-flight (TOF) analysers the mass measurement is determined upon measurement of the TOF of an ion in the analyser to measure the mass of product ions and/or precursor ions. The triple quadrupole analyser (Morris *et al.*, 1996; Loboda *et al.*, 2000) consists of four parallel and

hyperbolic rods, with oscillating voltage switching between opposite pairs of rods, in which some gas phase ions reach a stable trajectory. Ions traversing the space between the rods will only pass through the rods to reach to the detector if they have certain m/z values, where a range of voltages allows a wide m/z and absolute mass range to be observed. The triple quadrupole analyser coupled with ESI has been demonstrated to be of high utility for proteomics (von Haller et al., 2001) including additional fragmentation, for additional structural information with tandem mass spectrometry (MS/MS) using the first and final quadrupoles as mass filters and the middle quadrupole as a collision cell for further fragmentation. In the collision cell the ions collide in gas phase with neutral gas at an increased pressure, which fragments the ion by collision-induced dissociation (CID). Ions are accelerated by electrical potential to a high kinetic energy for the collision. During the collision some kinetic energy converts to internal energy resulting in bond breakage, for fragments to be analysed and detected. MS/MS leads to unique fragment ions, which have utility for identification, structural information and identification and structural determination in complex samples where the likelihood of precursor ions with identical mass is increased. CID also has utility for precursor ion scanning MS modes where it is important to determine which precursor the product originated from as a means of identifying products by their unique precursors and precursor fragments.

The presence of isotopes in the detected amino acids will produce several characteristic peaks, of differing mass, for isotopes of atoms such as carbon or nitrogen. The monoisotopic mass may be utilised for identification in cases where it is the largest peak due to ^{13}C abundances, as is checking for characteristic peak distributions.

For MS/MS analysis, m/z ratios are informative for *in silico* prediction of the amino acid sequence of the peptide and peptide modifications, when compared to peptide and protein databases with informatics protocols. Protein identification

analysis takes the form of a selection of or combination of peptide mass fingerprinting, and tandem mass spectrometry. The peptide mass fingerprint (PMF) technique of digested proteins and sequence database search algorithms consists of *in silico* digest of every protein in the database with the same digestion reagent that is used in the *in vitro* digestion, and then comparing the theoretical *in silico* digestions to the experimentally obtained peptide masses from the MS spectrum (Pappin et al., 1993; Henzel et al., 1993; Mann et al., 1993; Yates et al., 1993; James et al., 1993). The matches are then scored, with scores reflecting the number of times the peptide mass was observed and matched and how accurate the match was in terms of masses. In order to perform PMF the knowledge of peptide modifications is also required, as is the error tolerance for the accuracy of the mass measurement which is dependent on MS calibration and mass accuracy. In order for PMF to give an unambiguous result, a significant number of experimental masses should match the expected masses for the cleavage specificity of the digestive enzyme used. MS/MS allows for product and precursor ion scan analysis. Product ion scans use the first MS to specifically select the precursor ion/s of interest. The precursor ion is then allowed into the collision cell for CID. The products of the CID are resolved by MS/MS, and are then detected to produce a product ion spectrum. The low energy fragmentation leads to precursor ion fragments that fragment predictably at peptide amide bonds along the peptide backbone, which leads to a two series of ions being produced. The N-terminal ion series is formed from the peptide N-terminal amino acids and its extensions, the C-terminal ion series is denoted as the y-ion series and is formed from the peptide C-terminal amino acid and its extensions. Sequence information has been demonstrated to be able to identify a protein from a few peptides from a well-characterised genome (Susin et al., 1999). Precursor ion scanning mode has the first part of the MS analyser transmit all ions into the collision cell for CID, with the final MS/MS analyser being fixed for a specific mass to detect the fragments.

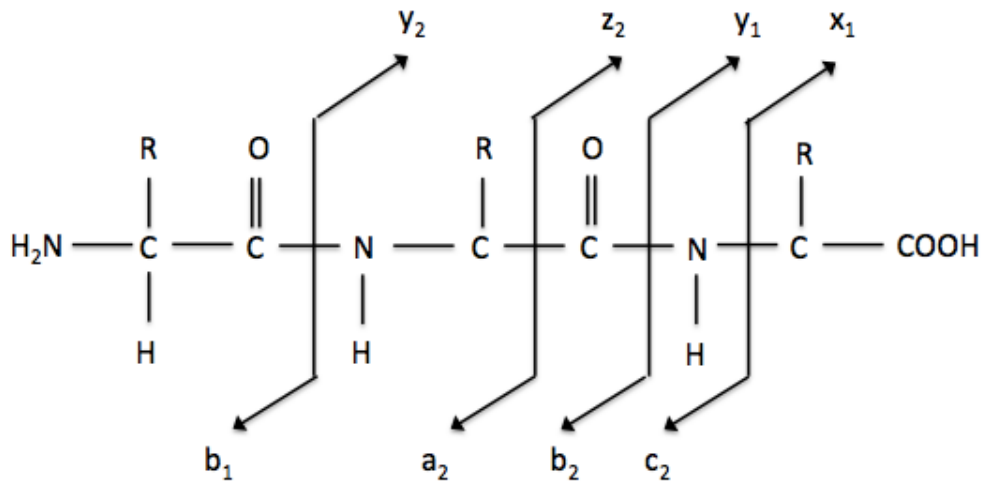


Figure 8. Fragmentation pattern and nomenclature

Figure adapted from Peptide Fragmentation (2016). Nomenclature of fragment ions from Roepstorff & Fohlman (1984).

Sequence validation and searching for sequences not predicted by informatics

requires *de novo* sequencing of a peptide fragmentation spectrum, where the complimentary b-ion and y-ion spectra are used to reconstruct the sequence from amino acid and fragment masses.

MS has the capability to identify proteins and their PTMs. In order to attain functional information with utility for therapy development and/or theranostics development techniques such as protein arrays and co-immunoprecipitation can be performed.

1.1.4.2. Biochips, biosensors and bioprinting

Biochips and miniaturisation innovation has enabled miniaturised systems that can be performed on the surface of a chip or slide, and for the development of biosensors.

Biochips primarily consist of a slide, commonly a glass slide, coated with a polymer or matrix layer or a silicon wafer, referred to as the substrate. Multiple component biochips can be designed with channels, spots, reaction chambers, filters and other

compartments to perform single or multiple sets of reactions on biological objects in serial or parallel. Advantages of biochips include their size, small sample size required for detection, high-throughput and multiplex experimentation. Biochips and the miniaturisation of assays permit biomarker assays and theranostics to be performed nearer the patient at point of care, as demonstrated by biosensor bioelectronic graphene oxide nanoribbon analysis of amino acids by Martin *et al* detecting H₂O₂ with pulse voltammetry (2015) and by point of care immunoassays and peptide assays for infectious diseases with antibodies to infectious diseases as reviewed by Su *et al* (2014). Biosensors also have the potential to be performed from a patient's personal items as demonstrated by the mobile monitoring of heart rate variability (HRV) and application of HRV signal algorithms to detect seizures (Jeppesen et al., 2014), From inside the patient, there is potential with an implant or on-board a patient's artificial systems, as demonstrated with artificial heart monitoring systems that relay artificial organ information as well as blood flow data from the organ to external devices (Chung et al., 2004).

Microarray biochips technologies are based on a microscope slide format. Proteins or other moieties are arrayed upon membrane substrates in small volumes in spots, which will show the intensity of the signal and interaction upon binding of probe/s and spectroscopic detection.

Microscope slide coatings include nitrocellulose, which binds biomolecules. Nitrocellulose has superior binding to glass and is protective of the protein tertiary structure. Proteins can be arrayed onto slides with a variety of arraying technologies, including nanolithography and piezoelectric spotting. Piezoelectric spotters utilise electrical charge to deposit droplets of biomolecule containing solution containing onto the slides in an array pattern. Probing of arrays occurs with probes of interest, including cell lysate solutions, antibodies and other biomolecules.

Microarray biochips has been used for medical profiling has been demonstrated using biochips for genotyping alongside protein microarrays for autoantibody profiling (Chen et al., 2012). Biochips can also be used to assess therapeutic effect of an intervention and as part of therapeutic development, by discovering interacting moieties or changes in amounts and properties of moieties present, Akbani *et al* (2014, review) state that protein biochips have been used to dynamically profile post-translational signalling events, and characterised the effect of inhibition of epidermal growth factor on sensitisation of cancer cells to genotoxic drugs. Akbani et al (2014, review) also state that protein arrays may be used to detect levels of protein and protein PTMs in order to identify sets of protein markers that predict sensitivity and resistance to a therapeutic moiety.

Protein-protein microarrays describe arrays, which have proteins spotted on an array substrate, and are probed with protein, which may bind to the spotted protein on the array. Protein-protein microarrays are a sub-set of protein microarrays that screen for protein-protein interactions and sample a nearby space to gene transcript arrays although they are more expensive to produce due to the complexity of proteins and elegant biochemical structure of DNA. Protein-protein microarrays have multiple distinct features from gene transcript arrays, including ability to directly assess which proteins are expressed, as many RNA fragments are non-translated through degradation pathways, competitive inhibition and some never being translated, and do not assess protein PTMs. For performing functional proteomics and identifying which proteins interact under particular conditions, protein-protein microarrays have potential utility for understanding signalling dynamics and monitoring functional changes and PTMs including phosphorylation, ubiquitinylation, acetylation and nitrosylation (Hu et al., 2001).

Protein-protein interactions (PPIs) that are measured in protein microarrays are the physical contacts between two or more proteins due to chemical events or

electrostatic forces. Proteins can have stable and transient interactions occurring over different time scales, and thus measured by different and appropriate methods.

Longer, or stable interactions as they are referred to, can be probed and assessed via protein-protein microarray library screening. The PPI interface can be modified by the environment the interaction is taking place in as well as PTMs. Aberrant PPIs and signalling have the potential for proteins to interact with other partners, or not interact with partners, and thus reduce their function, or have additional functionality. Protein-peptide interactions can also be performed to assess the interactions between a partial protein sequence which has utility for therapeutic molecule screening and identifying protein interactions with consensus sequences (Landgraf et al., 2004).

PPIs may also be assessed via non-biochip methods including immunoprecipitation techniques such as tagging the protein or peptide of interest with subsequent immobilisation to beads covered in a corresponding tag, which are then probed with protein. Bound proteins may then be identified via technologies including Western blotting or mass spectrometry (Schulze et al., 2005).

1.2. Aims

The aims of this project are i) to show as proof-of-principle that protein oxidative modifications from a variety of sources can be mapped with regards to their location, abundance, effects on activity and protein-protein interaction ii) to determine the extent of oxidation and nitration of nitrating species, including the abundances of modification associated with nitrating species iii) develop the knowledgebase of VHR and PTEN with regards to their oxidations, peptide fragments, interactors, oxidations of residues with known function and to explore the relationship of function and activity for VHR and PTEN to understand their fundamental biology to advance the knowledgebase for biomarker and therapeutic target identification iv) Develop and assess workflows for mass spectrometric identification of protein-wide systematic identification of protein oxidative modifications, abundances and validation of modifications for both research, development and diagnostic purposes. By using mass spectrometric techniques to identify multiple previously uncharacterised peptide modifications, these modifications may be statistically correlated with changes in activity and the peptides responsible for these changes can be identified, paving the way to searching for them in novel and more complex biological samples. Enzymatic assays of phosphatase activity will be used to determine the effect on activity of variable oxidative agents at variable concentrations, and the effect of the specific peptide modifications found at those molar concentrations of oxidant. By using protein-protein arrays, and co-immunoprecipitation we can find what interacts with our candidate proteins of interest, and from the interactome, literature analysis of candidates and modification mapping – develop synthetic modified peptides to challenge protein libraries, with as well as oxidise proteins before a protein-pair array to research the effect of oxidation on protein interaction. Co-immunoprecipitation in

combination with mass spectrometry will also be used to detect candidate interactors as a comparative and combinational method.

Chapter 2

Materials and Methods

2. Materials and Methods

2.1. Methods Summary

This project focuses on functional proteomics, which is defined as the functional effect of a particular protein or protein post-translational modification and builds upon the importance of not only identifying aspects of a proteome and but their functional role, role as a biomarker and role as a target in health and longevity. Functional proteomics has previously been used to identify how genetic modifications affect the proteome in cancer (Gonzalez-Angulo et al., 2011; Kolch & Pitt, 2010).

All reagents were stored at their recommended temperatures and conditions. All work that needed to be sterile was done under a blue Bunsen burner flame. Proteins were stored at -80°C (New Brunswick ultra low temperature freezer, U725 innova®) and kept on ice or in a cold room at all times. All reactions where temperature is not stated were performed at room temperature.

2.2. Methods

2.2.1. Plasmid constructs

Plasmid constructs were used to express test proteins (PTEN, VHR) for subsequent purification and *in vitro* analysis via 3-*O*-methyl-fluorescein phosphatase (OMFP) release assay, protein-protein interaction microarrays and MS/MS analysis. For full plasmid construct sequences refer to appendix (Appendices 3, 4, 5, 6.).

Protein encoded	Taxonomy	Plasmid vector	Fusion protein
PTEN	<i>Homo sapiens</i> <i>sapiens</i>	pGEX-4T1	GST
VHR	<i>Homo sapiens</i> <i>sapiens</i>	pGEX-4T1	GST
VHR	<i>Homo sapiens</i> <i>sapiens</i>	pcDNA 3.1	Flag

Table 1. Plasmid constructs

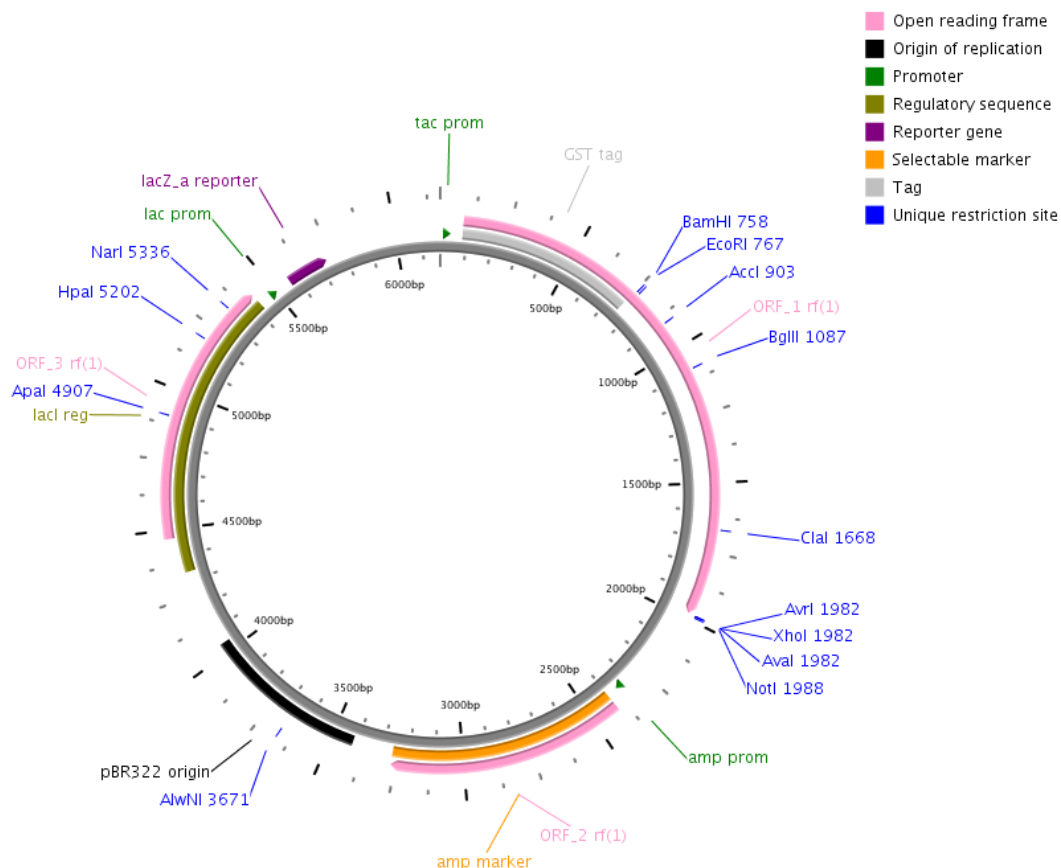


Figure 9. pGEX-4T1 vector map Vector map for pGEX-4T1. Inserted gene designed as a GST fusion with a linker sequence in open reading frame (ORF) 1. pGEX-4T1 also contains Lac promoter and ampicillin resistance gene. Drawn using PlasMapper online (<http://wishart.biology.ualberta.ca/PlasMapper/index.html>).

2.2.2. Minipreps and Maxipreps

Plasmid DNA for future transformations was miniprepmed using the GeneJET™ Plasmid Miniprep Kit (Thermo Scientific, EU) and standard kit protocol. PTEN-GST and VHR-GST in pGEX plasmid constructs were miniprepmed and the plasmid DNA was stored at -80°C, VHR-Flag pcDNA 3.1 plasmid constructs were maxiprepmed using the PureYield™ Plasmid Maxiprep System (Promega, USA) and the plasmid DNA stored at -80°C. A Maxiprep system was used for VHR-Flag pcDNA 3.1 for larger yields required for HCT 116 cell line transfection. Miniprep and Maxiprep kits used according to availability.

2.2.3. Transformation of PTEN and VHR

The PTEN-GST and VHR-GST containing pGEX plasmids (Figure 9.) were transformed into transformation competent DH5 α *E.coli* cells (See 2.2.3.1. Generating competency in *E.coli* cells). All transformation and expression procedures were carried out in sterile conditions. DH5 α *E.coli* cells were used for expression, replicating the protocol from Imperial College London collaborator Doctor Lok Hang Mak (See 2.2.4. Expression of PTEN and VHR).

Luria Broth (LB) growth medium was prepared using 5g yeast extract, large granules (Fisher Scientific, UK), 10g bacto-tryptone, large granules, microbial media, (Fisher Scientific, UK), 10g NaCl (Sigma Aldrich, US), pH 7.5, made up to 1L with high quality distilled water, autoclave). 100mg/mL ampicillin sodium salt (Sigma, US) was added to medium on the day of experimentation. Agar for agar plates was made using LB medium with the addition of 15g bacto-agar, (DIFCO, US) to make 1L, autoclave). Agar was microwaved (Pacific™) then cooled to 50°C in a water bath (Clifton) before the addition of 100mg/mL ampicillin sodium salt (Sigma, US) and pouring into petri dishes.

2.2.3.1. Generating competency in *E.coli* cells

DH5 α *E.coli* cell transformation competency was achieved via rubidium chloride (RbCl). A 5mL LB medium culture of *E.coli* cells was grown for 24hr. The 5ml LB culture was then used to inoculate a 250mL culture, which was grown at 37°C to an Optical Density (OD) of 0.5 Absorbance (A). The 250mL culture was then cooled on ice for 15min then transferred to centrifuge bottles. The culture was centrifuged for 10min at 4.5K RPM in JSA J-20 rotor (Beckman) and cells formed pellets. The

supernatant was discarded and the pellet was resuspended in 30mL of Tfb1 rubidium chloride medium (RbCl 100mM, manganese chloride $\text{MnCl}_2 - 4\text{H}_2\text{O}$ 50mM, potassium acetate 30mM, $\text{CaCl}_2 \cdot 2\text{H}_2\text{O}$ 10mM, Glycerol 15% final volume, H_2O 500mL final volume). Cells were put on ice and then centrifuged for 5min at 4K RPM. The pellet was then resuspended in 6ml Tfb2 medium on ice (0.2M 3-(N-morpholino) propanesulfonic acid (MOPS) (Good et al., 1966) 10mM, RbCl 10mM, $\text{CaCl}_2 \cdot 2\text{H}_2\text{O}$ 10mM, Glycerol 15% final volume, 400mL final volume). 0.2M MOPS buffer (20.93g MOPS in 500mL H_2O , pH6.5, filter sterilise). Cells were then aliquoted on dry ice and stored at -80°C until use.

2.2.3.3. Transformation

Competent DH5 α *E.coli* cells were transformed with pGEX-4T1 plasmids containing PTEN or VHR attached to a glutathione-S-transferase with a linker region, ampicillin resistance and an IPTG inducible promoter (Gift from Doctor Woscholski's laboratory, Imperial College London) (see Table 1, Figure 9, Appendices 4, 5, 6.). 100 μL competent cells and 1 μL of miniprepmed plasmid were used for transformation. The plasmid DNA was mixed with the competed cells and left on ice for 30min. The competent cell and plasmid DNA containing suspension was heat shocked at 42°C for 90sec using a heat block (Grant). The transformed cells were then cooled on ice for 2min. Next 0.5mL of LB medium was added to transformed cells to rescue them. The transformed cells were then incubated at 37°C for 1hr in MAXQ 8000 incubator (Thermo Scientific) at rotation speed 180. Transformed cells were plated onto agar plates containing ampicillin (10 $\mu\text{g}/\text{mL}$) plates were then sealed and then incubated at 37°C for 16hr.

2.2.4. Expression of PTEN and VHR

Sufficient quantities of PTEN and VHR proteins were required for *in vitro* studies. The pGEX vector system (Figure 9.) with ampicillin resistance and an IPTG inducible promoter for the gene of interest was used, and DH5 α *E.coli* were used as previous experimental data and experiment optimisation by Doctor Lok Hang Mak had shown that the pGEX vector system with DH5 α *E.coli* had produced sufficient protein for assaying and additional studies (communication with Doctor Lok Hang Mak, Imperial College London; data not shown).

Transformed DH5 α *E.coli* cells plated on LB agar with 100 μ g/mL of ampicillin were taken out of the plate incubator. Several colonies were picked using a pipette tip. Next 10mL LB Broth mini-cultures were grown with pipette tip with colonies inserted into LB Broth with 100 μ g/mL of ampicillin. The mini-cultures were grown for 16hr at 37 $^{\circ}$ C in a MAXQ 8000 incubator (Thermo Scientific) at rotation setting 180. After 16hr the 10mL mini-culture of transformed *E.coli* cells were used to inoculate a 1L growth culture in 2L shaker flasks (Fisherbrand). The growth medium consisted of LB medium with 100 μ g/mL of ampicillin. The 1L growth cultures were grown at 37 $^{\circ}$ C until an Optical Density (OD) of 0.5-0.6 Absorbance (A) was reached. OD was measured, at multiple timepoints, using 1mL fraction of growth culture on a UV/VIS spectrophotometer (PerkinElmerTM instruments, PTP-6 Peltier System with Perkin Elmer precisely, Lambda 35 UV/VIS Spectrophotometer, US) at an absorbance of 600nm, with H₂O and LB medium as blanks. When the OD reaches 0.5-0.6A, 1mL 1M per 1L Isopropyl beta-D-1-thiogalactopyranoside (IPTG) was added to induce expression of the protein of interest. At the point of IPTG induction, the cultures were incubated at 23 $^{\circ}$ C for 24hr in a shaking incubator (MAXQ 8000, Thermo Scientific) at 180-rotation speed. After 24hr the OD of the cells was measured by spectrophotometer. The cultures were then transferred to 1L centrifuge

bottles to fit FIBERLite® F8-61000y rotor (Piramoon Technologies Inc.). Cultures were centrifuged for 30min at 1.9K RPM with refrigeration at 4⁰C in Sorvall EVOLUTION RC centrifuge (Thermo Scientific). The supernatant was discarded keeping the cell pellets. 20mL of 20mM TRIS (Trizma® base, Sigma Aldrich, US) including 50µL protease inhibitor cocktail (Protease Cocktail set III EDTA-free, CALBIOCHEM®, US) was added to cell pellets to protect expressed protein and be able to further concentrate pellet in Oakridge centrifuge tubes (QuickSeal™, Beckman) using a JA-20 J series rotor (Beckman) and an Avanti® J-E centrifuge (Beckman coulter) at 10K RPM, for 15min at 4⁰C. The supernatant was discarded and the pellet was stored at -20⁰C until purification.

2.2.5. Bradford assay for the determination of protein concentration

Bradford assays were used to determine the concentration of proteins before oxidation, OMFP assay, arraying, array probing and after filtration and concentration. Bradford assay assays were carried out using the Thermo Scientific Coomassie Stain Plus Bradford Assay protocol (<http://www.piercenet.com/instructions/2160229.pdf>) in addition to the Coomassie Plus™ Protein Assay Reagent kit (Thermo Scientific, US). The microtiterplate version of the protocol was carried out to minimise protein usage. The BSA protein standards and experimental samples were analysed in triplicate wells, and 5-fold dilutions of the protein were carried out to find values in the middle of the BSA standard curve. The BioTek® plate reader (Biotek, UK) was used to analyse the wells. Protein concentration was found by creating a standard curve from the BSA protein samples, finding the equation for the values plotted, and then rearranging equation to find the unknown (X).

2.2.6. Purification of PTEN and VHR

Pellets of transformed DH5α *E.coli* cells containing pGEX-4T1 vector including gene of interest and expressed protein of interest were defrosted on ice. A cell lysis solution was prepared with 2mg/mL Lysozyme, 1μL /1mL protease inhibitor cocktail (Roche), 10 μL/1mL Triton-X 100 (BDH, UK), 50mM TRIS (Trizma® base, Sigma Aldrich, US), 2mM chelating agent Ethylenediaminetetraacetic acid (EDTA, BDH limited, UK) 2mM of reducing agent DL-Dithiothreitol (DTT, Fisher Chemical, US). 50mL of lysis solution was added to pellets per 1L of culture that formed pellet. The pellet in lysis solution was stirred with a magnetic stirrer in a glass beaker for 1hr in a cold room.

5mL of Glutathione Sepharose™ 4B column beads (GE Healthcare), for affinity purification, were added to a gravity column. Glutathione Sepharose beads consist of reduced glutathione covalently coupled to Sepharose® beads via a 10-carbon spacer arm. The column beads were equilibrated with 60mL of equilibration buffer consisting of 50mM TRIS, 140mM NaCl and 2.7mM KCl (Fisher Scientific), pH 7.4. The lysed cell solution was homogenised X10 using manual homogeniser apparatus to suspend the protein in solution. Next the lysed and homogenised sample was sonicated. Experiments carried out based on optimised protocol by Doctor Lok Hang Mak (Imperial College London). Sonication of samples was performed using a UP50H, ultrasonic processor (Hielscher ultrasound technology). Sonication was performed on ice. The cell and protein suspension was sonicated for 30sec, and then rested for 1min X10 cycles. The sonicated suspension was then spun down in a centrifuge in a JA-20 rotor at 15K RPM, for 60min at 4°C. Samples of pre- and post-sonication were stored in freezer, along with the pellet from the centrifugation for SDS-PAGE and Coomassie staining analysis. The supernatant after centrifugation which contained the soluble protein was filtered in a 0.45μm syringe filter tip (Millex® Syringe-driven

filter unit, 0.45µM, Millipore, Ireland). A sample was taken post-filtration for SDS-PAGE and Coomassie staining analysis.

The filtered supernatant was then loaded onto the Glutathione Sepharose™4B column and slowly gravity filtered. The column was then washed with a series of wash buffers including surfactant in the first wash, with increasing amounts of salt. The column was first washed with 25mL of 50mM TRIS, 140mM NaCl, 2.7mM KCl, 1% Triton X-100, 2mM DTT, and pH 7.4. The column was then washed with 40mL 50mM TRIS, 140mM NaCl, 2.7mM KCl, 2mM DTT and pH 7.4. The column was finally washed with 40mL of 50mM TRIS, 500mM NaCl, 2.7mM KCl, 2mM DTT and pH 7.4. The wash buffer was then collected for analysis with SDS-PAGE and Coomassie staining for presence of protein in flow through. An elution buffer of 50mM TRIS, 20mM L- glutathione reduced (Sigma Aldrich, US), 250mM NaCl and 2mM DTT at pH7.4 was then added to the column, 2mL of this was allowed through the column then the column cap was securely fastened and the elution buffer was incubated on the column with the protein and beads overnight in the cold room.

After overnight cold room incubation the protein was eluted by collecting it into a suitable vessel. The protein was then concentrated if less than 1mg/mL as concentrated protein meant less additional compounds at final concentration in the 3-O-methylfluorescein phosphate (OMFP) activity assay, and smaller volumes for oxidation experiments. 50% glycerol (Analytic reagent grade, Fisher Chemical, UK) was then added to the protein and the protein was stored at -80°C.

The volume of the protein solution was recorded, and then a Bradford assay (Thermo Scientific, US) of protein concentration determination was performed.

To assess protein activity an OMFP assay of phosphatase activity (See 2.2.11. OMFP assay of phosphatase activity) was performed. Following the Bradford assay estimation of concentration of the protein the specific activity (nMole/min/mg protein) was calculated. The specific activity of that protein batch was then used to compare

activities between batches. The specific activity of a batch was also used to compare to the specific activity of the same batch after subsequent concentration, freeze-thaw cycles and filtrations when comparing treated (oxidised) versus control samples.

In order to ascertain the purity of the sample an SDS-PAGE and Coomassie stain were performed. Adequate purity of the sample was inferred by the presence of a single band on the gel. The identity of the protein could also be inferred by the size of the band relative to the protein ladder marker (PageRuler™ Plus, Fermentas), although this would be confirmed later by MS/MS analysis and Mascot software protein predictions. Adequate purity was required for attaining the specific activity of the protein, and for array interactions. The collected samples from all the stages of the purification procedure were also run via SDS-PAGE and Coomassie stained to assess whether protein produced was transferred onto the column, had bound to the column, and had eluted appropriately. The gel was kept to test fragments from fractions and stages of purification.

The Glutathione Sepharose™ 4B column material was regenerated after each use. The column was first washed with 10mL of 0.1M TRIS, 0.5M NaCl and pH 8.5 wash solution. The column was then washed with 10mL 0.1M sodium acetate (BDH, UK), 0.5M NaCl, pH 4.5 wash solution. These wash steps were then repeated twice in an alternating fashion. Next the column material was washed with 10mL of 6M chaotrope guanidine hydrochloride (Sigma Aldrich, US), and then immediately followed by a wash with 30mL of TRIS column equilibration buffer. Next 15mL of 70% ethanol (Fisher Scientific) was used to wash the column, immediately followed by a wash with 50mL of column equilibration buffer. To store the Glutathione Sepharose™ 4B column, 15mL of 20% ethanol was added, 10mL was allowed to flow through the column, then the column was closed and the wet column was stored in the cold room.

2.2.7. SDS-PAGE and Coomassie staining

2.2.7.1. SDS-PAGE

Sodium dodecyl sulphate polyacrylamide gel electrophoresis (SDS-PAGE) separates proteins by electrophoretic properties, and thus proteins with different masses separate in space when ran on an SDS-PAGE gel. SDS-PAGE was used as part of multiple protocols, including in-gel digest and analysis of protein purity.

The BIORAD SDS-PAGE gel tank system was used (BIO RAD, US) in combination with a power pack (Consort, E844). 12% acrylamide resolving gels were made with 4.2mL H₂O, 2.5mL 1.5M TRIS-HCl pH8.8, 3.1mL 40% acrylamide/bis 37.5:1 (Sigma, US) and 100µL 10% sodium dodecyl sulphate. (SDS), 50µL 10% oxidising agent ammonium persulfate (electrophoresis grade >= 98% pure, Sigma, US) and 20µL TEMED ((NNN'-N' Tetramethylethylenediamine, BDH Limited, UK) were used added to catalyse polymerisation of acrylamide. 6.7% acrylamide stacking gels were made using 980µL H₂O, 440µL 1.5M TRIS-HCl pH6.8, 300µL 40% acrylamide/bis 37.5:1, 18µL. SDS gel running buffer was made as a 10X solution (30g TRIS, 144g glycine (Fisher Scientific, UK), 100mL SDS, final volume 1L made up with H₂O) and diluted to 1X before running gel.

10µL samples were mixed with 10µL Sample Buffer and Laemmli 2X Concentrate (Sigma Life Science, US) then boiled on a heat block for 10min and loaded into wells in gel. 10µL of PageRuler™ Plus Prestained Protein Ladder (Thermo Scientific, US) was loaded as visible marker including proteins of known molecular weights. Gel electrophoresis was run at 120V until visible loading buffer dye front had reached the bottom of the gel, thus maximally separating out proteins on gel by their electrophoretic qualities.

2.2.7.2. Coomassie staining

For in-gel digestion and assessment of protein purification SDS-PAGE gels were stained with Coomassie stain solution made with 0.5g Coomassie dye per 100mL of 45% methanol (Fisher Scientific), 45% H₂O and 10% acetic acid.

Gels were stained for 12hr and then destained using a destain solution consisting of 45% methanol, 45% H₂O and 10% acetic acid. This was done on a rotational shaker plate (Mini orbital shaker, SSM1, Stuart®). An appropriate amount of stain and destain was used to fully submerge the gel. Gels were destained until bands appeared and could be resolved with low noise from the background. Gels were then photographed using the G:BOX (SYNGENE) fluorescence and natural light gel photography device and associated software.

Densitometry on Coomassie stained SDS-PAGE gels was performed by using ImageJ (<https://imagej.nih.gov/ij/>). A rectangle selection tool was used to create blocks around either Coomassie stained gel bands or around the complete SDS-PAGE gel lane, where controls for non-stained areas were selected from empty SDS-PAGE gel lanes. ImageJ profile plots were created for each sample and background noise was cut off manually using the ImageJ 'straight line selection tool' where profile plots do not reach the baseline. Next the ImageJ 'wand' tool was used to select the area inside the profile plots representing the densities from the gel bands and lanes, and the ImageJ 'label peaks' tool was used to label each peak with a percentage of the total size of all the highlighted peaks that represent gel band and lane densitometry. The percentage densitometry compared to the control band or lane was then calculated.

2.2.8. Filtration

Illustra™ NAP™-5 columns (GE Healthcare, UK) were used to buffer exchange protein samples (PTEN-GST, VHR-GST) into non-reducing buffer for subsequent oxidation and OMFP assay. The standard Illustra™ NAP™-5 column protocol was followed (http://www.gelifesciences.co.jp/tech_support/manual/pdf/17085301.pdf). Protein was filtered into phosphate buffer (50mM, pH7.4)

Slide-a-Lyzer dialysis cassette (Thermo Scientific, US) membrane filtration was also used to buffer exchange protein samples (PTEN-GST and VHR-GST) into non-reducing buffer. The standard Slide-a-Lyzer protocol was followed (<http://www.piercenet.com/instructions/2160729.pdf>), Protein was filtered into phosphate buffer (50mM, pH7.4) Microcon centrifugal filter devices (Millipore, US) were also used for protein ultrafiltration.

2.2.9. Oxidation

Protein was oxidised over a range of oxidant concentrations. The amount of protein added was determined by the amount needed for the downstream reactions. Reducing agents were removed prior to oxidation via filtration. Filtration was performed at 4°C.

The amounts of OMFP assay protein used were previously determined via optimisation by Doctor Lok Hang Mak (Imperial College London). Protein amounts to for digestion experiments to yield sufficient protein for downstream experiments where experimentally determined by Oxidative Stress Group, Aston University. Protoarray probing protein amounts required for experimentation were determined experimentally by the Invitrogen Protoarray Human Microarray standard protocol in combination with Dynamic Bioarray silicon dioxide chip technology which determined

liquid volumes of sample. Values of protein concentration are for proteins as fusion constructs with GST.

20% Trichloroacetic acid (TCA, Sigma-Aldrich, US) kept at 4°C was added (incubate oxidation reaction on ice for 20min with TCA), then a centrifugation step (5min, 13K RPM), then the pellet was washed with 1ml ice-cold acetone and then re-pelleted. The pellet was spun until dry using a vacuum centrifuge. An alternative reaction stopping method of adding excess L-Methionine (Sigma, US) was used with Lysozyme to co-optimize reaction stopping and mass spectrometry sequence coverage. Protein that was to be assayed in the OMFP assay was not stopped, but reactants would have been diluted in OMFP master mix.

2.2.9.1. Hypochlorous acid (HOCl) oxidation

Protein samples were treated with Hypochlorous acid (HOCl, Sigma-Aldrich, US), incubating at room temperature for 1hr with a range of concentrations and molar ratios (See 3.4.1. Oxidation of PTEN-GST with HOCl and sin-1 generated peroxynitrite and 3.4.5 Oxidation of VHR-GST with HOCl, sin-1 generated peroxynitrite and tetranitromethane), and was adapted from Mouls et al (2009).

HOCl may react with amino group side-chains, including the chlorine from the HOCl displacing a hydrogen (Dychdala, 1991).

As HOCl degrades over time when stored at 4°C, in order for an accurate molar ratio of oxidant to protein oxidation to be carried out, HOCl stock which varied in concentration over time was regularly empirically determined on a UV/VIS spectrophotometer (PerkinElmer™ instruments, PTP-6 Peltier System and Perkin Elmer precisely, Lambda 35 UV/VIS Spectrophotometer, US) at 292nm wavelength.

Phosphate buffer (50mM, pH7.4) was used as a buffer for the oxidation as TRIS buffer has a primary amine that reacts with HOCl (Fu et al, 2001).

2.2.9.2. 3-Morpholinosydnonimine (SIN-1) oxidation

Samples were treated with sin-1 (Sigma-Aldrich, US) incubating at 25^oC using a heating block (Grant) for 1hr with a range of concentrations (protocol from personal communication with Doctor Corinne Spickett and Doctor Karina Tveen Jensen, Oxidative Stress Group Aston University). Phosphate buffer (50mM, pH7.4) was used for sin-1 oxidation.

Kirsch *et al* (1998) state that sin-1 releases nitric oxide and superoxide, and is used as a source for peroxynitrite. Peroxynitrite is an oxidant formed in the diffusion-controlled reaction of superoxide and nitrogen monoxide.

2.2.9.3. Tetranitromethane oxidation

Samples were treated with tetranitromethane (Sigma, US) incubating at 25^oC using a heating block (Grant, UK) for 1hr as per sin-1 oxidation. Ammonium bicarbonate (10mM, pH 7.8) was used for tetranitromethane oxidation which was the buffer used by Ghesquiere *et al* (2009). Tetranitromethane was used for increased nitration of tyrosyl residues, through the nitration of phenol groups to form 3-nitrotyrosine (Sokolovsky, Riordan, & Vallee, 1966).

2.2.10. Digestion protocols

In order to detect protein identity, and the identity and abundance of modifications by bottom-up MS based MS/MS proteins need to be fragmented to sizes that can be ionized by electrospray ionisation (ESI), and be manipulated in the quadrupoles. Two digestion protocols were used to digest protein, in-gel digestion and in-solution digestion.

In-gel digestion can be performed with less protein sample, with increases in the effective concentration and K_m of the trypsin digestion enzyme, but is subject to selection bias as only the protein that is present in the band that is cut out and analysed is detected by subsequent MS/MS analysis. As modification of protein structures by oxidation, nitration and chlorination may include changes in mass by addition of molecules to amino acid side chains, fragmentation and aggregation, these changes may affect the electrophoretic properties of sub-populations of protein molecules which may or may not be selected for by the cutting out and digestion of a Coomassie stained gel section.

2.2.10.1. In-gel digestion

Load and run purified, oxidised protein samples and controls onto an SDS-PAGE gel in 2X loading buffer. Next Coomassie stain the protein in the SDS-PAGE gel (See 2.2.7.2. Coomassie staining).

Coomassie stained sample bands were excised from gel lanes with a scalpel. Gel pieces were dissected further into smaller segments. The gel pieces were then transferred to a microcentrifuge tube. Gel pieces were washed in 500 μ L of 100mM ammonium bicarbonate with (Mini orbital shaker, SSM1, Stuart®) shaking for 30min. Next the wash solution was pipetted off and discarded. Then 500 μ L of 50% Acetonitrile in 100mM ammonium bicarbonate was added, submerging the gel pieces, and then washed with rotational shaking (Mini orbital shaker, SSM1, Stuart®) for 30min. Next the wash solution was discarded.

A reduction step with 100mM and 10 μ L 45mM DTT (Sigma) was then performed, in order to chemical reduce any cysteine disulphide bridges that may form between and within denatured protein strands. The incubation of the gel pieces with DTT was done at 60°C for 30min using a heating block (Grant).

Next an alkylation step was performed to alkylate the free cysteines carbamidomethyl cysteine so that cysteine disulphide bridges do not reform. Note that this prevents the detection of cysteine disulphide bridges in CX₅R proteins such as PTEN, which has a redox sensitive cysteine disulphide bridge nucleophile in its active site. Other, further oxidised forms such as sulphinic acid (dioxidised cysteine side chain) and sulphonic acid (trioxidised cysteine side chain).

The alkylation step was performed using 100mM iodoacetamide (Sigma, US) incubation at room temperature for 10min followed by incubation in the dark for 30min. Afterwards the supernatant was discarded.

The gel pieces were then washed in 50% acetonitrile, 100mM ammonium bicarbonate for 30min with rotational shaking (Mini orbital shaker, SSM1, Stuart®) Next the gel pieces were dried by the addition of 50µL acetonitrile for 10min. A solution of trypsin was then added to digest the protein. Trypsin was added in excess to protein (1:50) in a 25mM ammonium bicarbonate. The gel pieces were covered and protein was heated at 37⁰C on a heating block for 12hr.

After 12hr samples were taken off the heat block and centrifuged for 5min at 13K RPM to collect liquid at bottom with protein and gel pieces. Transfer liquid into a new microcentrifuge tube. Then add 20µL 5% Formic acid to gel pieces, and then incubate for 20min at 35⁰C. Next 40µL acetonitrile was added to gel pieces and then they were incubated at room temperature for 20min. Next the samples were centrifuged (5min, 13K RPM). All liquid was then transferred to the centrifuge tube containing the collected digested protein sample. Next a drying step was performed to the digested protein sample using a Concentrator plus vacuum centrifuge (Eppendorf) and samples were stored at -20⁰C until use in MS experiments.

2.2.10.2. Double digestion

In order to improve sequence coverage, and/or total between runs sequence coverage, a sequential double digestion protocol was implemented with two digestion enzymes. The enzymes were selected after the ExPASy Peptide Cutter *in silico* digestion software (http://web.expasy.org/peptide_cutter/) suggested a suitable candidate peptide (NGRVLVHCR) given the requirements of peptides of a suitable length and mass for detection via MS. The GluC/AspN (Sigma-Aldrich, US) procedure for the double digest used in investigation of VHR sequence coverage and active site coverage was adapted from Ragan (2002). Followed in-gel digestion protocol (2.2.10.1. In-gel digestion) for first digest, with the following adaptations of 300ng GluC in 100mM ammonium bicarbonate. The second digestion was an in-solution digest with sample incubated overnight at 37°C with 80ng AspN added to 2µL of 100mM ammonium bicarbonate.

2.2.11. OMFP assay of phosphatase activity

The 3-*O*-methylfluorescein phosphate (OMFP) assay of phosphatase activity was used as the primary method of determining protein activity of a known amount of PTEN or VHR protein. The OMFP substrate undergoes cleavage to OMF + P via phosphatase activity and OMF fluorescence intensity is detected.

Firstly an SDS-PAGE and Coomassie staining analysis of protein was performed to determine the purity of the sample by visual inspection of the Coomassie stained proteins for presence of any Coomassie-binding moieties not of the expected size (See 2.2.7. SDS-PAGE and Coomassie staining), from which to calculate a specific activity of the protein construct rather than just of a certain concentration of protein

containing enzymatic activity. A Bradford assay (Thermo Scientific, US) was performed to calculate the concentration of protein in sample.

The OMFP reagent was prepared by addition of 3-*O*-methylfluorescein phosphate cyclohexylammonium salt (Sigma-Aldrich) powder to dimethyl sulfoxide (DMSO, Fisher BioReagents®, US), fresh on the day of experimentation (0.0025g in 250µL DMSO). OMFP DMSO solution was mixed using a TopMix FB15024 vortex mixer (Fisher Scientific), and then sonicated using a sonicating water bath (Ultrawave limited, UK) for 30min.

Master mixes contained OMFP assay buffer (TRIS 100mM, pH 7.0) 1mM DTT, protein for four wells and the final volume of the master mixes is 600µL.

The experiment was carried out in white 96 well plates using a Spectra MAX GEMINI XS Fluorescence plate reader (Molecular Devices).

and associated Softmax Pro® Software for Spectra MAX GEMINI XS Fluorescence plate reader. Reactions were carried out in triplicate with blanks containing the OMFP assay buffer and reaction mix but without protein. In order to start the reaction 50µL of reaction mix (TRIS 100mM, 2µL DMSO OMFP solution) was added to the wells containing 150µL of master mix, and the reaction was recorded via the plate reader immediately following the addition of the OMFP. The reaction kinetics were monitored over the course of 20min.

Usage of plate reader and plate reader software including optimisation of settings. The maximum relative fluorescence unit (RFU) threshold was increased so that the readings would not saturate (increased to 40K RFU threshold) and sensitivity of reading was reduced to low to prevent background noise fluctuations. Plate reader settings were optimised for the concentrations of protein and the activities of the particular proteins used. A maximum amount of readings, and thus minimal time between reading intervals was used for reaction monitoring and kinetics.

In order to calculate the specific activity of the protein sample, a 3-*O*-Methylfluorescein (OMF) standard curve was produced using OMF powder (Apollo Scientific Limited).

The specific activity of the protein was used to determine the quality of protein expression and purification, the effects of buffers and filtration methods, the effects of oxidation treatments and to ensure that the protein is in an active conformation for protein-protein interaction microarray arraying and probing.

2.2.12. Liquid chromatography coupled mass spectrometry

2.2.12.1. TOF MS/MS

An ABSciex quadrupole time of flight (QTOF) 5600 time of flight analyser mass spectrometer (ABSciex, Warrington, UK) was used to perform experiments.

20µg protein samples were resuspended up to a volume of 30µL with Eluent A (98% acetonitrile, 2% H₂O, 0.1% formic acid) prior to LC-MS analysis, which allowed for technical replicates or usage for a different MS experiment as 10 µL of resuspended sample was used per MS experiment. Eluent A and Eluent B (98% H₂O, 2% acetonitrile, 0.1% formic acid) were used in the HPLC system to separate the peptides.

The custom on-line system included a Dionex Ultimate 3000 (Dionex, Camberley) High-performance liquid chromatography (HPLC) system on-line to QTOF 5600 to separate peptides connected via a New Objective PicoTip emitter (FS360-20-10-N, Woburn, MA, USA). The peptides were captured and desalted on a C18RP pre-column (C18 PepMap™ 5 µm, 5mm x 0.3 mm i.d. Dionex, Bellefonte, PA, USA). Peptides were separated on a C18 nano-HPLC column (C18 PepMap™ 5 µm, 5mm x 0.3 mm i.d. Dionex, Bellefonte, PA, USA) using a gradient elution running from 2% to 45% aqueous acetonitrile (0.1% formic acid) in 60min and a final washing step

running from 45% to 90% aqueous acetonitrile (0.1% formic acid) in 1min. The system was then washed with 90% aqueous acetonitrile (0.1% formic acid) for 5min and then equilibrated with 2% aqueous acetonitrile (0.1% formic acid) (See Appendix 7). Chromeleon Xpress software was used for controlling the Dionex Ultimate 3000 HPLC system and Analyst® TF 1.5 software (ABSciex, Warrington) was used to control and record the QTOF. The computer controlling the online system was a DELL Precision T3500 with Intel® Xeon® Inside™.

Ionisation of the peptides as achieved with a spray voltage set at 2.4KV, a source temperature set at 150°C, declustering potential set at 50V and a curtain set at 15. Survey high resolution. The MS method was run in independent data acquisition (IDA) with dynamic exclusion for 20s, 250ms acquisition time and rolling collision energy following from Moulis et al (2011) with a duration setting of 60min per sample, synchronization mode set to LC Sync, and the Original Configuration set to 'instrument signature' TripleTOF 5600, and 'ion source' Nanospray, and 'device methods' set to Dionex Chromatography MS link. The scan type was set to TOF MS, accumulation time to 0.200031s, polarity was set to positive. For the period, the cycle time was set to 2.2503, period was set to 1, cycles were set to 1600 and delay time was set to 0sec. The IDA experiment was set to scan in positive ion mode for TOF Masses (Da) of minimum of 350 and maximum of 1250. For 'advanced MS' settings, Analyst was set to 'Auto Adjust with mass', with a Q1 transmission window of Mass (Da) 330.0000, 100%, with an acquisition parameter of 'time bins to sum' of 4. TOF extraction parameters were set to settling time (ms) of 0 and pause between mass ranges (ms) of 1.028. Time-to-digital converter channels 1,2 3 and 4 were checked. Switch criteria for Survey scan for IDA were set to 'for ions greater than 350m/z, for ions smaller than 1250m/z, with a charge state of 2 to 5, which exceeds 250 counts per second and excludes isotopes with 4Da. Mass tolerance was set to 50mDa, and maximum number of candidate ions to monitor per cycle was set to 10. Exclude

former target ions was set to for 40sec. Raw data files were converted to .mgf files via PeakView® software (<http://www.absciex.com/products/software/peakview-software>).

The mass spectrometer was calibrated by disconnecting the HPLC from the needle and connected to a syringe pump (Harvard Apparatus, MA, US) containing tuning solution for the AB SCIEX TripleTOF™ System (AB SCIEX, UK). The spray was then started via the Chromeleon Xpress software and the spray was checked via the needle camera on the ABSciex 5600. The spray was left until stabilisation. The 829 Dalton peak from the tuning solution (AB SCIEX, UK) was optimised to be 10^4 signal intensity via Analyst® TF 1.5 software. The total ion chromatogram (TIC) was optimised to be 10^6 signal intensity. The accumulation time for the calibration was set to 1sec, the period duration to 5min, ion source voltage to 2400, ion source gas 1 was set to 12 and ion source gas 2 was set to 0. The TIC of the positive TOF was selected for TOF calibration with the ALILTLVS reference tuning solution. The calibration was calculated for the spectrum. The calibration was also performed for MS/MS product ions with high sensitivity selected and a collision energy of 50, then the needle was reconnected to the HPLC.

The position of the needle was moved and optimised per run, and calibrations were optimised for each run and needle. Replicates were run in serial in a single batch where possible, which was optimised for analysis with Progenesis QI for proteomics software (Nonlinear Dynamics, UK) for optimised Progenesis file alignments. The source and needle were optimised for the HPLC Dionex Ultimate 3000 HPLC system and for the properties of the specific independent data acquisition run.

2.2.12.2. Targeted ion scan

The precursor ion scan experiment scanned for selected product ion masses which had either been previously detected in a standard MS/MS experiment or calculated

based on predicted mass and charge if unable to detect them or not present in standard MS/MS experiment results.

The acquisition method was set to a duration of 60min, Original Configuration was set to Instrument signature: TripleTOF 5600, Ion source was set to: Nanospray and Device methods were set to Dionex Chromatography MS link. The scan type was set for TOF MS, the accumulation time: 0.2000031, TOF Masses (Da) were set to min:350 and max: 1250. IDA was unchecked. Polarity was positive. The period had a cycle time of 1.8503sec, cycles set to 1946, period 1 and a delay time of 0sec. Analyst was set to 'Auto Adjust with mass', with a Q1 transmission window of Mass (Da) 330.0000, 100%, with an acquisition parameter of 'time bins to sum' of 4. TOF extraction parameters were set to settling time (ms) of 0 and pause between mass ranges (ms) of 1.028. TDC channels 1,2 3 and 4 were checked.

For the product ion scan experiments scan type Product Ion was selected, TOF masses (Da) min: 100 to max: 2000 were selected with high resolution settings. Auto-adjust with mass was checked. The Q2 transmission window was set to 50% 80(Da) and 50% 230 (Da), and resolution was set to 'unit'.

2.2.12.3. *In silico* identification of modified peptides

2.2.12.3.1. Mascot *in silico* identification

Mascot software

(http://www.matrixscience.com/cgi/search_form.pl?FORMVER=2&SEARCH=MIS)

was run on MS raw data that had been converted to .mgf files by Peakview® version 1.0.0.3 (ABSciex).

Variable modifications were searched for in groups of modifications on Mascot.

The first modification set searched for was carbamidomethylation as a fixed

modification, and as variable modifications of methionine oxidation, nitrotyrosine oxidation, nitrotyrosine (or chlorotyrosine for HOCl treated samples) cysteine dioxidation, cysteine trioxidation. The second search performed was for histidine oxidation, tryptophan oxidation, lysine oxidation, proline oxidation and methionine dioxidation. Additional modifications were searched for including allysine, tryptophan dioxidation and tryptophan nitration. Error tolerant search was also performed after targeted searches as an unbiased and due diligence approach to check for other PTM modifications that may have occurred that we did not identify as targets to search for.

For Mascot protein database settings the SwissProt non-redundant database was used as a database of protein sequences to search against. For Mascot taxonomy settings the nearest taxonomy to the protein of interest was selected, for PTEN and VHR this was *Homo sapiens*. For enzyme settings trypsin was inputted as the digestion method. The peptide tolerance used was +/- 0.8 Da, so as have a tolerance value smaller than a hydrogen atom, peptide charges of 2+, 3+ and 4+ was used, MS/MS ion search was selected. All other settings were appropriate to instrument used and standard settings.

The Mascot score and protein sequence coverage for the protein was used to comparatively assess MS/MS runs, oxidant treatments, tryptic enzymes and oxidant treatment concentrations. The 'score distribution' window was used to assess 'Peptide score distribution' for the ion score for that Mascot search that corresponds to a *P* value of $p < 0.05$, which was noted, yet all modifications were checked on Mascot for their sequencing and y-ion series, in addition to searches in the raw data via Peakview. Rare or unexpected peptides were sequenced using *de novo* sequencing in cases where systematic manual or automated modification searching was performed, for experiments searching for particular peptides or modification, in these cases all modifications were sequenced *de novo*.

The output retrieved from Mascot included the sequence coverage, peptide sequences containing the modified and unmodified residue, modifications found, statistical likelihood of the modification as an ion score, and retention times of the ion. Data was retrieved for peptides with multiple modifications, fragmentation patterns and charge states, and all non-modified versions. Peptides found in one search, were recorded to be searched for in the downstream raw data analysis of other samples, were that peptide may not have been detected by Mascot in that sample, and may not have been covered by the sequence coverage for that sample. For eXtracted Ion Chromatograph (XIC) the mass, charge and retention times of the peptides of interest (non-modified and modified intra- and inter-sample) were recorded. The search results for each Mascot run were also analysed for the error range and drift for quality control purposes.

The peptides predicted by Mascot were investigated using the detailed view for each Mascot peptide query. The Mascot sequencing graph in the 'peptide view' was used to assess whether the peaks picked by Mascot were above the noise. Mascot was also used to predict the likelihood of modifications being false positives using the Mascot sequencing tool. Peptide sequences were checked for i) peaks that could be differentiated from noise ii) whether the modification was covered in the sequence by assessing the y ions and the extent of coverage of y ions over the peptide and oxidative modification/s, including continuous y ion coverage, and coverage of other amino acids that could also be modified with the modifications that are being searched for in the search parameters.

2.2.12.3.2. Progenesis *in silico* identification

Progenesis LC-MS (Nonlinear Dynamics, UK) was used to search multiple replicates and perform *in silico* experiments to find the abundances of modifications automatically and provide statistics for the modifications. Progenesis was used in combination with Mascot, where modifications were predicted by Mascot and uploaded into Progenesis as a batch before the automated Progenesis XIC. A threshold was applied to the results with a cut off recommended by Mascot for the appropriate 0.05 significance p-value. Progenesis modifications still required manual validation and *de novo* sequencing in Peakview® version 1.0.0.3 analysis suite (AB SCIEX, UK).

Data was imported in the AB SCIEX .wiff format. All runs for varying concentrations and replicates were attempted to be aligned as part of an *in silico* experiment. The chromatography was then aligned in the import data window for similarities, artefacts and manual quality control. The imported data was then aligned. Samples with an alignment score of lower than 30% were removed from the alignment, or if a sample was empirically found to be reducing the overall alignment and number and quality of modifications found, it was also removed. The experimental design setup separated samples out by treatment condition and added replicates samples to the condition. Peptides were identified via the exporting of the mass spectra to Mascot in the 'identify peptides' panel and then imported as 'import search results'. Statistical significance cut offs were applied in the 'refine identifications' window, with a score less than suggested by Mascot and then deleted from the search. A report was then generated with all features extracted from Progenesis for downstream data analysis. Standard settings for Progenesis were used, and automated alignments were used.

2.2.12.3.3. Analysis of raw MS data

2.2.12.3.3.1. Extracted ion chromatography

The PeakView® version 1.0.0.3 analysis suite was used to analyse MS/MS data for each predicted ion of interest previously identified in the Mascot search, Progenesis or from product ion scanning. It was used to convert files to .MGF for Mascot searching, to assess the spread of the MS/MS data via Independent Data Acquisition (IDA) view. Standard options were used for Peakview analyses, with 'peak labelling & finding' with spectra default threshold of 5%, maximum charge state for peak finder of 6, 'centroid height percentage' of 50%, and with chromatogram settings of area set to 5%, noise percentage set to 40%, baseline subtraction window set to 40% and peak splitting factor set to 10 points. Gaussian smoothing peak integration was applied for purposes of presentation and not for analysis.

To assess the intensity of the peaks and quality of the run, the TIC view was used to make sure that the majority of the peptides from the on-line HPLC run have been ionised and detected by the MS program.

The total intensity within a mass tolerance window around a mass-to-charge (m/z) ratio of predicted peptide of interest is plotted. The size of the mass tolerance used was 0.2 either side of m/z value. XICs are used to determine the intensity, and thus abundance, of a specific m/z ratio ion. The predicted mass, charge and time the ion where observed are needed to perform an XIC. By first finding the ion that has the closest m/z and appears at the time expected (data obtained from Mascot search), the peak that this ion is part of can be found, as well as the area of this peak which is an accurate measure of abundance of that ion.

The numerical area under the peak from all unmodified versions of a peptide and other modifications can then be compared to the area under the peak from the

modified peptide of interest, and a percentage abundance for each modification can be found. This can be performed intra-sample to determine the modification level in a sample, and inter-sample when comparing varying treatments or comparing to controls. The numerical percentage abundances were found for varying oxidising and nitrating agents and over varying molar ratios and plotted as a landscape to visualise global oxidative PTMs and their abundances.

For each oxidised peptide, there may also be a non-oxidised version of the peptide. There may also be non-standardly cleaved versions of the peptide, both oxidised and non-oxidised. Some versions of a peptide may be present in some samples and not in others. In order to perform quantitative analysis, all relevant versions of peptides must be searched for in all sample data files.

2.2.12.3.3.2. *De novo* sequencing

Peptides of interest were sequenced via *de novo* sequencing from raw data, whereby the masses of individual amino acids and modified amino acids are known and for a particular MS ion, its MS/MS fragments were analysed in a way where the fragmentation was analysed to see whether the fragments matched the amino acids and modified amino acids expected, calculated or predicted by Mascot. A full *de novo* sequencing was used as an additional check for the validity of the predicted results, or in cases where predictive software did not show the peptides that were expected for a particular protein, product ion scan or digestion that were of particular interest.

Peakview *de novo* sequencing was performed as the final *in silico* validation assessment; where the validation of modified residues within an identifiable section of amino acids from the peptide in question being searched for. The first *de novo* sequencing attempt for each peptide was done as a blinded experiment not knowing or being able to refer to the peptide sequence looking for, only having access to the

Peakview *de novo* sequencing panel and a lookup table of amino acid masses. A second pass *de novo* sequencing was then attempted with the peptide sequence available if *de novo* sequencing without knowledge of the peptide sequence was not possible. For *de novo* sequencing sequence coverage was not relevant for the purposes of searching for sequences not detected by Mascot.

2.2.12.3.4. Computational modeling

2.2.12.3.4.1 Mediator modeling

The mean of the technical replicates from the VHR phosphatase percentage activity, micromolar concentration of treatment and total percentage modification of amino acid residues were used. The mean activity level is defined as the model dependent variable and the input is the modification level. Each amino acid is treated separately in the analysis, where assume the percentage modification for each amino acid is independent to the other amino acids. Resampling was used with $n = 10000$ random samples added, to calculate 95% confidence intervals for single mediator analysis. A resampling method was applied due to sample and sample variable numbers, for attainment of statistical significance (Based on communication with Doctor Alexis Boukouvalas, Aston University School of Engineering and Applied Science).

For multiple mediator modeling a forward effect is calculated which captures the effect of the first mediator on the second mediator with the total indirect effect being the total effect of the first and second mediators minus the relationship between the percentage phosphatase activity and the treatment molarity. Resampling was used with $n = 5000$ random samples to calculate 99% confidence intervals for the multiple mediator analysis.

2.2.13. Protein-protein interactions

2.2.13.1. Arraying protein and antibody spots onto substrate using sciFLEXARRAYER S3

Arrays were spotted with antibodies and proteins for several uses including testing and optimising antibody-protein interactions, protein-protein interactions, oxidised protein-protein interactions, as well as testing biochips for probing and incubation (Dynamic Bioarray).

Arrays were spotted using sciFLEXARRAYER S3 (Scienion AG, Germany). Spots were arrayed in 10-by-10 grids with 4-by-8 blocks of grids. Each block had an identical layout (Figure 10.) The spotting pattern used enabled multiple replicates of the same experiment to be spotted in parallel as well as enabling positive and negative controls and different spotting and probing concentrations and treatments to be applied. The spotting pattern also fitted the Dynamic Bioarray biochips used which either had one hydrophilic chamber that covered all blocks and grids (Figure 10), or one individual hydrophilic chamber per block (Figure 11). The sciFLEXARRAYER software and hardware was used as recommended in the Scienion S3 Quickstart Guide and Operations Manual obtained with the sciFLEXARRAYER.

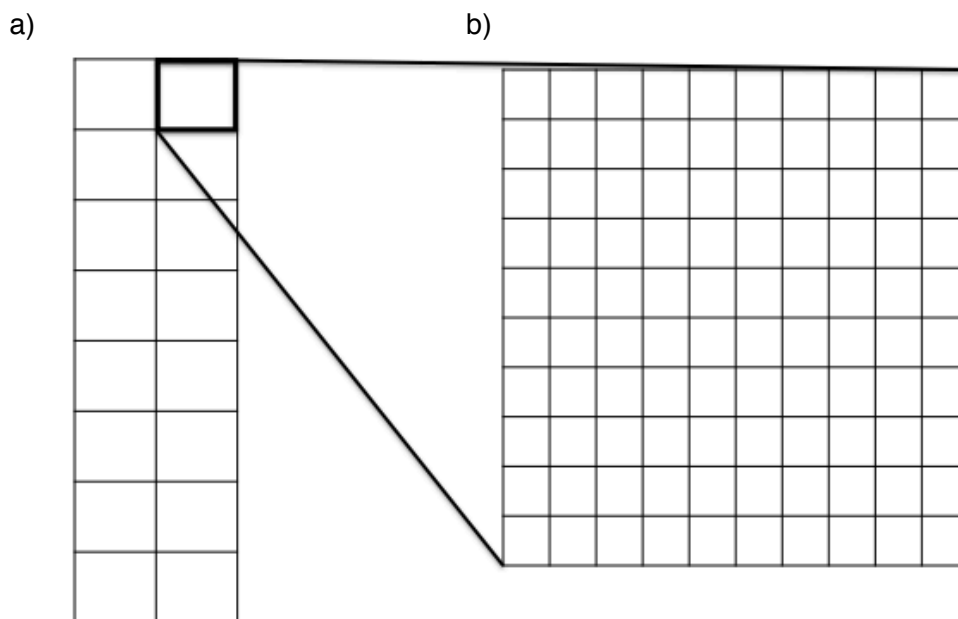


Figure 10. Array spotting layout schematic

a) Arrays were spotted in a 2-by-8 grid pattern onto substrate **b)** Array spots were spotted in 10-by-10 blocks in each 2-by-8 or 2-by-12 grid pattern. 2-by-8 pattern shown in schematic. b) is a close-up view of a single section of the 2-by-8 grid pattern in a).

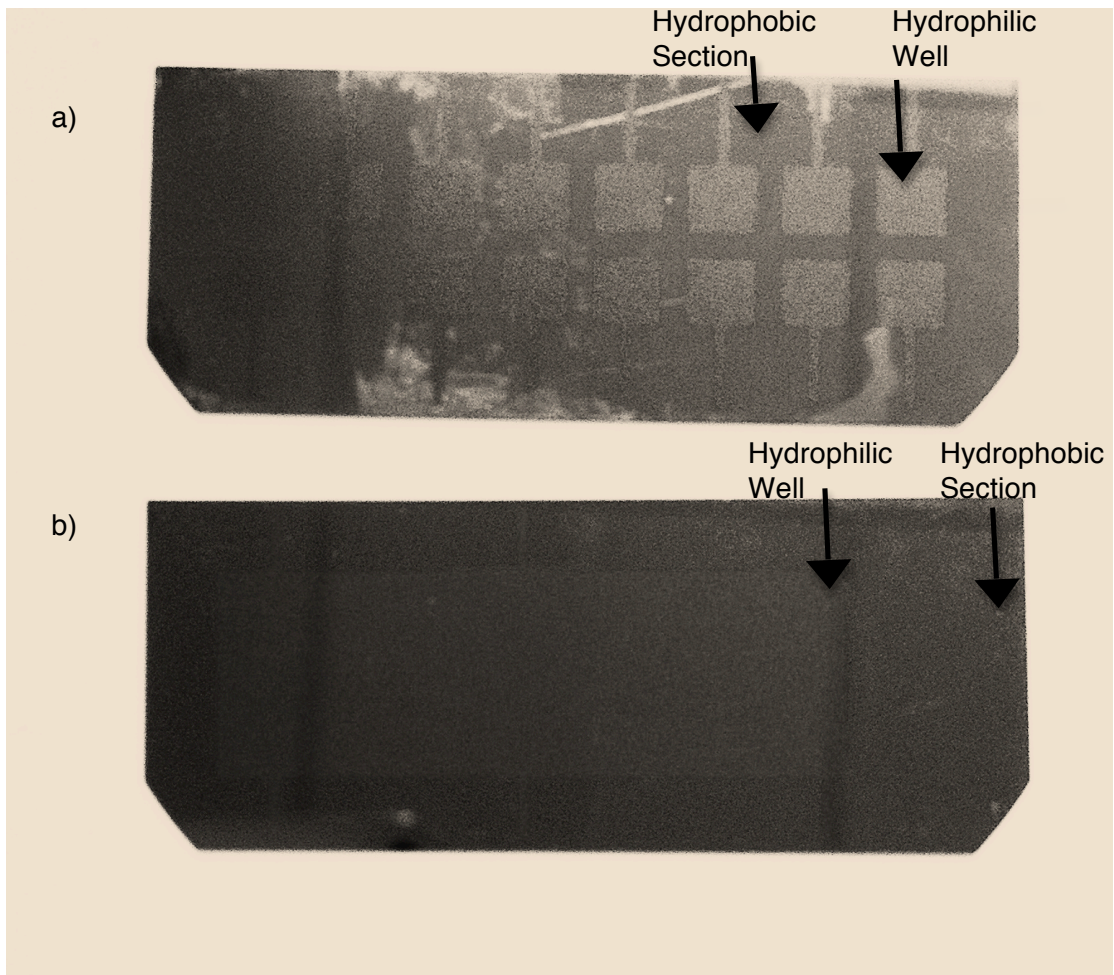


Figure 11. Dynamic Bioarray chip configurations

a) Multi-well Dynamic Bioarray chip b) Single well Dynamic Bioarray chip. (See protocol usage in 2.2.13.2. Protoarray probing for antibody-protein, protein-protein and protein-peptide arrays using Dynamic Bioarray biochip and lifterslip technologies)

Positive and negative controls were spotted on arrays in a similar block design to Protoarray® with positive and negative controls at the beginning and end of each block. Positive controls were antibodies with fluorescent probes (Molecular Probes, Cell Signalling Technologies).

Negative controls included PBS and a negative control protein Albumin, from bovine serum (BSA, Sigma, US) or VHR-GST. VHR-GST was used as a negative control for PTEN-GST; VHR is also a part of the PTP superfamily with CX₅R phosphatase motif homology, so this should detect non-specific binding that a standard BSA positive control may not.

The piezo tip settings were set to 92V, 48 pulse, Frequency 500 Hertz, LED delay 500. These contribute to the droplet formation and shape and should be optimised for spot shape, spot size, reduction of satellite spots and the uniformity within and between spots. Samples were aliquoted into 96 or 386 well, V-shape, Greiner PP-Microplates (Greiner bio-one, Germany). Wash procedures were performed prior to arraying. 1X PBST (0.1% Tween-20) washing the inside and outside of the piezo tip, then 1X Doctor Ekaterina McKenna's proprietary array tip cleaning detergent solution, then 1X HPLC grade water wash, then 1X PBST (0.1% Tween-20). Between samples 2 wash cycles of 1XPBST (0.1% Tween-20) were performed to avoid contamination and to clean piezo tip for high quality arraying. The array tip was washed with 1XPBST after the arraying procedure.

Arraying was performed on a clean bench, and extra care was taken to minimise dust and particulate matter using the following techniques and preventative measures: dusting, cleaning down surfaces, regularly swapping nitrile gloves, tying hair back, lab coats, minimising exposure of substrates in open environment, handling substrates by edges, minimising traffic in laboratory, creation of a designated clean bench. Quality control procedure was performed and analysed using the sciFLEXARRAYER (Scienion AG, Germany) camera system and quality control software to diagnose and minimise spotting error, and optimise quality. After arraying and drying, slides were sealed in 5-place slide mailer tube (Fisherbrand, UK) with nitrogen and stored in the fridge for use the next day when they were equilibrated to room temperature.

2.2.13.2. Protoarray probing for antibody-protein, protein-protein and protein-peptide arrays using Dynamic Bioarray biochip and lifterslip technologies

Arrays were probed with the biomolecules of interest to detect interactions between proteins and peptides and the spotted proteins and antibodies. Probing was performed using a modified version of the Invitrogen Protoarray® protein-protein interaction (PPI) application notes

(http://www.invitrogen.com/etc/medialib/en/filelibrary/protein_expression/pdfs.Par.73773.File.dat/Application-Note-Protein-Protein.pdf) and short protocol

(http://tools.invitrogen.com/content/sfs/manuals/protoarrayPPI_short_protocol.pdf) .

Modifications were made through communications with, knowledge transfer from and on request of industrial research partner Doctor Ekaterina McKenna who had pre-optimised protocol for usage with Dynamic Bioarray chips based on proprietary intellectual property (Dynamic Bioarray).

Modifications to the Invitrogen Protoarray® protocol are:

- Primary probe was incubated in proprietary Dynamic Bioarray hydrophilic silicon dioxide microfluidic system (Dynamic Bioarray, Doctor Ekaterina McKenna). A minimum of 180ul of primary probe (protein or primary antibody) was used per slide (PATH™ *plus* Protein Microarray Slide, Silver Quant®). This proprietary technology (subject to non-disclosure agreement whilst incorporating) uses less probe, lowering amount of protein needed to be expressed, and less primary antibody, which minimises expense, and also minimises total harm to animals antibodies raised in. For comparative analysis, the standard Lifterslip™ (Thermo Scientific) technology was used in parallel.
- Buffers used were as follows. Washing, protein suspension and antibody buffer (1XPBS, 0.1% Tween 20), Blocking buffer (1XPBS, 1% BSA). Notable

differences include a lack of blocking reagent in washing buffer, lack of reducing agents in blocking buffer and lack of detergent in blocking buffer.

- Air dry blocked slides for 30min in dark rather than proceeding directly to probing.
- Incubated Protoarray with protein at RT for 1hr rather than 90min at 4^oC.
- Wash 4X 15min after primary antibody with washing buffer rather than 4X 5min.
- Array drying was performed ON, although submerging in deionised water and drying by centrifugation preferential.
- Arrays were imaged the day after the array probing procedure. Arrays were kept in a slide mailer tube in the dark.

Modifications to standard Human Protoarray® v5.0 were recommended in knowledge transfer from Doctor Ekaterina McKenna (Dynamic Bioarray), as to be suitable for Dynamic Bioarray technology (Figure 11.), but further empirical tests would be carried out to determine the suitability of the standard Human Protoarray® v5.0 buffers with the Dynamic Bioarray technology.

Bespoke arrays were probed using the same modified Protoarray® Human Protoarray v5.0 (Invitrogen, US) probing protocol to maintain consistency and to be able to undergo parallel testing and optimisation with the bespoke PATH™ *plus* Protein Microarray Slide (Gentel Biosciences, US) substrate array results in order to optimise probe protein concentrations to minimise background, minimise sample usage and increase resolution.

2.2.13.3. Array Scanning

A GenePix® 4300A array reader (Molecular Devices) with associated GenePixPro 7 software (Molecular Devices) was used to image both Protoarrays® (Invitrogen, US) and bespoke arrays on PATH™ *plus* Protein Microarray Slide (Gentel Biosciences, US) and Silver Quant® microarray slide (Intuitive Biosciences) substrates.

Arrays were scanned following the GenePix® 4300A array reader manual combined with the Protoarray® Human Protein Microarray short protocol manual. Resolution settings of either 5-10nm were used. Single colour images were imaged as using Alexa Fluor® 647. Files were saved and exported as JPEG and TIFF files.

2.2.13.4. Array data acquisition and analysis

Software for array data acquisition and analysis included the Invitrogen ProtoArray® Prospector Imager and Prospector. Prospector Imager was used to align the GAL files with the database of which proteins are arrayed in which spot, and Prospector was used to statistically analyse the probability of the positive interaction between protein of interest and arrayed protein on ProtoArray® library.

Array data acquisition and analysis was carried out according to the following instruction manuals.

- The ProtoArray® Human Protein Microarray Protein-Protein Interaction short protocol.
- ProtoArray® Prospector Imager v4.0 user manual.
- ProtoArray® Prospector v5.2 User Guide.

2.2.14. Molecular Biology

2.2.14.1. Sub-cloning tagged VHR for mammalian expression system and immunoprecipitation experiments

Plasmids were digested with tags and VHR plasmid with BamH1 and Xho1 restriction enzyme sites. Next plasmids were ligated and transformed. Overnight *E. coli* growths of pcDNA 3.1 N-terminal FLAG and pGEX VHR were grown. A FLAG tag was used as a smaller tag than GST so as to reduce obstruction of epitopes, domains, or alter function of fusion protein. A Miniprep kit (Promega, UK) was used to extract plasmid DNA using the standard kit and instructions (<https://www.promega.co.uk/~media/files/resources/protocols/technical%20bulletins/101/pureyield%20plasmid%20miniprep%20system%20protocol.pdf>).

2.2.14.2. Digestion

Plasmid DNA was digested by BamH1 and Xho1 using the New England Biolabs restriction enzyme protocol (<https://www.neb.com/protocols/2014/05/07/double-digest-protocol-with-standard-restriction-enzymes>). The digestion mix of BamH1-HF (1 µL), Xho1 (1 µL), 10X Cutsmarter buffer (5 µL), plasmid DNA (1 µg) in distilled H₂O (50 µL) was incubated for 10 minutes at 37°C in a water bath.

The digested DNA was then run on an agarose gel to separate digested plasmid sections as well as to validate a successful digestion. The agarose gel was run as a 1% agarose gel with TBE buffer (Tris-borate-EDTA) (Tris Base 890mM, Boric acid 890mM, EDTA 20mM, pH 8.3). To stain the DNA in the agarose gel, Sybersafe was used rather than Ethidium Bromide to reduce risk and danger of the experiment.

Bands were cut out using a gel extraction kit (Thermo, US) for subsequent purification of the DNA.

2.2.14.3. Ligation

Ligation was performed using 10ng of vector plasmid (pcDNA 3.1) as well as 60ng insert (VHR that was previously in pGEX). The protocol was for New England Biolabs T4 DNA ligase, T4 DNA ligase. The ligation reaction was left at room temperature for 4hr.

2.2.14.4. Transformation

Transformation was performed with 5µl of ligation reaction with 50µl of competent cells. The transformed DNA was checked for correctness via gene sequencing (Eurofins, UK) and then a Maxiprep (Promega, UK) was performed to produce the yields of DNA required.

2.2.14.5. Cell culture

2.2.14.5.1. Culturing HCT 116 cells for transfection and co-immunoprecipitation

H. sapiens colon carcinoma HCT 116 cell line derivative was used for *in vivo* study (C. Lee et al., 2004; Mendes-Pereira et al., 2009). This cell line was used by our collaborators across the Proxomics Project and was gifted by the Professor David Klug and The Molecular Dynamics Group from Imperial College London. The gifted HCT 116 cells were at passage 10 on receipt.

Standard aseptic technique was used to handle cells. Cells were handled in an aseptic and sterile flow hood and incubated under standard temperature, O₂ and CO₂. Cells were grown in Dulbecco's Modified Eagles Medium (DMEM) (Life Technologies, UK) supplemented with 10% Fetal Bovine Serum (FBS) (Life Technologies, UK) and 1% penicillin-streptomycin (Life Technologies, UK) antibiotics. Cells were grown in an incubator, in flasks (Life Technologies, UK) and passaged and split prior to confluence.

2.2.14.5.2. Cell passaging

Cells were washed with sterile PBS prior to passaging, splitting and changes of media. Medium was incubated to 37°C prior to contact with cells. Numbers of passages were counted for the information of the laboratory.

Media from cells was removed, cells washed with PBS. PBS was removed and then 0.25% trypsin EDTA (Gibco, UK) was added, at 1-3mls for 10min at RT. After cells were checked for visual detaching from flask surface 5ml of DMEM 10% FBS medium was added to the cells. Cells in medium were split between canted neck pyrogenic flasks (Corning, US) in appropriate quantities. Additional cells were safely disposed of. New medium was added to fully cover the adherent cells in the flask.

2.2.14.5.3. Adherent cell transfection

Adherent cells were transfected by re-plating cells 24hr prior to transfection in DMEM supplemented with 10% FBS after plating at 50-70% confluence. pcDNA 3.1 containing FLAG-tagged VHR was added to 1.5ml of Opti-MEM® (Life Technologies, UK) at varying concentrations (35µg, 52.5 µg, 70µg). Diluted lipofectamine 2000 (Life Technologies, USA) reagent was added to 1.5ml of Opti-MEM® to create

differing concentrations (112.5µl, 168µl, 225µl). For each transfection 9mls of Opti-MEM® was added as per manufacturers instructions to tube containing both lipofectamine and DNA, after separate incubation as per lipofectamine manufacturer standard protocol. The lipofectamine, DNA, Opti-MEM® transfection mix was incubated for 30min at RT. DMEM medium with FBS was removed from the cells to be transfected and DMEM minus serum was added ensuring cells were covered before adding the contents of the lipofectamine, DNA, Opti-MEM® transfection mix. After 5hr transfection mix and medium was replaced with DMEM medium supplemented with 10% FBS.

2.2.14.5.4. Cell harvesting

Cells were harvested for lysis and downstream experimentation and analysis, by removing the media, washing with refrigerated PBS, then applying NP-40 lysis buffer consisting of NP40 (Life Technologies, USA) 1%, NaCl 150mM, Tris-Cl 50mM, pH 8.0. Flasks with transfected cells on ice were incubated with NP40 lysis buffer for 20min. Cells were collected and then centrifuged at 16,000G at 4⁰C for 10mins. After centrifugation, supernatant was removed and transferred to new centrifuge tubes.

2.2.15. Co-immunoprecipitation

Dynabeads® Protein G (Life Technologies AS, Oslo) were resuspended in a vial and mixed via a vortex shaker for ~30sec. Dynabeads® (50µl) were added to centrifuge vials per sample including replicates. The centrifuge tubes containing Dynabeads® were placed on a rack with a magnet at the bottom (Millipore, UK) to separate the Dynabeads® from the Dynabead® solution. The Dynabead solution was removed leaving the Dynabeads®. The Dynabeads were then pre-equilibrated via a series of

washes (x4) with PBS supplemented with 0.02% Tween. Next the antibody (FLAG® M2 mouse monoclonal primary antibody DYKDDDK tag (Sigma-Aldrich USA) was added at the maximum suggested concentration from the Dynabead® standard protocol to PBS supplemented with 0.02% Tween. The antibody in solution was added to the Dynabeads and incubated with rotational shaking at RT for 10min. After incubation of antibody with Dynabeads the centrifuge tube containing them was placed on the rack with the magnet to pull down the magnetic Dynabeads with antibody bound and the supernatant was removed. The antibody bound Dynabeads® were resuspended in 200µl PBS supplemented with 0.02% Tween and washed gently with pipetting. To immunoprecipitate target antigen the centrifuge tube containing the antibody bound Dynabeads® was placed upon the rack with magnetic pull down, supernatant was removed then lysate from cell culture, adherent cell transfection and cell harvesting was added to the centrifuge tube and gently resuspended. The lysate, with the antibody bound Dynabeads® was incubated with rotation ON in a cold room. After ON incubation the antibody bound Dynabeads® with lysate was added to the rack with the magnetic bottom and the supernatant was removed and transferred to separate centrifuge tubes for subsequent analysis. The Dynabeads® with antibody and bound material from lysate was washed with 200µl of PBS and then supernatant was removed whilst on magnetic rack. 100µl of PBS was added to the sample and transferred to new centrifuge tubes. To elute the target antigen, the sample tubes on the rack with magnetic bottom, remove supernatant then add 30µl of Laemmli sample buffer per sample to 30µl of sample for SDS page electrophoresis, Coomassie staining, MS and Western blotting. Incubate samples with rotation for 2min, heat samples in heating block for 10min at 70°C, place sample tube on rack with magnetic bottom and then transfer supernatant to a new centrifuge tube before transferring samples minus Dynabeads® to gels.

Crosslinking the antibody to the Dynabeads was performed using a BS³ conjugation buffer (20mM sodium phosphate, 0.15M NaCl, pH 7.9) and BS³ quenching buffer (1M Tris HCl, pH 7.5) and carried out as per the Dynabead standard protocol.

2.2.16. Western Blotting

Western blotting procedure was performed by taking an SDS-PAGE gel that contains protein samples and transferring it to an activated polyvinylidene fluoride membrane that had been soaked in methanol for 15min. Filter papers and sponges were soaked prior to usage in transfer buffer (28.8g glycine, 6.04g TRIS, 200mL methanol, 1.6L H₂O) for 15min. A Western blotting tank and cassette kit was used (BIO RAD). The cassette was constructed as sponge, filter paper, gel, membrane, filter paper, and sponge, making sure that the protein would travel with the electric current onto the membrane. The cassette was submerged in transfer buffer in the Western blotting tank and then 70V were applied for 1hr. After 1hr the membrane was removed, checking that the visible protein ladder marker proteins (Page Ruler™ Plus Protein Ladder, Fermentas) had transferred to the membrane. Next the membrane was incubated with shaking for 2hr at room temperature in TBST with milk powder blocking solution consisting of 8.8g NaCl, 0.2g KCl, 3g TRIS, 500µl Tween-20 (Fisher Scientific, UK), 50g milk powder (Marvel), pH 7.4, final volume of 1L made up with H₂O. Next the primary antibody against the protein of interest was added in a 5% BSA TBST solution (8.8g NaCl, 0.2g KCl, 3g TRIS, 500µL Tween-20). The primary antibody was added at a 1:1000 dilution of the stock. The membrane was incubated with the primary antibody solution for 2hr with shaking. Next the membrane was washed X2 10min with TBST. Next a HRP system secondary antibody (1:1000) against the primary antibody rose in a different animal species was applied in 5%

BSA TBST and incubated for 1hr with shaking. After the membrane was washed for 15min with X2 TBST with shaking.

The detection of protein of interest-primary antibody-secondary antibody-HRP complex was achieved by addition of 5ml of chemiluminescent substrate (super signal west picochemiluminescent substrate, Thermo Scientific). The chemiluminescent substrate was incubated with membrane for 5min. G-box detection hardware and software was used to capture an image (using auto-exposure and visible marker settings) of the chemiluminescence, putting the membrane between copier transparency film (Niceday).

2.2.17. Informatics analysis

2.2.17.1. ExPASy ProtParam

ProtParam (<http://web.expasy.org/protparam/>) was used to predict molecular weight of PTEN, VHR and GST.

2.2.17.2. NCBI BLAST local alignment search tool

Used NCBI portal to search for plasmid sequences versus NCBI protein database (<http://blast.ncbi.nlm.nih.gov/>). Plasmid sequences supplied by Doctor Lok Hang Mak, for additional details including taxonomy of proteins and homology between related mammalian proteins.

2.2.17.3. Protein-protein interaction databases

The following databases were used to assess current openly available data on the protein-protein interactors with the proteins of interest:

PSIQUIC database

(<http://www.ebi.ac.uk/Tools/webservices/psicquic/view/main.xhtml>)

EMBL-EBI IntAct database (<http://www.ebi.ac.uk/intact/>)

STRING database of known and predicted interactions (<http://string-db.org/>)

PIPS database (<http://www.compbio.dundee.ac.uk/www-pips/>),

MINT (<http://mint.bio.uniroma2.it/mint/Welcome.do>)

APID (<http://bioinfow.dep.usal.es/apid/index.htm>)

Reactome (<http://www.reactome.org/ReactomeGWT/entrypoint.html>)

Irefindex (<http://irefindex.uio.no/wiki/iRefIndex>)

Biogrid (<http://thebiogrid.org/>)

SPIKE (<http://www.cs.tau.ac.il/~spike/>)

UniPROT (<http://www.uniprot.org/>)

BIND (<http://bond.unleashedinformatics.com/>)

PANTHER (<http://www.pantherdb.org/>)

Protein-protein interaction databases were searched to determine the amount of previous research already conducted and accessible in public and publicly known pay-for-access databases. These databases contained known and predicted interactors and these lists of proteins were used to compile cross-database lists (Appendix 1, 2.) of protein interactors with which to compare and contrast our protein-protein interaction array work, including Protoarray® Human Protein Microarray library screens. The databases were also useful to determine with which techniques protein-

protein interactors were found by, as some techniques may give technique specific results that may be due to resolving power of technique or technique specific errors.

2.2.17.4. Molecular viewers

2.2.17.4.1. Chimera

Chimera (<http://www.cgl.ucsf.edu/chimera/>) by Pettersen *et al* (2004) was used to visualise the 3D structure from X-ray crystallography data of the proteins of interest. Protein 3D structure data was retrieved from the Protein Data Bank (<http://www.pdb.org/pdb/home/home.do>). This was done in order to make informed predictions about which amino acids and side chains might be important structurally for protein-protein binding, enzymatic regulation and may be easier to modify due to their positioning near the surface of the protein, or the location of other amino acids nearby which may facilitate a reaction.

3D protein structure images could also be used to map any modifications that were predicted by MASCOT software. The data used from the Protein Data Bank was as follows: PTEN structure data, 1D5R (Lee *et al.*, 1999) and VHR structural data, 1VHR (Yuvaniyama., *et al*, 1996).

Preface

The following research details the experimentation to develop a series of methods to correlate detection of specific oxidative modifications with detection of changes in enzymatic activity and protein-protein interaction.

Experiments:

- Transformation, expression and purification of proteins of interest
- Development of oxidation protocols to generate and detect oxidative modifications in PTEN and VHR
- Oxidation with HOCl, sin-1 and tetranitromethane
- Technology transfer and development of activity assay for phosphatase activity
- Analysis of activity versus gel densitometry
- Protocol optimisation to maintain activity in phosphatases during handling and experimentation
- Mass spectrometric analysis (MS/MS) of PTEN and VHR
- Mass spectrometric analysis (Product ion scanning) of proteins of VHR
- Systematic manual and automated semi-quantitative analyses of abundances
- *De novo* sequencing and validation of modifications
- Double digestion of VHR for increased coverage and search for VHR active site cysteine
- *In silico* analysis of modifications versus activity for correlation
- Technology transfer of arraying and array probing
- Analysis of array probing methods for Dynamic Bioarray
- Development of arraying protocols for VHR
- Library array of VHR with Protoarray for identification of potential interactors

- *In silico* and literature analysis of Protoarray potential interactors
- Investigating effect of oxidation of protein-pair interactions via protein-protein arrays
- Generation of VHR construct with appropriate tags for co-immunoprecipitation
- Transfection of cell line with VHR
- Co-immunoprecipitation of VHR with MS identification of potential interactors
- *In silico* analysis of co-immunoprecipitation gel bands to identify potential interactors
- Comparison of Protoarray and co-immunoprecipitation interactors and literature

Outcomes:

- Successfully generating active purified proteins of interest (PTEN and VHR)
- Quantifying the expression yields of protein of interest (PTEN and VHR)
- Successfully assaying phosphatase activity of proteins of interest
- Quantifying the specific activity of proteins of interest
- Successfully assaying proteins after removal of non-reducing buffer
- Successful identification of oxidations in protein of interest (PTEN and VHR)
- Successful identification of oxidations that occur differentially between oxidation concentrations in protein of interest (PTEN and VHR)
- Successful analysis of abundance of oxidative modifications in protein of interest (PTEN and VHR)
- Successfully assaying of proteins onto an array substrate
- Successfully probing library array with VHR to identify potential interactors
- Successfully co-immunoprecipitating potential interactors for VHR
- Experimental skills gaining in mass spectrometry, arraying, array probing, assaying phosphatase activity, oxidation of proteins, digestion of proteins, transformation of cells, expression and purification of proteins

- Technology and knowledge transfer from Imperial College London research partnership
- Technology and knowledge transfer from Dynamic Bioarray industry collaboration

Scientific knowledge that has been developed in this document includes the identification of oxidations in PTEN and VHR in specific residues, due to reaction with specific amounts of oxidants, correlating VHR activity with modifications and discovery of potential VHR interactors via protein-protein array and co-immunoprecipitation

Chapter 3

Oxidation of CX₅R phosphatases

3. Oxidation of CX₅R phosphatases

3.1. Introduction

3.1.1. Investigation of the effects of hypochlorous acid, sin-1 and tetranitromethane

The aims of this investigation include assessing the oxidative PTM signature for single proteins under a variety of treatments, assessing the specificity and differences between the commonly used *in vitro* nitrating agents tetranitromethane and the peroxyxynitrite generator sin-1, and the oxidising and chlorinating agent hypochlorous acid (HOCl). In particular, the aims are to explore whether oxidation, nitration and chlorination occurs on residues previously implicated in other types of signalling and novel residues, and whether, with global functional proteomic analysis, the importance and properties of these oxidants can be advanced by assessing the global effects on a single protein.

The study of HOCl on the function and activity of proteins, protein aggregation and protein fragmentation is important regarding what metabolites may be present in samples after bacterial infection (Thomas, 1979). Bacterial infection is important with regards to mitigating surgery risk, co-morbidities with non-communicable diseases and for communicable disease prevention. HOCl oxidation and chlorination was performed because it is present *in vivo*, generated by activated neutrophils by myeloperoxidase-mediated peroxidation of chloride ions. HOCl production is involved in the immune response to bacterial infection (Albrich et al., 1981; Harrison & Schultz, 1976; Thomas, 1979) and also ischemia-induced inflammation (Panizzi et al., 2009).

Concentrations in particular cellular locations during particular cellular phases and undergoing particular cellular processes are unknown – and so a range of *in vitro* concentrations will be employed so as to potentially cover the range of concentrations that occur *in vivo*.

Peroxynitrite is an oxidising and nitrating agent. Peroxynitrite is involved in multiple states associated with loss of homeostasis and ageing damage including stroke, myocardial infarction, chronic heart failure, diabetes, circulatory shock, chronic inflammatory diseases, cancer, and neurodegenerative disorders (Pacher et al., 2007). Oxidation and nitration were of interest as both are present *in vivo* (Pacher et al., 2007). For our *in vitro* studies proteins were oxidised and nitrated with 3-morpholinosydnonimine (sin-1) a peroxynitrite (ONOO⁻) generator, where peroxynitrite induces oxidative stress in neurons (Wallace et al., 2006) and contributes to the pathogenesis of neuropathological states (Jang et al., 2004). Sin-1 has been used in studies focused on protein tyrosine nitration and thiol oxidation, for example as demonstrated by Daiber *et al* (2013) with immunological and assaying techniques.

Tetranitromethane (TNM) is a non-biological oxidant, which was used as an alternative to sin-1 to generate high levels of nitration in an *in vitro* system. TNM has been demonstrated as a reagent for chemically altering proteins (Wormall, 1930), including for the nitration of tyrosyl residues in proteins to 3-nitrotyrosine (Sokolovsky et al., 1966; Riordan and Vallee, 1972). Sokolovsky describes TNM as a mild and specific nitrating reagent at pH 8, with cysteine being modified at pH 6 rather than tyrosine; its primary uses pertain to its residue specificity and to its acidic mildness for the treatment of enzymatically active proteins sensitive to pH (Roberts and Caserio, 1964). Exploration of the specificity and action of a range of biologically relevant oxidants and agents which may produce modifications that are biologically relevant may have importance for clinical applications involving cell signalling enzymes with cysteine active sites and phosphorylated tyrosine residues.

3.2. Results

3.2.1. Transformation, expression and purification of PTEN-GST and VHR-GST

PTEN-GST and VHR-GST were overexpressed in *E.coli* in pGEX-4T1 plasmid vectors (See 2.2.4. Expression of PTEN and VHR) and affinity purified using a GST and Glutathione Sepharose® 4B system via a gravity column. Samples and flow through from the purification procedure were run on SDS-PAGE (Figures 12,13.) and stained with Coomassie stain to assess efficiency of purification, purity of protein and to assess comparative yields and to detect stages of yield loss from samples taken over course of purification. Initial assessment of the purity of the protein was performed via manual inspection of the gel lanes for additional bands stained with Coomassie dye. Figure 12.c and Figure 13.c show an MS analysis of proteins used for further experiments, which demonstrates that protein of interest (PTEN, VHR) and the GST fusion tag are most abundant and that there are some contaminants and impurities from laboratory processing during in-gel digestion, MS instrumentation, and *E. coli* proteins with low Mascot scores from the MS analysis software Mascot.

The transformation, expression and purification protocol for PTEN-GST and VHR-GST was transferred from Doctor Lok Hang Mak, Imperial College London.

Bradford assays were performed on the purified protein to determine expression yields. Bradford assays were also performed post-filtration and prior to an OMFP assay of enzymatic function (See 3.3. Assaying phosphatase activity of CX₅R phosphatases).

The protein yields as determined by Bradford assay corresponding to the PTEN-GST expression in Figure 12 are 2.89mg per litre of culture, and 8.69mg total yield.

The yield corresponding to the VHR-GST expression in Figure 13 are 7.7mg per litre of culture and 15.4mg total yield. These represent exemplar yields.

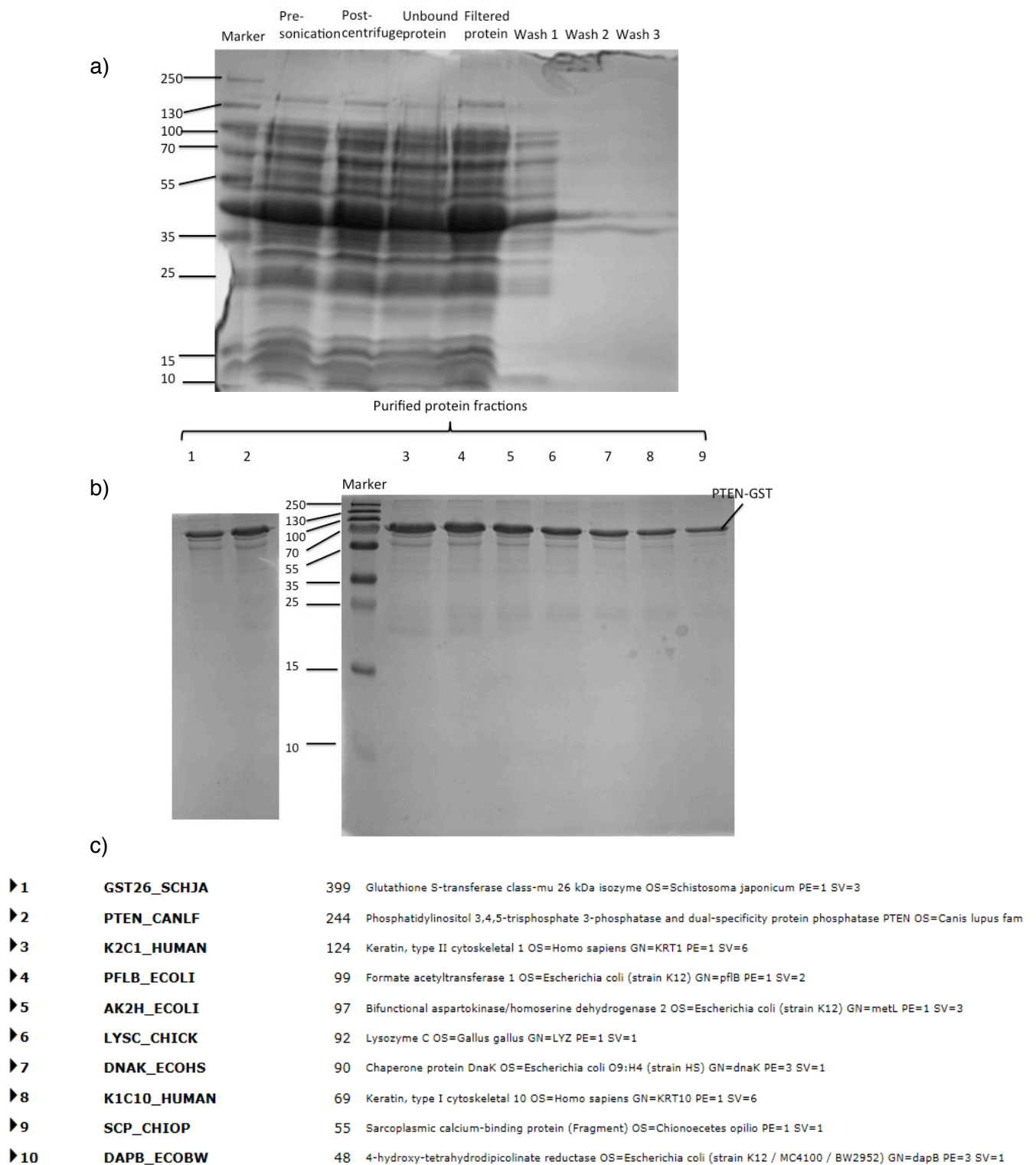


Figure 12. SDS-PAGE and Coomassie staining analysis of PTEN-GST expression and purification protocol and purified fractions

Purified protein fraction numbering indicates which 1ml fraction protein was obtained from. Marker bands have been labelled with masses of proteins in KDa. PTEN-GST was eluted from the column in 1ml fractions and run on an SDS-PAGE gel. a) Supernatants from procedure including from pre-sonication, pre-centrifugation, unbound protein and washes Filtered protein = Glutathione Sepharose 4B column filtered protein. Unbound protein = protein not bound to Glutathione Sepharose 4B column b) Purified protein fractions.. c) Mass spectrometric analysis and Mascot Search of final purified fraction. Numeric = Mascot Score for protein. OS= Organism, GN= Gene Name. (n=4)

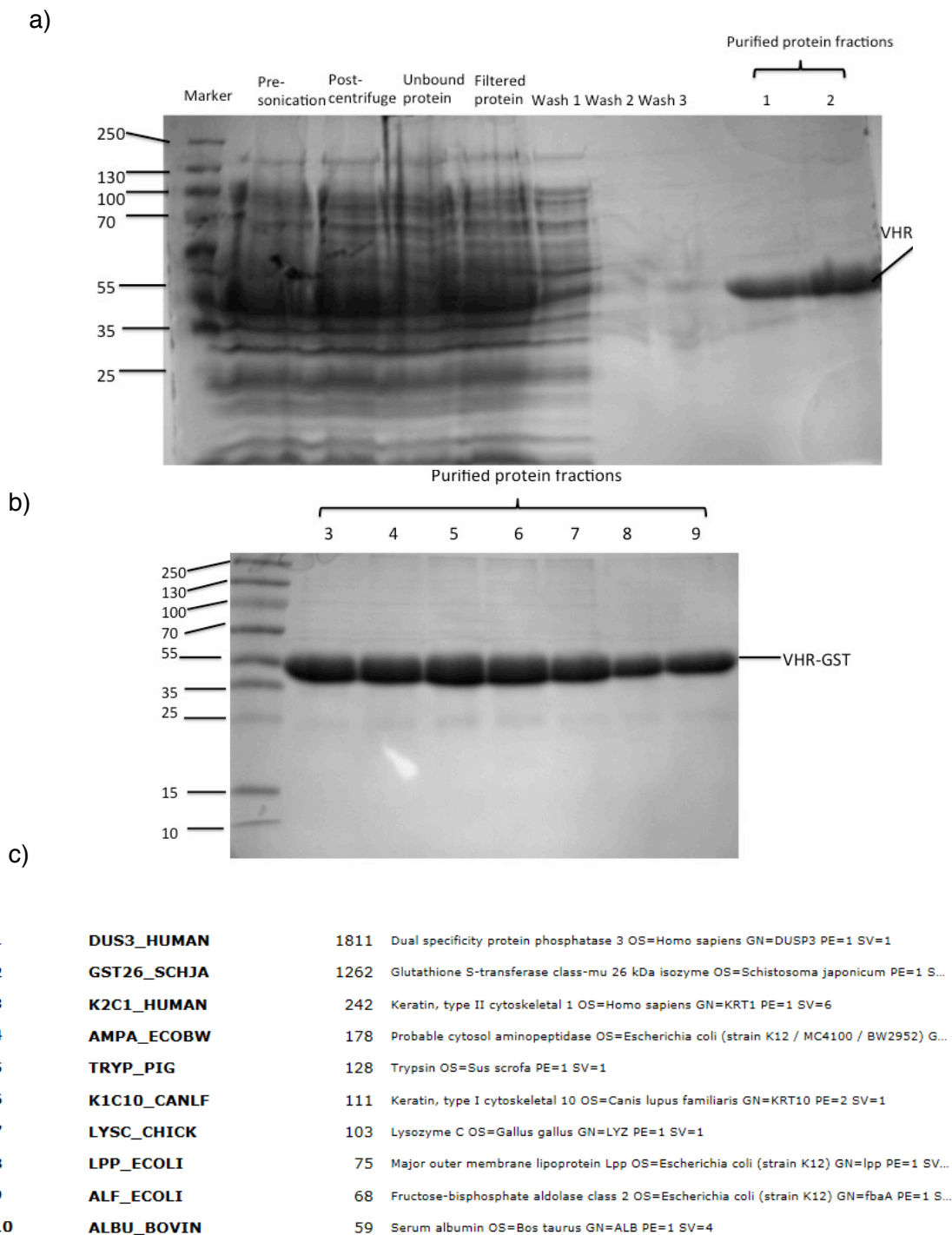


Figure 13. SDS-PAGE and Coomassie staining analysis of VHR-GST expression and purification protocol and purified fractions

VHR-GST was eluted from the column in 1ml fractions and ran on a gel via SDS-PAGE. Purified protein fraction numbering indicates which 1ml fraction protein was obtained from. Marker bands have been labelled with masses of proteins in KDa. Gel lane labels indicate when samples were taken in the purification processes. a) Supernatants from procedure including from pre-sonication, pre-centrifugation, unbound protein and washes and first purified protein fractions b) Additional purified protein fractions. Filtered protein = Glutathione Sepharose 4B column filtered protein. Unbound protein = protein not bound to Glutathione Sepharose 4B column c) Mass spectrometric analysis and Mascot Search of final purified fraction. Numeric = Mascot Score for protein. OS= Organism, GN= Gene Name. (n=4).

3.3. Assaying phosphatase activity of CX₅R phosphatases

3.3.1. Assessment of gel filtration and retainment of PTEN-GST and VHR-GST activity

An assaying for enzymatic phosphatase specific activity of PTEN and VHR was performed. A standard Bradford assay was used to determine protein concentration performed post-filtration, with the assumption that all the protein in the solutions was the protein of interest, an experiment to assess effect of gel filtration on enzyme phosphatase activity, and a measurement of enzymatic activity using the OMFP assay was performed prior to and post-buffer exchange, to compare between batches and between experiments carried out both at Aston University and our collaborators, the group of Dr Rudiger Woscholski at Imperial College London. The OMFP phosphatase assay system was used. An OMF standard curve was experimentally obtained for the calculation of specific activity (Figure 14., Table 2.), measurements of the activity of expression preparations (Figure 15., Figure 16.) and measurement of the activity of expression preparations prior to oxidative treatments and after filtration to remove reducing agents (Figure 17., Figure 18).

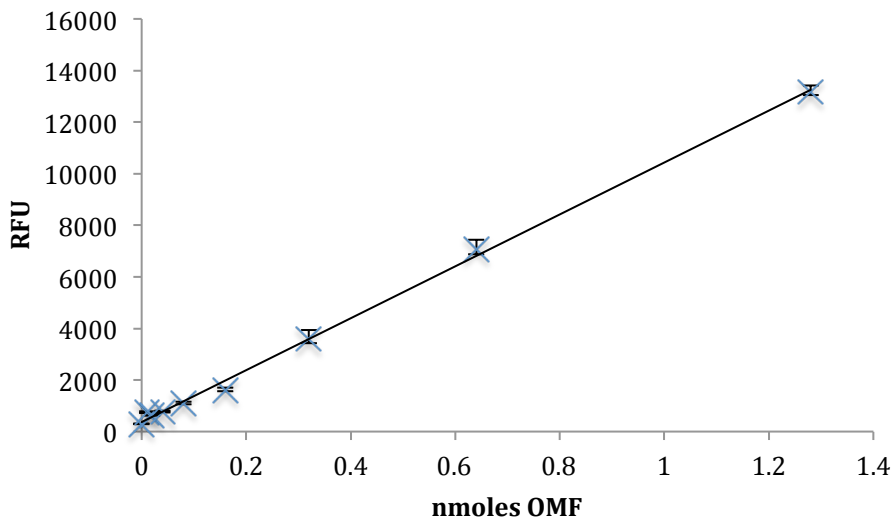


Figure 14. Representative OMF calibration curve
 r^2 values and formula as below

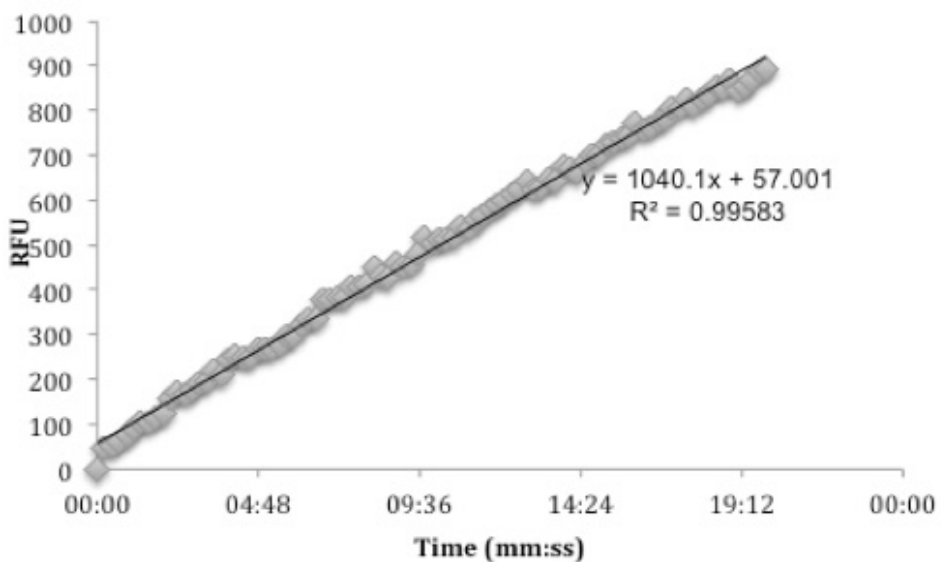


Figure 15. OMF assay for phosphatase activity of expressed and purified PTEN-GST in reducing conditions RFU displayed is mean rise in RFU of the experimental control minus the mean RFU in the no-enzyme negative control, over 20min, normalised to start at zero. Specific activity of PTEN-GST = 0.65 nMoles/min/mg protein, and 10.59 μ g PTEN-GST used per well for experiment shown (n=3).

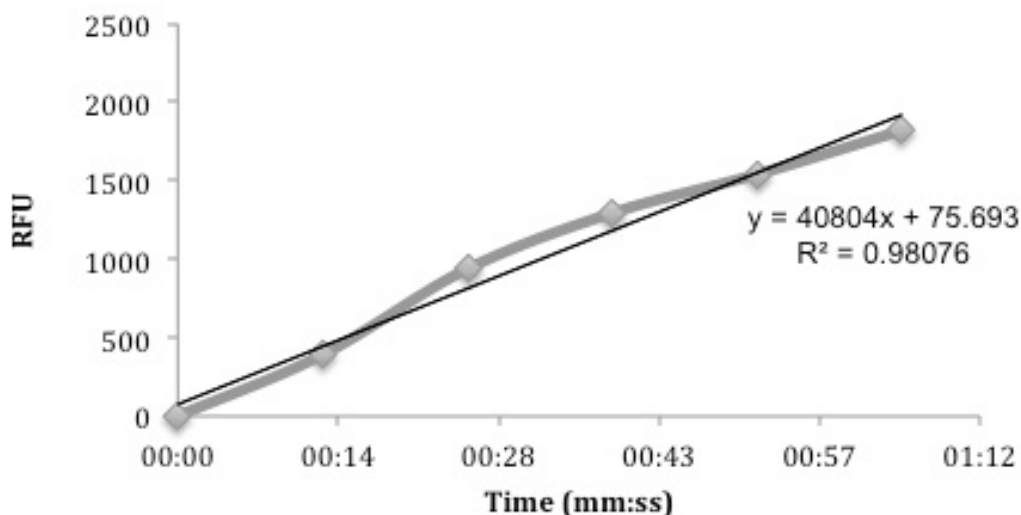


Figure 16. OMFP assay for phosphatase activity of expressed and purified VHR-GST in reducing conditions RFU displayed is mean rise in RFU of the experimental control minus the mean RFU in the no-enzyme negative control, over 1min, normalised to start at zero. Specific activity of VHR-GST = 298.46 nMoles/min/mg protein, and 0.0425µg PTEN-GST used per well for experiment shown (n=3).

Protein	Specific activity
PTEN-GST	0.65nMoles/min/mg protein
VHR-GST	298.46 nMoles/min/mg protein

Table 2. Specific activities of expressed and purified protein in non-reducing buffer.

3.3.2. Tests to assess the effect of different methods for buffer exchange on enzymatic activity as assayed by the OMFP activity assay

3.3.2.2. Column filtration

PTEN-GST and VHR-GST were stored with DTT (See 2.2.6. Purification of PTEN and VHR) and for subsequent oxidation studies with molar ratios of protein to oxidant, reducing agents needed to be removed prior to studies via gel filtration. A Bradford assay was performed on samples prior to filtration, to determine the volume of sample to use for experimentation, and post-filtration to determine losses during the filtration and to determine the amounts of oxidant to use for oxidation studies. Protein used for OMFP assay was assayed via Bradford assay post-filtration, to ensure that the difference in activity is not due to a loss of protein during gel filtration. Size exclusion gravity column filtration was tested for the effect of column gel filtration on PTEN-GST and VHR-GST activity as assayed by the OMFP assay. VHR-GST was column filtered and retained activity (Figure 17.), column filtration inactivated PTEN-GST (Figure 18.). Column filtration would be used on both proteins for comparable treatment and taken forward.

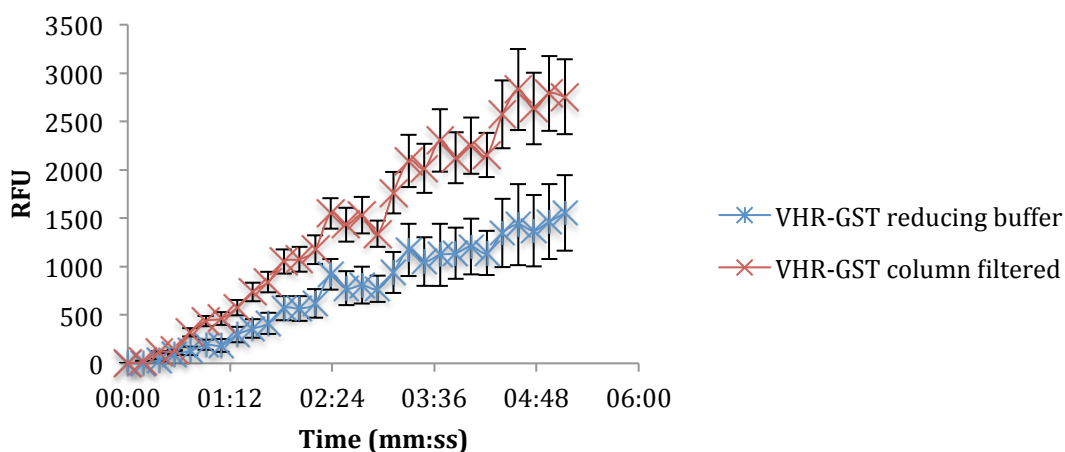


Figure 17. OMFP assay for phosphatase activity of VHR-GST after NAP-5 column filtration RFU displayed is mean rise in RFU of the experimental control minus the mean RFU in the in the no-enzyme negative control, over 10min, normalised to start at zero. Specific activity of VHR-GST in reducing buffer = 1371.55 nMole/min/mg protein. Specific activity of VHR-GST after column filtration of reducing agents = 1338.48 nMoles/min/mg protein. Error bars represent standard deviation (n=3).

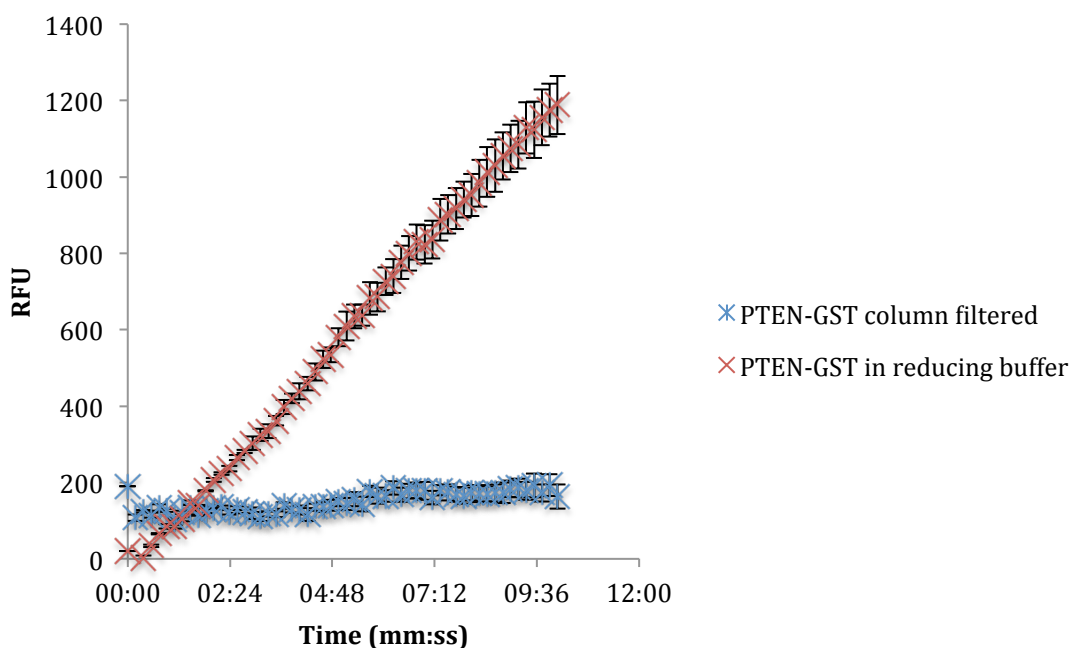


Figure 18. OMFP assay for phosphatase activity of PTEN-GST after NAP-5 column filtration RFU displayed is mean rise in RFU of the experimental control minus the mean RFU in the no-enzyme negative control, over 10, normalised to start at zero. Specific activity of PTEN-GST in reducing buffer = 1.15 nMole/min/mg protein. Error bars represent standard deviation (n = 3).

3.4. Oxidation of PTEN-GST and VHR-GST

3.4.1. Oxidation of PTEN-GST with HOCl and sin-1 generated peroxynitrite

Buffer exchanged PTEN-GST was oxidised with a range of molar ratios of oxidants HOCl and sin-1 with downstream assaying via the OMFP assay, and analysis by SDS-PAGE (Figure 19.). A range of oxidant molarities were used to detect oxidations that only occur at particular molar ratios and in order to optimise PTEN oxidation treatment for the repeatable generation of specific modifications and specific abundances of modifications. Ranges of oxidant molarities used may cover and exceed *in vivo* cellular molar ratios and concentration, which are currently unknown. Coomassie staining was performed on the gel. The bands corresponding to PTEN-GST were subsequently excised for in-gel trypsin digestion and MS analysis.

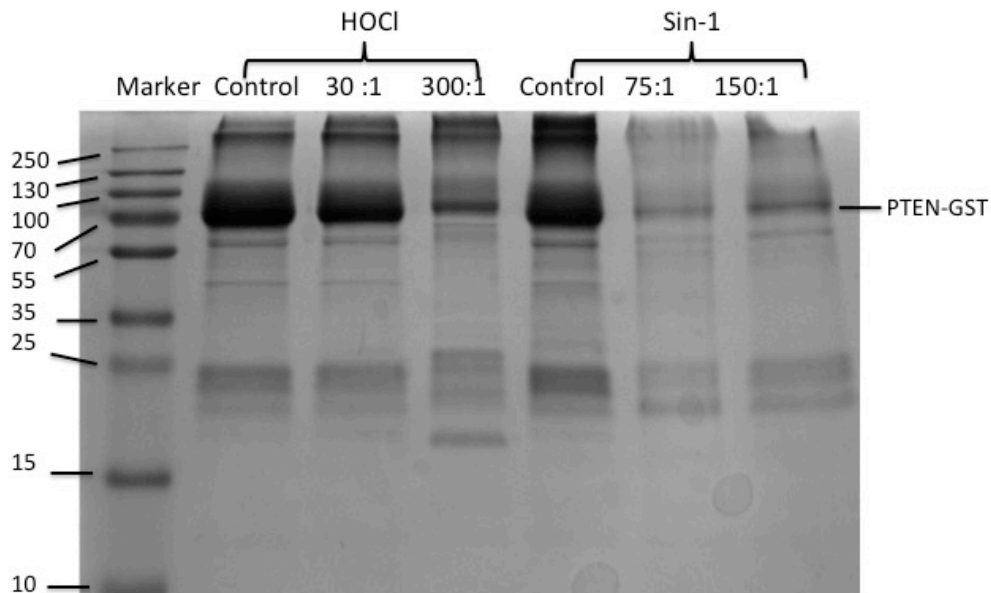


Figure 19. SDS-PAGE and Coomassie staining of PTEN-GST oxidised using 75:1 and 150:1 molar ratio sin-1 and 30:1 and 300:1 molar ratio HOCl

PTEN-GST was oxidised with HOCl at 30:1 and 300:1 molar ratio concentration to PTEN-GST for 1hr at room temperature. PTEN-GST was oxidised with SIN-1 at 75:1 and 150:1 molar concentration to PTEN-GST for 1hr at 37⁰C. The PTEN-GST band that has excised for in-gel digestion and identified as PTEN-GST by mass spectrometry has been indicated with an arrow. The masses of the bands in the protein marker lane have been indicated with arrows. Controls were non-treated PTEN-GST that were incubated at the same conditions as oxidised samples. Representative gel. Note high protein loading amounts necessary for sequence coverage upon high levels of treatment given loss of protein from bands.

The post-oxidation SDS-PAGE and Coomassie staining (Figure 19.) shows that bands corresponding to native protein change in intensity upon oxidation in comparison to control. The relative intensity of higher molecular weight bands can be seen near the intersection of the stacking and running gels (Figure 19). An additional low-molecular weight band can also be seen in the HOCl 300:1 sample in addition to variation in the levels of other low-molecular weight bands in high concentrations of treatment in comparison to the native protein control. Multiple additional bands are present in both the control and oxidised sample. Samples loading amounts in Figure 19. were optimised over a series of prior experiments (n=4) so bands could be observed in the most concentrated treatment sample, and detection of protein in all samples via MS, in addition to being optimised for sequence coverage and identification of oxidations with significant ion scores across the majority of samples

and treatments. Low molecular and high molecular weight bands were excised from the gel and MS analysis was also performed on these, including assessment of modifications present. At the time performed this experiment quantitative analysis via Progenesis software was not yet available.

3.4.2. Tandem mass spectrometry of PTEN

Tandem mass spectrometry (MS/MS) was performed in triplicate to assess which molar ratios of which oxidants oxidise the proteins of interest, which types of modifications specific oxidants cause, what the abundances of the modifications and relative abundances are and to assess which residues are most susceptible to oxidation. Also to be included in the assessment of protein oxidation via TOF MS/MS were those oxidations were sufficient to cause functional changes in the activity and interactions of the protein of interest, which modifications are correlated with changes in activity and what the different modification patterns between proteins, oxidants and oxidation ratios were. MS/MS was also used for the detection of specific instances of modifications that are correlated with changes of function so that these can be identified for later stage targeted scan MS techniques application.

Peptides from PTEN-GST were separated using reverse-phase liquid chromatography, ionised via electrospray ionisation before tandem MS. A representative total ion chromatogram (TIC) was obtained for each MS run (Figure 20.), displaying the gradient of the HPLC run and separation of peptides that was used for the standard TOF MS/MS runs and plotted as intensity versus time. The TIC was then visualised on Analyst or Peakview software prior to *in silico* analysis and manual validation to assess that the MS/MS run had detected the peptides from each run. Figure 20 shows a representative TIC intensity and representative exemplarily of peptide detection coverage within each run.

Mascot software analysis output was searching along with Peakview software search of raw data informed by Mascot output of TOF MS/MS of oxidant treated protein. Priority searches include searches for di- and tri-oxidation of active site nucleophilic and regulatory back-door cysteines of PTPs and tyrosine modifications including nitration which has been suggested may mimic phosphotyrosine (Mallozzi et al., 2001). The following additional modifications were also searched for: Methionine oxidation, methionine dioxidation, tryptophan oxidation, histidine oxidation, proline oxidation, lysine oxidation. In addition, error tolerant searches were performed, which predicts all modifications that match the query database (see Methods).

3.4.3. Mascot search of PTEN modification

Individual amino acid modifications predicted by Mascot analysis were confirmed in the following ways i) Experimental repeats from same oxidation concentration and range of concentrations of oxidant ii) Analysis of the raw data by the generation of extracted ion chromatographs for individual peptide mass-to-charge ratios for the modified and unmodified peptides in the control and experimental samples, regardless of whether they of their appearance in all Mascot searches.

Variable modifications: Dioxidation (C),Dioxidation (M),Dioxidation (Y),Trioxidation (C)
Cleavage by Trypsin: cuts C-term side of KR unless next residue is P
Sequence Coverage: 70%

Matched peptides shown in **Red**

```
1  MTAIIKEIVS RNKRRYQEDG FDLDLIYIYP NIIAMGFPPE RLEGVYRNNI
51  DDVVRFLDSK HKNHYKIYNL CAERHYDTAK FNCRVAQYPF EDHNPPQLEL
101 IKPFCELDLQ WLSEDDNHVA AIHCKAGKGR TGMICAYLL HRGKFLKAQE
151 ALDFYGEVRT RDKKGVITIPS QRRYVYYYSY LLKNHLDYRP VALLEFKMMF
201 ETIPMFSGGT CNPQFWCQL KVKIYSSNSG PTRREDKFMV FEPQPLPVC
251 GDIRVEFFHK QNKMLKKDKM FHFWMNTFFI PGPEETSEKV ENGSLCDQEI
301 DSICSIERAD NDKEYLVLT TLKNDLDFKANK DKANRYFSPN FKVKLYFTKT
351 VEEPSNPEAS SSTSVIPDVS DNEPDHYRYS DTTSDPENE PFDEDQHTQI
401  TKV
```

Figure 21. Representative sequence coverage analysis of PTEN after trypsin in-gel digestion. Sequence coverage for PTEN-GST. Mascot search results output including variable modifications searched for and enzyme proteins were cleaved with. Detected amino acids are highlighted in red and black amino acids were not detected.

The sequence coverage percentage for PTEN in Figure 21. is 70%, which represents exemplar sequence coverage for PTEN covered by assigned peptide matches (Exemplar sequence coverage in Table 3). Sequence coverage ranged from 10-70%, where 10% sequence coverage was upon treatment of PTEN-GST with 1:300 PTEN-HOCl molar ratio HOCl, average sequence coverage for unmodified PTEN-GST in triplicate was 49%. There are three large sections starting at amino acids 12, 85 and 350 of PTEN that are not detected with the amount of protein sampled, trypsin digestion and MS/MS TOF setup. The uncovered sequence sections contained residues known to be functional including the Cys124 the nucleophilic cysteine.

Treatment (Protein: Treatment)	Sequence coverage (%)
Untreated	48
Sin-1 1:75	55
Sin-1 1:150	47
HOCl 1:25	29
HOCl 1:100	44
HOCl 1:150	35
HOCl 1:300	10

Table 3. Exemplar sequence coverage versus treatment for PTEN

Sequence coverage for PTEN with the SCIEX 5600 LC-MS system and digestion protocol used, following treatment with sin-1 showed an increase at sin-1 1:75 molar ratio and a small decrease in sequence coverage at sin-1 1:150 (Table 3.). PTEN sequence coverage was reduced further on HOCl treatment, which at HOCl 1:300 reduced sequence coverage to 1/5 (Table 3.).

Mascot searching identified a number of predicted peptide modifications in PTEN (Figure 22a.). 'Start – End' corresponds to the N-terminal and C-terminal of the protein peptide sequence. The mass-to-charge ratio for the monoisotopic mass of the ion observed experimentally is displayed as 'Observed'. The mass of the peptide calculated from the observed m/z is displayed as 'Mr(expt)'. The theoretical mass of the peptide calculated based on its sequence is displayed as 'Mr(calc)'. The difference between the theoretical (Mr(calc)) and experimental (Mr(expt)) masses is expressed as 'Delta'. The number of missed enzymatic cleavage sites is represented as 'Miss'.

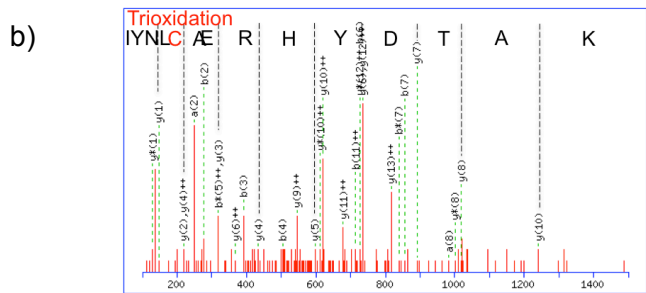
The Mascot 'ion score' for the likelihood that Mascot has correctly identified the peptide in question is displayed next to the peptide sequence in question and the modifications associated with that sequence. The Mascot ion score is calculated by the Mascot search engine for each peptide that is matched from the MS/MS list of peaks. The Mascot ion score is based on the probability that ion fragmentation matches are non-random. If the Mascot Ion Score is equal or greater than the Mascot Significance Level calculated for the search, this match is considered to be statistically non-random and statistically significant to 95% confidence.

Mascot displayed the MS/MS spectrum (Figure 22.b) including the masses that it has matched to ion fragments present in the experimental data (Figure 22.c table). MS/MS spectra are used for validation of Mascot predictions by ensuring that the modification predicted are well sequenced and covered by y and b ion series runs that correspond to peptide fragmentation patterns (Figure 22.c). Mascot ion tables (e.g. Figure 22.c) were used to manually assess the Mascot assignments for both unmodified and modified peptides; all modifications were taken forward to raw data analysis and XIC via Peakview.

Multiple modifications were predicted by Mascot upon sin-1 and HOCl treatment of PTEN including cysteine dioxidation and trioxidation, tyrosine oxidation, nitration and chlorination and methionine oxidation (see Tables 3, 4 and Appendices 8, 9.). Only modifications that were validated via manual assessment of the MS/MS spectra are shown and were chosen for extracted ion chromatogram generation. $n \Rightarrow 1000$ modifications were found and in silico validated via Mascot, Peakview XIC, and Peakview *de novo* sequencing and $n \Rightarrow 10000$ peptides were assessed via Mascot and Peakview XIC; for appropriate datasets where data was suitable for Progenesis software, Progenesis analysis of these modifications and peptides was also performed.

a)

Start - End	Observed	Mr (expt)	Mr (calc)	Delta	Miss Sequence		
67 - 74	519.8916	1037.7686	1038.4804	-0.7117	0	K.IYNLCAER.H	(Ions score 11)
67 - 74	519.8934	1037.7722	1038.4804	-0.7081	0	K.IYNLCAER.H	(Ions score 18)
67 - 74	520.3917	1038.7688	1038.4804	0.2885	0	K.IYNLCAER.H	(Ions score 20)
67 - 74	520.3927	1038.7708	1038.4804	0.2905	0	K.IYNLCAER.H	(Ions score 22)
67 - 74	520.3934	1038.7722	1038.4804	0.2919	0	K.IYNLCAER.H	(Ions score 14)
67 - 74	520.3946	1038.7746	1038.4804	0.2943	0	K.IYNLCAER.H	(Ions score 13)
67 - 74	520.3973	1038.7800	1038.4804	0.2997	0	K.IYNLCAER.H	(Ions score 20)
67 - 74	520.4524	1038.8902	1038.4804	0.4099	0	K.IYNLCAER.H	(Ions score 11)
67 - 74	520.4659	1038.9172	1038.4804	0.4369	0	K.IYNLCAER.H	(Ions score 25)
67 - 74	520.4659	1038.9172	1038.4804	0.4369	0	K.IYNLCAER.H	(Ions score 19)
67 - 74	520.4680	1038.9214	1038.4804	0.4411	0	K.IYNLCAER.H	(Ions score 10)
67 - 80	577.0903	1728.2491	1727.7937	0.4554	1	K.IYNLCAERHYDTAK.F	Dioxidation (C) (Ions score 20)
67 - 80	582.4235	1744.2487	1743.7886	0.4601	1	K.IYNLCAERHYDTAK.F	Trioxidation (C) (Ions score 58)
67 - 80	585.4297	1753.2673	1753.8093	-0.5421	1	K.IYNLCAERHYDTAK.F	(Ions score 38)
67 - 80	585.4358	1753.2856	1753.8093	-0.5238	1	K.IYNLCAERHYDTAK.F	(Ions score 34)
67 - 80	877.6564	1753.2982	1753.8093	-0.5111	1	K.IYNLCAERHYDTAK.F	(Ions score 84)
67 - 80	877.6578	1753.3010	1753.8093	-0.5083	1	K.IYNLCAERHYDTAK.F	(Ions score 65)
67 - 80	877.6587	1753.3028	1753.8093	-0.5065	1	K.IYNLCAERHYDTAK.F	(Ions score 75)
67 - 80	877.6591	1753.3036	1753.8093	-0.5057	1	K.IYNLCAERHYDTAK.F	(Ions score 74)
67 - 80	877.6598	1753.3050	1753.8093	-0.5043	1	K.IYNLCAERHYDTAK.F	(Ions score 76)
67 - 80	585.7695	1754.2867	1753.8093	0.4773	1	K.IYNLCAERHYDTAK.F	(Ions score 18)



Monoisotopic mass of neutral peptide Mr(calc): 1743.7886
 Fixed modifications: Carbboxymethyl (C) (apply to specified residues or termini only)
 Variable modifications:
 C5 : Trioxidation (C)
 Ions Score: 36 Expect: 0.0046
 Matches : 30/148 fragment ions using 79 most intense peaks (help)

c)

#	a	a ⁺⁺	a [*]	a ⁺⁺⁺	b	b ⁺⁺	b [*]	b ⁺⁺⁺	Seq.	y	y ⁺⁺	y [*]	y ⁺⁺⁺	#
1	86.0964	43.5519			114.0913	57.5493			I					14
2	249.1598	125.0835			277.1547	139.0810			Y	1631.7118	816.3596	1614.6853	807.8463	13
3	363.2027	182.1050	346.1761	173.5917	391.1976	196.1024	374.1710	187.5892	N	1468.6485	734.8279	1451.6220	726.3146	12
4	476.2867	238.6470	459.2602	230.1337	504.2817	252.6445	487.2551	244.1312	L	1354.6056	677.8064	1337.5790	669.2932	11
5	627.2807	314.1440	610.2541	305.6307	655.2756	328.1414	638.2490	319.6282	C	1241.5215	621.2644	1224.4950	612.7511	10
6	698.3178	349.6625	681.2912	341.1493	726.3127	363.6600	709.2862	355.1467	A	1090.5276	545.7674	1073.5011	537.2542	9
7	827.3604	414.1838	810.3338	405.6706	855.3553	428.1813	838.3287	419.6680	E	1019.4905	510.2489	1002.4639	501.7356	8
8	983.4615	492.2344	966.4349	483.7211	1011.4564	506.2318	994.4299	497.7186	R	890.4479	445.7276	873.4213	437.2143	7
9	1120.5204	560.7638	1103.4939	552.2506	1148.5153	574.7613	1131.4888	566.2480	H	734.3468	367.6770	717.3202	359.1638	6
10	1283.5837	642.2955	1266.5572	633.7822	1311.5786	656.2930	1294.5521	647.7797	Y	597.2879	299.1476	580.2613	290.6343	5
11	1398.6107	699.8090	1381.5841	691.2957	1426.6056	713.8064	1409.5790	705.2932	D	434.2245	217.6159	417.1980	209.1026	4
12	1499.6584	750.3328	1482.6318	741.8195	1527.6533	764.3303	1510.6267	755.8170	T	319.1976	160.1024	302.1710	151.5892	3
13	1570.6955	785.8514	1553.6689	777.3381	1598.6904	799.8488	1581.6638	791.3356	A	218.1499	109.5786	201.1234	101.0653	2
14									K	147.1128	74.0600	130.0863	65.5468	1

Figure 22. Representative Mascot output for Cys71 modification in sin-1 treated PTEN-GST a) Representative sample output from Mascot search for Cysteine di-, tri-oxidation and carbamidomethylation of PTEN active site regulatory cysteine Cys71 b) Representative MS/MS spectrum and sequencing of Cys71 trioxidation with the amino acids found via manual de novo sequencing added to the spectrum manually c) and ion table. Bold typeface in the ion table indicates non-redundant matches of fragment ions used to generate score. Red typeface in the ion table indicates the highest scoring match to a particular query. n=>1000

Amino acid residue in PTEN	Control	75:1 Sin-1 : PTEN	150:1 Sin-1 : PTEN
Y68			
Y138			
C71			
Y155			
Y46			
M134			
Y225			
M239			
Y336			
Y76			

Table 4. Summary of unique residue modifications predicted by Mascot for sin-1 oxidation found in 1:75 and 1:150 sin-1 oxidation at 37°C for 1 hour
 Grey highlighting indicates residue oxidatively modified in sample. See Appendix 8 for Mascot information regarding peptides.

Mascot search for modified peptides in PTEN following sin-1 oxidation at 1:75 and 1:150 sin-1 oxidation at 37°C for 1 hour identified modifications that occurred in all samples including non-treated control, modifications that occurred at both 1:75 and 1:150 sin-1 molar ratio concentration and modifications that only occurred at the highest level of sin-1 oxidation (see Table 4 and Appendices 8.). The higher the oxidant concentration, the greater the range of different oxidations and nitrations were predicted, including modifications not seen in lower treatments regardless of the decreasing sequence coverage for the protein. As table 4 and appendices 8 show modifications found in the

control were also found in the treated samples. Untreated control samples were run first on MS to avoid any potential cross contamination of modified peptides from treated samples. Variability of occurrence of modifications between treatments was analysed and visualised to detect non-linear and non-exponential patterns in the increased occurrence of modifications, in addition to assessing between-sample comparative presence of the modification. Minimal oxidation is expected in non-treated control, and minimisation of adventitious oxidation was attempted by following protocols that minimise protein contact with oxygen. PTMs in non-treated control will serve as background PTM during quantitative analysis.

Amino acid residue in PTEN	Control	30:1 HOCl : PTEN	300:1 HOCl : PTEN
C71			
M134			
Y138			
Y177			
Y178			
Y180			
M205			
M239			
M270			

Table 5. Summary table of unique residue modifications predicted by Mascot for HOCl oxidations found in 1:30 and 1:300 molar concentration HOCl oxidation at room temperature for 1 hour Grey highlighting indicates residue oxidatively modified in sample. See Appendix 9 for Mascot information regarding peptides.

A Mascot search for modified peptides in PTEN following HOCl oxidation at 1:30 and 1:300 molar concentration at room temperature for 1 hour found that Cys71 oxidative modifications occurred in all samples including non-treated control. Modifications that occurred at both 1:30 and 1:300 molar HOCl concentrations and modifications that occurred in either the higher and lower concentration (see Table 5 and Appendices 9). The HOCl modifications in Table 5 show less linear or exponential increase in identification of modifications by Mascot with increasing treatment molar ratio; where the HOCl treatment molar ratios are different to the sin-1 molar ratios and HOCl band Coomassie staining intensity and sequence coverage were lower.

3.4.4. Extracted Ion Chromatography (XIC) of PTEN modifications induced by SIN-1 and HOCl oxidation

Preliminary studies of protein oxidation abundance were carried out using PTEN. XIC were generated from the data as a validation and assessment step for Mascot, to assess whether ions predicted by Mascot were present. XICs were also used to assess whether the masses found by Mascot and predicted via calculations were due to a peptide, with characteristic isotopic distributions (Figure 23.b). The abundance of oxidative modification was quantified for oxidation treatments of PTEN to be further utilised downstream for assessing the practical suitability of PTEN for analysis of the effect of OxPTM on PPI, and optimisation of oxidation protocols for generating a range of OxPTM appropriate for altering PPI, whilst maintaining the PTEN structure as seen by Coomassie stained SDS-PAGE.

If the abundance of modification was similar to the difference in activity observed via the parallel OMFP assay, the oxidative modifications could account for the changes in activity. XIC would also be useful to determine when amino acid side

chain modifications are not sufficient in abundance to account for changes in activity (Table 6, Figure 25.), which would suggest that alternative mechanisms such as backbone cleavage and aggregation are being induced by oxidation and causing changes in activity.

To quantify the abundance of 1) oxidised to 2) unmodified peptides XICs were generated (see Methods) for each version of the modified and unmodified peptide. Versions of the peptides included modifications other than the one quantifying that are present on the same peptide sequence, incomplete trypsin digestion fragments, different sized fragments caused by modification changing trypsin cleavage sites and peptides modified with the modification of interest. The peak areas of the unmodified and modified fragments were obtained using Peakview®, and spectra were generated to confirm the presence of the peptide mass to further validate the peptides identity by confirming an isotopic fingerprint, and to further validate that the ions are indeed part of that XIC peak (Figures 23, 24.). *De novo* sequencing was also performed as part of the XIC workflow whilst using Peakview® and searching for a particular peptide and modification.

PTEN was treated with sin-1 1:10, 1:75 and 1:150 molar ratio of PTEN: treatment, and HOCl 1:30 and 1:300 PTEN: treatment. After the modifications had been determined via Mascot and a table of peptides including modified peptides had been built (Appendices 8, 9.) XICs of the relevant peptides were generated and *de novo* sequencing of modifications were performed. A representative XIC of the peptide containing Cys71, the PTEN resolving active site cysteine, with masses for the unmodified and trioxidised form is displayed in Figure 23 alongside the spectra. Figure 23.a displays the XICs of 585.77 +/- 0.01Da and 582.43 +/- 0.01Da, with intensities (abundance) plotted against retention time as the XIC output of Peakview. In the representative example the modified residue is lower abundance and has higher noise-to-signal ratio. The peaks that were first assessed via manual validation

of the XIC spectra using Peakview were the ones at the retention time identified via Mascot or calculated based on the shift in retention time observed in other peptides with that modification in the same sample or another sample. For each XIC peak the spectra was generated (Figure 23.b.). The spectra was checked for the m/z of the peptide being the monoisotopic peak, the presence of the characteristic isotopic distribution, isotopic peak differences in masses, and that peaks were not being combined to give a false negative. A representative XIC and spectra is also shown for Tyr336 as an example of a tyrosine nitration including the tyrosine-containing peptide isotopic distribution (Figure 24).

Mascot prediction and XIC analysis of Cys71, the PTEN non-nucleophilic active site cysteine, showed some trioxidation modification in the untreated sample (Table 6.). The intensity of signal, and thus presumably the abundance, of Cys71 trioxidation increased upon treatment with sin-1 and HOCl, with a linear dose-response correlation for HOCl and a non-dose dependent response for sin-1.

Due to the loss of activity of PTEN-GST upon filtration, its low absolute activity compared to VHR-GST as measured by the OMFP assay, and its lower protein expression as compared to VHR-GST made VHR-GST the primary candidate to take forward to further functional proteomics mass spectrometry and protein-interaction studies. After initial PTEN-GST oxidation experiments, the decision was taken to not pursue studies of PTEN-GST beyond initial oxidation studies, due to amount of protein expressed and loss of activity upon column filtration when compared to VHR-GST, including not performing PTEN-GST oxidation studies on PTEN-GST in reducing buffer.

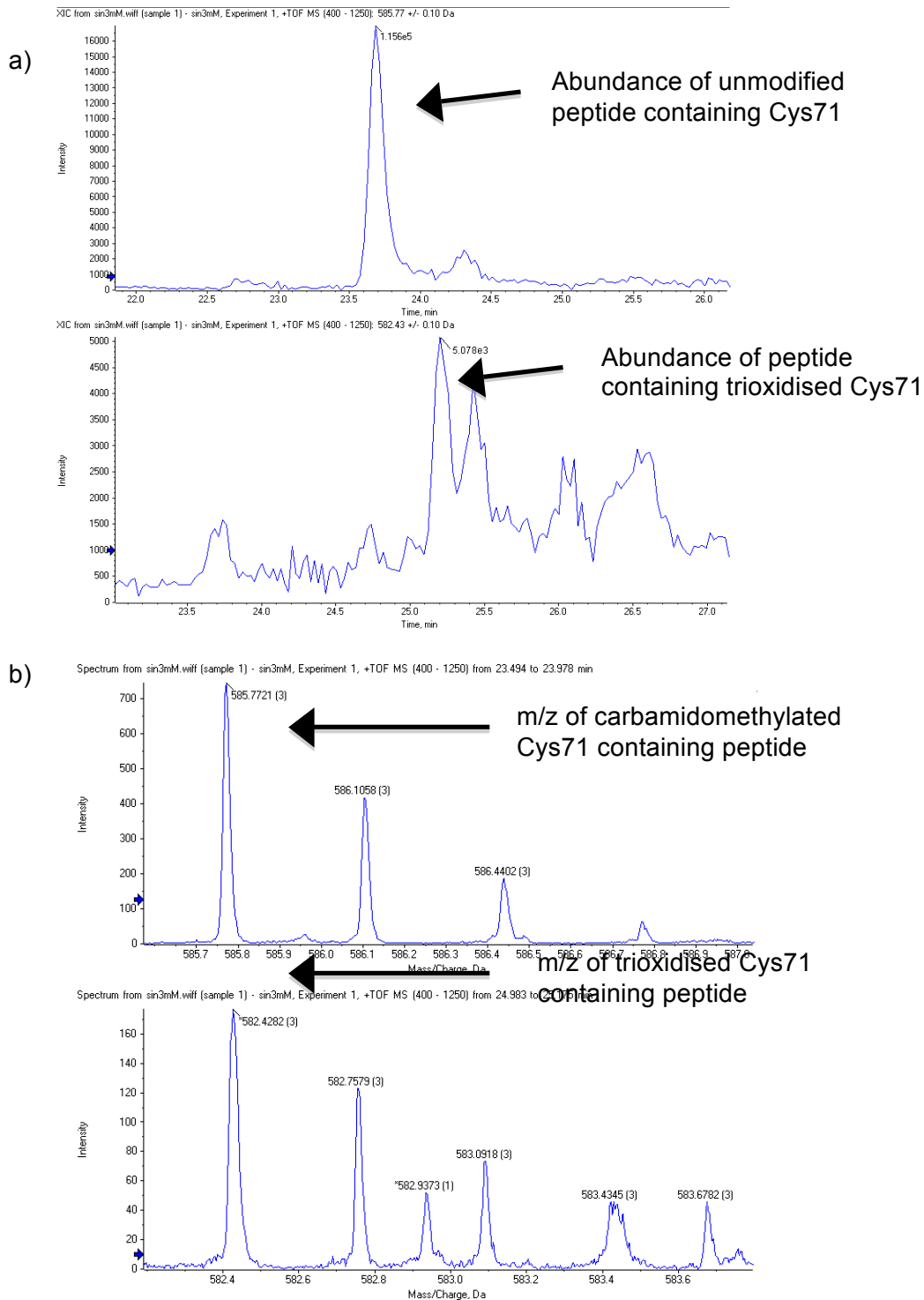


Figure 23. Representative extracted ion chromatograms and spectra of peptides containing trioxidised versus unmodified Cys71 in 1:150 molar concentration sin-1 treated PTEN a) Extracted Ion chromatogram (XIC) of unmodified and modified Cys71 b) Spectra of unmodified and modified Cys71. Asterisk (*) points to monoisotopic peak. XICs were generated with Peakview, parameters were standard, with peaks +/- 0.1Da of inputted value shown. Areas under peaks were calculated by Peakview for ions and read off.

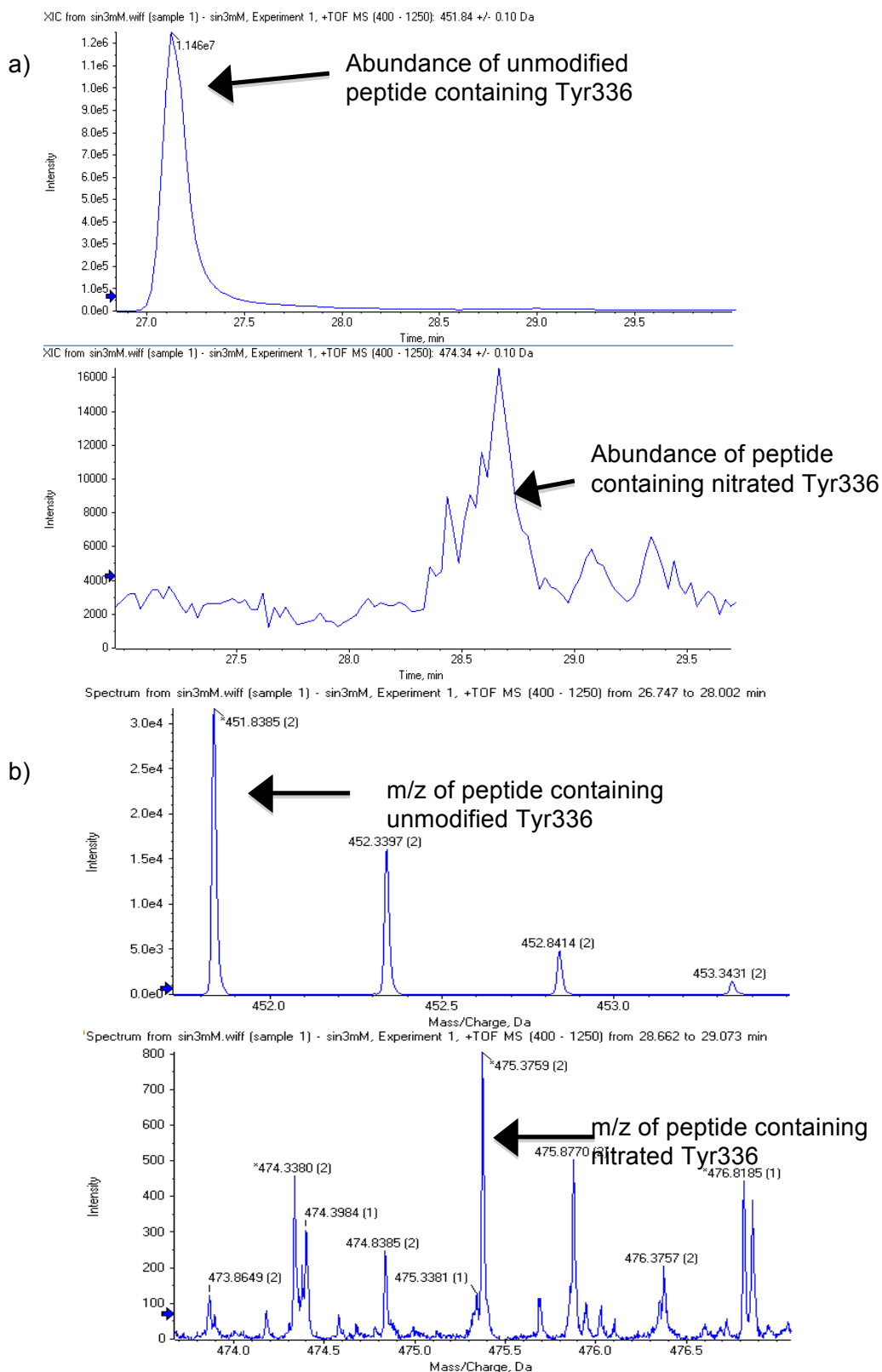


Figure 24. Representative extracted ion chromatograms and spectra of peptides containing nitrated versus unmodified Tyr336 in 1:150 molar concentration sin-1 treated PTEN

Extracted Ion chromatogram (XIC) of unmodified and modified Tyr336 b) Spectra of unmodified and modified Tyr336. Asterisk (*) points to monoisotopic peak. XICs were generated with Peakview, parameters were standard, with peaks +/- 0.1Da of inputted value shown. Areas under peaks were calculated by Peakview for ions and read off.

Ratios of Cys71 trioxidation in PTEN treated with sin-1		
PTEN non-oxidised control	PTEN treated with SIN-1 1:75 molar ratio concentration	PTEN treated with sin-1 1:150 molar ratio concentration
0.003%	0.026%	0.007%
Ratios of Cys71 trioxidation in PTEN treated with HOCl		
PTEN non-oxidised control	PTEN treated with HOCl 1:30 molar ratio concentration	PTEN treated with HOCl 1:300 molar ratio concentration
0.003%	0.0035%	0.009%

Table 6. Relative modification levels for non-nucleophilic active site regulatory cysteine Cys71 modifications from oxidation by sin-1 and HOCl
Ratios of trioxidised versus non-oxidised PTEN active site Cys71 in oxidised and control sample.

3.4.5. Oxidation of VHR-GST with HOCl, sin-1 generated peroxynitrite and tetranitromethane

3.4.5.1. SDS-PAGE and Coomassie staining of oxidised VHR

VHR was treated with a series of VHR-GST:reagent molar ratios of sin-1, TNM and HOCl. For Sin-1 (Figure 25a.) and tetranitromethane (Figure 26a.) the decrease in percentage OMFP activity was greater than the decrease in the percentage full lane densitometry. For sin-1 treatment the band percentage intensity shows a decrease similar to the percentage OMFP activity (Figure 25a). For tetranitromethane, the percentage OMFP activity decreases at a different rate to the percentage band intensity (Figure 26a.)

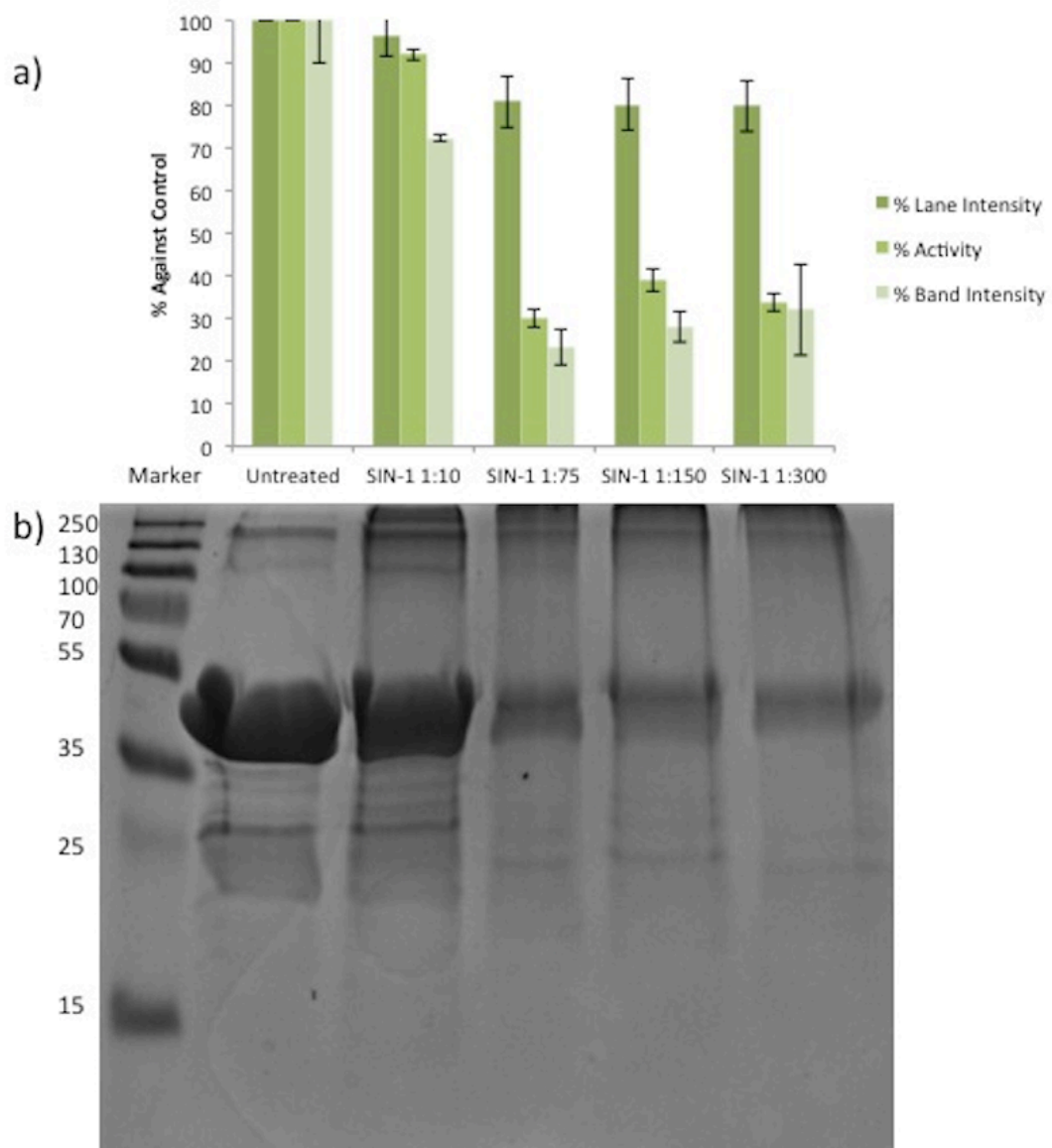


Figure 25. OMFP activity assay of phosphatase activity, densitometric analysis of SDS-PAGE and Coomassie stained SDS-PAGE of VHR upon treatment with *sin-1* a) OMFP activity is plotted versus the densitometry of the full gel lane, and b) densitometry for the main VHR gel band for *sin-1* treatment Coomassie stained SDS-PAGE for VHR treated with *sin-1*. Note high protein loading amounts necessary for sequence coverage upon high levels of treatment given loss of protein from bands. n=3

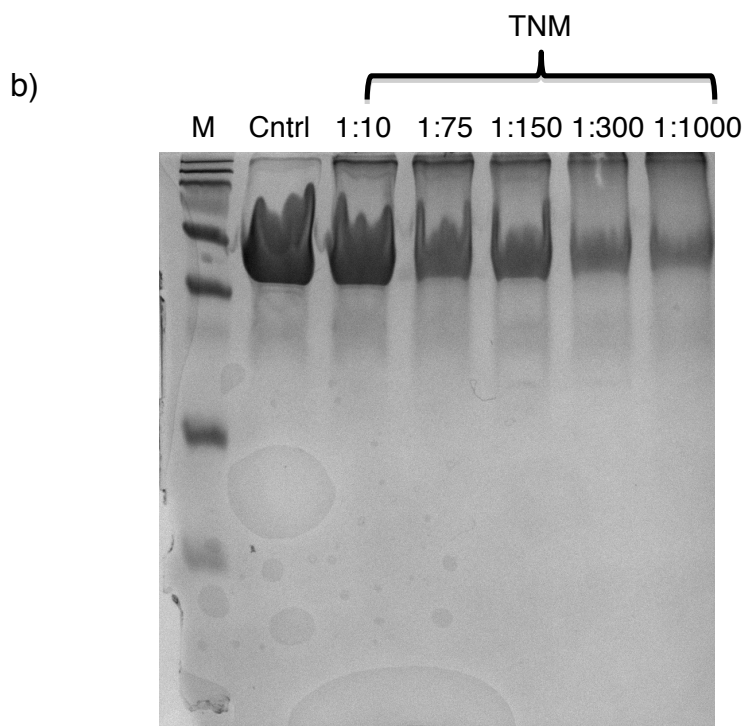
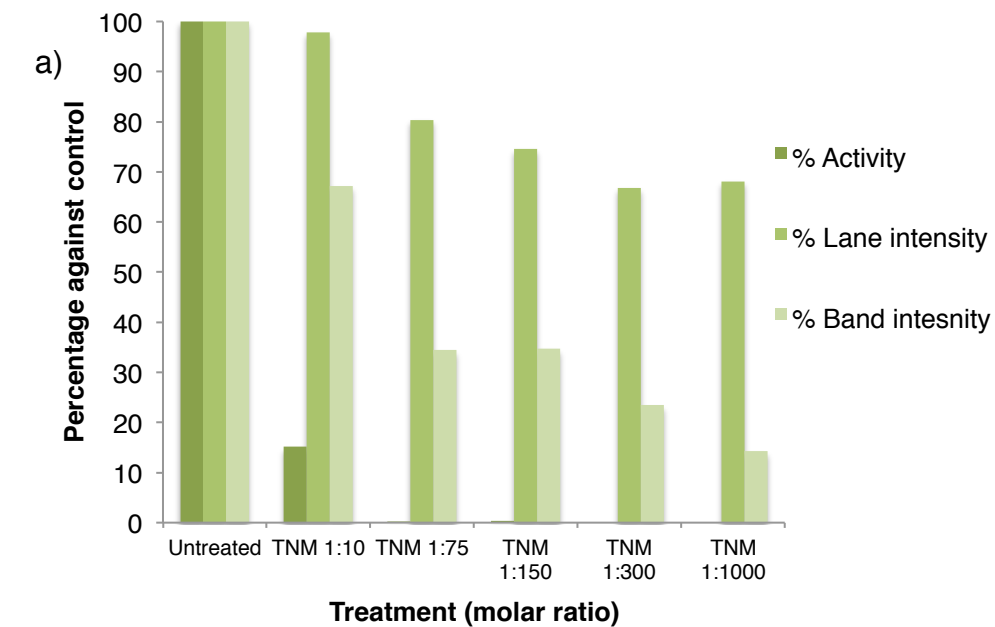


Figure 26. OMFP activity assay of phosphatase activity, densitometric analysis of SDS-PAGE and Coomassie stained SDS-PAGE of VHR upon treatment with tetranitromethane a) OMFP activity is plotted versus the densitometry of the full gel lane, and b) densitometry for the main VHR gel band for tetranitromethane treatment Coomassie stained SDS-PAGE for VHR treated with tetranitromethane. Exemplar result shown. Note high protein loading amounts necessary for sequence coverage upon high levels of treatment given loss of protein from bands.

3.4.5.2. Tandem mass spectrometry of VHR

VHR was treated with a series of VHR-GST:treatment molar ratios of sin-1, TNM and HOCl and then analysed via tandem LC-MS after cutting bands from the gel. The sequence coverage for VHR for the different treatments is presented in Table 7, with the corresponding Coomassie stained SDS PAGE and enzyme activity, where obtained, given in Figure 25 and 26. The sequence coverage for VHR drops by a maximum of ~15%, which upon treatment with HOCl, at 1:150 VHR: HOCl. TNM sequence coverage is increased from the untreated (Table 7, Figure 27a).

VHR upon increased oxidative treatment with HOCl gives an oxidation signature showing that particular regions exhibit increased oxidation and oxidation abundance including Pro49-Met69 and Tyr138-Met141, that also exhibit a waveform-like bell curve phenomenon. Novel modifications of note taking the body of literature into account would be Tyr138 chlorination showing that HOCl chlorination leads to the chlorination of the residue that interacts with ZAP-70 for VHR activation. Using Progenesis to analyse the data abundances gave a time saving of over x1000.

A comparative analysis of sin-1, tetranitromethane and HOCl insult indicates that there are common residues and also common regions of VHR that are modified such as the regions Pro49-Met69, a beta-sheet region, and Tyr138-Met141 which is an external end of an alpha-helix. There are also residues that have a higher abundance upon insult by a particular oxidising species. Tyr101 and Cys171 modification abundance show a tendency to be increased upon tetranitromethane treatment and Tyr85 shows a tendency for increased modification abundance. This particular comparative analysis of oxidative modification profiles if extrapolated could show promise for predicting or diagnosing what type of insult or stressor was being applied, as well as stratifying types of insults although this would require further *in vivo* experimentation and mathematical modeling.

Sequence coverage for VHR was higher than for PTEN under similar digestion, LC-MS and treatment protocols (Table 5 compared to Table 7). VHR sequence coverage decreases upon sin-1 and HOCl treatment, although not to the lowered levels that HOCl lowered sequence coverage in PTEN. TNM treatment increased sequence coverage, where sequence coverage remained high over treatments.

VHR modification abundances, as percentages of the unmodified peptides, alongside VHR activity were plotted for sin-1, TNM (Figure 28) and HOCl (Figure 29) treatment. Sin-1 and TNM abundance percentages were identified and calculated via Mascot and manual XIC, HOCl results were identified and performed with Progenesis and Mascot tools. The bands excised for the HOCl Progenesis automated analysis are present in Appendices 13, which are instructive of the excision method for all VHR LC-MS and areas selected for densitometric analysis, unless otherwise stated. VHR modification abundances plotted with standard error for select residues are plotted in Figure 30.

Treatment	Sequence coverage (%)
Untreated	69
Sin-1 1:10	69
Sin-1 1:75	67
Sin-1 1:150	64
Sin-1 1:300	64.5
HOCl 1:30	68.5
HOCl 1:150	59
HOCl 1:300	60
TNM 1:10	76
TNM 1:75	76
TNM 1:150	76
TNM 1:300	74
TNM 1:1000	75

Table 7. Sequence coverage versus treatment for VHR
Sin-1 n=3, HOCl n=3, TNM n=1

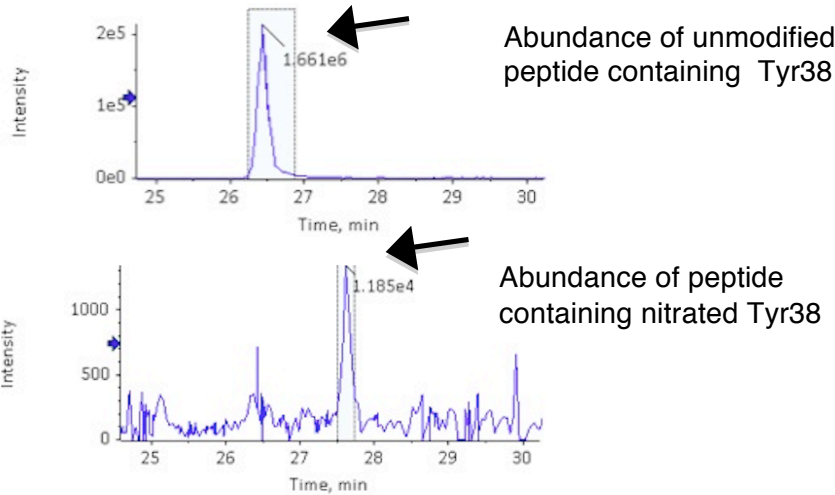
Variable modifications: [Oxidation \(M\)](#), [Oxidation \(Y\)](#), [Nitro \(Y\)](#), [Dioxidation \(C\)](#), [Trioxidation \(C\)](#)

a) **Protein sequence coverage: 74%**

Matched peptides shown in **bold red**.

1 MSGSFELSVQ DLNDLLSDGS GCYSLPSQPC NEVTPRIYVG **NASVAQDIPK**
 51 **LQKLGITHVL** NAAEGRSFMH VNTNANFYKD SGITYLGIKA NDTQEFNLSA
 101 **YFERAADFID** QALAQKNGRV LVHCREGYSR SPTLVIAYLM MRQKMDVKSAA
 151 **LSIVRQNRREI** GPNDGFLAQL CQLNDRLAKE GKLKP

b)



c)

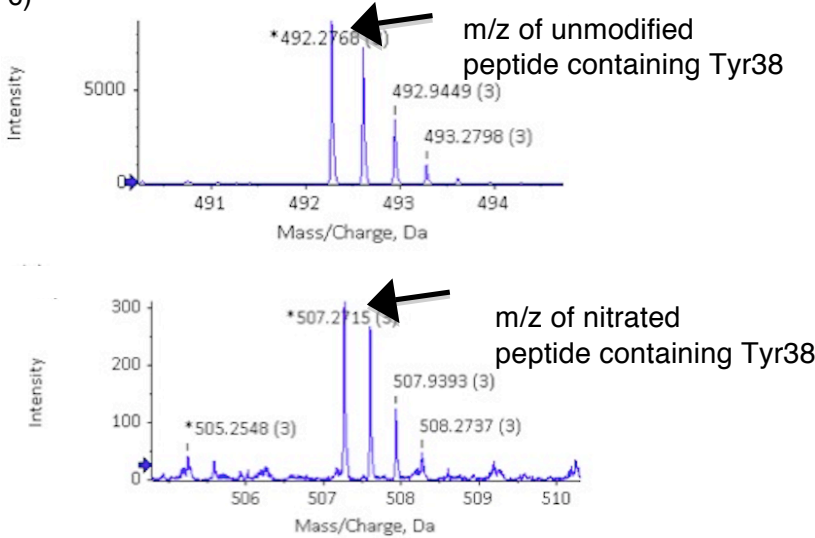


Figure 27. Representative sequence coverage of VHR after trypsin in-gel digestion and representative extracted ion chromatograms and spectra of peptides containing nitrated versus unmodified Tyr38 in sin-1 treated VHR
 a) Sequence coverage for VHR-GST. Mascot search results output including variable modifications searched for and enzyme proteins were cleaved with. Detected amino acids are highlighted in red and black amino acids were not detected.
 b) Extracted Ion Chromatogram (XIC) of unmodified and modified Tyr38 c) Spectra of unmodified and modified Tyr38. The mass windows that generated the spectra are shown. Mass windows were selected for the whole peak. XICs were generated with Peakview, parameters were standard, with peaks +/- 0.1Da of inputted value shown. Areas under peaks were calculated by Peakview for ions and read off.

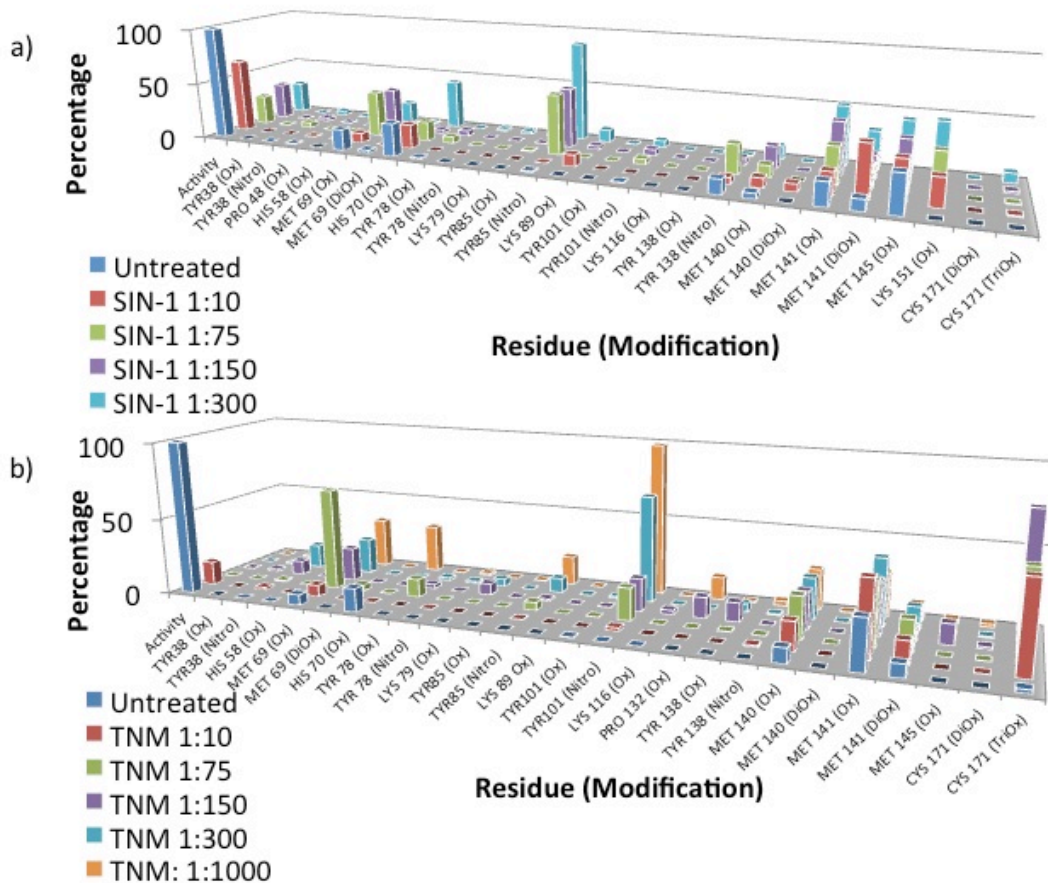


Figure 28. Functional proteomics of VHR upon oxidative treatment with sin-1 and TNM and phosphatase assay and in-gel digest of the major band corresponding to the molecular weight of the intact and active protein a) sin-1 treatment for 1hr at 37 degrees Celsius at 1:10 (21 μ M), 1:75 (80 μ M), 1:150 (160 μ M), 1:300 (320 μ M) protein: oxidant molar ratios. Relative abundance of modified to un-modified residues were calculated as a percentage and plotted alongside percentage phosphatase activity. n=3. b) tetranitromethane treatment or 1hr at 37 degrees Celsius at 1:10 (33 μ M), 1:75 (275 μ M), 1:150 (550 μ M), 1:300 (1.1mM) and 1:1000 (3.3mM) protein: oxidant molar ratios. Relative abundance of modified to un-modified residues were calculated and plotted as a percentage alongside percentage phosphatase activity. Ox= Oxidation. Nitro= Nitration. DiOx = Dioxidation. TriOx = Trioxidation. Representative study.

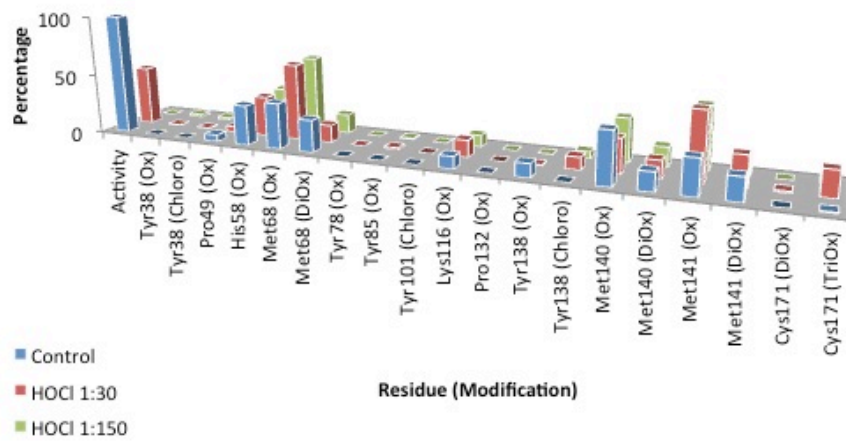


Figure 29. Functional proteomics of VHR upon oxidative insult of HOCl and phosphatase assay and in-gel digest of the major band corresponding to the molecular weight of the intact and active protein a) HOCl treatment for 1hr at 37 degrees Celsius at 1:30 (64 μ M), 1:150 (320 μ M), protein: oxidant molar ratios. Relative abundance of modified to un-modified residues were calculated as a percentage and plotted alongside percentage phosphatase activity. n=3. Data analysed with Progenesis software. Ox= Oxidation. Chloro= Chlorination. DiOx = Dioxidation. TriOx = Trioxidation. Representative study. Modifications thresholded to p-value 0.05 using Progenesis software.

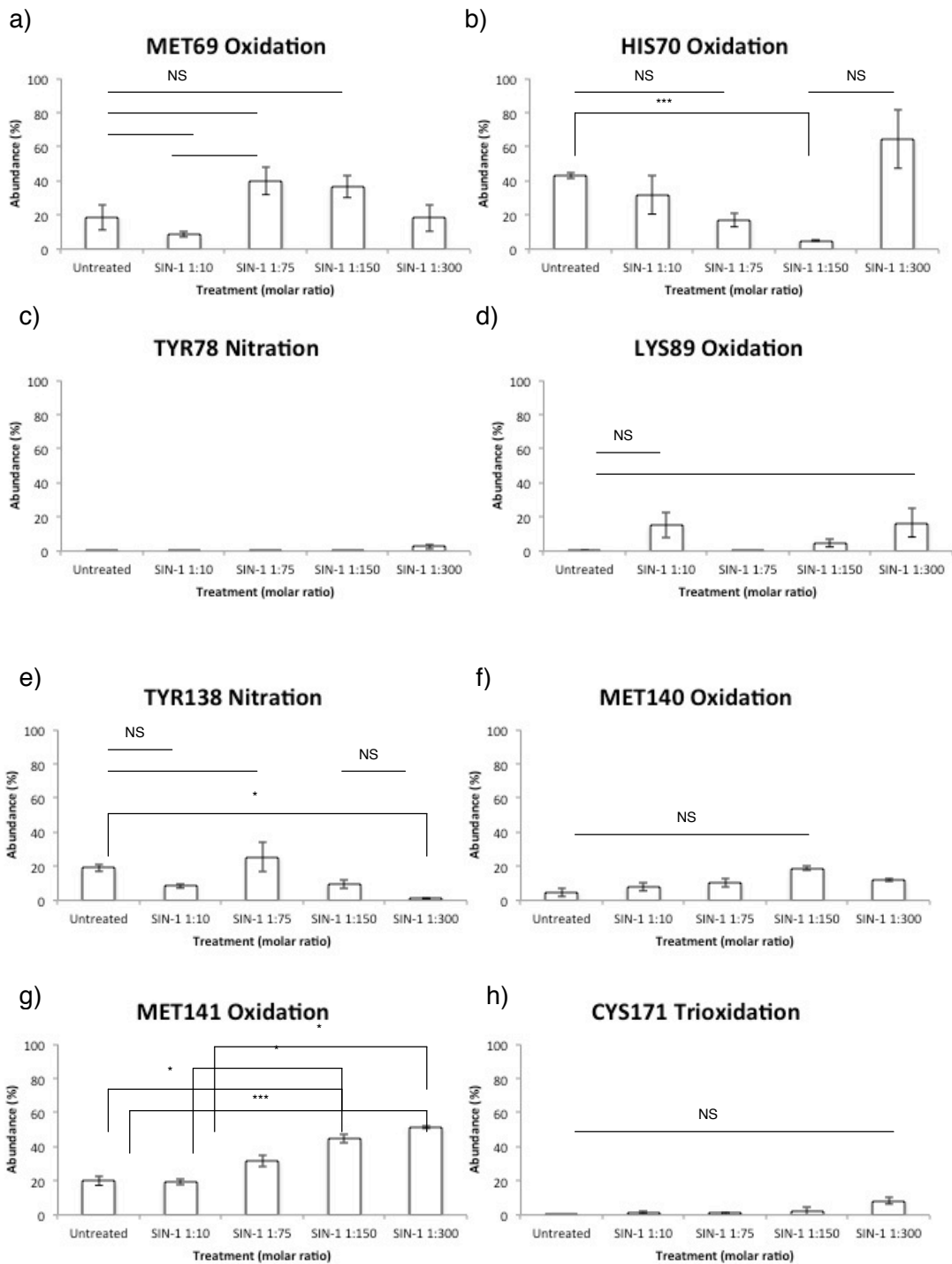


Figure 30. Select residues from functional proteomics of VHR upon oxidative treatment with sin-1 and in-gel digest of the major band corresponding to the molecular weight of the intact and active protein. Sin-1 treatment for 1hr at 37 degrees Celsius at 1:10 (21 μ M), 1:75 (80 μ M), 1:150 (160 μ M), 1:300 (320 μ M) protein: oxidant molar ratios. Relative abundance of modified to un-modified residues were calculated as a percentage and plotted alongside percentage phosphatase activity. Error bars = standard error. Unpaired *t* test * = 95% confidence interval, *** = 99.9% confidence interval NS = Not Significant (n=3).

3.4.5.2.1. Correlation of VHR activity and oxidative modifications via mediation modeling method

Computational modeling of VHR activity and modifications was performed to model the mediation effect of modifications on activity. Sin-1 data was used for mediation modeling; sin-1 data had the most replicates and was generated via Mascot searches and manual XIC. The mediation modeling shows the potential mediation effect of any one modification on the gross activity measure from the OMFP phosphatase assay from an aliquot of the same protein treatment batch as was run on the LC-MS (Figure 31). It can be seen that Lys116 upon mediation modeling shows a potential effect of increasing VHR activity with a large positive potential effect size, and Tyr138 showing a potential effect with a large negative potential effect size. Met141 has a smaller comparative negative effect size in the mediation model, yet has a mean value that has lower bounds furthest into having a negative effect on activity in the model.

Computational mediation modeling of VHR modeling was performed with a model with 2 mediators, with percentage abundances of modifications modeled for the forward mediation effect of the first mediator on the second mediator, and the potential effect size of this forward effect as a total indirect effect, as a multivariate model (Table 8).

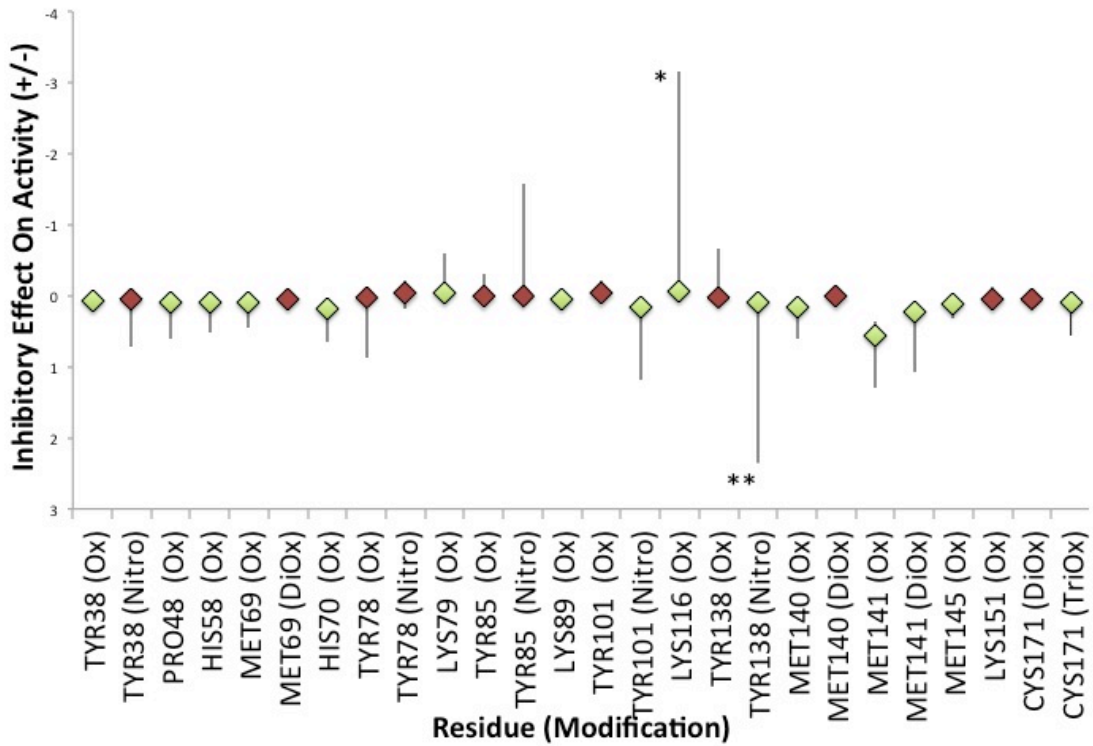


Figure 31. Mediation modeling for modified amino acids in VHR on phosphatase activity upon sin-1 treatment displaying inhibitory effects on activity. 95% confidence intervals displayed. Bootstrapping with N = 1000 random sample was used to calculate 95% confidence intervals. Diamonds represent mean value with bars displaying lower and upper bounds of potential effect size. Green diamonds are significant and red diamonds are non-significant. Y axis describes positive or negative mediation effect of modifications on phosphatase activity. * Lys116 modification predicted to increase VHR activity with large potential effect size. **Tyr138 regulatory residue modified with large potential effect size (n=10).

Mediation Effect Tested (X mediates Y)	Mediator I	Mediator II	Forward Effect of Mediator I on Mediator II (Minimum forward effect, Total magnitude of forward effect)
	(Mean mediation effect, Potential effect size)		
LYS70 Oxidation -> MET141 Oxidation	-0.0, 8.2	0.1, 4.5	767.1, 66436.8
TYR138 Oxidation -> MET141 Oxidation	-0.2, 5.8	0.2, 3.5	738.2, 889.7
LYS79 Oxidation -> TYR85 Nitration	54980.7, 60498.1	92204.2, 95929.2	548.2, 180277.6
TYR138 Oxidation -> MET141 Oxidation	14.3, -2.09e14	0.1, 2.5	369.3, 560.3
LYS116 Oxidation -> MET141	-0.1, 6.3	0.2, 2.6	246.7, 4292.9
TYR138 Oxidation -> MET140	0.5, 2363.7	0.2, 1099.8	196.9, 206.6
LYS116 Oxidation -> LYS151	-0.0, 33.7	-34.6, 0.1	186.1, 12616.7
TYR138 Oxidation -> MET145 Oxidation	-3.0, 0.0	0.0, 2.3	170.6, 565.2
LYS116 Oxidation -> MET141 Oxidation	-0.2, 7.0	0.1, 3.3	157.7, 3266.6
LYS116 Oxidation -> MET140 Oxidation	42014.3, 42014.3	0.4, 1107.0	86.1, 1738.5
HIS58 Oxidation -> MET69 Oxidation	-57.9, 0.1	0.0, 16.5	65.8, 414.2
HIS58 Oxidation -> TYR138 Nitration	-2.7, 0.2	0.0, 2.9	50.2, 779.3
LYS79 Oxidation -> LYS151 Oxidation	0.0, 222.2	-304.0, -0.0	47.4, 167917.8
LYS79 Oxidation -> LYS89 Oxidation	-28704.8, -28704.8	3104.7, 5132.1	39.9, 71035.7
TYR138 Oxidation -> TYR138 Nitration	3.2, - 6.2e16	0.0, 2.8	38.6, 155.0
TYR101 Oxidation -> MET141 Oxidation	-0.0, 1.1	0.3, 1.6	38.2, 587.4
HIS58 Oxidation -> MET141 Oxidation	-0.2, 1.9	-0.0, 3.0	35.0, 636.3
MET69 Dioxidation -> HIS70 Oxidation	-0.1, 0.1	0.0, 11.5	29.6, 23333.9
HIS58 Oxidation -> MET141 Oxidation	-0.1, 17.9	0.0, 3.9	26.2, 411.9
TYR101 Oxidation -> MET141 Oxidation	24.1, 589.3	-0.1, 1.5	0.1, 1.8

Table 8. Multivariate mediation modelling for modified amino acids in VHR on phosphatase activity upon sin-1 treatment displaying inhibitory effects on activity

The top 20 mediator combinations in terms of the magnitude displayed sorted by minimum forward effect, total magnitude of forward effect and total isolated mediator effects as the sum of the individual mediation effects of modification abundance on OMFP measured gross phosphatase activity. The magnitude of the forward effect is defined as the sum of the absolute values of the 99% confidence intervals. N =3, Resampling = 5000.

3.4.5.2.2. Search for modified and unmodified VHR active site nucleophilic residue and peptides

The active site nucleophilic Cys124 had been detected only in a modified state and only upon oxidative treatment (Figure 27a, Figure 32). The active site nucleophilic Cys124 peptides were searched for, including Cys124 in an unmodified, carbamidomethyl and modified state. VHR-GST treated with HOCl and sin-1 had yielded an instance in sin-1 treated VHR digested with trypsin of a Cys124 trioxidation (Figure 32a.). Sin-1 and HOCl treatments, trypsin digest and corresponding Mascot and systematic *de novo* manual searches did not identify uncarbamidomethylated miscleaved VLVHCREGYSR peptide with unmodified Cys124.

The uncarbamidomethylated miscleaved Cys124 containing peptide was not present in the same sample as the modified miscleaved and tryptically digested peptides for calculation of relative abundances between modified and unmodified, and between residues, samples and treatments, nor was the uncarbamidomethylated miscleaved Cys124 containing peptide present in all other samples and replicates obtained apart from one (Table 9, Figure 32, Figure 33).

TNM treatment and subsequent Mascot search led to the identification of additional instances of Cys124 identification in only modified forms of dioxidation and trioxidation (Table 9, Figure 32, Appendix 12), within multiple peptides, including both miscleaved peptides and with additional oxidation and nitration modifications at the distal tyrosine of the nucleophilic Cys124-containing peptide (Figure 33b.). Figure 32a. and 33b. y ions cover the Cys124, whereas Figure 32c. does not cover the y ions for Cys124.

A Mascot search with cysteine carbamidomethylation as a variable modification identified an unmodified, miscleaved instance of Cys124 in a single replicate of a single sample – which was subsequently verified via XIC and *de novo* sequencing (Table 9, Figure 32c, Figure 33.). This identification did not allow for relative quantification of

unmodified to modified active site residues to determine whether active site Cys124 modification was correlated to enzymatic activity loss by OMFP assay.

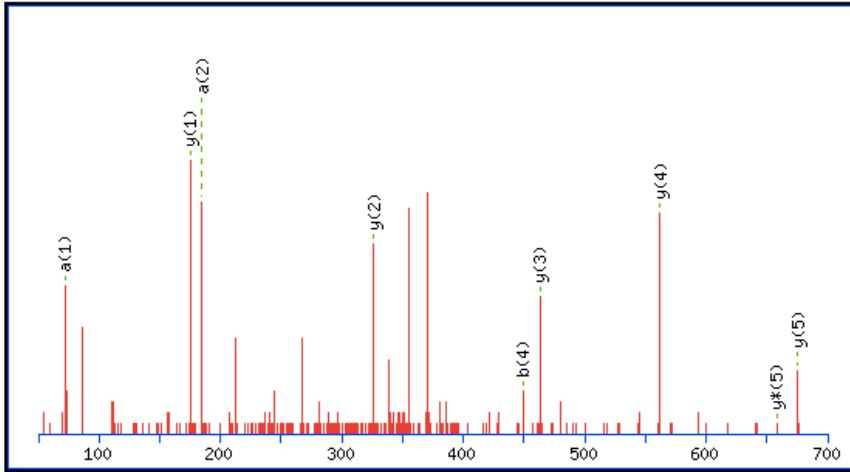
Table 9 displays peptides predicted *in silico* via EXPASy Bioinformatics Resource Portal tools, peptides calculated manually that may be expected, and the peptides identified via LC-MS. The peptides predicted *in silico* without being miscleaved were not identified in samples. Manual analysis of TIC included scanning XICs for peptides predicted and expected, at appropriate charge states, across the TIC.

Figure 34 displays the *de novo* identification window for the mass-to-charge ratio and retention time identified by Mascot search as displayed in Peakview, where SRYGER in y ion sequence of VLVHCREGYSR was sequenced *de novo* with assistance from Doctor Karina Tveen-Jensen, giving a partial *de novo* sequencing of the unmodified, miscleaved, uncarbamidomethylated Cys124 active site peptide.

Peptide sequence	Expected ion (m/z)	Retention time (mins)	Charge
<i>In silico</i> tryptic digest			
VLVHCR	363.95	Unknown	2
VLVHC*R	392.7	Unknown	2
<i>In silico</i> GluC/AspN digest			
NGRVLVHCR	526.786	Unknown	2
NGRVLVHC*R	541.786	Unknown	2
Calculated and identified unmodified residues (additional to <i>in silico</i> tryptic digest)			
VLVHCREGYSR	440.2789	Unknown	2
VLVHC*REGYSR	688.3342	Unknown	2
Calculated and identified modified residues (additional to <i>in silico</i> tryptic digest)			
VLVHC(O3)R	387.7313	Unknown	2
VLVHC(O3)REGYSR	712.3327	Unknown	2
VLVHC(O3)REGY(O)SR	691.9548	Unknown	2
Calculated and identified modified residues (additional to <i>in silico</i> GluC/AspN digest)			
NGRVLVHC(O3)R	1079.0734	Unknown	2
Tryptic digest (Identified via Mascot)			
VLVHCREGYSR	440.2789	19.36	2
VLVHC(O2)REGY(Nitro)SR	698.4565	23.82	2
VLVHC(O3)REGY(Nitro)SR	706.4507	26	2
VLVHC(O3)REGY(Nitro)SR	471.2828	24.51 to 25.19	3
VLVHC(O2)R	379.7315	17.81	2
VLVHC(O3)R	387.7313	18.36	2
VLVHC(O3)REGY(O)SR	461.6081	18.74 to 20.89	3
VLVHC(O3)REGY(O)SR	691.9548	20.63	2
GluC/AspN digest (Identified via Mascot)			
NGRVLVHC(O3)R	1079.0734	Unknown	2

Table 9. *In silico* digest, tryptic digest and GluC/AspN digest VHR peptides
*=carbamidomethylated.

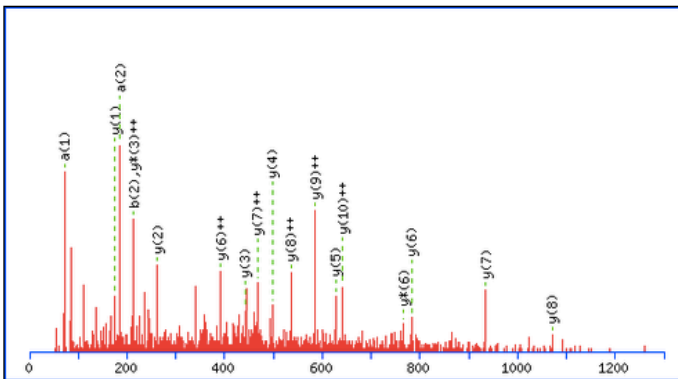
a)



Monoisotopic mass of neutral peptide Mr(calc): 773.3854
 Variable modifications:
 C5 : Trioxidation (C)
 Y9 : Oxidation (Y)
 Ions Score: 36 Expect: 0.36
 Matches : 9/40 fragment ions using 14 most intense peaks (help)

#	a	a ⁺⁺	b	b ⁺⁺	Seq.	y	y ⁺⁺	y*	y ⁺⁺⁺	#
1	72.0808	36.5440	100.0757	50.5415	V					6
2	185.1648	93.0861	213.1598	107.0835	L	675.3243	338.1658	658.2977	329.6525	5
3	284.2333	142.6203	312.2282	156.6177	V	562.2402	281.6237	545.2137	273.1105	4
4	421.2922	211.1497	449.2871	225.1472	H	463.1718	232.0895	446.1452	223.5763	3
5	572.2861	286.6467	600.2810	300.6441	C	326.1129	163.5601	309.0863	155.0468	2
6					R	175.1190	88.0631	158.0924	79.5498	1

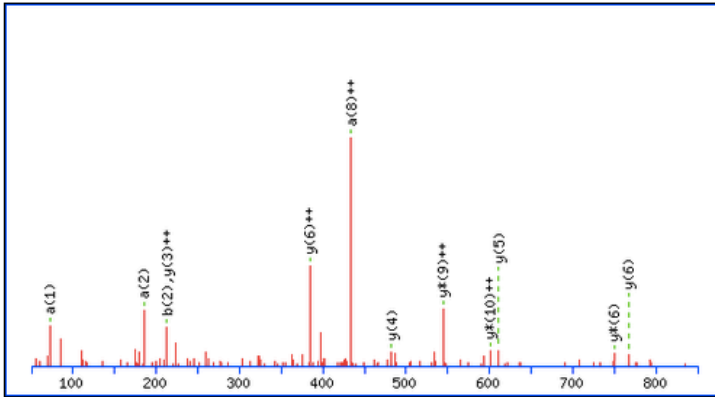
b)



Monoisotopic mass of neutral peptide Mr(calc): 1381.6408
 Variable modifications:
 C5 : Trioxidation (C)
 Y9 : Oxidation (Y)
 Ions Score: 32 Expect: 0.014
 Matches : 18/100 fragment ions using 46 most intense peaks (help)

#	a	a ⁺⁺	a*	a ⁺⁺⁺	b	b ⁺⁺	b*	b ⁺⁺⁺	Seq.	y	y ⁺⁺	y*	y ⁺⁺⁺	#
1	72.0808	36.5440			100.0757	50.5415			V					11
2	185.1648	93.0861			213.1598	107.0835			L	1283.5797	642.2935	1266.5532	633.7802	10
3	284.2333	142.6203			312.2282	156.6177			V	1170.4956	585.7515	1153.4691	577.2382	9
4	421.2922	211.1497			449.2871	225.1472			H	1071.4272	536.2173	1054.4007	527.7040	8
5	572.2861	286.6467			600.2810	300.6441			C	934.3683	467.6878	917.3418	459.1745	7
6	728.3872	364.6972	711.3607	356.1840	756.3821	378.6947	739.3556	370.1814	R	783.3744	392.1908	766.3478	383.6776	6
7	857.4298	429.2185	840.4032	420.7053	885.4247	443.2160	868.3982	434.7027	E	627.2733	314.1403	610.2467	305.6270	5
8	914.4513	457.7293	897.4247	449.2160	942.4462	471.7267	925.4196	463.2135	G	498.2307	249.6190	481.2041	241.1057	4
9	1093.5095	547.2584	1076.4830	538.7451	1121.5044	561.2558	1104.4779	552.7426	Y	441.2092	221.1083	424.1827	212.5950	3
10	1180.5415	590.7744	1163.5150	582.2611	1208.5364	604.7719	1191.5099	596.2586	S	262.1510	131.5791	245.1244	123.0659	2
11									R	175.1190	88.0631	158.0924	79.5498	1

c)



Monoisotopic mass of neutral peptide Mr(calc): 1317.6612
 Ions Score: 18 Expect: 0.5
 Matches : 12/100 fragment ions using 16 most intense peaks ([help](#))

#	a	a ⁺⁺	a [*]	a ⁺⁺⁺	b	b ⁺⁺	b [*]	b ⁺⁺⁺	Seq.	y	y ⁺⁺	y [*]	y ⁺⁺⁺	#
1	72.0808	36.5440			100.0757	50.5415			V					11
2	185.1648	93.0861			213.1598	107.0835			L	1219.6001	610.3037	1202.5735	601.7904	10
3	284.2333	142.6203			312.2282	156.6177			V	1106.5160	553.7616	1089.4894	545.2484	9
4	421.2922	211.1497			449.2871	225.1472			H	1007.4476	504.2274	990.4210	495.7142	8
5	524.3014	262.6543			552.2963	276.6518			C	870.3887	435.6980	853.3621	427.1847	7
6	680.4025	340.7049	663.3759	332.1916	708.3974	354.7023	691.3708	346.1891	R	767.3795	384.1934	750.3529	375.6801	6
7	809.4451	405.2262	792.4185	396.7129	837.4400	419.2236	820.4134	410.7103	E	611.2784	306.1428	594.2518	297.6295	5
8	866.4665	433.7369	849.4400	425.2236	894.4614	447.7344	877.4349	439.2211	G	482.2358	241.6215	465.2092	233.1083	4
9	1029.5298	515.2686	1012.5033	506.7553	1057.5248	529.2660	1040.4982	520.7527	Y	425.2143	213.1108	408.1878	204.5975	3
10	1116.5619	558.7846	1099.5353	550.2713	1144.5568	572.7820	1127.5302	564.2688	S	262.1510	131.5791	245.1244	123.0659	2
11									R	175.1190	88.0631	158.0924	79.5498	

Figure 32. Representative Mascot output from identification of VHR active site Cys124 peptides

a) Trioxidised Cys124 containing peptide b) Miscleaved Cys124 containing peptide with additional Tyr nitration c) Unmodified, miscleaved, uncarbamidomethylated Cys124 containing peptide. Representative MS/MS spectrum and sequencing with ion tables. Bold typeface in the ion table indicates the first time a peptide match to a query appears in the report. Red typeface in the ion table indicates the highest scoring match to a particular query. n=>1000.

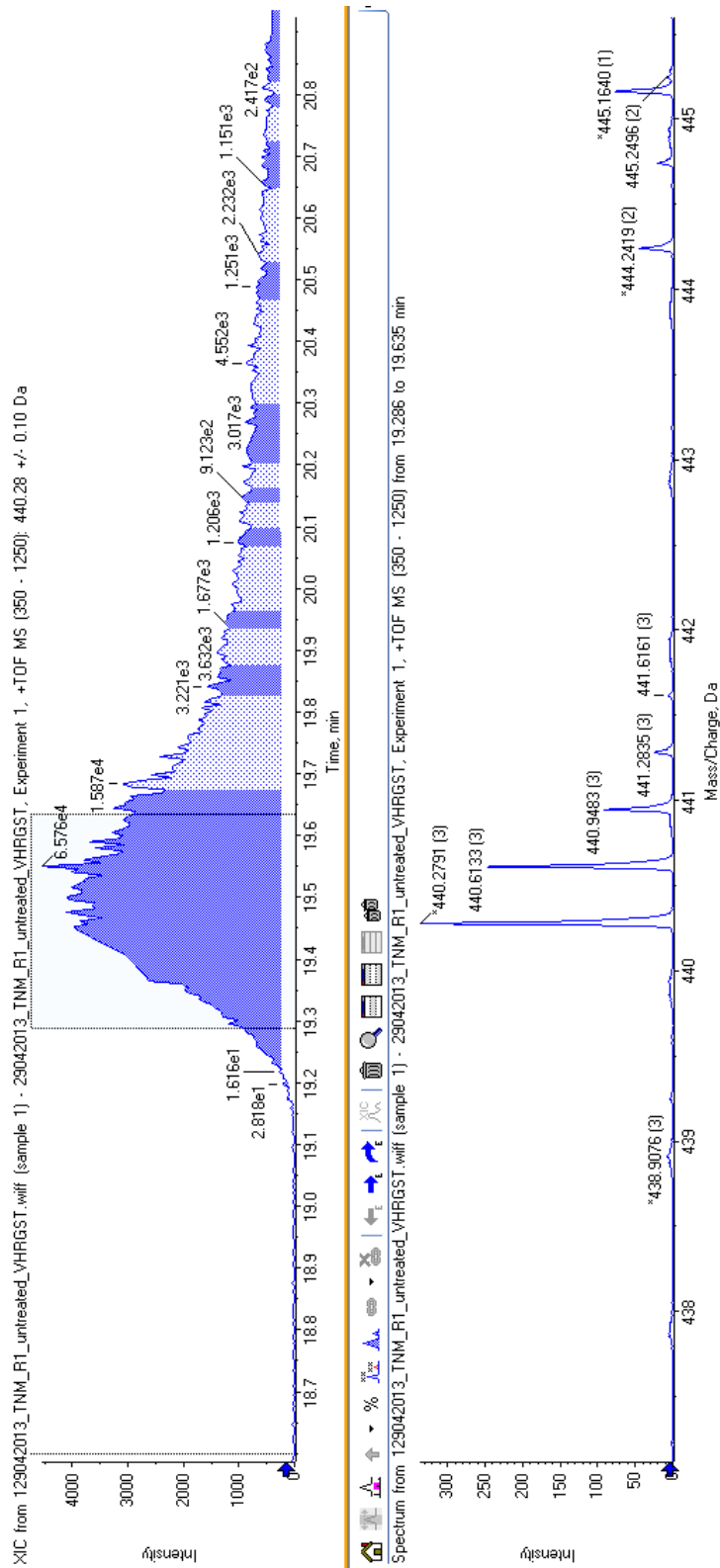


Figure 33. Extracted ion chromatography and spectra for identification of Cys124 unmodified, uncarbamidomethylated peptide in Peakview
Total ion chromatography and spectra from Peakview.

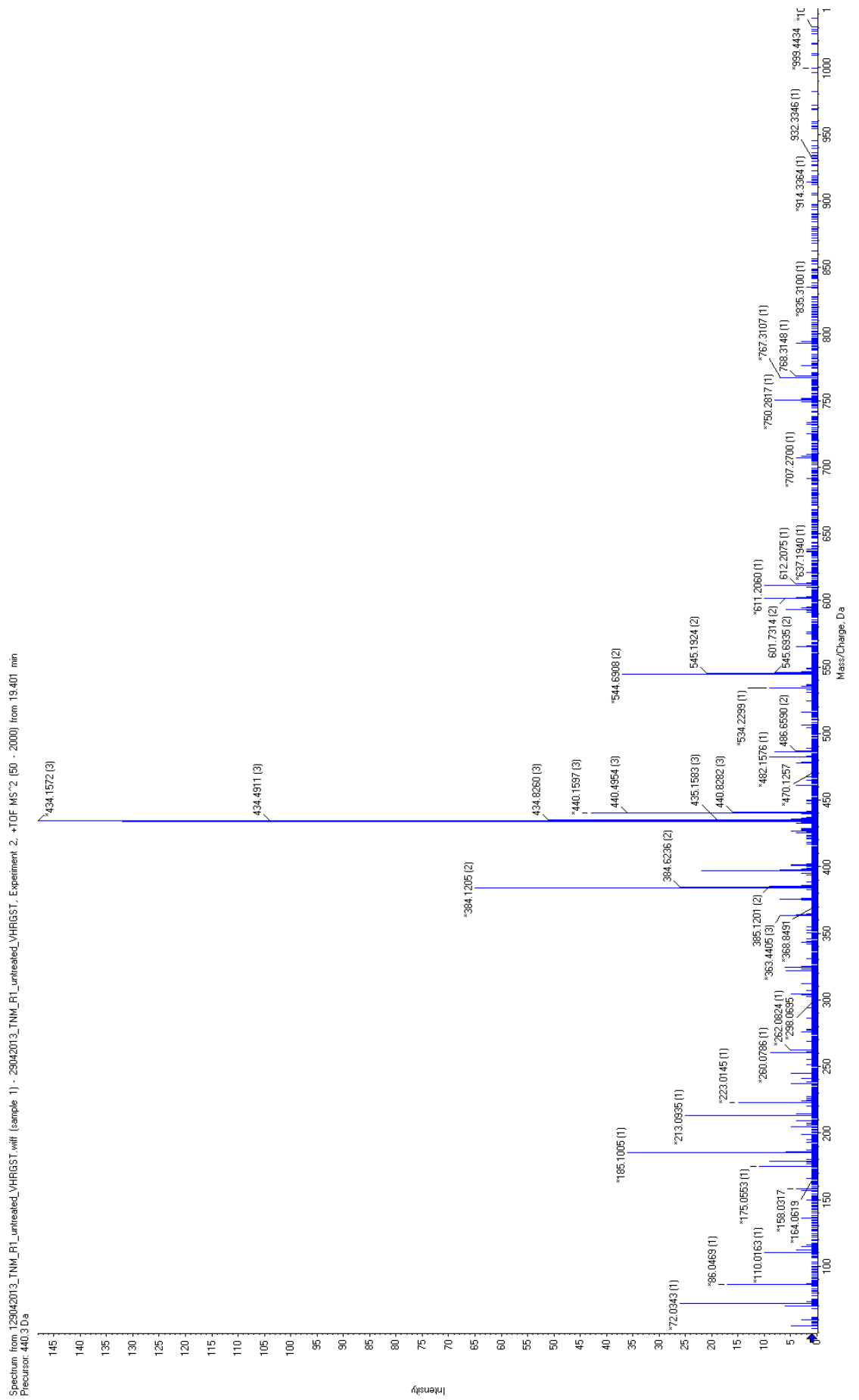


Figure 34. De novo sequencing for identification of Cys124 unmodified, uncarbamidomethylated peptide in Peakview

After Mascot search and manual analysis of tryptic digests of VHR-GST, a targeted ion scanning method was performed to scan for ions of specific mass-to-charge ratios with optimised MS settings (see Methods). A series of ions were selected to be analysed via targeted scans, including control ions seen at high abundances between tryptic digest samples (Table 10), and samples where the active site had been seen were used - TNM 1:1000 and untreated VHR, and a 1:1 1:1000 (VHR:TNM) to untreated mix. The results of the target scan were that the modified residues were identified; yet the unmodified Cys124 residues were not identified with manual *de novo* sequencing.

After a targeted scan approach was applied to the TNM treated tryptic digests, an alternate double digest approach was then attempted. Sequential AspN and GluC digests were performed on sin-1 treated VHR, at molar ratios that previously led to the identification of a trioxidised Cys124 peptide. The AspN and GluC digest did not identify the modified or unmodified Cys124 residues as present upon Mascot search or subsequent manual analysis of TIC and spectra, including searching for peptides predicted via *in silico* digests, previously identified or expected.

Target ion scanning method ions			
Peptide sequence	Expected ion (m/z)	Previously Identified retention time (mins)	Charge
VLVHCR	363.95	Unknown	2
VLVHC*R	392.7	Unknown	2
VLVHC(O3)R	387.7313	18.67	2
VLVHCREGYSR	440.2789	19.36	2
VLVHC*REGYSR	688.3342	Unknown	2
VLVHC(O3)REGYSR	712.3327	Unknown	2
VLVHC(O3)REGY(O)SR	691.9548	20.63	2
EIGPNDGFLAQLCQLNDR	1001.7266	43.61	2
EIGPNDGFLAQLC*QLNDR	1030.7413	46.04 to 46.93	2
EIGPNDGFLAQLC(O3)QLNDR	1026.2285	41.49 to 46.22	2

Table 10. Target scan method ion selection for search for VHR active site peptides

*=carbamidomethylated.

3.5. Discussion

3.5.1. Discussion of purification and expression of PTEN-GST and VHR-GST

In order to investigate how differences in oxidation states correlate to activity, aggregation and fragmentation for proteins of interest cells needed to be transformed, proteins expressed and purified in sufficient quantities, to a sufficient purity and quality. The protein produced per litre for PTEN-GST and VHR-GST was sufficient for activity assay, oxidation study and arraying and array probing needs. PTEN-GST and VHR-GST fusion proteins were selected as model candidates to be expressed and purified because of their oxidation sensitive active sites, the role of PTEN in cell signalling and cell survival (Rodriguez & Huynh-Do, 2012), role of PTEN in cancer (Silva et al., 2008), previous evidence of PTEN active site proneness to oxidation (Covey et al. 2007; Pei et al., 2009; Yu et al., 2005) and inhibitors of PTEN active site (Rosivatz et al., 2006; Mak et al., 2010). VHR was selected due to involvement in EGFR signalling (Ishibashi et al. 1992) and role in cancer (Wang et al., 2011), yet VHR and PTEN dioxidation and trioxidation had not been studied with the present literature focusing on reversible oxidation (Kim et al., 2000; Lee et al., 2002).

There are additional bands in the fractions (Figure 12, 13), including bands that are directly below the bands identified as the protein of interest by MS; these may be incomplete expression products, co-purifying proteins, as could the additional bands, this was not confirmed with MS due to the size of band not accounting for differences in yield.

As a control for the potential oxidising effect of 1)sonication of samples and 2) use of SDS-PAGE, LC-MS data attained for untreated/native protein, demonstrated that sonication and SDS PAGE do not yield high abundances of oxidative

modifications (Table 4, Table 5, Figure 28, Figure 29, Appendix 9, Appendix 10, Appendix 11, Appendix 12).

PTEN-GST and VHR-GST purification and expression was performed as part of a knowledge transfer agreement with Imperial College London as part of the Proxomics Project, and the protocol used, including sonication and use of SDS-PAGE was not adapted so that results could be compared with collaborators and protein samples could be shared between collaborators.

3.5.2. Discussion of assaying enzymatic activity of PTEN-GST and VHR-GST before and after filtration

The OMFP enzymatic assay was optimised with regard to the amount of protein added to the assay wells. The specific activity of PTEN-GST produced is within the range of PTEN-GST specific activity (0.5-1.5 nMoles/min/mg protein) gained from different expressions calculated by Doctor Lok Hang Mak, Imperial College London (personal communication). Thus the phosphatases expressed gave expected activity levels. Note that PTEN activity appears lower than VHR due to low substrate specificity of OMFP for this enzyme when compared with PIP₃ (Mak et al., 2010). Verrastro *et al* (2016) demonstrates a PTEN-GST specific activity of 0.57 nMoles OMF/min/mg protein, as a comparison of activity.

The OMFP assay would detect the total amount of activity of a known amount of protein, but did not resolve between inactivity of sub-populations and individual molecules of PTEN-GST that correspond to modification, aggregation or fragmentation.

A step to remove reducing agents was required for the quantification of the abundance, type and location of oxidative modifications for a particular molar ratio of oxidant added can be performed. It was necessary to remove reducing agents

because they would have reacted with the oxidant that was being added which would have meant would not know how much oxidant there was in treated samples. Mak *et al* (2010) also stores the expressed PTEN-GST fusion protein in reducing agents.

NAP5 column filtration was attempted as a method of buffer exchanging VHR-GST (Figure 17). NAP5 column filtration inactivated PTEN-GST (Figure 18). Mak *et al* (2010) who assayed PTEN-GST with OMFP substrate did not require a reducing agent removal step as they were assessing PTEN inhibitor action rather than oxidant effect. Routine Bradford assays prior to and after column filtration ensured that protein was not being lost during filtration and reduced OMF production was due to loss of activity of PTEN.

The combination of PTEN-GST inactivation by NAP-5 column filtration, inability to detect the active site nucleophilic Cys124 by MS/MS, lower comparative protein expression yields than VHR, lower comparative OMFP activity compared to VHR were the reasons to not take PTEN forward for systematic for systematic detection of a larger range of modifications, calculation of the abundances of these modifications, and correlation of these modifications to OMFP activity. PTEN was taken forward to MS and initial oxidation as the first candidate based upon historic reasons in the collaboration with Imperial College. For PTEN data shown, this was from PTEN-GST batches, which were active (Figure 15) yet without corresponding OMFP assays of column filtered PTEN-GST, where removal of reducing agents would be required for molar ratio oxidant studies. Thus we focussed on VHR for optimising and developing a functional proteomics workflow, after getting results, learning and making needed conclusions and looking at potential lines of inquiry for within the timeframe.

3.5.3. Discussion of SDS-PAGE and Coomassie staining of oxidised PTEN-GST and VHR-GST

Multiple additional bands are present in both the control and oxidised PTEN-GST sample (Figure 19.). The additional bands may be due to: I) incomplete/partial expression products II) protein backbone breaking and fragmentation III) oxidised protein that is preferentially oxidising at specific points having different electrophoretic properties IV) impurities from expression and purification process. Bands that appear at a higher molecular weight than PTEN-GST may be due to aggregation of protein due to oxidation or handling, or are incomplete protein expression productions and expression fragments of PTEN and/or GST.

Coomassie stained bands at the size appropriate to PTEN-GST or VHR-GST were excised. The rationale for this was that the majority of the peptides would be found in this band, and that peptides found in this band were more likely to be from the protein of interest. This band was also cut out so that the modifications that were present in intact protein could be analysed – these would be the modifications in the intact protein that may affect function and protein-protein interaction. Cutting out the gel band for PTEN-GST and VHR-GST selects against modifications that may be important in the formation of aggregates and fragments that aggregate. SDS-resistant protein aggregation behaviour has been demonstrated (Sagné et al., 1996), and Coomassie stained moieties that move more slowly through the SDS-PAGE gel is suggested of moieties being aggregates due to molecules being separated by mass as well as charge (Figure 19).

The effect sin-1 to create additional bands may have important roles in proteopathies such as Alzheimer's disease, Parkinson's disease, type 2 diabetes and other proteopathies; and offers an additional hypothetical mechanism for how oxidation, nitration and chlorination may be involved in the proteopathic mechanisms

of age-caused diseases and increases in morbidity, mortality and inability to maintain homeostatic capacity. Smith *et al* (1997) found protein nitration in neurons containing neurofibrillary tangles, which is an indicator of peroxynitrite involvement in Alzheimer's disease and the sin-1 gel band patterns (Figure 19) could be suggestive of a mechanism in Alzheimer's aggregate formation.

The decision to focus on the gel bands, rather than digest the whole SDS PAGE lane, was to determine which modifications occur to intact PTEN and VHR. Whereby modifications found would be more correlated or causal to the changes in activity seen or protein-interactions seen in the counterpart experiment with the same protein or same treatment regimen used. An assessment was also made to downgrade the priority of whole gel lane MS analysis as performing the XICs and *de novo* sequencing would have been inappropriate for the timescale, method and human resources available.

Importantly, although there was some loss of signal from densitometry of the whole gel lane for VHR (Figure 25., 26) the loss in densitometry signal from the lane is less than the loss in activity, and the protein appears to be still present in the gel lane if not in the excised major protein band. Therefore loss in activity (Figure 25., 26) does not appear to be due to loss of protein from the gel.

3.5.4. Discussion of oxidative treatment of PTEN

3.5.4.1. Discussion of the combinatorial bottom-up mass-spectrometric analysis and phosphatase assays of oxidised PTEN

The unique contribution to knowledge for PTEN is the identification of oxidations, nitrations and chlorinations previously uncharacterised. These were generated *in vitro* but may have relevance *in vivo* – as peroxynitrite and HOCl are biological oxidants

(Albrich et al., 1981; Harrison & Shultz, 1976; Spickett et al., 2006; Thomas, 1979; Waldow et al., 2004,). The results may be of utility for designing PTEN and PTP inhibitors, and the functioning of PTEN and PTP inhibitors (Mak et al., 2010) in an oxidative environment.

Probably the most important amongst the unique contributions to knowledge is the discovery of the Cys71 non-nucleophilic active site cysteine trioxidation, which has been detected, sequence validated by *de novo* sequencing, and its abundance characterised for specific treatments. Cys71 is capable of forming a disulphide bond with Cys124 upon oxidative stress (Lee et al., 2002). Salmena *et al* (2008) demonstrate reversible inactivation of PTEN, yet if Cys71 di-oxidation or trioxidation were to occur *in vivo* this may disable the reversible oxidative inactivation of PTEN, and could keep PTEN in a constitutively active state where Cys124 was no-longer forming disulphide bonds with Cys71, which would be an interesting subject of future study.

The low abundance of the Cys71 oxidation present within the excised band fragment may be suggestive of Cys71 not having a major role in inactivation of intact PTEN (Table 6), unless biological regulation of PTEN through binding partners and intracellular concentrations of oxidant enhanced the production of trioxidised Cys71 through altering access to the site and reaction kinetics, where changes in protein conformation on access to active site have been demonstrated (Świderek et al., 2015).

The trioxidation of Cys71 may represent a form of oxidative damage from oxidative stress rather than reversible redox sensing in short time scales that includes chemically or biologically reversible reactions without the degradation of a protein – where the redox sensing is on the protein level, rather than redox sensing at a cellular locale or cellular level – if there were no possible biological reactions to reverse trioxidation *in vivo*.

Discovery of the trioxidation of redox sensitive and redox sensing residues may lead to a wider understanding and utilisation of both the inter-relation between reversible oxidation and non-reversible oxidations, and how non-reversible oxidations may be part of oxidation sensing over longer timescales and at a level higher than the individual protein level. Trioxidation of the active site Cys71 may be adaptive and provide regulation at the signalling network level, or over long periods of time, rather than the individual protein level in addition to roles in oxidative stress and oxidative damage, or could be found to be reversible – posing a similar scientific enquiry as the enquiry into the regulatory effect and reversible nature of histone methylation as described by Bannister and Kouzarides (2005).

To obtain a higher sequence coverage than 70% for the most heavily oxidised samples for PTEN under treatment conditions (Figure 21), the follow may be of utility – increasing protein loaded onto an already heavily overloaded SDS PAGE gel, digesting protein from whole gel lane, and further optimisation of oxidant concentration, oxidant-to-protein molar ratio, pH and temperature and the use of alternative protein digestion enzymes, and non-gel based digests – to be able to detect all the appropriate residues and modifications.

This unique contribution to knowledge for PTEN in context of known PTMs, particularly phosphorylation and ubiquitination, and known PPIs adds to the knowledge base for PTEN which can be utilised during *in silico* therapy design, and could be of utility to appropriately build a list of PTEN-related biomarkers to search for, that may have association with cancer or age-related diseases. To elaborate, if peptide biomarkers related to PTEN are being searched for *in vivo* and not found, they may differ in masses due to the presence of the oxidative modifications herein identified. Thus being able to build a more comprehensive list of potential peptides to search for, may allow the complete *in vivo* search space to be queried, even if many modifications in the PTEN PTM list built for biomarker discovery do not occur *in vivo*

or are not related to the relevant clinical and health outcomes, searching for modifications found *in vitro* may assist finding the modification which do occur *in vivo*. Such a systematic analysis may have challenges regarding how many variable modifications to search for accurately, both during MS scans, and software searches, and thus may require appropriate sample sizes and automation of many variable modification searches..

Multiple new sites of oxidative modification have been identified, and validated in PTEN treated with the *in vivo* oxidants peroxynitrite and HOCl (Table 4., Table 5.). Oxidative modifications in the active site non-nucleophilic regulatory counterpart Cys71 as well as Tyr76 and Tyr46 have been identified which are spatially near to the PTEN active site (Figure 36, 37), although it has not been established experimentally or by molecular dynamics that Tyr47 and Tyr76 are near enough to affect phosphatase activity. Molecular dynamics would assist in modelling how close residues may move to each other, which could be cross-referenced with how close they may need to be in order to interact, which is demonstrated by Margreitter *et al* (2013). There is an overlap in residues oxidised between sin-1 and HOCl, however sin-1 oxidation caused a greater variety of modifications (Tables 4, and 5 and Appendices 8 and 9), the gel bands after oxidation were weaker (Figure 19.).

Additional studies would be required to confirm the relevance of the importance of non-reversible oxidation *in vitro* and *in vivo* applications, and will need to be repeated, supported and validated by additional mass-spectrometric techniques such as targeted mass spectrometry to provide greater accuracy validation. Note that the reason that singly oxidised Cys71 is not observed in the experiments utilising iodoacetamide and DTT is because of the reduction and alkylation steps of the digestion protocol that reduce cysteine disulphide bridges and add an adduct via carbamidomethylation.

Increasing concentrations of sin-1 oxidation of PTEN showed an increase in the presence of particular modified residues according to oxidation concentration (Tables 5 and 6, Appendices 8 and 9.), which may represent which residues may be more readily modified, or are more likely to be present at that concentration, in the band excised. Where other modifications associated with this concentration may be present outside the band excised. The existence of more readily modified residues for PTEN may include residues that have the higher chance of being modified that changes with concentration of oxidant – and may have evolved a sensitivity to oxidation, for functional reasons such as scavenging, active site regulation, conformational change, regulation by protein degradation or non-oxidative PTM interaction or PPI – and may be sensitive to specific levels of oxidation for variable functionality. These evolved functions may not PTEN specific, yet PTEN data demonstrating residues more readily modified and to a greater abundance (Tables 5 and 6, Appendices 8 and 9.), may add to the body of evidence for such mechanisms, and builds on the hypothesis of Levine et al (1996) who propose methionine residues in proteins to be an important antioxidant defence mechanism.

The limitation to sequence coverage of 70% or less for oxidised samples may limit the identification and quantification of all modified residues, in particular Cys124 and parts of the C-terminal tail sequence, which includes phosphorylation sites and a PDZ binding domain. To speculate, oxidative modifications to the C-terminal sequence may be cause changes in activity, as phosphorylation of the C-terminal tail was shown by Bolduc *et al* (2013) to induce conformational change to a conformation closure with reduced catalytic activity. Bolduc *et al* (2013) speculate that the phosphorylated C-terminal tail may interact with the C2 domain for this conformational change to occur. Thus oxidation of the C2 domain or C-terminal tail, may be relevant for functional catalytic changes in PTEN.

Multiple overlapping different sized peptides covering the same residues were seen following both sin-1 and HOCl in-gel digestion (Tables 5 and 6 and Appendices 8 and 9.) indicating trypsin digest miscleavage. Miscleavage can occur due to incomplete digestion by trypsin, which may indicate sub-optimal trypsin concentration, peptide sequence (Šlechtová et al., 2015), or oxidative modifications may alter the structure of the trypsin cleavage site so it is no longer recognised by the digestive enzyme.

A comparative analysis of PTEN to the PTP VHR may yield insights into PTEN function, given the conserved features and function of VHR, both at a functional level including changes of conformation, translocation and Cys124 nucleophilic activity (Denu & Tanner, 1998). VHR has a Tyr138 residue that has been identified as involved in PPI with ZAP-70 through phosphorylation (Alonso et al. 2003), this residue has also been identified as oxidised and nitrated *in vitro* (Figure 28, Figure 29, Figure 30). As PTEN has a corresponding Tyr and this has been found to be both oxidised and nitrated, the oxPTM of residue may also have functional, regulatory and PPI importance in PTEN. Literature evidence of the importance of Tyr138 and adjacent Gly139 includes Stumpf & Hertog (2016) and Leslie et al (2007), who demonstrate effects of Tyr138 mutants *in vivo* for vascular hyperbranching, and state that Tyr138 mutation is selected for in the metastatic small cell lung cancer cell line NCI-H196. Due to Tyr138 involvement in cancer in PTEN, oxidation and nitration of this residue, peptide fragments pertaining to this residue, and other non-active site residues and their modifications, may be important for cancer therapeutic development and biomarker development. This analysis highlights the potential importance of comparative PTM omics, and for the parallel querying of multiple biomolecules.

Regarding the PTEN active site Cys124, as the VHR Cys124 has been detected as trioxidised (Figure 32), one may speculate that the PTEN Cys124 may also be capable of trioxidation, *in vitro*, *in vivo* and via intervention.

3.5.4.2. Discussion of domain regions of PTEN oxidised and nitrated by sin-1 and HOCl

Mapping modifications to domain structure (Figure 36.) indicates that the phosphatase domain of PTEN is susceptible to modification. To speculate, phosphatase domain modifications may affect enzymatic activity of PTEN *in vivo*. There are multiple modifications in the C2 domain at M205, M225, M239, M270, Y316 (Figure 35., Appendices 8.,9.) Bolduc *et al* (2013) suggest that the C2 domain may interact with the C-terminal tail for an activity modifying conformational change, thus the C2 domain modifications found may have an affect on conformational change. There is a modification of a tyrosine in the phosphorylation domain. To speculate, modification of Tyr336 may have additional *in vivo* importance as tyrosine phosphorylation of PTEN (Lu et al., 2003) and nitrotyrosine mimicking of phosphotyrosine (Mallozzi et al., 2001). Modifications in the C2 domain can also be important as it is a binding domain that also has auto-inhibition functionality (Odriozola et al., 2007).

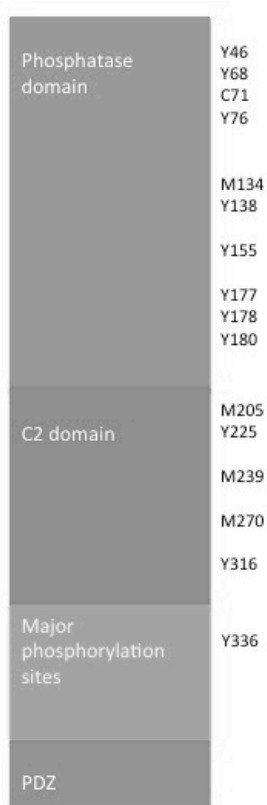


Figure 35. Mapping of all residue modifications predicted by Mascot search from oxidation of PTEN by sin-1 and HOCl oxidation and nitration
Phosphatase domain sequence 15-186, C2 domain sequence 186-403 and major phosphorylation sites 352-403.

3.5.4.3. Discussion of oxidative and nitrative modifications in the context of crystal structure information for PTEN

Mapping the modifications identified onto the crystal structure of PTEN (Figures 36., 37.) allowed for the secondary and tertiary structure to be taken into account when assessing the putative effect of oxidative modifications on protein function, and to inform decision making as part of the screening process. Tyr46 and Tyr155 oxidation and nitration modifications were identified (Tables 5 and 6, Appendices 8 and 9.) are spatially situated near to the active site (Figure 36.) and they could have an affect on PTEN activity through a direct or in-direct action on the active site cysteines or the amino acids that form the active site cleft and create the physicochemical properties of the active site cleft. Note that the presence of Tyr46 on an unstructured sequence

that, to speculate, may have the ability and propensity to interact with the active site, where informatic and physical analysis may query this. Tyr76 is situated on an unstructured sequence region, where to speculate, modified Tyr76 may affect PPI as unstructured and loop regions may be involved in PPI due to their movement and varied conformations that they may take. Tyr138 appears to be an outwards facing residue on an α -helix, flanked by two α -helices that may constitute an α -helix domain. Tyr138 may be of relevance, due to VHR Tyr138 being involved in the phosphorylation-activation of VHR by ZAP-70. When the crystal structure of PTEN is cross-referenced, comparatively, with the crystal structure of VHR it can be seen that the α -helix Tyr138 is present on appears evolutionarily and structurally conserved, as does the potential α -helix domain, as well as the Tyr138 sequence and the ability for Tyr138 to be oxidised and nitrated *in vitro*. Tyr155 is situated on an α -helix and adjacent to an α -helix and β -sheet, in addition to being outwards facing, and thus modification of this residue, may alter the conformation, with regards to interact with the adjacent α -helix and β -sheet which may affect protein translocation, function, or affect PPI binding. Tyr225 is situated at the start of an unstructured region and thus may affect PPI through either a docking site or altering the movement and direction of movement of the unstructured region. Tyr336 is situated on an unstructured loop region, at the hinge of the loop, which may both directly affect a docking site for PPI and also the movement direction, movement range and vibrational frequency of the loop region, which may affect further complex formation and PPI. The Cys71, in addition to being a partner for Cys-Cys disulphide bridge formation with the nucleophilic Cys124 (Figure 37), is situated at the start of an unstructured region, which, may also affect the movement and shape of this region and thus PPI interactions and PTEN conformation.

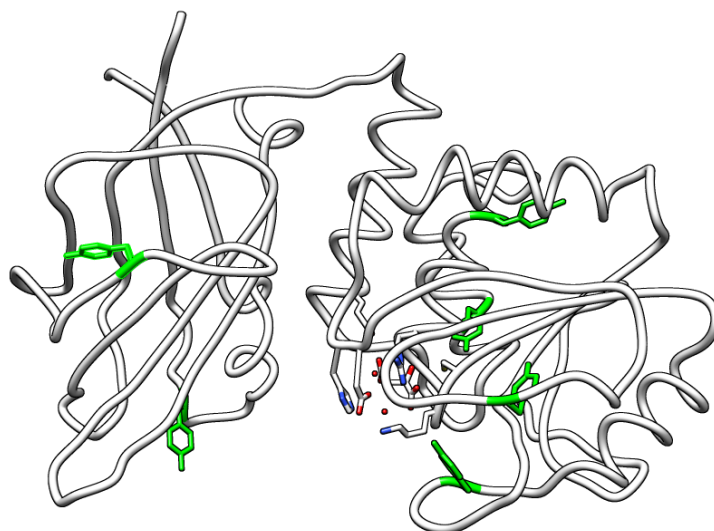


Figure 36. Tyrosine modifications found in sin-1 oxidation of PTEN mapped onto PTEN crystal structure model

Tyrosines identified as modified by Mascot search are highlighted in green on the 3D structure of PTEN (1D5R), Tyr46, Tyr76, Tyr138, Tyr155, Tyr225 and Tyr336. The structure is based on PTEN X-ray crystallography data (Lee et al., 1999) and displayed using UCSF Chimera (Pettersen et al., 2004).

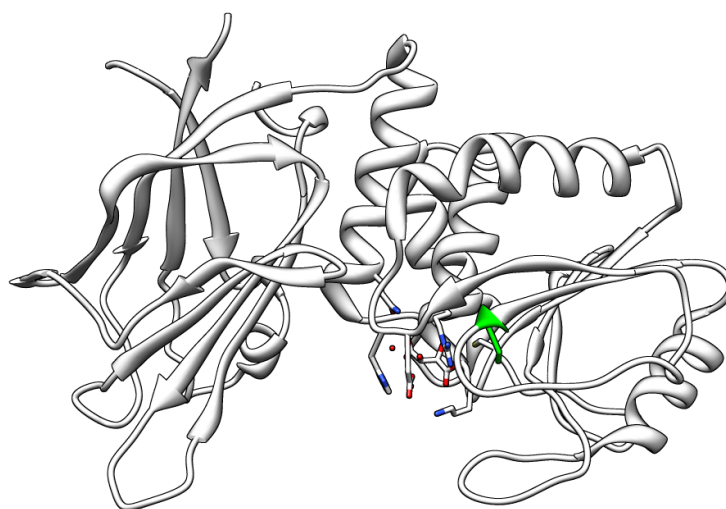


Figure 37. Cysteine modifications found in sin-1 oxidation of PTEN mapped onto PTEN crystal structure model

The non-nucleophilic regulatory active site cysteine identified as modified by Mascot search is highlighted in green on the 3D structure of PTEN. The structure is based on PTEN X-ray crystallography data (1D5R) (Lee et al., 1999) and displayed using University of California San Francisco Chimera (Pettersen et al., 2004).

Without the identification of Cys124 with tryptic digests of treated and untreated PTEN, low protein expression and purification yields of PTEN and the lower OMFP phosphatase activity of PTEN both comparative to VHR and absolutely, the line of inquiry was pivoted towards VHR functional proteomics. Due to this pivoting of line of inquiry and the time constraints of manual analysis of XICs and *de novo* sequencing, the other modifications and residues apart from Cys71 were not analysed via a systematic analysis of all PTEN residues and their percentage abundances between treatments and treatment molarity ratios with PTEN. Additional replicates would be required for Progenesis automated analysis, and further PTEN study was assessed to be an alternate line of inquiry to the one taken to deliver a systematic functional oxidation analysis and correlate function to the oxidation of key residues involved in activity and regulation of function, which was performed using VHR.

3.5.5. Discussion of oxidative treatment of VHR

3.5.5.1. Discussion of the combinatorial bottom-up mass-spectrometric analysis and phosphatase assays of oxidised VHR

This *in vitro* study is important for understanding the signalling of VHR and the potential for VHR *in vivo* to be oxidised upon damage from oxidative stress, inflammation and ageing. Having used a systematic, protein-wide approach to detected modifications *in vitro*, a novel, proof-of-principle workflow to quantify and visualise oxidative PTMs has been developed (Figure 28, Figure 29). A protein-wide, systematic functional oxidation analysis of a single protein also yielded multiple oxidised residues, which would be obvious targets to take forward for mutation analysis to determine whether the modifications seen may have an effect on OMFP

activity or on *in vivo* function, such as Leslie *et al* (2007) and Stumpf & Hertog (2016) demonstrate with PTEN as well as peptide ions to detect in *in vivo* samples using targeted mass spectrometry or multiple reaction monitoring.

Di- and Tri-oxidation of the Cys124 active site nucleophilic residue of VHR is a novel finding (Appendices 10, 11, 12), which indicates that biologically irreversible oxidation is possible for the active site of VHR, which could have implications in pathology as an epigenetic and pathogenic event, given the involvement of VHR in diseases such as non-small cell lung cancer (Wang *et al.*, 2011) and given that PTP active site modification can occur in cancer cells (Lou *et al.*, 2008). Lou *et al* (2008) demonstrate reversible and irreversible oxidation of PTP1B in cancer cells from intrinsic reactive oxygen species production, and assess *in cellulo* oxidation of PTP active site in relationship to cancer via immunoprecipitation of PTP1B and mass spectrometry analysis of abundance ratios between oxidised and non-oxidised active site residues.

The active site of VHR is comparatively less complex with regards to cysteine redox regulation (Denu *et al.*, 1998; Yuvaniyama *et al.*, 1996) than other PTPs, such as PTEN, as it has one active site nucleophilic cysteine without another local cysteine within 9Å with which to form a cysteine disulphide bridge, making intramolecular disulphide bridges improbable (Denu & Tanner, 1998).

Lou *et al* (2008) discuss the finding of irreversibly oxidised PTP1B active site Cys in a cancer cell line as having potential for signalling, including their finding that the active site Cys of PTP1B was preferentially oxidised, showing some level of selectivity as may be the case with a regulatory mechanism or may promote cancer progression, unless this merely shows a susceptibility damage of PTP active site Cys in cancer cells with high levels of reactive oxygen species.

The Cys124 residue was only detectable via TOF MS/MS due to the added mass of the modifications and a miscleavage event (Figure 32.), which may have been due

to the oxidation or nitration of a tyrosine on the Cys124-containing peptide interfering with the trypsin cleavage. Detecting the Cys124 peptide more frequently when it contains modifications (Appendices 10, 12) yet the peptide occurring at low abundances suggests an interaction between the phenomenon. Modifications are known to affect digestion such as methylation of lysine (Zee and Garcia, 2012). The trioxidised Cys124 was not seen in untreated controls suggesting that Cys124 oxidation was not a result of handling and methods. The non-modified Cys124-containing peptide was neither identified by Mascot®, via searching the XIC and spectra, or after both double digestion with an enzyme combination predicted *in silico* to yield an appropriate sized Cys124-containing peptide, or via a product ion scan of VHR for Cys124-containing peptides of varying cleavages, charge states and modifications. Although the Cys124 di- and tri-oxidation were identified, the abundance and relative abundance to other modifications is unconfirmed via ratios of modified to un-modified peptides due to the absence in reliable detection of the unoxidised control. A single instance in a single untreated control sample of an uncarbamidomethylated peptide was found for the cysteine of interest, which was not appropriate for the calculation of relative abundances. This information may be needed to assess the role of the active site Cys124 nucleophilic residue di- and tri-oxidation in the loss of activity recorded (Figure 25a., 26a.), and whether the active site nucleophilic residue is responsible, in part, alone or to what degree in the loss of activity upon treatment, regardless of the computational modeling correlations to non-nucleophilic residues (Figure 31.). To speculate further regarding the importance of Cys124 in the inactivation of VHR, VHR is known to form VHR-VHR dimers (Pavic et al, 2014) if this is still possible and favorable *in vitro* with GST tagged VHR, this points to the potential of non-nucleophilic residues in the activity reduction of VHR upon treatment with oxidants, by the action of modified residues to reduce or increase VHR dimerization, where VHR dimerization can reduce VHR activity (Pavic et al., 2014).

The identification of oxidation, chlorination and nitration of Tyr138 (Figures 28, 29, 30; Appendices 11, 12) may merit further investigation of this residue due to Tyr138 phosphorylation by ZAP-70 being involved in VHR activation (Alonso et al., 2003) and the mediator modeling indicating Tyr138 is a significant mediator between oxidant concentration and VHR phosphatase activity (Figure 31.), and given that nitrotyrosine is suggested to mimic phosphotyrosine (Mallozzi et al., 2001).

Finding multiple modification classes, that of oxidation and nitration on the same residue of known functional importance (Alonso et al., 2003), also suggests the potential the possibility of competitive PTM processes *in vitro* and, to speculate, suggests the potential for interaction between multiple signalling pathways – oxidation, phosphorylation and nitration *in vivo*, given that Tyr138 is phosphorylated *in vivo* (Alonso et al., 2003). Evidence for interaction between PTM types has been suggested between phosphorylation and methionine oxidation for proximal methionines to serine, threonine and tyrosine (Rao et al., 2013), and also between phosphorylation and ubiquitination (Nguyen et al., 2013), yet these examples are of interactions between pathways and for a protein, not on the same residue. Chiarugi & Buricchi (2007) review the interaction of tyrosine phosphorylation and reversible oxidation and the potential opposite effects of these signalling pathways, and Mallozzi et al (2001) discuss potential for nitrotyrosine to mimic phosphorylation.

Further research would need to be carried out to see whether oxidation and nitration of Tyr138 have an effect on activity, deactivate VHR, permanently activate it or affect VHR PPI. To support speculation regarding *in vivo* function, there is already precedent for this with the tumour suppressor signalling protein p53 where nitration of Tyr327 promotes p53 oligomerisation and activation (Yakovlev et al., 2010), which was nitrated with the NO donor diethylenetriamine.

Activity of VHR upon sin-1 oxidation decreased to a similar percentage to multiple oxidations abundances- whereby, the level of abundance of particular modifications

are correlated with the level of activity loss. Multiple oxidations were present at a higher abundance percentage than the percentage loss of phosphatase activity. Thus, the abundance and activity measurements do not allow the resolving of which residues and modifications alone, or in concert, have a role in one or multiple mechanisms of inactivation or loss of activity of VHR. Without further investigation, further statistical modeling, and deletion analysis, the modifications which affect enzymatic activity are not readily discernable.

Activity of VHR upon TNM oxidation of a comparable molar ratio to sin-1 produced a larger array of modified residues, as well as increased abundances, particularly for the Tyr101 and Cys171 residues, specifically Tyr101 nitration and Cys171 trioxidation. TNM treatment inactivated the enzymatic activity of VHR at all molar ratios of treatment used (Figure 26a.). TNM and TNM molar ratios used were rationally selected to generate levels of tyrosine nitration that would be discernible and statistically significant from the noise for their effect on PPI arrays, where effects may be linear and non-multiplicative. The TNM molar ratios were also selected after having performed the sin-1 and HOCl treatments noting the effects of these treatments on band loss, activity loss, and percentage abundances of the modifications identified via XIC, comparatively. In order to generate nitrations of the abundance intensity for PPI arrays protein loss, fragmentation and aggregation can be seen (Figure 26b.), therefore a strategy to separate sufficiently nitrated, intact VHR from both aggregates and fragments, to assess the effect of modified VHR with substantial nitration would be required. This in itself, may not be sufficient to identify and resolve the specific effects of specific tyrosine nitration, or whether those PPI identifications would be due to a phosphate mimicking or phosphate-analogous property. TNM modification provided the identification of the VHR active site nucleophilic residue, where there is reason to suggest that the additional modification to the Cys124-containing peptide was due to the abundance levels of modification

from the TNM, and the properties of TNM as an oxidant. Utilising compounds that do not exist without intervention *in vivo* such as TNM have utility, as their chemical properties have potential to investigate potential biological interactions. Comparative information regarding compounds found *in vivo* such as peroxynitrite and HOCl to TNM also provides some context as for the modifications found and the abundances they are found at, and allows the *in vitro* modification space of a protein to be more fully searched and mapped, as well as profiling the damage of a compound not found without intervention in biology with regards to its aggregates, fragments and modifications and peptides associated with this non-biological compound.

Protein loss from the VHR-GST gel band (Figure 25b, 26b.) along with marked aggregation and fragmentation, including for treatment regimes that did not produce high abundances of modifications, does not enable the elucidation of what activity loss was due to the modifications, and what activity loss may be due to aggregation or fragmentation – although the result from the TNM densitometry and percentage OMFP activity (Figure 26a.), may suggest that as a larger decrease in activity is seen comparatively to the full lane densitometry and VHR-GST band densitometry, that the differences in activity may not be entirely correlated to the loss in band intensity.

Between sin-1 and TNM treatment of VHR-GST similar fragmentation and aggregation patterns, and fragments and aggregates are observed (Figure 25b., 26b.) regarding the sizes and appearance of non-VHR-GST bands in the Coomassie stained gel. Where both sin-1 and TNM treatment of VHR-GST displays multiple higher-than-VHR-GST molecular weight bands at the entrance of the running gel, that is not present in the untreated, and also decreases in intensity upon increased treatments, following a trend of all bands decreasing in intensity. Comparatively between sin-1 and TNM the lower-than-VHR-GST molecular weight bands appear similar, and also display a reduction in intensity as treatment molar ratio increases (Figure 25b., 26b.).

Patterns of oxidation between residues, as the molar ratios increase, are, for some cases, non-linear which, to speculate, may suggest properties such as specificity, hyper-reactivity or conformational change of the protein (Figure 27, 28).

The TOF MS/MS experiments performed suggest that tyrosine nitration, via sin-1 and TNM are partially selective, with some residues having a higher relative abundance of modification than others – but against a background of additional tyrosine nitrations and tyrosine oxidations. TOF MS/MS and other methods that assess protein-wide, individual residue resolving modifications, are suitable for the assessment of treatment specificity and residue selectivity of oxidants. Further, the results of TNM and sin-1 treatment showing numerous oxidations, and only partially selective nitration, which would inform future experimental design, as TNM and sin-1 have been previously characterised as selective nitrating agents, and the effects of TNM and sin-1 associated with the nitrating selectivity that was characterised without protein-wide, individual residue resolving. Whereby some of the functional differences observed upon tetranitromethane and sin-1 treatment, one could reasonably hypothesise is due to either modifications that are not presently searched for or due to multiple modifications.

Peroxynitrite has been shown to react with thiols and nitrate tyrosines (Radi, 2013), which confirms predictions from MS and analysis software. For a more selective nitration in order to selectively modify particular residues, it has been reported that electrochemical treatment (Kendall et al., 2001; Richards et al., 1994) has greater selectivity although additional validation may need to be done to investigate whether other methods are as selective as has been previously reported. Comparative analysis of treatments that was comprehensive would contain searches for all modifications known via a systematic use of multiple searches and error tolerant searches to search for all possible modifications and higher resolution and

accuracy MS, in addition to flagging un-identified ions and *in silico* prediction based on the masses of un-matched peptides.

The systematic approach to mapping and quantifying protein modification that has been outlined imposed time constraints for a skilled operator. The ability of a skilled operator versus an automated analysis may be investigated to differentiate between medical classes of patients, and if and where a manual approach outperforms, and what the costs and risks of this are within the clinical pipeline and healthcare delivery. Taking into account the number of PTMs, treatments, treatment ratios, proteins and *in vitro* and *in vivo* sample types – a systematic functional analysis with relative quantifications may require automation at the bench top with liquid handling robots, an automated pipeline between predictive algorithms and raw data analysis programs, automated validation of peptides, automated relative quantification and modeling and data visualization software build into the pipeline downstream, with a focus on clinical development and outcomes.

The modifications discovered for VHR (Figures 28, 29, 30; Appendices 10, 11, 12), independently of the availability of the active site modification abundance data, have potential value for modifying VHR at other residues of importance such as Tyr138, and as potential VHR-based peptides to search for *in vivo* that may be correlated or causative for that *in vivo* state. If the VHR active site peptide identification is a constraint, other VHR peptides may be an appropriate proxy as a biomarker. Other signalling proteins in the cell signalling pathways of interest could also be assessed as proteins to sequence via MS and points to intervene in, within the cell signalling pathways.

In the context of VHR primary structure, and specific oxPTMs, modified residues were identified between Tyr38 and Cys171 (Figure 28., 29., 30; Appendices 10, 11, 12). The range in number of modifications identified between sin-1, HOCl and TNM may have been influenced by the concentration and molar ratio of the treatment,

including peroxyxynitrite concentration over time via sin-1 generation, and that the HOCl data was analysed via Progenesis and thus was not manually searched for modifications and peptides that had been predicted and previously seen in other samples, as was implemented in the manual analysis. Proceeding along the VHR primary sequence Tyr38 oxidation, Tyr38 nitration, Pro49 oxidation and His58 oxidation were identified at a <10% abundance with all sin-1 treatments implemented. For Tyr38 nitration, TNM treatments of over 1:150 produced dose dependent increases in TNM >1% with TNM 1:300 producing an abundance of >5%. HOCl treatment yielded Tyr38 chlorination identification, automated analysis of abundances identified <10% chlorination. HOCl produced >10% oxidation at His58 for all treatment molar ratios. Met69 is the amino acid across the sin-1, TNM and HOCl treatment replicates to give a >10% modification, with Met69 dioxidation upon sin-1 treatment of 1:300. The HOCl replicates show an increased Met69 dioxidation in the control of >10% with decreased Met69 dioxidation in treated, alongside an increase in Met69 oxidation in the HOCl treatment replicates. Along the primary sequence of VHR, His70 for both the sin-1 and TNM treatment replicates exhibits a pattern of low His70 oxidation in the control, with dose-dependent decrease in sin-1 and <1% modification in TNM, followed by a spike at sin-1 1:300, and TNM 1:1000, displaying a pattern of decrease (including dose-dependent decrease) followed by a spike in modification abundance. This could be part of a larger pattern, and may be due to either competitive local scavenging and reaction with oxidants, may be due to initiation of oxidant requiring a local oxidation at a local residue, or a conformational change only present at the higher concentrations which increases oxidant access or alters local reaction kinetics. Tyr78 has low levels of oxidation, and low levels of nitration across the treatments and treatment molar ratios – as Tyr85 and Tyr101 are oxidised and nitrated – this points to sequence and conformation specific factor involvement at this residue. Lys79 modification levels are low in both sin-1 and TNM and the modification

was not identified in HOCl by Mascot and Progenesis analysis alone. Tyr101 has <10% oxidation and nitration identified upon the sin-1 treatment molar ratios and replications performed, and <10% chlorination for the HOCl treatments. The TNM treatments performed, for Tyr101, yielded a dose-dependent, non-linear increase in Tyr101 nitration, reaching near-saturation of Tyr101 residues, and doing so preferentially versus Tyr101 oxidation. Lys116 has low levels of oxidation across sin-1, TNM and HOCl, with HOCl having increased Lys116 oxidation comparatively; noting that the HOCl untreated samples also have a baseline Lys116 oxidation higher than all the other treatments. Pro132 oxidation is not identified as modified in the sin-1 treatment replicates, Pro132 oxidation is identified at <5% in the HOCl treatments and replicates, and the TNM treatments identifies Pro132 oxidation in the TNM 1:150 and TNM 1:1000 treatment samples at below <10%, with some dose-dependent features. Tyr138, the residue known to interact with ZAP-70 and involved in the activation of VHR, shows <1% oxidation in sin-1 treatments and replicates, with Tyr138 showing nitration in the sin-1 untreated control, and >10% nitration in the 1:75 sin-1 treatment. The Tyr138 nitration was not seen in the TNM untreated control so, to speculate, may have been artefactual, and may be due to the residues reactivity to RNS. Met140 oxidation in the sin-1 treatments and replicates takes a dose-dependent increase at <10% with the exception of the sin-1 1:300 samples. To speculate, the decrease in the sin-1 1:300 Met140 oxidation, given the linear and dose-dependent increase may be due to the reduced sequence coverage and reduced identification of peptides, and the reduced sample protein in the band cut out for MS analysis. Met140 dioxidation in sin-1 is <10% and variable between treatment molar ratios. Met140 oxidation in TNM displays some oxidation in the untreated control, similar to the sin-1 replicates, yet at increased abundance, with Met140 oxidation increasing dose-dependently until a plateau after TNM 1:75, which to speculate, may be due to another modification that occurs at this TNM 1:75 and after that changes VHR conformation and thus reducing

the availability of the VHR molecules Met140 to oxidation and further oxidation to methionine sulphone. In the HOCl treatments and replicates Met140 oxidation is higher in the untreated than the other treatments and controls, where the abundance is variable around ~40% across the treatments, showing a plateau and/or abundance-limiting factor. Met140 dioxidation, whilst being <1%, excluding sin-1 1:10, exhibits an abundance of ~10% in the HOCl replicates including the untreated control, and this Met140 dioxidation abundance also exhibits a constancy or plateau feature, which may support speculation around a conformational change that may occur upon oxidation. Met141 oxidation follows a dose dependent increase across sin-1 molar ratios, and is also modified in the untreated, reaching a ~50% abundance at sin-1 1:300. Upon TNM treatment, Met141 has a variable, plateaued modification profile at <50%, and HOCl Met141 oxidation also reaches a plateau at ~50%, this plateauing feature and maximum abundance between treatments and the range of molar ratios used, given the differences in oxidation treatment reaction mechanisms, may, to speculate, further suggest a structural-conformational change occurring. Met141 dioxidation in sin-1 was identified in the untreated control, with a variable-function increase in the treated samples, with a peak abundance in sin-1 1:10 higher than all the recorded Met141 abundances. For sin-1, combining the Met141 oxidation and dioxidation there is a dose-dependent combined increase, alongside TNM. In both sin-1 and TNM 1:10 and 1:300 these treatments show higher peaks comparatively with regards to the other treatment ratios, to speculate, this may be due a property of the ratios used, or may indicate multiple distinct conformational changes that occur around these molar ratios between these treatments. Comparatively there is a general trend for Met141 oxidation to be increased compared to Met141 oxidation, and this is also true for Met141 dioxidation. Met140 and Met141 modifications, may, to speculate, affect ZAP-70 interaction with Tyr138, through potentially altering the local thermodynamic conditions or by being involved in Tyr138 modification.

Met145 was identified as oxidised in sin-1 with a dose dependent increase with a high starting percentage in the untreated control, which was the highest starting modification abundance across modifications for sin-1, and small increases in abundance, with Met145 dioxidation not being identified in the treatments and replicates. Met145 in TNM exhibits <10% modification, and does not exhibit the high abundance in the untreated control – however the abundances of Met oxidation across the VHR sequence – Met69, Met140, Met141 and Met145 do, when their abundances are combined, appear to show a trend for the basal level or opportunistic and artefactual level of methionine oxidation, which, to speculate, may point to the gross scavenging properties of methionine in VHR and gross artefactual oxidation in the experimental workflow used. HOCl treatments and identification via Mascot and Progenesis without searching the TIC manually for both peptides predicted *in silico* or seen in other samples, did not identify Met145 oxidation. Cys171 was found to be dioxidised at ~<1% for sin-1, TNM and HOCl, which, to speculate may be due to the dioxidation being further oxidised to trioxidation, and the stability of dioxidised cysteine. Sin-1 exhibited, for the treatments and replicates, <10% Cys171 trioxidation, TNM exhibited a low Cys171 trioxidation in the untreated, that was higher than the sin-1 or HOCl untreated control, with TNM treatment Cys171 trioxidation increasing to ~75% at TNM 1:150. The abundance of Cys171 upon TNM treatment both demonstrates the capacity of TNM as an oxidant in addition to being a nitrating agent, displays the potential for high abundance cysteine modifications in VHR and in VHR following TNM treatment, and shows the sensitivity of this particular cysteine, Cys171 which may have a regulatory role.

From the perspective of the protein sequence of VHR, the limitations of identifying amino acid modifications leaves out information as to which amino acids are in the vicinity of other amino acids in the secondary and tertiary structure, which may have a role in altering the environment for reaction to oxidants, acting as a catalyst, and

which also may have a role in secondary oxidation from other amino acids in the secondary and tertiary structure. The crystal structure of VHR is available (Yuvaniyama et al., 1996) but a molecular dynamic study with the modifications found would need to be performed, and may be an area for future study. Primary structure information, of identifying amino acids at a distal time-point to the modification process also does not query the order or reaction mechanism for the modification, or the changes in which amino acids may be in the appropriate range from the amino acid of interest when any secondary, tertiary and conformational changes occur. Some amino acid modifications, due to the characteristics of the peptides they are present on, the charge and polarity of the peptide and amino acid, may be less likely to be identified, and some modifications may have less unique characteristics to assist in validation – or may be present at levels that do not assist identification. In addition to Tyr138, to speculate, other tyrosines within VHR may also be involved in regulation of VHR activity and conformational change, and these may involve PTM competition and regulation dynamics between oxidation, nitration and phosphorylation. By comparative analysis to PTEN, and the mapping of PTEN PTMs, as a comparative PTP speculative analysis, lysine residues within VHR, may be relevant as these have been identified as modified in PTEN (Salmena et al., 2008) – and may have similar roles, particularly as VHR and PTEN have been identified as having translocated to the nucleus – this comparative PTM analysis may apply across residue types.

The challenge to get relative-quantification and thus differential relative-quantification data for VHR Cys124 may have importance for any biomarker approach that included a relative quantification of unmodified to modified Cys124 containing residues. The intensity of the signal and rarity of the peptide, in the data collected, may also pose challenges if the Cys124 peptide were to be utilised as a biomarker peptide.

Alternative and additional avenues, that were close in scope and process to what was performed, were as follows: An extensive manual analysis of HOCl XIC, additional treatment concentrations optimising intactness and/or protein or co-optimising intactness of protein and the abundances of Cys trioxidation and Tyr nitration, co-optimisation for selective nitration, nitration abundance and intactness of protein, H₂O₂ treatment of VHR, more extensive machine learning and computational modelling may be alternative and additional avenues of development. The avenues of development taken were taken in context of both the multi-centre collaboration with Imperial College, and their development of active site cysteine inhibitors for PTPs, and in the potential of the discovery of the effect of oxPTMs upon protein function, both enzymatically and on PPIs.

The avenues that were taken that did not yield results or were deemed, from the experiments performed, ineffective were as follows: The in solution digestion of proteins, as this gave a lower sequence coverage, in addition to not allowing visualisation via Coomassie-stained SDS PAGE. The double digestion of VHR for the purpose of identification and relative quantification of the Cys124 active site peptides, for the elucidation of the modification state/s Cys124 takes, and specifically what modification states/s Cys124 takes in the context of functional proteomics and the corresponding phosphatase activity for a particular treatment regimen. The product ion scanning for the purpose of identification of the Cys124 after single enzyme and double enzyme digestion.

Modelling of the relationship between the percentage abundances of modifications relative to the relationship between the percentage OMFP phosphatase specific activity and molarity of the treatment yielded models of relationships for the effects of modified amino acids as single mediators of activity and the effects of modified amino acids were the effect of one mediator had a forward effect on the second mediator amino acid, as multivariate analysis. The single mediator model

gave significant mediation effects for Tyr38 (Ox), Pro49 (Ox), His58 (Ox), Met69 (DiOx), His70 (Ox), Lys79 (Ox), Lys89 (Ox), Tyr101 (Nitro), Lys116 (Ox), Tyr138 (Nitro), Met140 (Ox), Met141 (Ox), Met141 (DiOx), Met145 (Ox), and Cys171 (Ox). The mediation model may assist with prioritisation of screening and validation of amino acids for functional effects and for building predictive models for functional predictions (Figure 31). Multiple mediation effect modelling of amino acid modifications on OMFP phosphatase specific activity in relationship to molarity of treatment modelled many relationships above a 99% confidence level (Table 8). The multivariate modelling of multiple mediators gave the following relationships: A forward effect of Lys70 (Ox) on Met141 (Ox) had the largest forward effect, yet Met141 is on an α -helices with Lys70 being part of an unstructured loop region at a distal location. The second largest forward effect was that of Tyr138 (Ox) on Met141 (Ox), which may be of interest as both are located in an adjacent position on the same side of the same α -helices. Given the role of Tyr138 in ZAP-70 mediated VHR activity, a greater understanding of the oxidation dynamics of Tyr138 may be of utility with regards to the potential role of the environment of Tyr138 on Tyr138 regulation, and the role of oxidation in both regulation of phosphatase activity, phosphorylation and nitration of Tyr138. To speculate, as there are 3 methionine residues (Met140, Met141, Met145), there may have been an evolutionary pressure for readily oxidised residues to be co-located with the regulatory Tyr138 residue. Lys79 (Ox) has the third largest forward effect in the model (Table 8) on Tyr85 (Nitro), which to speculate may be due to the dynamic, entropic, vibrational and flexible properties of the region, which is partially identified as an unstructured loop in the crystal structure, and partially a β -sheet flanked by unstructured regions. Tyr138 (Ox) also has a forward effect on Met140 (Ox) and Met145 (Ox) in addition to Met141 (Ox), which is located on the same α -helices, although Met140 (Ox) is on the other side of the α -helices, and Met145 (Ox) is in the unstructured sequence prior to the α -helices. Tyr138 (Ox)

has a forward effect on Tyr138 (Nitro), which to speculate may be of interest to understand and utilise the inter-relation between oxidation and nitration of Tyr138 for VHR activity, VHR phosphorylation and signalling pathway predictions and modulation. Met69 (Diox) also has a forward effect on His70 (Ox) the sequential residue in the multiple mediator model. To conclude, mediator modelling may direct further efforts regarding the elucidation and effective use of the relationships between amino acids, the mediator model also highlights that whilst some mediators have may have a low, negligible or non-significant mediation effect, they may mediate a forward effect in combination with a partner mediator.

The forward effects in the mediator model may be due to correlation due to advanced modification occurring at both residues at specific molarities, due to the direct effect of a residue on another residue by creating an environment for the modification of the second residue that is sequentially next to amino acid or adjacent to the amino acid in secondary or tertiary structure, or where a modification in the first residue may modify the secondary or tertiary structure which either exposes a residue to the reactant or creates an environment that increases the susceptibility to reaction.

Regarding biological validation – with the *in vitro* first approach, there are multiple avenues for biological validation – revolving around assessing which modifications occur during *in vivo* states, whether delivering modified protein or inhibiting residues modified has an *in vivo* effect that is relevant and valuable. Additional biological information on the VHR interactome was gathered to discover VHR PPI via *in vitro* protein-protein arrays and *in cellula* VHR co-immunoprecipitation, to create additional biological context.

The relevance of the systematic functional proteomics of PTEN and VHR oxPTMs to the body of work was for the treatment of samples that would be suitable for assessing the effects of oxPTM and specific oxPTMs in PTEN and VHR upon

PPI, through sample generation with the appropriate modifications, appropriate purity and intactness of the protein. PPI arrays may provide both a platform to query with protein modified with oxPTMs that had also been analysed via MS, and would also yield potential interactors to further screen and utilise in bespoke arrays to query the effects of the oxPTMs of the protein of interest against the interaction candidates – where sin-1 was first selected for PPI investigation, with a pivot in the line of inquiry to investigate TNM treatment prior to potential PPI investigation utilising TNM after results showed higher percentages tyrosine nitration, although these increases in tyrosine nitration were coupled with i) using a non-biological treatment and ii) substantial activity reductions that may be inappropriate for correlating activity changes to modifications, and these modifications to PPI interactions by correlation. Co-immunoprecipitation may provide a platform to discover potential interactors that are not present on a PPI array, and yield candidates for further study on bespoke arrays queried against protein samples with oxPTMs. As oxidations have been generated at levels that may be sufficient to query PPI arrays for differential signal intensity, in particular Tyr101 upon TNM treatments of 1:150, 1:300 and 1:1000 molar ration, for nitration, Cys171 trioxidation upon HOCl treatments of 1:30 and TNM 1:10, 1:75, 1:150 and 1:300 and Tyr85 nitration from the TNM treatments of 1:75, 1:150, 1:300 and sin-1 treatments of 1:75, 1:150 and 1:300. Challenges for these treatment samples analysed by MS would be similar to that of functional proteomics challenges when comparing MS to OMFP phosphatase assay, in that there are multiple amino acids and peptide regions not identified and multiple residues modified to large percentages, making the discernment between the effects of several modifications challenging without resolving the differences empirically or via modelling.

3.5.5.2. Discussion of domain regions of VHR oxidised and nitrated by sin-1, HOCl and tetranitromethane

Multiple, novel *in vitro* oxidative modifications of VHR have been elucidated. The modifications have a distribution, this includes regions that are more heavily modified such as the regions between Tyr138-Cys171 and His58-Tyr78 indicative of hyper-reactivity of the residues or specificity on the part of the oxidants (Figure 28, 29, 30). These modifications appear to fall within the major catalytic unit of VHR, with the residues His58-Tyr78 being on a putative β -domain, taking into account that the β -sheets are parallel and not anti-parallel. The modifications in the Tyr138-Cys171 appear to be within a α -domain consisting of 3 α -helices, with no modifications identified in the C-terminal tail region. To speculate, oxPTMs may alter the domain structure, domain-domain interaction, PPI, VHR-biomolecule interaction, VHR-inhibitor interaction, catalytic function and complex formation through altering the distance between and angle of domains, altering whether a domain is formed from primary sequence and the distance and angles between domain regions and unstructured regions including unstructured loops. Evidence of nitrotyrosine oxPTM affecting protein function include Cassina *et al* (2000) who demonstrate tyrosine nitration inhibiting protein function via altering protein conformation and steric hindrance in Cytochrome c. There is also evidence of the effect of protein oxidation on protein interactome, including protein therapeutics, whereby methionine oxidation weakened binding to protein binding partners, which was assessed via surface plasmon resonance (Pan *et al.*, 2009).

3.5.5.3. Discussion of oxidative and nitrative modifications in the context of crystal structure information for VHR

Mapping the modifications on the crystal structure of VHR (Figure 38, 39) may have utility for assessing the location, co-location and distribution between residues and treatments – taken alongside the informatic mediator modelling (Figure 31, Table 8) represents an informatic, physical and chemical approach.

If the two outermost α -helices that flank the α -helices where the Tyr138 is situated were to alter their position in relationship to the Tyr138 α -helix this may alter ZAP-70 binding, Tyr138 phosphorylation and the binding specificity and interaction likelihood with ZAP-70, which on a cell signalling level, may downregulate ERK and the Raf/MEK/ERK pathway, and downregulate cell growth, angiogenesis, survival and cell motility. Modifications to the domains surrounding Tyr138 may, to speculate, affect the binding of a Tyr138 inhibitor.

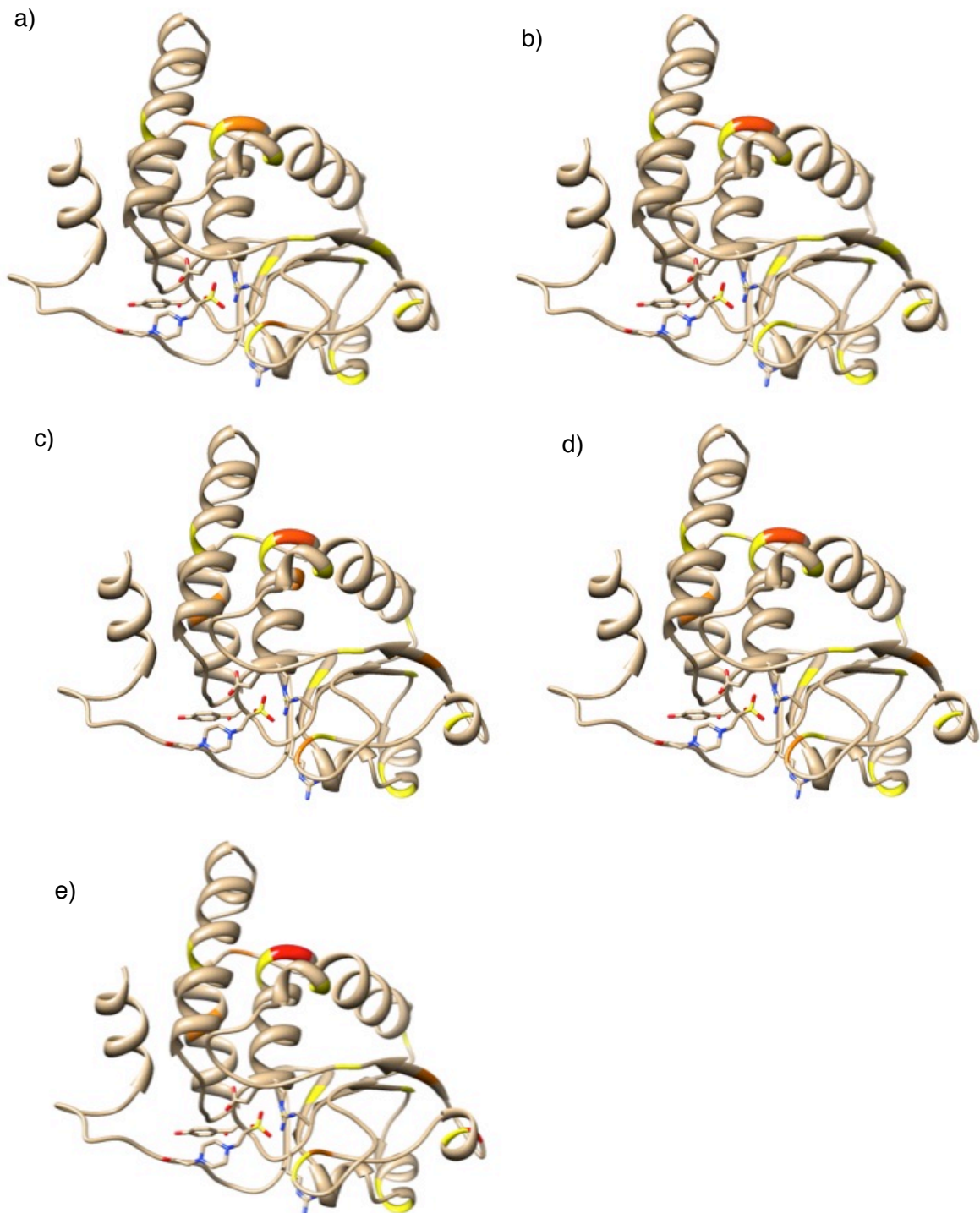


Figure 38. Modifications found in sin-1 treatment of VHR mapped onto VHR crystal structure mode

The non-nucleophilic regulatory active site cysteine identified as modified by Mascot search is highlighted in green on the 3D structure of VHR. The structure is based on VHR X-ray crystallography data (UniPROT, 1VHR) and displayed using University of California San Francisco Chimera (Pettersen et al., 2004). a) VHR-GST untreated b) sin-1:VHR-GST 1:10 c) sin-1:VHR-GST 1:75 d) sin-1:VHR-GST 1:150 e) sin-1:VHR-GST 1:300 Modified residues are coloured with Identified-24% as yellow, 25-49% as orange, 50-74% as orange-red and 75-100% as red; active site residues coloured and active site residue structure shown along with substrate. The percentage abundances of different modifications were aggregated for each residue.

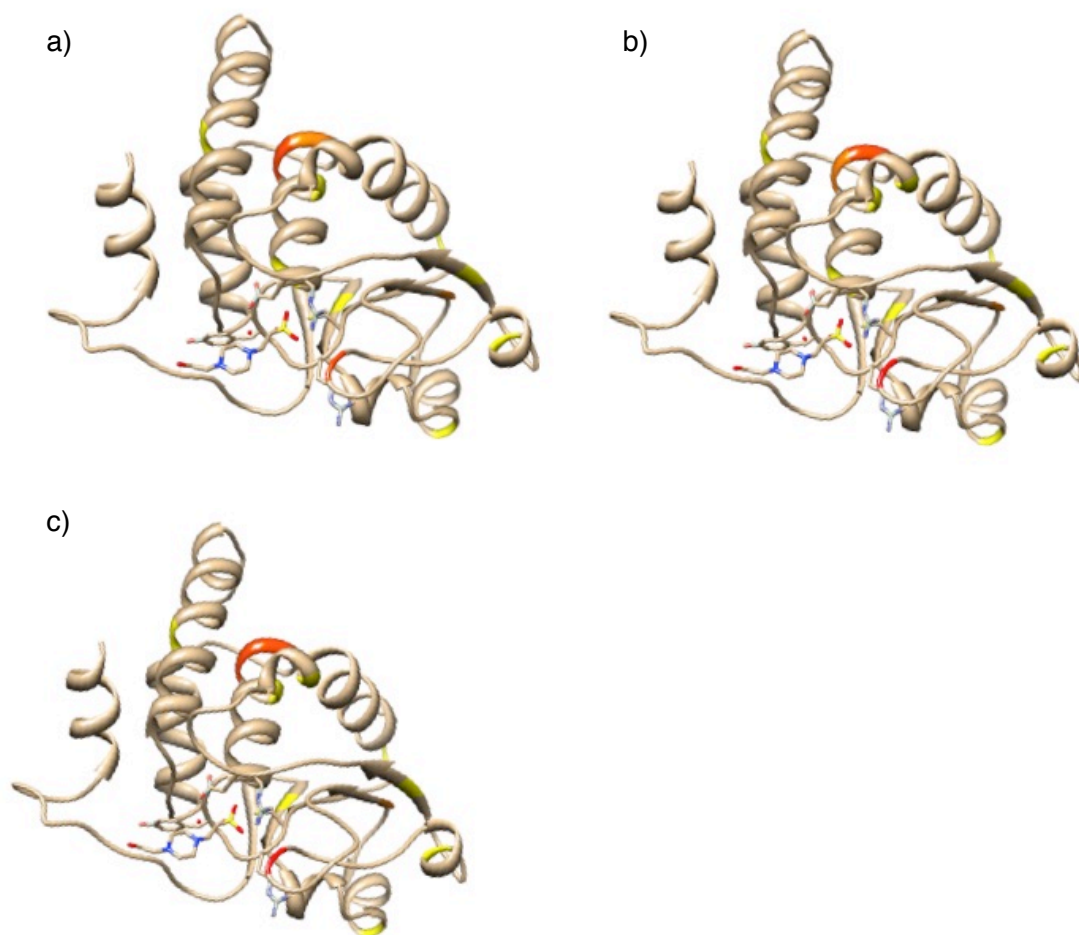


Figure 39. Modifications found in HOCl treatment of VHR via automated analysis with Mascot and Progenesis mapped onto VHR crystal structure mode
 The non-nucleophilic regulatory active site cysteine identified as modified by Mascot search is highlighted in green on the 3D structure of VHR. The structure is based on VHR X-ray crystallography data (UniPROT, 1VHR) and displayed using University of California San Francisco Chimera (Pettersen et al., 2004). a) VHR-GST untreated b) HOCl:VHR-GST 1:30 c) HOCl:VHR-GST. Modified residues are coloured with Identified-24% as yellow, 25-49% as orange, 50-74% as orange-red and 75-100% as red; active site residues coloured and active site residue structure shown along with substrate. The percentage abundances of different modifications were aggregated for each residue. Modifications were identified by Mascot search, and parsed to Progenesis for automated extracted ion chromatography.

Figure 38 and Figure 39 map oxidative modifications at different residues, with their abundances (colour coded) across a range of oxidative treatment molar ratios. The unstructured loops of VHR appear locally to the active site cleft, and to speculate these may have importance for binding, where the residue most local to the active site is modified by both sin-1 and HOCl treatments over a range of concentrations (Figure 38, 39.). Additional molecular modelling and biophysical analysis may be required for

validation of movement constraints of the loop region and any putative inhibitor or regulatory role.

To speculate, from analysis of the crystal structure there appears to be two tertiary putative domains, -a β -domain and α -domain - of VHR with the VHR active site residues situated at the nexus of two putative secondary structure domains – to speculate further – this differential and dual domain dynamic at both the secondary and tertiary level may aid regulation and be mechanistically explanatory as to how non-active site PPI and modifications may regulate the active site residue and active site cleft – where the one putative domain –contains the β -domain of four parallel β - sheets and one anti-parallel β sheet and another putative domain with five α –helices.

3.6. Conclusions on the novel discovery, workflow and process for functional proteomics of PTEN and VHR

The advances in both the results from functional proteomics utilising TOF mass spectrometry, SDS PAGE and assaying of enzymatic activity, and understanding of the applications for and limitations of these techniques as part of a pre-clinical workflow and platform can be seen to have implications and potential for other proteins, omes, and clinical applications. In particular this research points to the building of screening lists to extract value from *in vitro* results for *in vivo* peptide and oxidation screening by way of building lists of candidates to search for *in vivo* (Table 11, Appendices 8, 9, 10, 11, 12). This would not be an extrapolation of *in vitro* results to *in vivo* but a utilisation of *in vitro* and *in silico* techniques to search for *in vivo* peptides and oxidations where attempting to find *in vivo* peptides and oxidants of low abundance in mixed samples without a list of potential peptides and oxidants to scan or probe for, may be challenging depending on the technology used. For clinical

utility, additional workflows would be required, and would involve simplification and automation.

Protein	Number of residues identified as modified	Number of types of modifications identified
PTEN	10	6
VHR	16	12

Table 11. Summary of residues identified as modified and number of types of modifications identified in PTEN and VHR

Operationally, non-sequenced PTEN and VHR regions including the active site residue, manual sequencing and XIC, non-robotic assaying and non-robotic pipeline were operational constraints to deliver the potential. Constraints on manual validation were considered prior to further investigation with computational modeling and selection of protein and peptide candidates for PPI investigation, and prior to incorporation in databases of modifications (Appendices 9., 10., 11., 12) and comparative analysis with protein crystal structures. With automated XIC and an automated pipeline, more focus could be applied downstream with additional treatments, additional proteins, and *in vivo* samples.

Future work to assess PTEN and VHR modifications *in vivo* would be an interesting next step, in addition to the understanding *in vitro* of the interactomes of PTEN and VHR, and how oxidation affects the interactomes of PTEN and VHR.

Chapter 4

CX5R phosphatase arraying and array interactions

4.1. Introduction

4.1.1. Development of high resolution, low sample size antibody and protein pair arrays for protein interaction and oxidation studies

To improve the reproducibility, resolution and sample requirements of protein-protein array technology the factors that are available for optimisation are the workflow, sample type and quality, and the technology used. To develop an understanding of oxidation on protein interaction, samples and reagents are required to be developed that are suitable for the robust detection and investigation within an array platform and workflow.

Technology to develop includes the delivery of sample and probing solution to the surface of the array without the introduction of artifacts that might obscure array spots and signal, produce false-positives.

Sample size can be reduced, which would be beneficial for performing multiple experiments with a limited sample and with absolute sample size limitations for health and regulation of the patient or size of sample needed to be produced. Considerations for sample size including having enough sample to cover the spots and array without evaporation leading to salt crystal formation and unequal probing. Sample size reduction may also give cost benefits for the use of expensive reagents.

The aims of this research included developing arraying and array probing parameters and optimise them for studying protein-protein interactions with the Dynamic Bioarray biochip technology as well as optimise concentrations of arrayed and probing biomolecules. Dynamic Bioarray chips were tested versus the standard Lifterslip technologies for resolution and artifacts. Optimising the resolution and amounts of antibodies and proteins alongside the concentrations of the protein solution and arraying solution will be critical for proteins that have low binding affinity and to detect minor changes in protein-protein interaction.

Oxidised samples that were meaningful for testing specific hypotheses for oxidised protein-protein interactions may also be useful to develop. Considerations would include the mitigation or filtration of aggregates and fragments, in order for protein-protein interactions to be assessed for a specific protein and not an analysis of the fragments and aggregates of this protein, which would be testing different hypotheses. Utilising different oxidation treatments and profiling the modifications and modification abundances would also be a consideration for correlating specific modifications, modification signatures and modification abundance to protein-protein interaction signatures. Another consideration would be to be able to generate sufficient modification in residues of interest without aggregating or fragmenting the protein, whilst giving differences between samples that are detectable via a protein-protein array method.

4.1.2. Library array optimisation and screening for PTEN and VHR

The high-throughput screening of protein libraries for interactors for proteins of interest PTEN and VHR may be utilisable for understanding signalling pathways, additional protein functions for therapeutic use for regenerative therapies, and for the designing and engineering of artificial cells for industry and biotechnology. Additional utilisation of protein library arrays may be to screen peptides versus proteins, including peptides with oxPTMs.

Additional considerations for library array screening in addition to considerations for the improvement of protein-protein arrays in general are an increased focus on reproducibility and ability to extract value from the large-volume output, and to validate, perform complimentary experiments and act on information in a timely and effective manner for pre-clinical and clinical development.

4.2. Results

4.2.1. Dynamic Bioarray chip versus Lifterslip library screenings

Collaborating with Dynamic Bioarray (Doctor Ekaterina McKenna) who manufactured the Dynamic Bioarray slide, the Dynamic Bioarray chip was tested versus the Lifterslip coverslip (Thermo fisher, UK). Both the Dynamic Bioarray chip and the Lifterslip coverslip are technologies for incubation of protein-protein arrays that ensure that liquid samples cover the array spots with a particular volume of sample across the duration of the incubation period. Lifterslip coverslips have been demonstrated for use for protein arrays, an example of which is Feijs *et al* (2013), and Dynamic Bioarray sought to improve the quality and reproducibility of array incubation and also reduce sample sizes with the Dynamic Bioarray chip.

Prior to the optimisation of local spot conditions for arrays arrayed using the sciFLEXARRAYER and library array screening of Invitrogen ProtoArrays® for potential interactors and interaction dynamics, a comparison was performed between array incubation technology – Lifterslip cover slips compared to Dynamic Bioarray chips. The comparison was performed with arrayed PTEN-GST, with primary and secondary antibody probing of the array (Figure 40d, Figure 40h).

The Dynamic Bioarray slide incubation displays some global non-uniformity, including at the edge of the slide and chip, and a spot intensity that is stronger than the Lifterslip for Figure 40 a) and e) with increased uniformity at the block level in comparison to Figure 40 e). Lifterslip incubation displays regions of stronger and weaker spot intensity and smearing artifacts, dark regions and non-uniformity at the block level (Figure 40.). The decision was made to take forward the Dynamic Bioarray slide for use with arrays spotted with the sciFLEXARRAYER and library array screening of Invitrogen ProtoArrays®

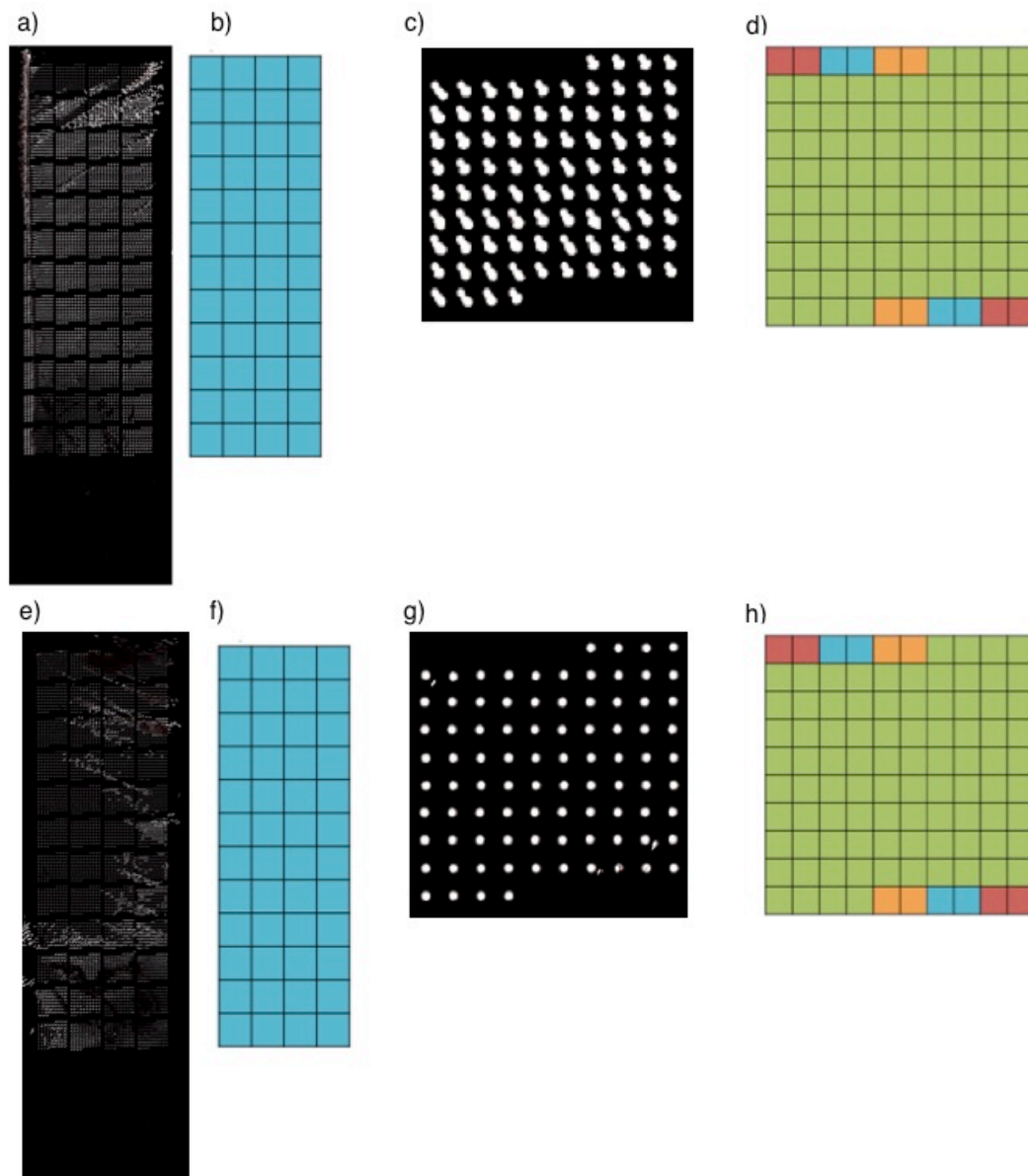


Figure 40. Anti-PTEN primary antibody and Alexafluor 647 conjugated secondary antibody probing 5μM PTEN-GST arrayed spots with Lifierslip™ and Dynamic Bioarray chip a) Fluorescence image of 4x12 array of 10x10 blocks incubated with Dynamic Bioarray chip b) Schematic of all blocks probed with 1:1000 anti-PTEN and 1:1000 Alexafluor 647 conjugated antibodies incubated with Dynamic Bioarray chip c) Fluorescence image of exemplar 10x10 block incubated with Dynamic Bioarray chip d) Schematic detailed protein arrayed as a 10x10 block onto array substrate with SciFLEXARRAYER. Red = Alexafluor 647 conjugated secondary antibody 1:500, Aqua = PBS Yellow = 5% BSA in PBS, Green = 5μM PTEN-GST in PBS incubated with Dynamic Bioarray chip. e) Fluorescence image of 4x12 array of 10x10 blocks incubated with Lifierslip™ cover slip f) Schematic of all blocks probed with 1:1000 anti-PTEN and 1:1000 Alexafluor 647 conjugated antibodies g) Fluorescence image of exemplar 10x10 block incubated with Lifierslip™ cover slip h) Schematic detailed protein arrayed as a 10x10 block onto array substrate with SciFLEXARRAYER. Red = Alexafluor 647 conjugated secondary antibody 1:500, Aqua = PBS Yellow = 5% BSA in PBS, Green = 5μM PTEN-GST in PBS incubated with Lifierslip™ cover slip. Scanned at 645nm, 5μm resolution, exemplar shown.

4.2.2. Optimisation of PTEN and VHR antibody and solution conditions for protein-protein interaction arraying and probing using Dynamic Bioarray chip

Optimisation and testing were performed to assess antibodies to PTEN, VHR and GST of the VHR-GST and PTEN-GST tagged constructs. The concentration of arrayed protein, probe protein, primary and secondary antibodies were tested, in addition to whether interactions were detectable, and how proteins and antibodies behaved as an arrayed solution and as a probe. Primary antibodies were tested via Western Blot to ascertain their capacity to bind to proteins of interest (Appendices 14).

PTEN-GST was arrayed at a range of concentrations (Figure 41.d.), and, with solution, antibodies, antibody concentrations, arrayer, slide, array and array reader configurations, 5 μ M had the highest signal without over-saturation (41.c.).

The protein probing concentration was also optimised, where 5 μ M VHR-GST, with solution, antibodies, antibody concentrations, arrayer, slide, array and array reader configurations had, with the anti-VHR antibody, had the highest signal without over-saturation (42.f.).

Antibody-protein-antibody sandwich formation were screened for compatible antibody-protein-antibody combinations (Figure 43.) where, anti-VHR monoclonal, anti-GST goat polyclonal 0.25mg/ml probed with 1 μ M VHR-GST, 1:500 anti-GST rabbit monoclonal and 1:1000 anti-rabbit Alexafluor 647 showed appropriate sandwich formation with the highest specificity out of the combinations screened.

With protein probing and antibody concentrations tested and optimised with SciFLEXARRAYER (Figure 43), could then proceed to probe Invitrogen Protoarrays with optimised proteins concentration and antibodies validated for work with protein-of-interest and the array technology used.

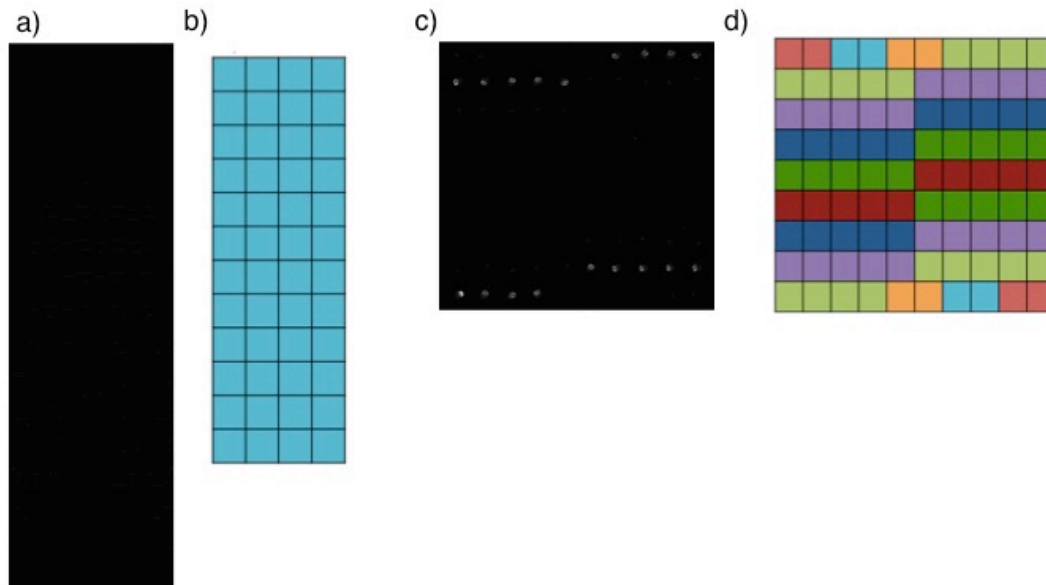


Figure 41. Arraying range of PTEN-GST concentrations on Path substrate slide array with sciFLEXARRAYER, probing with PTEN-GST and antibodies

a) Fluorescence image of PATH slide Global view of 4x12 array of 10x10 blocks b) Schematic of all blocks probed with 1µM PTEN-GST then 1:500 anti-PTEN then 1:1000 Alexafluor 647 conjugated antibodies c) Fluorescence image of exemplar 10x10 block d) Schematic detailed protein arrayed as a 10x10 block onto array substrate with SciFLEXARRAYER Red = Alexafluor 647 conjugated secondary antibody 1:250, Aqua = PBS Orange = BSA Lime green = 5µM PTEN-GST Purple = 1µM PTEN-GST Dark blue = 500nM PTEN-GST Green = 250nM PTEN-GST Dark red = 100nM PTEN-GST. Scanned at 645nm, 5µm resolution, 750 photomultiplier times (PMT), exemplar shown.

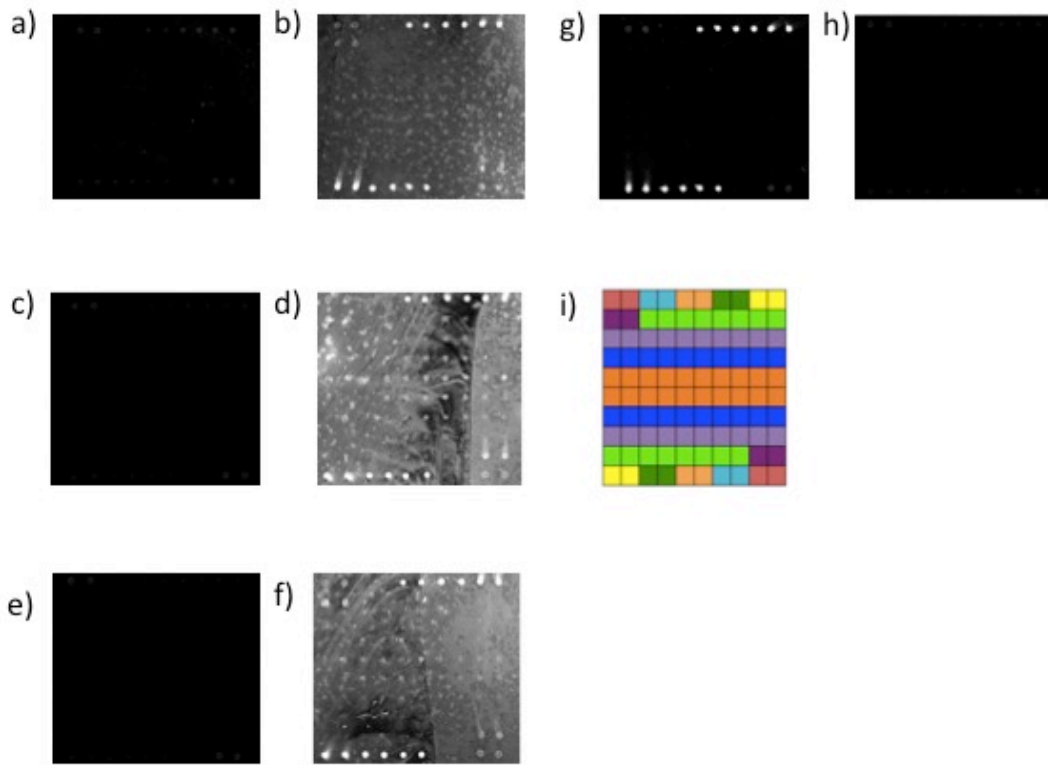


Figure 42. Anti-GST sandwich array probed with range of VHR-GST concentrations, anti-VHR primary antibody and Alexafluor 647 conjugated secondary antibodies a) Probed with 1 μ M VHR-GST b) Probed with 1 μ M VHR-GST and 1:500 anti-VHR c) Probed with 2.5 μ M VHR-GST d) Probed with 2.5 μ M VHR-GST and 1:500 anti-VHR e) Probed with 5 μ M VHR-GST f) Probed with 5 μ M anti-VHR and 1:500 anti-VHR g) No VHR-GST, 1:500 anti-VHR h) No VHR-GST No primary antibody i) Light Red = Alexafluor conjugated secondary antibody 1:250, Aqua = PBS, Peach = 1 μ M VHR-GST, Dark Green = 2.5 μ M VHR-GST, Yellow = 5 μ M VHR-GST, Purple = 1 μ M PTPMT1, Lime Green = anti-GST 1:100, Lilac = anti-GST 1:50, Blue = anti-GST 1:25 Orange = anti-GST 1:10. Scanned at 645nm, 5 μ m resolution, 750 photomultiplier times (PMT), 5 μ m resolution and 750 PMT, n=3, exemplar shown.

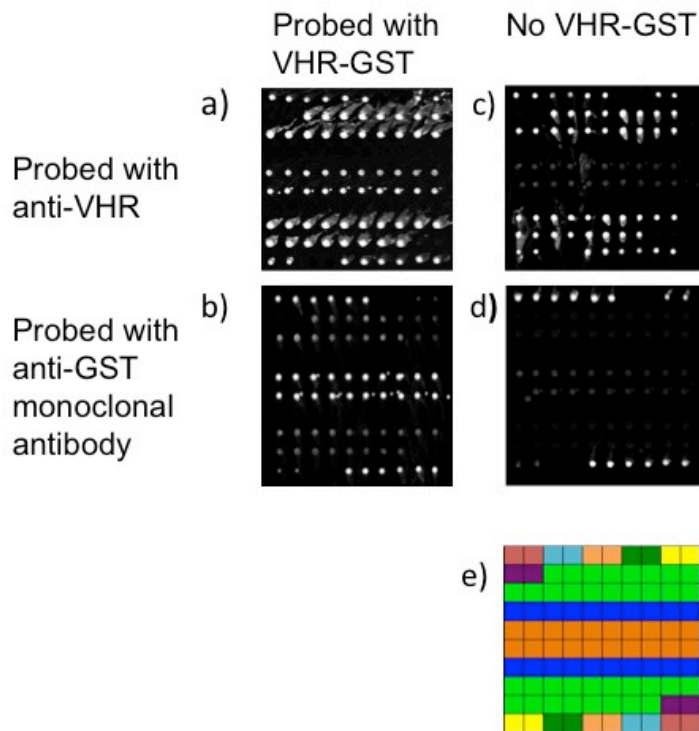


Figure 43. Anti-GST and anti-VHR sandwich array probed with VHR-GST, anti-VHR and anti-GST primary antibodies and Alexafluor 647 conjugated secondary antibodies a) Probed with 1 μ M VHR-GST, 1:50 Anti-VHR mouse monoclonal, 1:1000 anti-mouse Alexafluor 647 b) Probed with 1 μ M VHR-GST, 1:500 anti-GST rabbit monoclonal and 1:1000 anti-rabbit Alexafluor 647 c) Probed with 1:50 anti-VHR, 1:1000 anti-mouse Alexafluor 647 d) Probed with 1:500 anti-GST monoclonal rabbit and 1:1000 anti-rabbit Alexafluor 647 e) Arrayed protein layout: Red = Alexafluor 647 conjugated anti-mouse secondary antibody 0.5mg/ml Aqua = Alexafluor 647 conjugated anti-rabbit secondary antibody 0.5mg/ml Peach = Alexafluor 647 conjugated anti-goat secondary antibody 0.5mg/ml Dark green = PBS Yellow = 1 μ M VHR-GST Purple = 1 μ M PTPMT1-GST Light green = anti-VHR mouse monoclonal 0.5mg/ml Blue = anti-GST rabbit monoclonal 0.0033mg/ml Orange = anti-GST goat polyclonal 0.25mg/ml. Scanned at 645nm, 5 μ m resolution and 550 photomultiplier times (PMT). n=3, exemplar shown.

4.2.3. Protein library array screening of VHR using Dynamic Bioarray chip

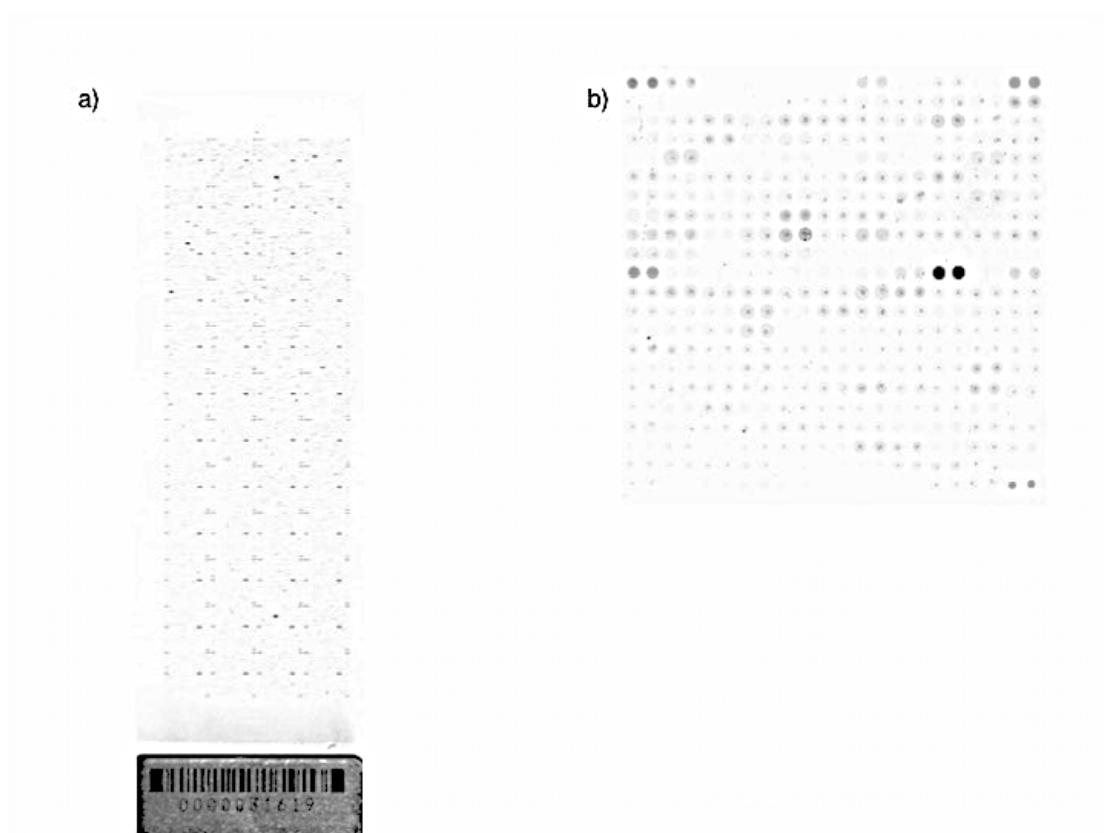
Library protein-protein screening arrays for VHR-GST were performed using Dynamic Bioarray chip for sample probing and incubation. Array incubation technology had been selected after comparative analysis, VHR-GST had been optimised for probing concentration and primary and secondary antibody selection for the VHR-GST protein-protein library-screening array. Invitrogen Human Protoarray® v5.0 were utilised for the protein-protein library array screening of VHR-GST. The Invitrogen Human Protoarray® v.5.0 contains over 9,000 human proteins printed in duplicate. The Protoarray proteins are produced from clones selected from Invitrogen's Ultimate™ open reading frame collection. Proteins on the Protoarray chip are expressed as N-terminal GST fusion proteins and purified under non-denaturing conditions. Protoarray proteins are printed on nitrocellulose to preserve native protein structure and protein interactions identified with Protoarrays have been validated with *in vitro* and *in vivo* assays (Al-Mulla et al., 2011; Fenner et al., 2010; Tong et al., 2008).

VHR-GST protein-protein arrays were performed with control arrays for the interaction of the secondary antibody with fluorescent conjugate with the arrayed proteins, and the effect of the primary antibody and secondary antibody with conjugate fluorophore (Figure 44). Figure 44 shows global and block view of proteins from Protoarray for the purpose of demonstration of quality of probing at the level of the whole array slide and for protein spot pairs. The array signal spots were compared between secondary antibody only, primary and secondary antibody only and VHR-GST, primary and secondary antibody arrays, and spot signals that for the scanning wavelength and photomultiplier times (PMT) displayed a differential signal, these differential signals were compiled in a list of putative VHR interactors (Table 12). Putative VHR interactors in Table 12 were selected via manual spot inspection between replicates and controls.

The list of putative VHR interactor candidates from the protein-protein library array screen (Table 12) was screened via protein analysis through evolutionary

relationships (PANTHER) modeling to assess the functions and roles of the putative VHR interactors, range of functions and roles of the putative VHR interactors and vicissitude and proportionality between the functions and roles (Figure 45.).

After Protoarray library screening of VHR-GST a complimentary screening of VHR interactors *in cellulo* as an initial *in vivo* study via immunoprecipitation and MS (See Chapter 5)



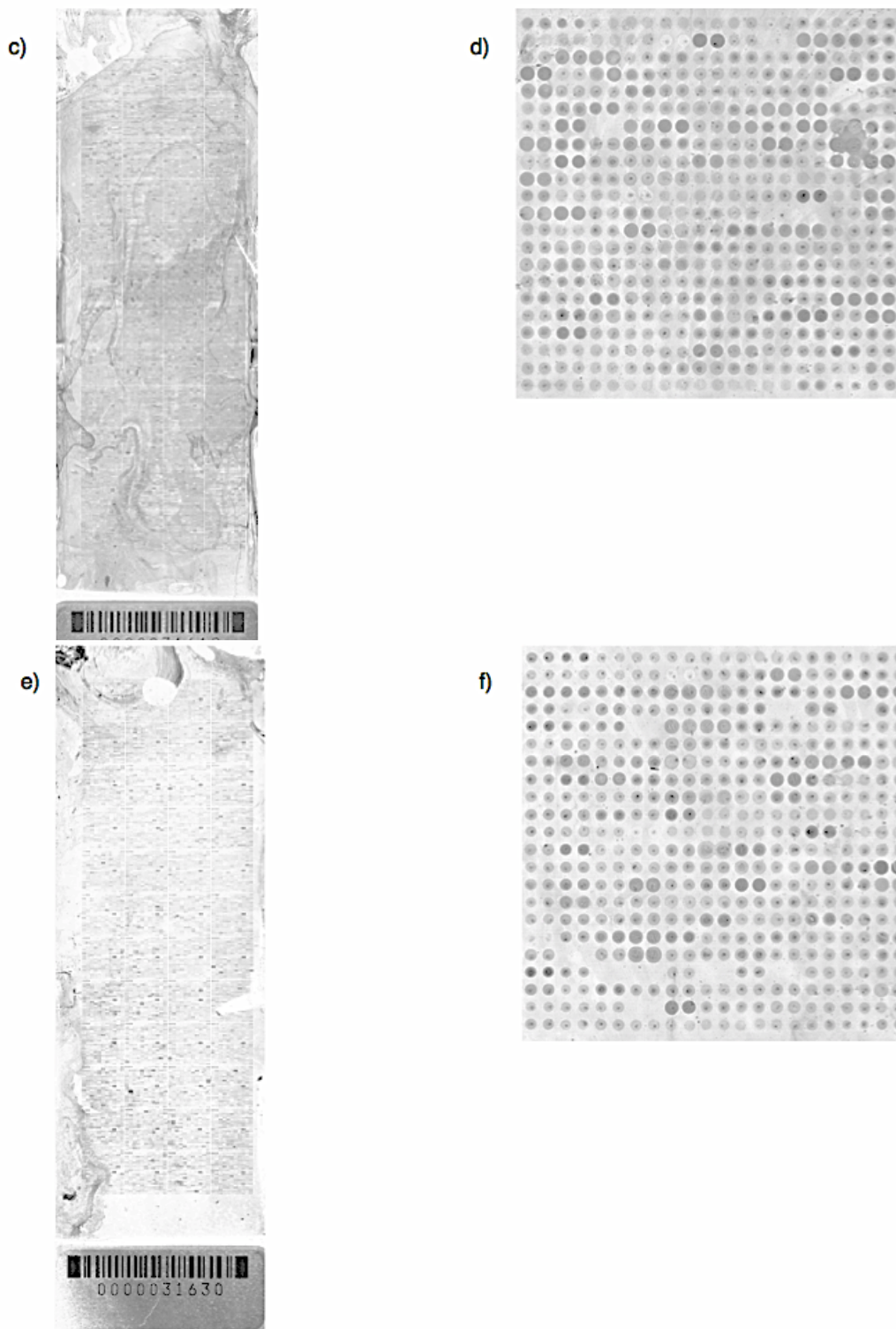


Figure 44. Protoarray protein-protein library screening of VHR-GST

a) Global view of Protoarray slide primary antibody control probed with Alexafluor 647 secondary antibody 0.5mg/ml b) Example block view of Protoarray slide primary antibody control probed with Alexafluor 647 secondary antibody 0.5mg/ml c) Global view of Protoarray slide no protein control probed with anti-VHR monoclonal antibody 1:50 dilution of 1mg/ml in PBS and Alexafluor 647 secondary 0.5mg/ml d) Example block view of Protoarray slide no protein control probed with anti-VHR monoclonal antibody 1:50 dilution of 1mg/ml in PBS and Alexafluor 647 secondary 0.5mg/ml e) Global view of Protoarray slide probed with VHR-GST 5 μ M, anti-VHR monoclonal antibody 1:50 dilution of 1mg/ml in PBS and Alexafluor 647 secondary 0.5mg/ml f) Example block view of Protoarray slide probed with VHR-GST 5 μ M, anti-VHR monoclonal antibody dilution of 1mg/ml in PBS and Alexafluor 647 secondary 0.5mg/ml. Scanned at 645nm, 5 μ m resolution and 450 photomultiplier times (PMT). n=3., exemplar shown.

Protoarray® Position			Potential Interactor Identification	
Block	Row	Column	Gene Name	Gene Identifier
2	16	5	SDF1A	NM_199168.2
5	13	1	GAGE7	NM_021123.1
5	19	7	PSMA5	NM_002790.1
6	9	21	CDK10	NM_003674.2
6	12	9	IDI2	NM_033261.2
7	4	17	TERF1	20810195
8	8	5	PLOD3	NM_001084.2
8	15	5	ASF1A	NM_014034.1
10	6	5	CSNK2A2	NM_001896.2
10	13	17	PAIP2	12804590
10	14	3	HSH2D	NM_032855.1
10	18	3	RPS28	NM_001031.4
11	8	13	ZAP70	NM_207519.1
12	12	21	USP2	34193195
12	14	21	RAB33A	NM_004794.1
12	20	21	RAD1	NM_002853.2
13	10	5	CCDC28A	BC013019.1
14	8	21	RGS3	NM_134427.1
14	12	19	BC009010.1	14290483
15	18	15	PAIP2A	25059069
17	7	11	NDRG4	NM_020465.2
17	2	15	KIAA1618	NM_020954.1
19	7	17	LOC401052	NM_001008737.1
19	13	1	GNL1	BC013959.1
20	8	21	KIAA0859	NM_014955.2
21	3	1	C8orf33	NM_023080.1
21	9	13	C14orf131	NM_018335.2
21	17	19	LMO4	NM_006769.2
23	12	5	ASS1	NM_054012.1

23	7	19	SLC22A18AS	BC030237.1
24	21	5	ERP27	NM_152321.1
26	16	5	CCL19	NM_006274.2
28	16	1	IL4	NM_000589.2
28	17	21	CAST	NM_173060.1
28	18	5	NM_001003704.1	NM_001003704.1
28	19	5	CARD9	BC008877.2
28	15	13	PTK6	NM_005975.2
28	15	21	RPS6KA4	NM_001006944.1
29	3	3	SPIRE1	BC016825.1
30	18	7	SNAP	NM_003826.1
30	9	13	ALKBH7	NM_032306.2
31	6	17	LCE3D	NM_032563.1
33	21	11	DTNA	NM_032981.2
33	7	11	SPRR4	NM_173080.1
35	19	1	HMGN1	NM_004965.3
35	6	17-18	USP28	BC065928.1
35	8	21-22	GDPD5	NM_030792.4
36	5	11	RLBP1	NM_000326.3
36	7	7	EPB41L4A	NM_022140.2
37	9	13	C9orf72	NM_018325.1
37	21	11	RCN2	NM_002902.1
38	3	15	SAMD3	NM_152552.1
38	6	11	ELOF1	NM_032377.2
38	6	13	UBE2S	BC004236.2
38	14	3	DUSP3/VHR	NM_004090.1
39	14	9	TRIP6	BC002680.1
40	3	13	SHOT1	NM_018330.2
40	8	7	RASGRP2	NM_005825.2
41	3	3	GAK	BC008668.1
41	15	11 12	SRrp35	NM_080743.2
43	6	11	FLJ37078	NM_153043.3

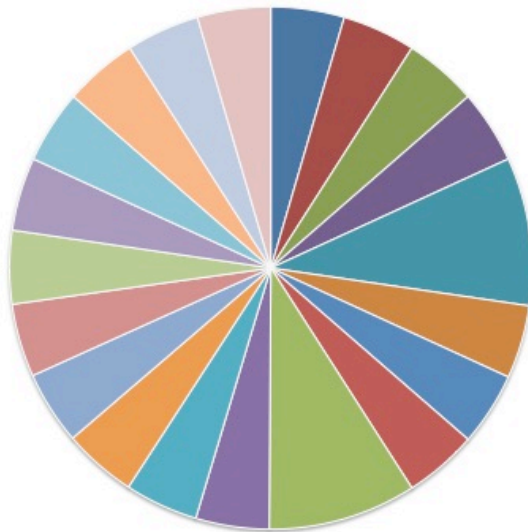
43	7	3	RSBN1I	NM_198467.1
44	6	9	MTG1	BC026039.1
45	8	19	VPS29	NM_016226.2
45	12	21	PECR	NM_018441.2
46	2	21	MP1	BC031630.1
46	10	3	STK17B	NM_004226.1
47	3	13	NARFL	NM_022493.1
47	14	9	FHL1	NM_001449.2
47	16	5 6	PPARA	BC000052.1
47	21	15	ADAT3	NM_138422.1
47	21	13-14	RNF135	NM_197939.1
48	8	7	C7orf27	NM_152743.2
48	12	17	RFC5	NM_007370.2
48	13	11	NAPG	BC001889.1
48	17	17	LIMS2	NM_004987.3
48	19	13	PGM3	NM_015599.1

Table 12. Selected putative interactors from VHR-GST Protoarray protein-protein library array screening

Systematic manual selection of proteins putative interactors utilising multiple blind manual analyses discounting proteins with spot signals in the controls. n=3

a)

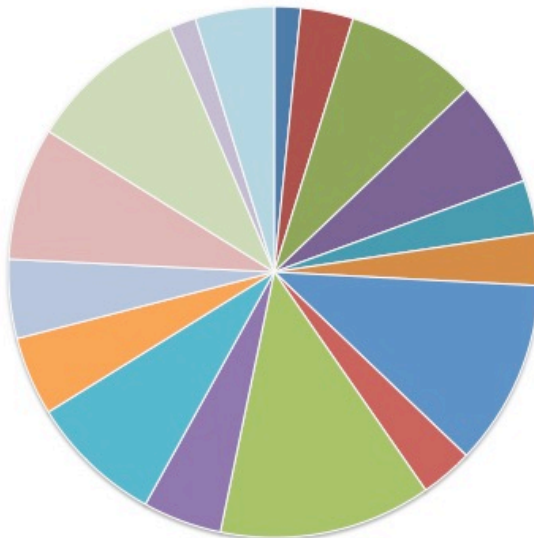
Pathways



- Axon guidance mediated by Slit/Robo (P00008)
- p38 MAPK pathway (P05918)
- Angiogenesis (P00005)
- Interleukin signaling pathway (P00036)
- Integrin signalling pathway (P00034)
- Insulin/IGF pathway-mitogen activated protein kinase kinase/MAP kinase cascade (P00032)
- De novo pyrimidine deoxyribonucleotide biosynthesis (P02739)
- Dopamine receptor mediated signaling pathway (P05912)
- Parkinson disease (P00049)
- PDGF signaling pathway (P00047)
- Nicotine pharmacodynamics pathway (P06587)
- Oxidative stress response (P00046)
- Cholesterol biosynthesis (P00014)
- Cadherin signaling pathway (P00012)
- Salvage pyrimidine ribonucleotides (P02775)
- Salvage pyrimidine deoxyribonucleotides (P02774)
- Wnt signaling pathway (P00057)
- VEGF signaling pathway (P00056)
- T cell activation (P00053)
- Arginine biosynthesis (P02728)

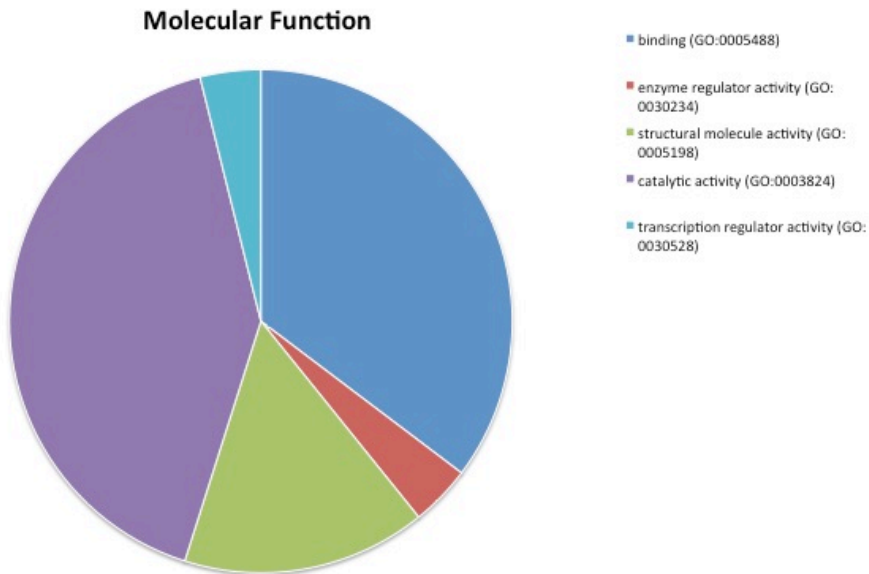
b)

Protein Class



- phosphatase (PC00181)
- membrane traffic protein (PC00150)
- hydrolase (PC00121)
- oxidoreductase (PC00176)
- enzyme modulator (PC00095)
- transfer/carrier protein (PC00219)
- transferase (PC00220)
- transcription factor (PC00218)
- nucleic acid binding (PC00171)
- ligase (PC00142)
- kinase (PC00137)
- calcium-binding protein (PC00060)
- isomerase (PC00135)
- cytoskeletal protein (PC00085)
- structural protein (PC00211)
- protease (PC00190)
- signaling molecule (PC00207)

c)



d)

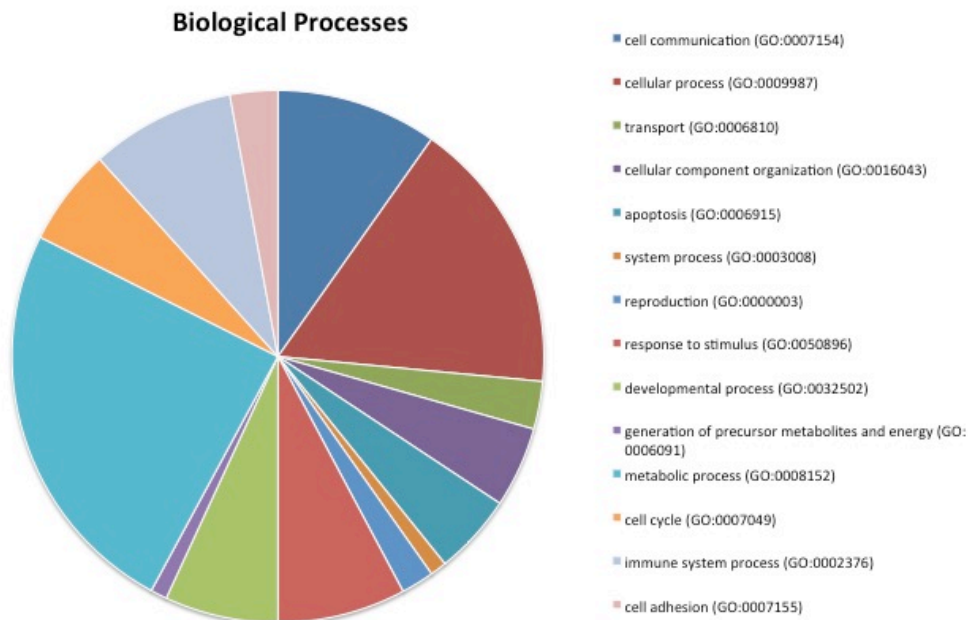


Figure 45. Protein analysis through evolutionary relationships of VHR-GST protein-protein Protoarray library screening of selected putative interactors
 Protein analysis through evolutionary relationships (PANTHER) analysis was performed (pantherdb.org) a) Pathways associated with protein-protein interactions with VHR-GST and proteins from Protoarray library screening and percentage ratios of associations between pathways b) Protein class associated with protein-protein interactions with VHR-GST and proteins from Protoarray library screening and percentage ratios of associations between protein classes c) Molecular functions associated with protein-protein interactions with VHR-GST and proteins from Protoarray library screening and percentage ratios of associations between molecular functions d) Biological processes associated with protein-protein interactions with VHR-GST and proteins from Protoarray library screening and percentage ratios of associations between biological processes.

4.3. Discussion

4.3.1. Discussion of technology selection and protocol optimisation for PTEN and VHR arraying and probing

The comparison of the Dynamic Bioarray chip versus the Lifterslip (Figure 40.) displayed a range of artifacts between the two array slide incubation technologies. Artifacts may have been due to specific handling errors linked to the technology regarding both the incubation procedure and engaging and dis-engaging the array slide and substrate from the incubation technologies, whereby both the Dynamic Bioarray chip and Lifterslip could slide and smear samples when handled manually.

The Dynamic Bioarray chip required appropriate activation of the hydrophilic-hydrophobic surface (Figure 11). The Dynamic Bioarray chip may offer higher resolution, and increased regularity of incubation intra-block and inter-block, in addition to the low and adjustable liquid probing volume the technology offers.

The arrayed protein, arrayed antibody and protein probes were optimised and screened for appropriate selection and forwarding down the pipeline for protein-protein library array probing (Figure 41., 42.,43.). Where optimisation was performed for VHR as this was the protein to be taken forward for protein-protein library screening with a replicate set of library arrays, due to VHR having higher activity than PTEN and larger protein expression yields and having performed a more extensive oxidative modification analysis on VHR.

It was decided that the arraying would be conducted with Dynamic Bioarray technology to take forward to library array screening to find putative VHR interactors.

4.3.2. Discussion of the protein-protein array VHR interactome screening

The unique, substantial and stand alone contribution to knowledge from the protein-protein array library screening work were the VHR-GST protein-protein array spot signals and corresponding lists of putative VHR interactors (Figure 44., Table 13). The putative VHR interactors were analysed for involvement in phosphorylation and kinase pathways and involvement in pathways and functions related to mammalian VHR-knockout phenotype to assess the putative functions of the interactors under adaptive and maladaptive conditions, and for prioritising for validatory screening.

The sciFLEXARRAYER and Protoarray library protein-protein arrays (Figure 40., 41., 42., 44.) were historically performed as optimisation and control experiments for an oxidised and nitrated protein interactome study, utilising VHR to screen for interactions that may be lost, altered or gained between cell signalling molecules and their interactors, and for functional correlation between interactions lost, altered and gained, with oxPTMs, oxPTM combinations, oxPTM abundances and oxPTM combination abundances. This direction was not carried forward as there were fragments and aggregates remaining in protein stock after treatment with oxidant and filtration attempts, which would render the samples unsuitable for protein-protein library array screening for the effect of intact proteins with oxPTMs on the interactome of a protein. The unfiltered treated protein with oxPTMs including states of fragmentation and aggregation, if arrayed, may have been similar to screening the effect of advanced oxidation end products (AOPP) on the cellular interactome and cellular signalling, which to speculate further, may elucidate the effect of AOPP on interactomes and cell signalling for errors and indications related to proteopathies and amyloidoses. AOPP have been demonstrated for use as a biomarker for monitoring oxidative stress in patients (Selmececi et al, 2005). The treatment molar concentrations and protein: treatment ratios that produced the fragments and aggregates were used in order to produce oxidation and nitration of amino acid side chains, both in

residues of interest, and to levels that may be distinguishable via fluorophore-tagged antibody array probing and imaging based on abundances of nitration observed in earlier experiments (Figure 28., 29).

The historic number of library arrays available and the variability between the replicate library arrays with regards to probing led to parts of the protein library array not having replicates. These areas were discounted from library array analysis. The manual probing and incubation of the array screening procedure was identified as a source of quality control risk that robotic procedure could mitigate, and manual screening was used due to historic shortage of arrays. False negatives and false positives may have been introduced through the probing and incubation procedure, presence of the GST tag, the antibodies utilised, incomplete optimisation and manual analysis. False coverage, the false-discovery rate (FDR) and false-positive rate (FPR) would be effected by procedural variation, GST tag, antibodies, manual analysis and historical numbers of replicate arrays.

VHR was found as a putative interactor on the array (Table 12), which is a confirmation of previous evidence of VHR dimerisation (Appendix 2), and ZAP-70, a known VHR interactor (Alonso et al., 2003) was also found (Table 12) as a putative potential interactor, which confirmed previous evidence via Invitrogen Protoarray technology and gave confidence to the arraying protocol. Additional interactors of VHR (Appendix 2) were not identified as putative interactors via Invitrogen Protoarray.

An initial literature search and database analysis was performed on the list of putative protein interactors (Table 12). Initial criteria for interest during literature search and database analysis were 1) Potential relationship to VHR knockout phenotype as assessed via the Mouse Genome Informatics database (www.informatics.jax.org, Skarnes et al., 2011) 2) Evidence of being phosphorylated 3) Evidence of involvement in kinase and phosphatase signalling pathways 4) Similarity to known VHR interactors (Appendix 2) and 5) Involvement in diseases of ageing and age-related pathology.

Peroxisome proliferator activated receptor alpha (PPARA) was identified as a putative interactor of potential interest due to PPARA involvement in fatty acid oxidation and transcriptional response to fasting which involves release of fatty acids from adipose tissue (Kersten et al., 1999). The VHR knockout phenotype reported abnormal adipose tissue phenotype and abnormal growth/size/body phenotype, and as such PPARA and VHR may be involved in a signalling pathway that regulates adipose tissue function. Additionally PPARA is also a target of phosphorylation by mitogen-activated kinase ERK (Burns et al., 2007), which is a substrate for VHR (Todd et al, 1999). Also note that there are a large amount of the putative interactors involved in metabolic processes as identified by PANTHER analysis (Figure 45).

Thyroid hormone receptor interactor 6 (TRIP6) was identified as a putative interactor of potential interest due to the role of the thyroid on growth rate (Symczynska et al., 2010), and the role of thyroid hormone receptors in visceral adiposity in mice (Liu et al., 2003), which may be associated with the VHR knockout phenotype reported abnormal adipose tissue phenotype and abnormal growth/size/body phenotype. TRIP6 also undergoes tyrosine phosphorylation (Lai et al, 2005) and is a signalling component of the ERK pathway (Li et al., 2005). TRIP6 also interacts with receptor interacting protein 2, which is involved in adaptive immune responses and inflammation (Li et al., 2005) where abnormal immune function was listed as in the VHR mouse knockout.

Calpastatin was identified as a putative interactor of potential interest due to calpastatin's role in inhibition of motor neuron death (Rao et al., 2016), where nervous system abnormalities were reported in the VHR mouse knockout phenotype. Chen *et al* (2010) also demonstrate that calpastatin and phosphorylated ERK may collaborate to promote the generation of a constitutively active androgen receptor in prostate cancer, where ERKs are substrates for VHR (Todd et al., 1999).

As a comparative and validatory analysis to the library array screening, co-immunoprecipitation of VHR with cellular contents was to be performed.

4.4. Conclusions for optimisation and development of arraying technologies for the investigation of oxidised protein-protein interactions and protein-protein library screenings of VHR

The Dynamic Bioarray hydrophilic-hydrophobic chips point to the potential of chips for further miniaturisation and parallelisation of screening technologies, liquid handling and reaction chambers and the range of uses these may have.

Protein-protein library array screening for functional interactome screening may yield results for proteins that may not be present or detectable via co-immunoprecipitation and downstream techniques from co-immunoprecipitation such as MS analysis.

Arraying, array probing and incubation and array analysis workflow would benefit from full robotic automation.

The library array screening of VHR added to the putative interactors list for VHR to develop knowledge of VHR, signalling pathways and cellular interactome. The putative interactors would need to be validated, and PPARA, TRIP6 and calpastatin may be priority candidates.

Chapter 5

VHR immunoprecipitation with mass spectrometric analysis

5.1. Introduction

5.1.1. Comparative analysis, discovery and validation of protein-protein interactors of VHR

To further investigate the protein-protein interactome of VHR in a *in cellula* context, and also to compare to *in vitro* protein-protein array library screening – co-immunoprecipitation may be appropriate. Co-/immunoprecipitation using a cell line offers advantages that it has a different and may have a possibly more comprehensive or alternate set of proteins to interact with than the 9,000+ proteins on the Protoarray. It may offer the advantage of screening for tertiary and additional interactors that are not direct interactors – this modifies what hypothesis is being questioned and what questions can be asked of the data. Immunoprecipitation coupled to MS offers an automated *in silico* identification of interactors. *In cellula* analysis may yield an interactome more homologous to the *H. sapiens in vivo* VHR interactome than the *in vitro* protoarray library interactome, taking into account the considerations that 1) the cell line is immortalised, 2) that the proteins over-expressed, with a tag, 3) the presence of plasmid constructs in the cell and 4) potential effects of transfection and transfection reagents on the interactome present at the timepoint of experimentation. Limitations of co-/immunoprecipitation and protein-protein array as comparative and combinatorial methods revolve around the validation of the interactor or relevant effect of interactor for pre-clinical or pre-clinical utility or efficacy. Patient outcomes and presence and absence of binary outcomes for clinical and biotechnological processes may be kept in view to assess validation studies.

The aims of this research were to explore the protein-protein interactors of VHR, with which to compare to the literature, expand fundamental knowledge of the protein

of study, and identify proteins to further explore protein-protein interactions with after exploratory studies. In order to explore the interactome and advance scientific knowledge – the interactome would be identified via immunoprecipitation experiments. Interactomes with the complimentary array library screenings and immunoprecipitation would be compared and validated via this second technique linked to semi-quantitative MS.

5.2. Results

5.2.1. Transfection of HCT116 cells with VHR-Flag

HCT116 cells were transfected with pcDNA3.1-VHR-Flag after ligation and transformation as part of an artificial over-expression system (see Methods). A range of amounts of pcDNA3.1-VHR-Flag DNA were screened for effects on protein content (Figure 46) and transfection success (Figure 48). 35µg from screening experiments (Figure 46) displayed larger protein yields than higher concentrations of 52.5µg and 70µg. Western Blot of transfected cell lysates for Flag tag with anti-flag antibody (Figure 47) was performed with successful binding of anti-flag antibody to moiety in lysate.

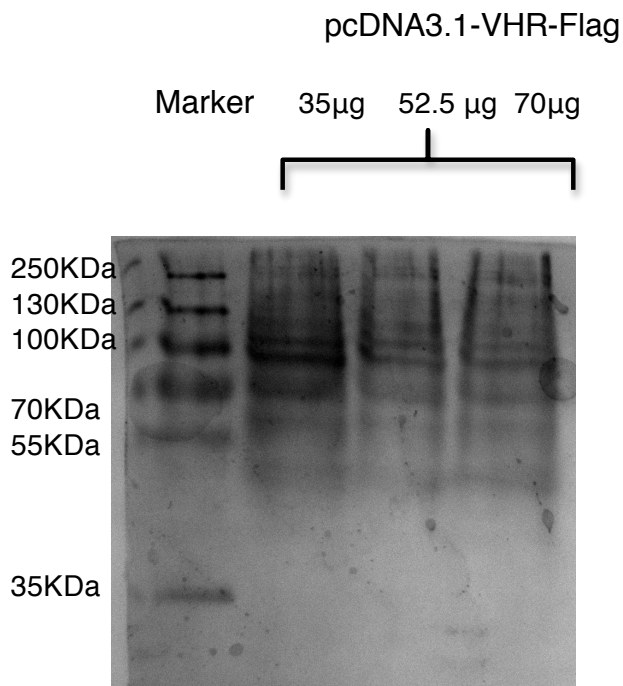


Figure 46. Coomassie staining of HCT116 cells transfected with range of quantity of pcDNA3.1-VHR-Flag

HCT116 cells grown with DMEM supplemented with 10% fetal calf serum (FCS) after reaching 70% confluence had 35µg, 52.5µg, 70µg pcDNA3.1-VHR-Flag in 1.5ml Opti-MEM® with 225µl Lipofectamine 2000 added to the cells with 9mls Opti-MEM®. Cells had DMEM medium minus FCS prior to addition of DNA and transfection reagent. Cells were incubated for 30min at room temperature. 5hr post-incubation medium was removed from cells and replaced with DMEM supplemented with 10% FCS. Cells were harvested for lysis and staining by removing media, washing with PBS then applying NP-40 lysis buffer 1%, NaCl 150mM, Tris-Cl 50mM, pH 8 for 20min prior to centrifugation at 20,000G, 4°C. Exemplar shown.

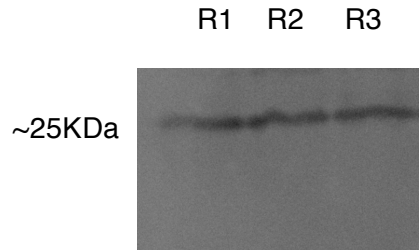


Figure 47. Western blot of transfection of HCT116 cells with pcDNA3.1-VHR-Flag 35µg of pcDNA3.1-VHR-Flag. 225µl Lipofectamine 2000. Anti-flag monoclonal primary antibody 1:1000. R1-3 = Transfection replicates. n=3.

5.2.2. Immunoprecipitation of VHR interactors

HCT116 cells were transfected with pcDNA3.1-VHR-Flag and then immunoprecipitated with Dynabeads® with anti-VHR antibody bound. The following lysate bound to the beads was loaded onto a SDS PAGE gel, stained with Coomassie blue stain and the whole gel lane was cut out into similar sized pieces for LC-MS analysis (Appendices 15). Controls used for immunoprecipitation were HCT116 cells transfected with pcDNA3.1 minus VHR-Flag, control cell lysates were used for immunoprecipitation and MS, where putative interactors that were found in empty vector control and experimental were removed from Table 13.

5.2.2.1. Mass spectrometric and *in silico* analysis of VHR interactors

Following immunoprecipitation of VHR-Flag with anti-VHR antibody, Dynabead and moieties bound to VHR-Flag from the HCT116 cells expressing the VHR-Flag from the pcDNA3.1-VHR-Flag construct, and from negative control cells with the pcDNA3.1 plasmid minus the VHR-Flag construct, and subsequent loading of the co-immunoprecipitated moieties onto a SDS PAGE gel, Coomassie staining – the gel

lane was cut into similar sized pieces, underwent trypsin digestion and LC-MS was performed.

The LC-MS sample data from each gel piece (see Appendices 15 for gel slicing) was analysed *in silico* via Progenesis, where all of the gel lane and all bands were sliced and taken forward for in-gel digestion. Results from all horizontal slices from replicates for each gel slice were combined in analysis. Potential interactors from each horizontal gel slice replicate set were combined along with averaging of the Exponentially Modified Protein Abundance (emPAI) confidence modeling score, whilst recording numbers of replicates identified in (Table 13). Potential interactors were found in multiple replicates (Table 13), with no set overlap with the Protoarray library screening of VHR-GST performed (Table 12).

Potential Interactor Identification		Number of replicates identified in	Average emPAI between replicates
Accession number	Gene Name		
S10A9_HUMAN	CAGB	2	0.26
H33_HUMAN	H3F3A	2	0.22
MUCL1_HUMAN	MUCL1	2	0.38
LTOR4_HUMAN	LAMTOR4	2	0.32
K1644_HUMAN	KIAA1644	2	0.15
ZFAN3_HUMAN	ZFAND3	2	0.13
ERMP1_HUMAN	ERMP1	2	0.03
CC135_HUMAN	CCDC135	2	0.03
ARG28_HUMAN	ARHGEF28	2	0.02
FUZZY_HUMAN	FUZ	4	0.07
LIPA2_HUMAN	PPFIA2	2	0.02
MYLK3_HUMAN	MYLK3	2	0.04
INTU_HUMAN	INTU	2	0.03
TRIB3_HUMAN	TRIB3	2	0.08
MAP6_HUMAN	MAP6	2	0.04

PININ_HUMAN	PNN	2	0.04
ATS1_HUMAN	ADAMTS1	2	0.03
KCC1B_HUMAN	PNCK	2	0.09
TNR16_HUMAN	NGFR	2	0.07
SPOT1_HUMAN	SPANXA2-OT1	2	0.26
WDR6_HUMAN	WDR6	2	0.03
CO4A4_HUMAN	COL4A4	4	0.02
TRDMT_HUMAN	TRDMT1	2	0.07
APR_HUMAN	PMAIP1	2	0.59
TSP3_HUMAN	THBS3	4	0.03
CJ068_HUMAN	C10orf68	2	0.05
RET_HUMAN	RET	4	0.03
ABC3D_HUMAN	APOBEC3D	2	0.07
DNMT1_HUMAN	DNMT1	1	0.02
CS045_HUMAN	C19orf45	1	0.06
RB22A_HUMAN	RAB22A	1	0.15
NBPFL_HUMAN	NBPF21	4	0.05
SCFD1_HUMAN	SCFD1	2	0.05
5NT3B_HUMAN	NT5C3B	2	0.1
CROL3_HUMAN	H7BZ55	2	0.01
DNMBP_HUMAN	DNMBP	3	0.02
PDZD2_HUMAN	PDZD2	2	0.01
TM63A_HUMAN	TMEM63A	2	0.04
K1C14_HUMAN	KRT14	2	0.36
NDKA_HUMAN	NDKA	2	0.43
RS23_HUMAN	RPS23	2	0.21
COF1_HUMAN	CFL1	2	0.39
RS20_HUMAN	RPS20	2	0.25
RL12_HUMAN	RPL12	2	0.19
PPIA_HUMAN	PPIA	2	0.67
CH60_HUMAN	HSPD1	2	0.05
RS15_HUMAN	RPS15	2	0.2

TBA3E_HUMAN	TUBA3E	2	0.07
RL34_HUMAN	RPL34	2	0.25
CC110_HUMAN	CCDC110	3	0.03
TBB4A_HUMAN	TUBB4A	3	0.07
IL25_HUMAN	IL25	2	0.16
PDS5B_HUMAN	PDS5B	2	0.02
MED13_HUMAN	MED13	2	0.01
RL35_HUMAN	RPL35	2	0.23
DESI2_HUMAN	DESI2	4	0.16
PDE11_HUMAN	PDE11A	2	0.03
HS74L_HUMAN	HSPA4L	2	0.03
VAPA_HUMAN	VAPA	2	0.12
CHD5_HUMAN	CHD5	2	0.01
RS17L_HUMAN	RPS17L	2	0.22
RWDD3_HUMAN	RWDD3	2	0.11
MAP1S_HUMAN	MAP1S	2	0.03
GTDC2_HUMAN	POMGNT2	2	0.05
ADAM2_HUMAN	ADAM2	2	0.04
GUAD_HUMAN	GDA	2	0.06
MARK4_HUMAN	MARK4	2	0.04
GBRR3_HUMAN	GABRR3	4	0.06
ANR11_HUMAN	ANKRD11	4	0.01
DOCK9_HUMAN	DOCK9	4	0.01
PAK4_HUMAN	PAK4	2	0.05
HMCN1_HUMAN	HMCN1	2	0.01
SMBT1_HUMAN	SFMBT1	2	0.03
PRCC_HUMAN	PRCC	2	0.06
F161A_HUMAN	FAM161A	2	0.04
PCD18_HUMAN	PCDH18	2	0.03
BBS10_HUMAN	BBS10	4	0.04
RBM22_HUMAN	RBM22	3	0.07
RPGP1_HUMAN	RAP1GAP	2	0.04

PXK_HUMAN	PXK	2	0.05
OSGI1_HUMAN	OSGIN1	2	0.05
GRIN1_HUMAN	GPRIN1	2	0.03
CJ071_HUMAN	C10orf71	2	0.02
CORA1_HUMAN	COL27A1	2	0.02
KI13B_HUMAN	KIF13B	2	0.02
GVIN1_HUMAN	GVINP1	2	0.01
KPRB_HUMAN	PRPSAP2	2	0.08
LGMN_HUMAN	LGMN	2	0.07
FINC_HUMAN	FN1	2	0.01
AKAP2_HUMAN	AKAP2	2	0.03
TCOF_HUMAN	TCOF1	2	0.02
PSMD1_HUMAN	PSMD1	2	0.03
BRE1B_HUMAN	RNF40	2	0.03
NOM1_HUMAN	NOM1	4	0.03
OSBL3_HUMAN	OSBPL3	2	0.03
LDHA_HUMAN	LDHA	2	0.19
H3C_HUMAN	H3F3C	2	0.22
LDHB_HUMAN	LDHB	2	0.09
KV116_HUMAN	P01608	2	0.29
TBA1A_HUMAN	TUBA1A	2	0.06
ANXA5_HUMAN	ANXA5	2	0.09
SPOC1_HUMAN	SPOCD1	2	0.02
BANK1_HUMAN	BANK1	2	0.04
RIMS3_HUMAN	RIMS3	2	0.1
NSUN4_HUMAN	NSUN4	2	0.08
ADNP_HUMAN	ADNP	2	0.03
HCN3_HUMAN	HCN3	2	0.04
KIF27_HUMAN	KIF27	2	0.02
DRD1_HUMAN	DRD1	2	0.07
TTC37_HUMAN	TTC37	2	0.02
SEN34_HUMAN	TSEN34	2	0.1

PGFRA_HUMAN	PDGFRA	2	0.03
CTU1_HUMAN	CTU1	2	0.09
PLCB4_HUMAN	PLCB4	2	0.02
TRPM3_HUMAN	TRPM3	2	0.02
IP3KA_HUMAN	ITPKA	2	0.06
APC1_HUMAN	ANAPC1	2	0.01
MOGT3_HUMAN	MOGAT3	2	0.08
MAGI2_HUMAN	MAGI2	2	0.02
IRX6_HUMAN	IRX6	2	0.07
OTUD4_HUMAN	OTUD4	2	0.03
NDRG1_HUMAN	NDRG1	2	0.08
LCE2A_HUMAN	LCE2A	2	0.28
FANCI_HUMAN	FANCI	2	0.02
RREB1_HUMAN	RREB1	2	0.02
ZNF268_HUMAN	ZNF268	2	0.03
ATL1_HUMAN	ADAMTSL1	2	0.02
ZNF473_HUMAN	ZNF473	2	0.03

Table 13. Putative interactors from VHR-Flag Dynabead-anti-VHR antibody immunoprecipitation from HCT116 cell screening using LC-MS and Progenesis analysis. n=6.

5.3. Discussion

5.3.1. Discussion of transfection of HCT116 cells with VHR-Flag

Transfection of HCT116 cells with pcDNA3.1-VHR-Flag was performed (Figure 48). HCT116 cells were used for historic reasons regarding collaboration with Imperial College London. Transfection DNA amount optimisation showed more intense staining with the least DNA used in the range (35µg) of DNA amounts screened, to speculate, this may be due to higher DNA concentrations being toxic or leading to toxic protein expression levels.

5.3.2. Discussion of immunoprecipitation of VHR interactors

The immunoprecipitation of VHR interactors and subsequent LC-MS analysis gave a list of putative VHR-Flag interactor proteins. Additional potential benefit of *in cellulo* approaches over protein array library screening is the potential proteins present in the cells. It may be difficult to speculate as to whether the proteins were bound by the protein of interest, bound to the Dynabeads, or in the case of the over-expression system or proteins in the library array, are within the actual interactome of a particular intact cell during health and disease. Current VHR interactors, even interactors obtained from *in vivo* sources (Appendix 2) may not represent the actual interactome of VHR during health and disease, only what interacts with VHR from a lysate of cells or other biological sample.

The interactomes of the VHR-GST library array and VHR-Flag immunoprecipitation were non-overlapping (Table 12., 13.). To speculate, the VHR-GST library array may have included GST interactors and interactors of the VHR-GST moiety that are unique to VHR-GST over VHR and GST alone.

An initial literature search and database analysis was performed on the list of putative protein interactors from the immunoprecipitation and MS (Table 13). Initial criteria for interest during literature search and database analysis were 1) Potential relationship to VHR knockout phenotype as assessed via the Mouse Genome Informatics database (www.informatics.jax.org, Skarnes et al., 2011) 2) Evidence of being phosphorylated 3) Evidence of involvement in kinase and phosphatase signalling pathways, 4) Similarity to known VHR interactors (Appendix 2), 5) The number of replicates of immunoprecipitation was identified in and emPAI score and 6) Involvement in diseases of ageing and age-related pathology.

S100 calcium binding protein A9 (S100A9) was identified as a putative interactor of potential interest due to involvement in immune function as a pro-

inflammatory molecule expressed in neutrophils and monocytes (Simard et al., 2010), where abnormal immune function is noted in the VHR knockout mouse. S100A9 was also shown to induce phosphorylation of MAPKs, ERK1 and ERK2, p38 and JNK (Simard et al., 2010), where ERK is a substrate of VHR and VHR has been shown to inactivate JNKs (Denu et al., 1999; Jacob et al., 2002; Todd et al., 1999).

Neuroblastoma breakpoint family 21 (NBPF21) was identified as a putative interactor of potential interest due to the number of replicates it was found in and because the NBPF family has a highly conserved domain of unknown function (Vandepoele et al., 2005) and little is known about NBPF21, thus taking this candidate forward may provide an opportunity to discover the function of this protein family.

Late endosomal/lysosomal adaptor and mitogen-activated protein kinase and mammalian target of rapamycin (mTOR) activator/regulator (LAMTOR) complex adaptor molecule 2 (LAMTOR2) was identified as a putative interactor of potential interest as it mediates the activation of ERK, which is a substrate of VHR (Todd et al., 1999). The mTOR pathway and the rapamycin compound are involved in the extension of maximum lifespan in a mammalian system, Ehninger *et al* (2014) states that this extension of mammalian maximum lifespan may be due to cancer suppression.

The VHR-Flag interactors may have included proteins interacting with the combination of the Dynabeads and VHR-Flag that would not bind to VHR-Flag, VHR or Dynabeads alone, or interact with VHR-Flag over VHR. Literature evidence for resin and beads having their own interactors includes Rees *et al* (2015) who demonstrate the proteins that bind non-specifically to resins from DT40 chicken B-cell line, which include high abundance proteins that may mask lower abundance proteins.

The decision to select the Flag tag over the GST fusion protein for VHR was made as the Flag tag is a short peptide, smaller than GST where the aim was to reduce non-VHR interactions. The flag tag has been used for immunoprecipitation

and subsequent MS including for the von Hippel-Lindau gene component of a ubiquitin ligase complex (Lai et al., 2011).

Putative interactors were, on mode, found in 2 replicates out of 6 (Table 13). Due to putative interactors being found in a variable amount of replicates, taking into account the mode of putative interactors being found in 2 replicates, the average emPAI confidence given by Progenesis was utilised as an interim confidence indicator.

5.4. Conclusion of immunoprecipitation and mass spectrometric VHR interactome discovery and protein-protein array comparative analysis

To conclude, the interactomic analysis of VHR via immunoprecipitation and protein-protein array library screening has yielded sets of putative interactors including proteins with kinase activity and phosphorylation. The putative interactors will require additional validation, where validation may include 1) that the proteins can interact, 2) proteins do interact under the state required, 3) interact appropriately under the state required for the output and outcomes required and 4) that the efficacy of this interaction and outcome occurs in the range of states and/or patients required. Thus validation type and degree requires directions and desired outcomes to be considered.

High-throughput screening methods of array libraries, and immunoprecipitation LC-MS of over-expressed protein *in cellulo* in cell lines distinct from patients allow for fundamentally different applications and cover a different sub-set/interactome of the hyper-interactome of VHR, where the hyper-interactome is defined as all moieties that can interact with VHR, where all other interactomes must specify the limits of the sub-set/interactome including cell types, gene expression, cell state and all relevant factors. The fundamentally different applications include discovery of unique signalling pathway networks and signalling pathway interactions, novel interactors that may not have a signalling or enzymatic function, and interactors from the hyper-interactome

that may not interact over the range of states VHR or the cell containing VHR usually takes, yet could be manipulated to take for the purposes of biological engineering.

High-throughput screening methods, to speculate, with regards to interactomics, offer starting at the hyper-interactome rather than selection of proteins in or related to known signalling pathway networks. Regarding screening of the hyper-interactome with the inclusion of PTMs, including oxPTMs, the potential may include discovery of unique signalling pathway networks and signalling pathway interactions, novel interactors that may not have a signalling or enzymatic function or role in health or disease, and interactors from the hyper-interactome that may not interact over the range of states VHR or the cell containing VHR usually takes, yet could be manipulated to take via a therapeutic intervention related to the existence of causation of the PTMs.

The immunoprecipitation may have been improved upon utilising primary cells such as diploid fibroblasts, old versus young fibroblasts and treated fibroblasts, for screening VHR interactors, and additional controls including multiple cell lines, multiple plasmids, alternate transfection protocol, control cells not transfected, and controls for proteins that bind to the beads rather than the protein-of-interest.

Over-expression models may exhibit non-overlapping interactomes with the interactome of a protein under the non-overexpressed interactome states it can take, due to over-expression models being artificial systems. Over-expression models, may offer additional information regarding moieties that may interact with the protein of interest that could be useful, and thus could give insight into the design of therapeutics though knowledge about the interaction properties of a protein for what it may interact with, and types of moieties it may interact with and their properties.

A major challenge of immunoprecipitation using lysate is the potential for non-specific binding partners and partners binding to the beads, as shown by Rees *et al* (2015) who show that 367 proteins bind the bead resins used, which accounts for

1.16% of the proteome of the chicken B-cell DT40 cells used, including highly abundant proteins.

To conclude, although over-expression systems are artificial, and non-specific binding is known to occur, immunoprecipitation offers the potential to identify protein interactors that may not be present on protein library arrays, including indirect binding partners.

Future work might include immunoprecipitation of proteins from lysate from cells after the application of oxidative stress, validation of interactors including S100A9, NBPF21 and LAMTOR2.

Chapter 6

Discussion

6. Discussion

6.1. Summary of Oxidation of VHR and PTEN results

Contained within this unique contribution is evidence that can enable us to consider more maturely the speed and throughput limitations of *de novo* sequencing and systematic mapping, the capacity for relevance of starting with *in vitro* techniques for biomarker discovery rather than directly sampling healthy young and diseased individuals, the selectivity of oxidising and nitrating agents and the potentially functional role of non-active site oxidations and more potential ways to modulate VHR and PTEN function.

The aim of this research was to reveal unique information in the proteome and for a particular protein show that it is possible to profile the oxidative and nitrative modifications of it, with *de novo* validation, and to discover what that looks like, regarding stochasticity, selectivity, characteristic signatures and make statistical predictions as to the functional proteomic effects of those modifications utilising appropriate mathematical modelling. This would be towards leveraging unique data in the proteome to be able to make more informed and prioritised decisions about the limitations and advantages of proteomics for biomarker discovery, drug design and to more pragmatically ask questions about what proteomic data we need to make decisions about care, therapy and health using omics approaches – and what protein oxPTMs can add to omic and multiomic approaches.

The identification of the nitration and oxidation of the VHR ZAP-70 interacting (Alonso et al., 2003) amino acid residue Tyr138 (Figure 28., 29., 30., Appendices 10., 11., 12) highlighted the potential for competitive PTM, therapeutic competitive PTM and phosphorylation mimics (Mallozzi et al., 2013) involved in cell signalling pathway network interactions and identification of the VHR Cys124 nucleophilic acid

trioxidation highlights the potential of multiple oxidations of VHR and CX5R phosphatases to be modified with the oxPTM property profile of trioxidation. Although it is not clear what the consequences of nitration mimicking phosphorylation *in vivo* may be or whether the Tyr138 residue is competitively nitrated or oxidised *in vivo*, which would require additional study.

6.2. Summary of nitration, chlorination and oxidation reagent results

Searching for multiple known modifications across the available primary sequence demonstrates the empirical specificity of peroxyxynitrite as generated by sin-1, HOCl and TNM under specific conditions is the primary contribution to knowledge regarding nitration, chlorination and oxidation of proteins (Figures 29., 30., Appendices 8., 9., 10., 11., 12) including the variability of specificity and the range of residues and modification types associated within those specific conditions. The peptide and modification identification and specificity creates a corpus of knowledge and datasets regarding oxPTM profiles. This data may lead to utility for future experimental design, optimisation of nitrating, chlorinating and oxidising agents having profiled PTMs generated under specific conditions, systematically, with specific appreciation of the inputs, outputs and correlations of such experimental systems.

6.3. Summary of interactome results

The interactomics screening of VHR via library array screening and immunoprecipitation yielded an array of uniquely identified putative interactors (Table 12., 13) not previously found, were previously found interactors are listed in Appendix 2, of which VHR and ZAP-70 were identified in by library array screening. Potential interactors found may have important functional roles in health and disease,

and validation of the interactors *in vivo*, and assessing their functional relevance *in vivo* would require additional study.

The combination of library array screening and immunoprecipitation with LC-MS offers a combinational high-throughput approach that may be appropriate for diagnostics and to be of an appropriate speed to the identification of modifications and analysis of enzymatic function, and to identify interactors not identified via other methods (Appendix 2).

6.4. Justification of methods

6.4.1 Treatments

6.4.1.1. Advantages of treatments

The advantages of the treatments used included that peroxynitrite has been investigated *in vivo* and associated with age-caused errors, damage and symptoms (Radi et al, 1991; Alvarez & Radi, 2003). The sin-1-caused modifications *in vitro* may translate to *in vivo* as those modifications occurring in age-caused diseases and oxidative stress that occur as a consequence of being alive from timepoint x to timepoint y.

An advantage of HOCl was that HOCl is involved in the myeloperoxidase response to bacterial infection, and thus the sub-set of modifications found could intersect with the sub-set of modifications caused by inflammation and the myeloperoxidase response to bacterial infection (Thomas, 1979).

An advantage of utilising TNM was that it yielded both higher abundance oxPTMs, it also generated multiple modifications and peptides not seen with HOCl or sin-1. An advantage of utilising multiple treatments is to screen a larger sub-set of

possible modifications of the protein of interest to find modifications that may be of clinical value.

6.4.1.2. Limitations of treatments

The limitations of sin-1 treatment included low comparative nitration compared to TNM, and sin-1 being a peroxynitrite generator and thus being an indirect model of peroxynitrite treatment. For modeling the effect of peroxynitrite oxidative damage on signalling proteins, the generation by sin-1 may produce a particular treatment effect given the rate of peroxynitrite generation as the concentration of protein to sin-1 molar ratio and concentration would differ including not being as high concentration and molar ratio of oxidising agent at the beginning of the reaction. Sin-1 treatment differs from peroxynitrite treatment, peroxynitrite *in vivo* and sin-1 *in vivo*, and this then creates a differing, potentially overlapping, set of hypotheses that can be tested by sin-1 *in vitro*. Sin-1 presented challenges to generating sufficient nitration abundance for PPI study via protein-protein array, in the intact-protein bands for PTEN and VHR.

The limitations of HOCl treatment for the study of the effect of HOCl on the activity of intact-yet-modified protein come from a property of HOCl to induce backbone cleavage and give high relative yields of protein fragments, and to speculate, potentially aggregates of fragments and aggregates with fragments, compared to intact-yet-modified protein. This limitation may suggest *in vivo* fragmentation and aggregate formation via HOCl, yet poses a challenge for the use of HOCl to assess the effect of oxidation on intact proteins.

HOCl in the context of the treatment molar ratios and concentrations used, gave low yields of modification abundance for chlorination, this meant that at the concentrations used, HOCl presented challenges for generating intact-yet-modified protein with sufficient chlorination abundance for PPI study via protein-protein array.

This does not however imply that HOCl is irrelevant to *in vivo* interaction, as HOCl may have a role in protein interaction of aggregates, or *in vivo* microenvironment kinetics and concentrations of HOCl may generate alternate modification abundances and likelihoods. HOCl has a limitation when comparing the treatment to that of sin-1 as, in addition to the different mechanism of action to compare, sin-1 and HOCl also produce different molar ratios and concentrations of oxidant, that are not equivalent for corresponding HOCl versus sin-1 and TNM molar ratios and concentrations – in terms of modifications produced, abundances, activity level differences and fragments and aggregates produced.

The limitations of TNM were that TNM, at the concentrations and molar ratios used, inactivated VHR, thus being unable to correlate specific modifications to specific decreases in enzymatic activity. To produce levels of tyrosine nitration predicted to be suitable for PPI protein-protein arrays TNM treatment also produced high yields of fragments and aggregates, which was a limitation for TNM and a challenge for PPI protein-protein arrays of intact-yet-modified protein filtered of aggregates.

A limitation of the treatments involves the oxidant titration, concentration, molar ratio and conditions, where, to speculate, the titration, concentration, molar ratios and conditions are not appropriate as an *in vivo* comparison, and *in vivo* empirical studies would be required for this.

The limitation of assessing a limited number of molar ratios, concentrations and treatments meant that clinically and therapeutically important modifications may still be available to be discovered via *in vitro* approaches alongside *in vivo* approaches, and may add to fundamental knowledge about PTEN, VHR, HOCl, TNM, sin-1, ageing, inflammation and oxidative stress that may have clinical relevance and value.

For generating modified peptides, oxidative treatments *in vitro* where the residues modified, the ratios of abundances and the off-site modifications are not controlled is

inappropriate for screening the effects of a single molecule type, or as part of a process to create a reproducible biologic product. Screening of synthetic modified proteins and the usage of targeted and specific modification techniques would be required to be developed and implemented if this avenue was assessed to be valuable for clinical outcomes.

For assessing the oxPTMs, and PPIs associated and correlated with oxPTMs *in vivo* during specific health states in specific patients, appropriate patient samples, handled appropriately, from the appropriate patient cell populations would be required.

For delivering an oxidative payload to specific molecules and cells, small molecule oxidising agents may be inappropriate.

Challenges may include altering relative fragment-to-modification and aggregate-to-modification levels, and screening a larger and wider number of treatments and molar ratios in a time-efficient manner. A particular sub-challenge would be to create time-efficient iterations of the workflow through treatment, through assessment of what modifications, aggregates and fragments are produced and their abundances.

6.4.1.2. Quality of treatments in thesis

Treatments in the thesis were repeated, with new stocks of oxidants created for each repeat. Some variability can be expected between treatment concentrations and molar ratios, and this variability would stack with variability of protein concentration, repeats and statistics were used to minimise and control the effect of variability.

HOCl was measured prior to experimentation, for its concentration, as HOCl degrades. Stocks of sin-1 and TNM were made up freshly prior to experimentation.

Additional technical repeats for each treatment stock and treatment reaction, for each and between each MS run would also be required to improve the quality of the treatments.

6.4.2. Mass spectrometry

6.4.2.1. Advantages of mass spectrometry for functional proteomics of oxidative modifications

In-gel digest for MS samples offers advantages of being able to visualise via Coomassie staining changes in protein band intensity, and protein fragmentation and aggregation. The usage of SDS-PAGE for in-gel digest did not appear, given oxidation occurrences and abundances in controls, appear to oxidise protein samples. Excision of bands from gels for in-gel digest offers several technical advantages. I) Any impurities, contaminants that are have a different electrophoretic property to the protein of interest are discarded from MS analysis. II) In-gel digestion increases the efficiency of the trypsin digestion due to the matrix gel structure and effective trypsin concentration III) Differences in the way proteins run on a gel gives additional information that not detected via in-solution digestion such as changes in mass-to-charge ratio IV) The full complement of protein biomolecules included in the phosphatase assay are not represented in the mass-spectrometric data unless entire gel lane is excised.

Mass spectrometric techniques to identify specific PTMs have advantages over immunostaining, immunohistological or fluorescence reporter assay techniques – whereby particular PTMs can be correlated and modeled to corresponding activities and functions. The systematic approach further highlights the complexity of oxidation signatures and what is not detected using immunostaining, immunohistological or fluorescence reporter assay procedures.

ESI LC-MS offers advantages for quantitative analysis, high-throughput and automation potential which may be appropriate for mapping the roles and extracting

the value of oxPTMs, given the range of oxPTMs, proteins and abundances possible in the protein-oxidation landscape. ESI LC-MS may also have the throughput appropriate for a clinical environment (Chen et al., 2012).

6.4.2.2. Limitations of mass spectrometry for functional proteomics of oxidative modifications

The disadvantages of SDS-PAGE, Coomassie staining and gel band excision for MS analysis are that if a high level of oxidation is required for abundant modification, in order to elicit changes in the proxome and interactome of the protein of interest, the more oxidant added, the less protein of interest in an identifiable band. Additionally by selecting a band, this selects against modified protein of interest that have attained different electrophoretic properties post-oxidation. Additional disadvantages of in-gel digest include contamination with keratins and trypsin autolysis products.

Limitations of mass spectrometric analysis of peptides for functional proteomics include the limitation of assessing multiple peptides as a population. MS/MS does not elucidate which peptides came from a single protein molecule, and thus which modifications are correlated or causal for other modifications on the same molecule and functional effects, and only detects peptides and modifications that are pooled from multiple proteins and multiple cells, where multiple cells are used. A certain oxPTM sub-set may yield specific functional changes – including novel PPI, increases in activity or novel decreases in activity and novel conformations – these will be undiscoverable via a peptide-only approach linked to functional assays and arrays that assess gross and mean functionality.

Limitations include the range of mass-to-charge ratios detected via MS – with small and large peptides not being detected, in addition to particular peptides without

sufficient charge. Additional limitations with MS are that MS detects all proteins including contaminants.

Limitations in the Progenesis software were the order in which Progenesis searches were performed to search for multiple modification types, increases the potential for misidentification of modifications, and misallocation of masses.

Samples that were heavily modified, as part of the treatment, in-gel digest, LC-MS workflow had lower sequence coverage and lower p-values and less modified and unmodified peptides covered, which has limitations for comparative analysis of MS results including XICs of oxPTM abundance. This limitation may also point to the limitation of the LC-MS TOF ABSCIEX 5600, Mascot and Progenesis to detect sequence coverage and oxPTMs, in a label-free approach, in a purified sample of a single protein – for the systematic screening of oxPTMs for a protein and their relative abundances between samples and treatments.

Mascot searches were used as initial data processing protocol in order to I) Determine the identity of the proteins in the sample (protein of interest, contaminants) II) Assess the sequence coverage of the sample (how much of the protein sequence could be detected in QTOF). III) Assess if and which peptides and amino acids were oxidatively modified by treatment. Effort was taken to combine modifications in groups that would minimise misclassification – such as testing different groupings and combining the modifications that Mascot mistakes for each other in the same group. Searching for more modifications in one set can decrease accuracy. Searching for modifications in groups still includes the limitation that some modifications are classified differently when searched together or apart, such as multiple types of oxidation of different residues on the same peptide – if the sequencing cannot accurately predict which residue the modification is on within the peptide.

Error tolerant searches showed more erroneous predictions of modification that had a low probability of existing in the sample due to being unrelated to the sample or

oxidant type, thus increasing noise and false positives, and also force fitting raw data to fit modifications in the Mascot database, error tolerant search provides a methodological approach to reduce bias in the data analysis process. This limitation may be offset by an alternative verification method such as heavy isotope labelled modification reagents.

All Mascot search results are dependent on the quality of the MS/MS method, calibration of the QTOF, concentration of the protein, length of the MS/MS method, number of ions detected, the size of the ions and the quality and completeness of the enzymatic digest.

The step of analysing the raw data for the abundance of the modification is critical to both determining the functional effect of that modification by comparing to OMFP activity assays, but also for method development to create a oxidising treatment that oxidises protein enough that the protein-protein binding interaction for that protein changes.

6.4.2.3. Quality of mass spectrometry in thesis

The mass spectrometric procedures performed were done so in a manner where calibration, operator vigilance, error-rate checking and manual validation were implemented and maintained. Manual validation, for some samples, were possible was re-screened via automated software, and important residues were re-sequenced by additional stakeholders from the Oxidative Stress Group, Aston University.

Sample consistency may have been improved, as some samples were run on separate days and MS runs – due to either time-availability of the MS resources and the uptime limitations of the LC-MS bespoke setup. To improve quality control, instruments were calibrated between runs, and where possible samples were run on the same day, and on the same gel.

TIC, as can be seen from Figure 20, shows an intensity sufficient to detect many modifications, with high ion scores in Mascot and to be *de novo* sequenced. Figure 20 shows an exemplar run of capturing the peptide ions within the run that correspond to the sizes of peptides.

Samples and batches were run strategically including ensuring the sorting of samples in order of least oxidised, and run samples in one batch with a single calibration, where this would be appropriate without calibration drift over an extended batch run. Excess sample was generated in order that samples could be re-ran and also further investigated.

Blanks were ran at the start of batches and between sample sets to reduce cross-contamination. Samples were stored at -20°C prior to running, and time-in-storage was minimised via a LC-MS booking system.

The LC-MS system was regularly visited for maintenance and software upgrade over the time-course of running the MS experiments to ensure and improve the quality of the LC-MS system and the improve system consistency.

Where appropriate, training was given, and analysis was analysed by Professor Andrew Pitt, Doctor Karina Tveen-Jensen and Doctor Ana Reis to ensure quality.

6.4.3. Protein arrays

6.4.3.1. Advantages of protein arrays

Protein-protein arrays deliver the following advantages: Protein-protein arrays query the direct and single interactions between proteins, when contrasted with co-immunoprecipitation studies whereby the method may also screen for indirect interactors that interact via other cellular moieties, and as part of biomolecule and protein complexes. Protein-protein library arrays, excluding the variability of spotting between arrays by a single manufacturer, can be screened and validated at multiple geographic locations. Protein-protein arrays also have advantages for miniaturisation, automation and chip-based microfluidic workflows.

6.4.3.2. Limitations of protein arrays

Protein tertiary properties provide challenges for accurate spotting and meaningful spot-to-spot comparisons between different proteins given their conformation, size, binding properties and solubilities.

Protein library arrays contain a limited number of proteins and do not represent the protein complexes and protein-biomolecule complexes that occur *in vivo*, with regards to folding, PTMs, conformations, and the aggregates and fragments that may occur and have relevance for health states.

Constraints in protein-solubilisation versus protein-activity versus detection limits versus may pose challenges in protein-protein array protocol optimisation. Detection limits versus experimental variation in protein spotting and concentrations of spots between proteins versus abundance of modifications may also be a constraint and challenge.

Manual probing of arrays, utilising Dynamic Bioarrays or Lifterslips™ may introduce experimental variation that may be a constraint regarding array quality and statistical validation. An integrated, automated, enclosed solution may be a way to introduce greater reproducibility within a geographical location and between locations and time-points – and reduce or remove risk and manual error whilst created a solution that is of clinical quality for both pre-clinical and clinical deployment.

For the assessment of oxPTMs on PPI a limitation of arrays of industry purchased protein libraries, may be that the batch of protein arrayed on the library has not been analysed for oxPTMs, and cannot be readily assessed for oxPTMs from opportunistic oxidation from storage and during the workflow.

The cost of protein-protein libraries arrays provides a challenge to protein-protein arrays versus comparative technologies, including cost-per-use.

Antibody based techniques have the limitation that antibody specificity is variable and antibody non-specific binding to proteins and primary antibodies poses challenges – this antibody specificity and limit of known antibody targets may be compounded by oxPTMs and novel workflows.

6.4.3.3. Quality of protein arrays in thesis

The quality of protein-protein arrays performed was constrained from a limited number of library arrays in stock and procurable and reduced by the introduction of artefacts by the manual probing process. The combination of the constraint on array replicate number and the consequences of introduced artefacts from the manual probing process made statistical and automated analysis of the arrays untenable – leading to a manual validation of the protein-protein array libraries, hence a challenge for providing statistical significance.

6.4.4. Immunoprecipitation

6.4.4.1. Advantages of immunoprecipitation

The advantages of co-immunoprecipitation for PPI discovery are that the proteins discovered are from a sample and thus cover the range of proteins present in a particular sample lysate. Co-immunoprecipitation also offers high-throughput analysis via MS-coupled co-immunoprecipitation, which offers an identification of many proteins, where generating and purchasing antibodies for all proteins may be untenable, and nanopore technology may be inappropriate.

6.4.4.2. Limitations of immunoprecipitation

Limitations of co-immunoprecipitation include non-specificity of antibodies, where antibodies may find PPI for proteins other than the protein of interest. The beads utilised may also have their own interactors, and these would need to be differentiated from the PPIs for the protein of interest. Co-immunoprecipitation with downstream Western blotting has limitations based on antibody size versus size of protein interactors of interest, antibody non-specificity and cost, scalability and throughput constraints and challenges, and automation constraints – making immunoblotting untenable for pre-clinical and clinical multi-omic multi-marker discovery, screening and diagnostics; MS-coupled-immunoprecipitation with automated robotic co-immunoprecipitation and automated software analysis of proteins and PTMs may overcome challenges.

6.4.4.3. Quality of immunoprecipitation in thesis

Co-immunoprecipitation was performed on lysed samples directly following sample lysis to minimise changes in protein conformation, PTM and/or PPI, which might occur during storage or prolonged processing.

6.4.5. Modelling

The standard modelling methods included standard error and standard deviation, the t test inbuilt p-value significance and probability scores in the software packages of Mascot and Progenesis, and collaboration with Doctor Alexis Boukouvalas using mediator statistics.

Mediator analysis was implemented due to the shape of the oxPTM MS XIC abundances, upon recommendation of Doctor Alexis Boukouvalas, which had a comparatively low n versus intra-sample variable number. It also allowed multivariate analysis on comparatively low n versus intra-sample variable number.

6.4.6. Justification of methods: Conclusions

To conclude the overarching theme of the justification of methods is focused on resolution, quality and throughput – where limitations are focused on how to improve resolution, quality and throughput further through robotic and artificial intelligence automation. Thus future method workflows may from the outset be designed strategically as to deliver appropriate improvements in resolution, quality and throughput that fully robotic and fully automated workflows may offer.

6.5. What are valuable factors in systematic functional proteomics of oxidation in protein tyrosine phosphatases?

Broadly, valuable factors in systematic functional proteomics of oxidation in protein tyrosine phosphatases include identification, sequence coverage, quality and validation.

Factors that one may wish to identify include 1) Identification of which modifications are present, 2) which modifications are functionally linked to a health state, which modifications are correlated to a health state, 3) which modifications are predictive of the occurrence of a future health state, 4) which modifications are detectable *in vivo*, 5) which modifications are therapeutically amenable via therapies acting directly on the modification, 6) therapies acting on the protein of interest, 7) therapies acting on the cell with the protein of interest with the modification of interest, and 8) therapies acting on the organ of interest. The results herein describe a potential systematisation of *in vitro* study with which to start to approach these factors of interest, with further *in vivo* study, whereby it may be of value to have pre-identified which residues may be modified and what peptides to search for in a targeted search *in vivo* to improve detection capability *in vivo*.

With regards to PTPs finding 1) which PTPs are modified with oxPTMs in a health state of interest, 2) which oxPTMs in PTPs are correlated to health states of interest, 3) which oxPTMs in PTPs are predictive of future health states, 4) which PTP oxPTMs are detectible *in vivo*, 5) which oxPTMs in PTPs are therapeutically amenable at the oxPTM level, PTP level, and at the level of cells, tissues and organs containing PTPs with oxPTMs are factors of interest. The relevance and priority of PTP oxPTM identification may be determined empirically and/or via informatic analysis of available datasets including literature databases as datasets, which may be accurately extrapolated to *in vivo* outcomes.

Sequence coverage may be a valuable factor – and is linked to both identification and quality of proteomics via MS as a class of protein-sequencing-based approaches. Whereby sequence coverage allows questions to be asked regarding the context which the PTP oxPTM appears in, which may assist in assessing the functional relevance of those PTP oxPTM upon covering the sequence of a single protein, or sub-set of proteins from a part of a cell, or selected sub-set of cells. Sequence coverage may not be valuable if PTP oxPTMs or other modifications or peptides have can be identified reliably with untargeted, targeted, labelled or unlabelled methods.

For asking questions about a particular oxPTM in a PTP, having full sequence coverage including residues of known functional importance has value. For approaches based on measuring the function of a population of PTP molecules sampled from a patient – full sequence coverage of the PTP would ensure that all oxPTMs could be identified and thus the relationship between the function and all modifications present could be elucidated.

Automation is a valuable factor in functional proteomics. Omic strategies were enabled by automated and high-throughput technology, and increased automation may deliver the full value of omics. For a given use-case, it may be empirically determined as to whether an automated identification of protein and PTMs identifies modifications and how, and when the approach out-performs manual analysis.

Automation potential for parts of a workflow and value chain around oxPTMs and PTP functional proteomics may include I) Automation of sample sorting and treatment II) Automation of digestion protocol in solution III) Automation of assaying IV) Automation of loading digested samples to LC-MS V) Automated *in silico* digests and automated building of targeted scanning protocols to search for modified peptides VI) Automated data conversion, modification identification, statistics and differential and multivariate analysis VII) Automated uploading of data and meta-data to online database. This may require an online-liquid handling robot setup and an automated

software workflow. Specifically for OxPTMs in PTPs this may allow the empirical search and multivariate modelling of a larger area of the PTP oxPTM space, and to increase statistical power and discover a larger number of sequence-function correlations and also may increase predictive power as to what to take forward to the next phase of pre-clinical validation, and such workflow innovation may translate to a clinical setting. Specifically, with larger datasets, automation, and greater statistical power – non-active site modifications contributing to functional differences, rare events, interactions between multiple residues, multiple residues altering functionality may also be identified.

An automation-first, and full-automation strategy, may be valuable, to automated everything that may be automated at every stage of the life science and healthcare workflow, supply chain and value chain – from investment and funding, through pre-clinical workflows in sample collection, sample handling and processing, screening, modelling, analysis, data and information sharing, and integrated downstream clinical trials, and automated preventative healthcare and health screening, with automated robotic surgery for regenerative and prosthetic medicine to produce exponential gains in health and longevity for value-based medicine.

6.6. Clinical potential for PTEN and VHR oxidative proteomics

PTEN and VHR are cellular signalling proteins that can undergo PTM including oxPTM, have the potential to act a signal or part of a signal or model that may be utilised in personalised diagnostics and personalised medicine. Evidence for this comes from residues in PTEN and VHR being mutated in cancer, including Tyr138 which was found to be mutated in a cancer cell line (Stumpf & Hertog, 2016), where these residues being found to be modified by oxPTM in this thesis. The role of PTEN and VHR molecules in a diagnostic or at point of inhibition in cellular signalling may

rely on both the empirical drug screening and effective signalling pathway intervention, abundance of signalling molecules, expression of those signalling molecules in the cells of interest related to the health state, and the amenability of the PTEN and VHR molecules to diagnostic tests given its molecular characteristics that may affect identification, and cost of the diagnostic. How many PTEN and VHR molecules *in vivo* are required to be modified in a health state, versus how many are required for identification of the molecules-of-interest for the diagnostic may be a factor. PTEN has shown, that one of its active site amino acids, Cys71, can be modified with a biologically long-term modification, trioxidised cysteine, alongside VHR being modified at active site nucleophilic Cys124, and this may be one class of modifications-of-interest to search for in an automation-first informatics-led approach. Additional modification-regions of interest that may be searched for in a screening and diagnostic dataset, utilising PTEN as an example, and utilising the oxPTM functional proteomics to inform the drug screening may be to search for modification of the domains and regions of known interest, residues with evidence of modification, such as the phosphatase domain, C2 domain and area of major phosphorylation sites and residues known to be phosphorylated and ubiquitinated, and also search for long-term modifications whose reversal biologically and chemically is unfavourable entropically and has a low likelihood, which may last through processing and have a lower likelihood of being introduced as an artefact. Label and hypothesis free functional proteomics linked multi-omics may also be utilised in drug screening of cell signalling pathway modifying drugs. To speculate, for PTEN, disease state samples, and priority samples to perform drug screenings for disease-modifying effects in, of which MS and oxPTMs may be a part of a multi-omic approach, may be samples from neuropathies and neurological cancer, given the role of PTEN in cancer (Li, 1997; Steck et al., 1997) and neuroregeneration (Liu et al., 2010). To speculate, PTEN may be druggable at the protein level, and utilising MS to understand the PTEN PTMs in

the PTEN-associated disease states, or PTEN-modifiable disease states may be of interest – knowledge of PTEN PTMs may have utility in this process, to assess the PTMs involvement in effectiveness of therapy, mimicking their role, delivering PTM payloads to PTEN, competing with PTM PTEN and competition with PTEN PTM processes. To speculate, neuro-geroprotective and neuroregenerative therapies to address neuropathy, brain trauma and time-dependent neural cell loss, may utilise the role of PTEN in neural growth and neuroregeneration (Liu et al., 2010), including small molecule approaches and gene and cell therapy approaches to neurodegeneration and neurological cancers, as part of a multi-candidate, multi-omic assessment. To speculate further, for health states of interest, specifically the CNS which is cannot be replaced through transplants or artificial systems in the same way as every other tissue and organ, MS and proteomics may have utility to focus further upstream of PTEN in the signalling pathway, including the extracellular signals that interact with the PTEN pathways, and to focus on more readily accessible patient samples for the brain, such as cerebrospinal fluid (CSF). Lehtinen *et al* (2011) show that Pten and Protein associated with Lin 7 have opposing roles in the localisation of the insulin growth factor receptor 1 to the apical, ventricular domain of the cerebral cortex progenitor cells, and that CSF-based signalling activities including insulin growth factor 2 has an effect on cerebral cortex proliferation via Pten regulation. In this way, MS and proteomics of CSF for upstream proteins and extracellular proteins at distal and more accessible locations may be strategic with regards to developing diagnostics and pathway-modifying disease-preventing and disease-modifying therapeutics, which may include an assessment of the PTM and oxPTM state of these upstream and distal samples and proteins.

For VHR, disease state samples, and priority samples to perform drug screenings for disease-modifying effects in, of which MS and oxPTMs may be a part of a multi-omic approach, may include samples related to neuropathies and neurodegeneration,

given the PPI with NEUROD1 (see Appendices 2) and potential role in neurogenic differentiation. PTEN and VHR may also have utility and potential druggability in non-neuronal geroprotection and non-neuronal cancers, including cell signalling-modifying compounds. The PTEN and VHR oxPTMs found are part of a class of potential targets, and further understanding the oxPTMs of proteins may lead to additional efficacy and specificity of drugs and more specific, effective biologic drugs that target oxPTMs or contain oxPTMs, in biologic drugs with oxPTMs may have different biological half-lives and toxicities.

6.7. Future paths

Future paths may include working on the strategy and experimental design, starting with patients and outcomes that need to create for patients and other healthcare value chain stakeholders, and then reverse engineering a workflow and to appropriately gather enough of the appropriate *in vivo* samples. This is non-trivial on multiple accounts – the first being that *de novo* validation of PTMs is time consuming and impractical for pre-clinical and clinical settings, if indeed it is even needed when peptide identification, *in silico* prediction and statistical correlation of peptides may suffice given an approach that starts with clinically relevant patient samples, with appropriate statistics and population data.

Starting with *in vitro* work may contain biases and assumptions and be at risk of not fitting into a clinical translation workflow and not finding clinically relevant peptides and modifications and could its effectiveness as a strategy that is clinically relevant, competitive, economically valuable use of scientists, machine time and funding within a fixed time frame should be carefully considered and acted upon.

Starting with a relevant sample and seeing what one can and cannot see in that particular sample and what one can and cannot use as a biomarker or drug target

could be a direct approach along the critical path to health and longevity outcomes to consider. If there are no biomarkers or drug targets identifiable with regards to the statistical and repeatability constraints needed for clinical practice or drug development, then more targeted approaches could be performed using *in silico* predictions of expected peptides, literature searches, fractionation and antibody enrichment experiments and potential stratification and bifurcation of health or disease states by peptide or PTM. If specific peptides or PTMs are useful, this research could then lead to new diagnostic and prognostic test development, deeper understanding of disease processes and mechanisms, as part of a timely and anti-fragile value chain and workflow to generate pre-clinical leads to feed into a clinical pipeline.

Western blots of the SDS-PAGE gels containing oxidised protein to check for aggregates and fragments may add utility, as an additional technique for determination of action of oxidants on proteins of interest.

More replicates and higher resolution experiments could be performed including determining the functional importance of the modifications. This could include more oxidation replicates and treatment regimes, and even synthetic proteins with specific PTMs, as and when the technology and funding is available to do this if it is deemed critical. Co-immunoprecipitation may also be performed on stressed and ageing cells.

To validate the VHR putative interactions additional VHR array screenings, co-immunoprecipitations with statistical analysis and bespoke arrays with the interactors as both probe and arrayed protein. To explore the relevance of that interaction for drug design and *in vivo* occurrence, *in vivo* relevance and *in vivo* relevance to the health and longevity outcomes that you need, knockout mice and patient samples may be needed.

Samples that may have utility screening with high mass accuracy MS and PTM analysis including oxPTMs could be stem cells for stem cell differentiation method

development and quality control, organ printing quality control, space radiation risk analysis and mitigation and profiling of young and calorie restricted individuals so you had proteomic baselines for therapies to return individuals to. By applying high-resolution oxidative modification mapping as part of a multi-omics workflow in key areas such as space exploration, regenerative medicine to rejuvenate or replace ageing cells and tissues to develop personalised and preventative medicines – the technologies detailed within could be more fully realised to create the future outcomes for individuals and our species that we may want.

Much of the work contained within could have been performed at over 10X the speed with an automated thermal oxidation device linked to HPLC and MS with automated modification detection and statistical analysis. A careful questioning of the value of manual validation, bespoke methodology, methodology that introduces multiple stages and types of human error and bias, non-linkage of research from clinical workstreams and outcomes and the utilisation and current role and efficiency of pre-clinical academic research, with inflexible projects funded and designed from the top down that are not sufficiently linked to patient outcomes for health and longevity in a reasonable timeframe, or making full use of the innovation and dynamic capacity of talent.

Manual validation needs to be questioned as manual validation of PTMs, apart from in select instances of pre-clinical research, is not practical and scalable to a healthcare solution. A careful focus on prognostic capability and false discovery rates from the beginning in pre-clinical research might allow for more full utilisation of all academic resources, capacity and capability. There may also exist scenarios whereby bespoke analysis and manual validation can be afforded, when linked to health outcomes for personalised medical healthcare for confounding cases or high value clients – rather than something implemented from the start by fiat.

By critically questioning the research, alternative options, the wider context of the research – asking what future research we can do becomes a wider and more useful question as to what we can do, together, to utilise the knowledge, people and resources available for health and longevity outcomes.

List of References

- Aaronson, D. S., & Horvath, C. M. (2002). A road map for those who don't know JAK-STAT. *Science (New York, N.Y.)*, *296*(5573), 1653–5. Retrieved from <http://www.ncbi.nlm.nih.gov/pubmed/12040185>
- Adey, N. B., Huang, L., Ormonde, P. A., Baumgard, M. L., Pero, R., Byreddy, D. V., Tavitigian, S. V., et al. (2000). Threonine phosphorylation of the MMAC1/PTEN PDZ binding domain both inhibits and stimulates PDZ binding. *Cancer research*, *60*(1), 35–7. Retrieved from <http://www.ncbi.nlm.nih.gov/pubmed/10646847>
- Akbani, R., Becker, K.-F., Carragher, N., Goldstein, T., de Koning, L., Korf, U., ... Zhu, J. (2014). Realizing the promise of reverse phase protein arrays for clinical, translational, and basic research: a workshop report: the RPPA (Reverse Phase Protein Array) society. *Molecular & Cellular Proteomics: MCP*, *13*(7), 1625–43. doi:10.1074/mcp.O113.034918
- Albrich, J. M., McCarthy, C. A., & Hurst, J. K. (1981). Biological reactivity of hypochlorous acid: implications for microbicidal mechanisms of leukocyte myeloperoxidase. *Proceedings of the National Academy of Sciences of the United States of America*, *78*(1), 210–4. Retrieved from <http://www.pubmedcentral.nih.gov/articlerender.fcgi?artid=319021&tool=pmcentrez&rendertype=abstract>
- Al-Mulla, F., Bitar, M. S., Al-Maghrebi, M., Behbehani, A. I., Al-Ali, W., Rath, O., ... Kolch, W. (2011). Raf kinase inhibitor protein RKIP enhances signaling by glycogen synthase kinase-3 β . *Cancer Research*, *71*(4), 1334–43. doi:10.1158/0008-5472.CAN-10-3102

- Alonso, A, Saxena, M., Williams, S., & Mustelin, T. (2001). Inhibitory role for dual specificity phosphatase VHR in T cell antigen receptor and CD28-induced Erk and Jnk activation. *The Journal of biological chemistry*, 276(7), 4766–71. Retrieved from <http://www.ncbi.nlm.nih.gov/pubmed/11085983>
- Alonso, Andres, Rahmouni, S., Williams, S., van Stipdonk, M., Jaroszewski, L., Godzik, A., Abraham, R. T., et al. (2003). Tyrosine phosphorylation of VHR phosphatase by ZAP-70. *Nature immunology*, 4(1), 44–8. Retrieved from <http://www.ncbi.nlm.nih.gov/pubmed/12447358>
- Alonso, Andres, Sasin, J., Bottini, N., Friedberg, I., Friedberg, I., Osterman, A., Godzik, A., et al. (2004). Protein tyrosine phosphatases in the human genome. *Cell*, 117(6), 699–711. Retrieved from <http://www.ncbi.nlm.nih.gov/pubmed/15186772>
- Alvarez, B., & Radi, R. (2003). Peroxynitrite reactivity with amino acids and proteins. *Amino acids*, 25(3-4), 295–311. doi:10.1007/s00726-003-0018-8
- Anisimov, V. N., Berstein, L. M., Egormin, P. A., Piskunova, T. S., Popovich, I. G., Zabezhinski, M. A., ... Semenchenko, A. V. (2014). Metformin slows down aging and extends life span of female SHR mice. *Cell Cycle*, 7(17), 2769–2773. doi:10.4161/cc.7.17.6625
- Amand, M., Epicum, C., Bajou, K., Cerignoli, F., Blacher, S., Martin, M., ... Rahmouni, S. (2014). DUSP3/VHR is a pro-angiogenic atypical dual-specificity phosphatase. *Molecular Cancer*, 13(1), 108. doi:10.1186/1476-4598-13-108
- Aulak, K. S., Miyagi, M., Yan, L., West, K. A., Massillon, D., Crabb, J. W., & Stuehr, D. J. (2001). Proteomic method identifies proteins nitrated in vivo during inflammatory challenge. *Proceedings of the National Academy of Sciences of the United States of America*, 98(21), 12056–61. doi:10.1073/pnas.221269198

- Bannister, A. J., & Kouzarides, T. (2005). Reversing histone methylation. *Nature*, 436(7054), 1103–1106. doi:10.1038/nature04048
- Bayden, A. S., Yakovlev, V. A., Graves, P. R., Mikkelsen, R. B., & Kellogg, G. E. (2011). Factors influencing protein tyrosine nitration--structure-based predictive models. *Free radical biology & medicine*, 50(6), 749–62. doi:10.1016/j.freeradbiomed.2010.12.016
- Bensaad, K., & Vousden, K. H. (2005). Savior and slayer: the two faces of p53. *Nature Medicine*, 11(12), 1278–9. doi:10.1038/nm1205-1278
- Biancotto, C., Frigè, G., Minucci S. (2010). Histone modification therapy of cancer. *Adv Genet* 70, 341-86. doi:10.1016/b978-0-12-380866-0.60013-7
- Bolduc, D., Rahdar, M., Tu-Sekine, B., Sivakumaren, S. C., Raben, D., Amzel, L. M., Devreotes, P., Gabelli, S, B., Cole, P. (2013) Phosphorylation-mediated PTEN conformational closure and deactivation revealed with protein semisynthesis *eLife*; 2: e00691. Published online 2013 Jul 9. doi: 10.7554/eLife.00691
- Buchczyk, D. P., Grune, T., Sies, H., & Klotz, L.-O. (2003). Modifications of glyceraldehyde-3-phosphate dehydrogenase induced by increasing concentrations of peroxynitrite: early recognition by 20S proteasome. *Biological chemistry*, 384(2), 237–41. doi:10.1515/BC.2003.026
- Burns, K. A., & Vanden Heuvel, J. P. (2007). Modulation of PPAR activity via phosphorylation. *Biochimica et Biophysica Acta*, 1771(8), 952–60. doi:10.1016/j.bbailp.2007.04.018
- Capeillere-Blandin, C., Delaveau, T., & Descamps-Latscha, B. (1991). Structural modifications of human beta 2 microglobulin treated with oxygen-derived radicals. *The Biochemical Journal*, 277 (Pt 1, 175–82. Retrieved from

<http://www.pubmedcentral.nih.gov/articlerender.fcgi?artid=1151207&tool=pmcentrez&rendertype=abstract>

Campisi, J. (2001). Cellular senescence as a tumor-suppressor mechanism. *Trends in Cell Biology*, 11(11), 27–31.

Camps, M., Nichols, A., & Arkinstall, S. (2000). Dual specificity phosphatases: a gene family for control of MAP kinase function. *FASEB journal: official publication of the Federation of American Societies for Experimental Biology*, 14(1), 6–16. Retrieved from <http://www.ncbi.nlm.nih.gov/pubmed/10627275>

Cassina, A. M., Hodara, R., Souza, J. M., Thomson, L., Castro, L., Ischiropoulos, H., ... Radi, R. (2000). Cytochrome c Nitration by Peroxynitrite. *Journal of Biological Chemistry*, 275(28), 21409–21415. doi:10.1074/jbc.M909978199

Chambers, A. G., Percy, A. J., Simon, R., & Borchers, C. H. (2014). MRM for the verification of cancer biomarker proteins: recent applications to human plasma and serum. *Expert Review of Proteomics*, 11(2), 137–48.
doi:10.1586/14789450.2014.877346

Chen, H., Libertini, S. J., Wang, Y., Kung, H.-J., Ghosh, P., & Mudryj, M. (2010). ERK Regulates Calpain 2-induced Androgen Receptor Proteolysis in CWR22 Relapsed Prostate Tumor Cell Lines. *Journal of Biological Chemistry*, 285(4), 2368–2374.
doi:10.1074/jbc.M109.049379

Chen, C. C., Tung, Y. Y., Chang, C. A lifespan MRI evaluation of ventricular enlargement in normal aging mice (2011). *Neurobiol Aging*, 32(12), 2299-307.
doi:10.1016/j.neurobiolaging.2010.01.013

Chen, R., Mias, G. I., Li-Pook-Than, J., Jiang, L., Lam, H. Y. K., Chen, R., ... Snyder, M. (2012). Personal omics profiling reveals dynamic molecular and medical phenotypes. *Cell*, 148(6), 1293–307. doi:10.1016/j.cell.2012.02.009

- Cheshire, J. 2012. Lives on the Line: Mapping Life Expectancy Along the London Tube Network. *Environment and Planning A*. 44 (7). Doi: 10.1068/a45341
- Chiarugi, P., & Buricchi, F. (2007). Protein tyrosine phosphorylation and reversible oxidation: two cross-talking posttranslation modifications. *Antioxidants & Redox Signaling*, 9(1), 1–24. doi:10.1089/ars.2007.9.1
- Chiarugi, P., Taddei, M. L., & Ramponi, G. (2005). Oxidation and tyrosine phosphorylation: synergistic or antagonistic cues in protein tyrosine phosphatase. *Cellular and Molecular Life Sciences : CMLS*, 62(9), 931–6. doi:10.1007/s00018-004-4448-1
- Chicco, A. J., & Sparagna, G. C. (2007). Role of cardiolipin alterations in mitochondrial dysfunction and disease. *American journal of physiology. Cell physiology*, 292(1), C33–44. Retrieved from <http://ajpcell.physiology.org/cgi/content/abstract/292/1/C33>
- Chu, G., Kerr, J. P., Mitton, B., Egnaczyk, G. F., Vazquez, J. A., Shen, M., ... Kranias, E. G. (2004). Proteomic analysis of hyperdynamic mouse hearts with enhanced sarcoplasmic reticulum calcium cycling. *FASEB Journal : Official Publication of the Federation of American Societies for Experimental Biology*, 18(14), 1725–7. doi:10.1096/fj.04-2025fje
- Chung, J., Lee, J. H., Choi, J., Lee, J., Kim, W. G., Sun, K., & Min, B. G. (2004). Home care artificial heart monitoring system via internet. *The International Journal of Artificial Organs*, 27(10), 898–903. Retrieved from <http://www.ncbi.nlm.nih.gov/pubmed/15560684>
- Claxton, J. S., Sandoval, P. C., Liu, G., Chou, C.-L., Hoffert, J. D., & Knepper, M. A. (2013). Endogenous carbamylation of renal medullary proteins. *PLoS One*, 8(12), e82655. doi:10.1371/journal.pone.0082655

- Cohen, P. (1999). The Croonian Lecture 1998. Identification of a protein kinase cascade of major importance in insulin signal transduction. *Philosophical Transactions of the Royal Society of London. Series B, Biological Sciences*, 354(1382), 485–95.
doi:10.1098/rstb.1999.0399
- Collado, M., Blasco, M. a, & Serrano, M. (2007). Cellular senescence in cancer and aging. *Cell*, 130(2), 223–33. doi:10.1016/j.cell.2007.07.003
- Collado, M., Gil, J., Efeyan, A., Guerra, C., Schuhmacher, A. J., Barradas, M., ... Serrano, M. (2005). Tumour biology: senescence in premalignant tumours. *Nature*, 436(7051), 642. doi:10.1038/436642a
- Corey, D. R. (2009). Telomeres and Telomerase: From Discovery to Clinical Trials. *Chemistry & Biology*. doi:10.1016/j.chembiol.2009.12.001
- Cox, J., & Mann, M. (2011). Quantitative, high-resolution proteomics for data-driven systems biology. *Annual Review of Biochemistry*, 80, 273–99. doi:10.1146/annurev-biochem-061308-093216
- Daiber, A., Daub, S., Bachschmid, M., Schildknecht, S., Oelze, M., Steven, S., Schmidt, P., Megner, A., Wada, M., Tanabe, T., Münzel, T., Bottari, S., Ullrich, V. (2013). Protein tyrosine nitration and thiol oxidation by peroxynitrite-strategies to prevent these oxidative modifications. *Int J Mol Sci*. Apr 8;14(4):7542-70. doi: 10.3390/ijms14047542.
- Dalle-Donne, I., Rossi, R., Colombo, R., Giustarini, D., & Milzani, A. (2006). Biomarkers of oxidative damage in human disease. *Clinical Chemistry*, 52(4), 601–23.
doi:10.1373/clinchem.2005.061408
- Dalle-Donne, I., Rossi, R., Giustarini, D., Milzani, A., & Colombo, R. (2003). Protein carbonyl groups as biomarkers of oxidative stress. *Clinica Chimica Acta; International Journal of Clinical Chemistry*, 329(1-2), 23–38. Retrieved from <http://www.ncbi.nlm.nih.gov/pubmed/12589963>

- Dalle-Donne, I., Scaloni, A., Giustarini, D., Cavarra, E., Tell, G., Lungarella, G., ... Milzani, A. (2005). Proteins as biomarkers of oxidative/nitrosative stress in diseases: the contribution of redox proteomics. *Mass Spectrometry Reviews*, *24*(1), 55–99.
doi:10.1002/mas.20006
- Davis, K. M., Pattanayak, V., Thompson, D. B., Zuris, J. A., & Liu, D. R. (2015). Small molecule–triggered Cas9 protein with improved genome-editing specificity. *Nature Chemical Biology*, *11*(5), 316–318. doi:10.1038/nchembio.1793
- De Martinis, M., Franceschi, C., Monti, D., & Ginaldi, L. (2005). *Inflamm-ageing and lifelong antigenic load as major determinants of ageing rate and longevity*. *FEBS Letters* (Vol. 579). doi:10.1016/j.febslet.2005.02.055
- Denu, J M, Stuckey, J. A., Saper, M. A., & Dixon, J. E. (1996). Form and function in protein dephosphorylation. *Cell*, *87*(3), 361–4. Retrieved from <http://www.ncbi.nlm.nih.gov/pubmed/8898189>
- Denu, J M, & Tanner, K. G. (1998). Specific and reversible inactivation of protein tyrosine phosphatases by hydrogen peroxide: evidence for a sulfenic acid intermediate and implications for redox regulation. *Biochemistry*, *37*(16), 5633–42.
doi:10.1021/bi973035t
- Denu, John M, & Tanner, K. G. (1998). Specific and Reversible Inactivation of Protein Tyrosine Phosphatases by Hydrogen Peroxide : Evidence for a Sulfenic Acid Intermediate and Implications for Redox, *2960*(16), 5633–5642.
- Devine, T., & Dai, M.-S. (2013). Targeting the ubiquitin-mediated proteasome degradation of p53 for cancer therapy. *Current Pharmaceutical Design*, *19*(18), 3248–62.
Retrieved from <http://www.ncbi.nlm.nih.gov/pubmed/23151129>

- Dey, S., Guha, M., Alam, A., Goyal, M., Bindu, S., Pal, C., ... Bandyopadhyay, U. (2009). Malarial infection develops mitochondrial pathology and mitochondrial oxidative stress to promote hepatocyte apoptosis. *Free Radical Biology & Medicine*, *46*(2), 271–81. doi:10.1016/j.freeradbiomed.2008.10.032
- Diepen, M. T. V., Parsons, M., Downes, C. P., Leslie, N. R., Hindges, R., & Eickholt, B. J. (2009). MyosinV controls PTEN function and neuronal cell size. *October*, *11*(10). doi:10.1038/ncb1961.nature
- Djuric, Z., Heilbrun, L. K., Reading, B. A., Boomer, A., Valeriote, F. A., & Martino, S. (1991). Effects of a low-fat diet on levels of oxidative damage to DNA to human peripheral nucleated blood cells. *Journal of the National Cancer Institute*, *83*(11), 766–9. Retrieved from <http://www.ncbi.nlm.nih.gov/pubmed/2041051>
- Dychdala, G. R. (1991). Chlorine and chlorine compounds. pp.131-151. In S. S. Block (ed.), *Disinfection, Sterilization and Preservation*. Lea & Febiger, Philadelphia. ISBN 0-693-30740-1
- Ehninger, D., Neff, F., & Xie, K. (2014). Longevity, aging and rapamycin. *Cellular and Molecular Life Sciences : CMLS*, *71*(22), 4325–46. doi:10.1007/s00018-014-1677-1
- Elchebly, M., Payette, P., Michaliszyn, E., Cromlish, W., Collins, S., Loy, A. L., ... Kennedy, B. P. (1999). Increased insulin sensitivity and obesity resistance in mice lacking the protein tyrosine phosphatase-1B gene. *Science (New York, N.Y.)*, *283*(5407), 1544–8. Retrieved from <http://www.ncbi.nlm.nih.gov/pubmed/10066179>
- El-Kouhen, K., & Tremblay, M. L. (2011). PTPMT1: connecting cardiolipin biosynthesis to mitochondrial function. *Cell metabolism*, *13*(6), 615–7. Retrieved from <http://www.ncbi.nlm.nih.gov/pubmed/21641541>
- Engelfriet, P. M., Jansen, E. H. J. M., Picavet, H. S. J., & Dollé, M. E. T. (2013). Biochemical Markers of Aging for Longitudinal Studies in Humans. *Epidemiologic Reviews*. doi:10.1093/epirev/mxs011

- Ewing, R. M., Chu, P., Elisma, F., Li, H., Taylor, P., Climie, S., McBroom-Cerajewski, L., et al. (2007). Large-scale mapping of human protein-protein interactions by mass spectrometry. *Molecular systems biology*, 3, 89. Retrieved from <http://www.pubmedcentral.nih.gov/articlerender.fcgi?artid=1847948&tool=pmcentrez&rendertype=abstract>
- Fan, X., Zhang, J., Theves, M., Strauch, C., Nemet, f I., Liu, X., Qian, J., et al. (2009). Mechanism of lysine oxidation in human lens crystallins during aging and in diabetes. *The Journal of biological chemistry*, 284(50), 34618–27. doi:10.1074/jbc.M109.032094
- Fedorova, M. (2011). Identification of protein carbonylation sites by two-dimensional liquid chromatography in combination with MALDI- and ESI-MS. *Journal of Proteomics*, 74(11), 2338–50. doi:10.1016/j.jprot.2011.07.002
- Fedorova, M., Bollineni, R. C., & Hoffmann, R. Protein carbonylation as a major hallmark of oxidative damage: update of analytical strategies. *Mass Spectrometry Reviews*, 33(2), 79–97. doi:10.1002/mas.21381
- Feijs, K. L., Kleine, H., Braczynski, A., Forst, A. H., Herzog, N., Verheugd, P., ... Dawid, I. (2013). ARTD10 substrate identification on protein microarrays: regulation of GSK3 β by mono-ADP-ribosylation. *Cell Communication and Signaling*, 11(1), 5. doi:10.1186/1478-811X-11-5
- Fenaille, F., Tabet, J.-C., & Guy, P. A. (2004). Identification of 4-hydroxy-2-nonenal-modified peptides within unfractionated digests using matrix-assisted laser desorption/ionization time-of-flight mass spectrometry. *Analytical Chemistry*, 76(4), 867–73. doi:10.1021/ac0303822

- Fenaille, F., Parisod, V., Tabet, J.-C., & Guy, P. A. (2005). Carbonylation of milk powder proteins as a consequence of processing conditions. *Proteomics*, 5(12), 3097–104. doi:10.1002/pmic.200401139
- Fenn, J. B., Mann, M., Meng, C. K., Wong, S. F., & Whitehouse, C. M. (1989). Electrospray ionization for mass spectrometry of large biomolecules. *Science (New York, N.Y.)*, 246(4926), 64–71. Retrieved from <http://www.ncbi.nlm.nih.gov/pubmed/2675315>
- Fenner, B. J., Scannell, M., & Prehn, J. H. M. (2010). Expanding the substantial interactome of NEMO using protein microarrays. *PloS One*, 5(1), e8799. doi:10.1371/journal.pone.0008799
- Fine, B., Hodakoski, C., Koujak, S., Su, T., Saal, L. H., Maurer, M., Hopkins, B., et al. (2009). Activation of the PI3K pathway in cancer through inhibition of PTEN by exchange factor P-REX2a. *Science (New York, N.Y.)*, 325(5945), 1261–5. Retrieved from <http://www.pubmedcentral.nih.gov/articlerender.fcgi?artid=2936784&tool=pmcentrez&rendertype=abstract>
- Forman, H. J., Fukuto, J. M., & Torres, M. (2004). Redox signaling: thiol chemistry defines which reactive oxygen and nitrogen species can act as second messengers. *American Journal of Physiology. Cell Physiology*, 287(2), C246–56. doi:10.1152/ajpcell.00516.2003
- Gems, D., & Partridge, L. (2008). Stress-response hormesis and aging: “that which does not kill us makes us stronger”. *Cell Metabolism*, 7(3), 200–3. doi:10.1016/j.cmet.2008.01.001
- Ghesquière, B., Jonckheere, V., Colaert, N., Van Durme, J., Timmerman, E., Goethals, M., ... Gevaert, K. (2011). Redox proteomics of protein-bound methionine oxidation.

Molecular & Cellular Proteomics: MCP, 10(5), M110.006866.

doi:10.1074/mcp.M110.006866

- Gella, A., & Durany, N. (2009). Oxidative stress in Alzheimer disease. *Cell Adhesion & Migration*, 3(1), 88–93. Retrieved from <http://www.pubmedcentral.nih.gov/articlerender.fcgi?artid=2675154&tool=pmcentrez&rendertype=abstract>
- Giot, L., Bader, J. S., Brouwer, C., Chaudhuri, A., Kuang, B., Li, Y., Hao, Y. L., et al. (2003). A protein interaction map of *Drosophila melanogaster*. *Science (New York, N.Y.)*, 302(5651), 1727–36. doi:10.1126/science.1090289
- Good, N. E., Winget, G. D., Winter, W., Connolly, T. N., Izawa, S., & Singh, R. M. (1966). Hydrogen ion buffers for biological research. *Biochemistry*, 5(2), 467–77. Retrieved from <http://www.ncbi.nlm.nih.gov/pubmed/5942950>
- Gow, A. J., Farkouh, C. R., Munson, D. a, Posencheg, M. a, & Ischiropoulos, H. (2004). Biological significance of nitric oxide-mediated protein modifications. *American journal of physiology. Lung cellular and molecular physiology*, 287(2), L262–8. doi:10.1152/ajplung.00295.2003
- Greenacre, S. A. B., & Ischiropoulos, H. (2001). Tyrosine nitration: Localisation, quantification, consequences for protein function and signal transduction. *Free Radical Research*, 34(6), 541–581. doi:10.1080/10715760100300471
- Grumont, R. J., Rasko, J. E., Strasser, A., & Gerondakis, S. (1996). Activation of the mitogen-activated protein kinase pathway induces transcription of the PAC-1 phosphatase gene. *Molecular and cellular biology*, 16(6), 2913–21. Retrieved from <http://www.pubmedcentral.nih.gov/articlerender.fcgi?artid=231285&tool=pmcentrez&rendertype=abstract>

- Grune, T., Jung, T., Merker, K., & Davies, K. J. A. (2004). Decreased proteolysis caused by protein aggregates, inclusion bodies, plaques, lipofuscin, ceroid, and “aggresomes” during oxidative stress, aging, and disease. *The International Journal of Biochemistry & Cell Biology*, 36(12), 2519–30. doi:10.1016/j.biocel.2004.04.020
- Gunaratne, J., Goh, M. X., Swa, H. L. F., Lee, F. Y., Sanford, E., Wong, L. M., Hogue, K. a, et al. (2011). Protein interactions of phosphatase and tensin homologue (PTEN) and its cancer-associated G20E mutant compared by using stable isotope labeling by amino acids in cell culture-based parallel affinity purification. *The Journal of biological chemistry*, 286(20), 18093–103. doi:10.1074/jbc.M111.221184
- Haass, C., & Selkoe, D. J. (2007). Soluble protein oligomers in neurodegeneration: lessons from the Alzheimer’s amyloid beta-peptide. *Nature Reviews. Molecular Cell Biology*, 8(2), 101–12. doi:10.1038/nrm2101
- Harris, M. E., Hensley, K., Butterfield, D. A., Leedle, R. A., & Carney, J. M. (1995). Direct evidence of oxidative injury produced by the Alzheimer’s beta-amyloid peptide (1-40) in cultured hippocampal neurons. *Experimental Neurology*, 131(2), 193–202.
Retrieved from <http://www.ncbi.nlm.nih.gov/pubmed/7895820>
- Harrison, J. E., & Schultz, J. (1976). Studies on the chlorinating activity of myeloperoxidase. *The Journal of biological chemistry*, 251(5), 1371–4. Retrieved from <http://www.ncbi.nlm.nih.gov/pubmed/176150>
- Harrison, D. E., Strong, R., Sharp, Z. D., Nelson, J. F., Astle, C. M., Flurkey, K., ... Miller, R. A. (2009). Rapamycin fed late in life extends lifespan in genetically heterogeneous mice. *Nature*, 460(7253), 392–5. doi:10.1038/nature08221
- Hayflick, L., Moorhead, P. S. (1961) The serial cultivation of human diploid cell strains. *Experimental Cell Research*. 25:585-621.

- Hecht, D., & Zick, Y. (1992). Selective inhibition of protein tyrosine phosphatase activities by H₂O₂ and vanadate in vitro. *Biochemical and biophysical research communications*, *188*(2), 773–9. Retrieved from <http://www.ncbi.nlm.nih.gov/pubmed/1445322>
- Henkens, R., Delvenne, P., Arafa, M., Moutschen, M., Zeddou, M., Tautz, L., Boniver, J., et al. (2008). Cervix carcinoma is associated with an up-regulation and nuclear localization of the dual-specificity protein phosphatase VHR. *BMC cancer*, *8*, 147. Retrieved from <http://www.pubmedcentral.nih.gov/articlerender.fcgi?artid=2413255&tool=pmcentrez&rendertype=abstract>
- Henzel, W. J., Billeci, T. M., Stults, J. T., Wong, S. C., Grimley, C., & Watanabe, C. (1993). Identifying proteins from two-dimensional gels by molecular mass searching of peptide fragments in protein sequence databases. *Proceedings of the National Academy of Sciences of the United States of America*, *90*(11), 5011–5. Retrieved from <http://www.pubmedcentral.nih.gov/articlerender.fcgi?artid=46643&tool=pmcentrez&rendertype=abstract>
- Hess, D. T., Matsumoto, A., Kim, S.-O., Marshall, H. E., & Stamler, J. S. (2005). Protein S-nitrosylation: purview and parameters. *Nature Reviews. Molecular Cell Biology*, *6*(2), 150–66. doi:10.1038/nrm1569
- Holmes, B. B., & Diamond, M. I. (2014). Prion-like properties of Tau protein: the importance of extracellular Tau as a therapeutic target. *The Journal of Biological Chemistry*, *289*(29), 19855–61. doi:10.1074/jbc.R114.549295
- Holmgren, A. (1989). Thioredoxin and glutaredoxin systems. *The Journal of Biological Chemistry*, *264*(24), 13963–6. Retrieved from <http://www.ncbi.nlm.nih.gov/pubmed/2668278>
- Houtkooper, R. H., & Vaz, F. M. (2008). Cardiolipin, the heart of mitochondrial metabolism. *Cellular and molecular life sciences : CMLS*, *65*(16), 2493–506. Retrieved from <http://www.ncbi.nlm.nih.gov/pubmed/18425414>

- Hu, S., Xie, Z., Qian, J., Blackshaw, S., & Zhu, H. (2011). Functional Protein Microarray Technology. *Wiley Interdisciplinary Reviews. Systems Biology and Medicine*, 3(3), 255–268. <http://doi.org/10.1002/wsbm.118>
- Ishibashi, T., Bottaro, D. P., Chan, A., Miki, T., & Aaronson, S. A. (1992). Expression cloning of a human dual-specificity phosphatase. *Proceedings of the National Academy of Sciences of the United States of America*, 89(24), 12170–4. Retrieved from <http://www.pubmedcentral.nih.gov/articlerender.fcgi?artid=50720&tool=pmcentrez&rendertype=abstract>
- Jang, J.-H., Aruoma, O. I., Jen, L.-S., Chung, H. Y., & Surh, Y.-J. (2004). Ergothioneine rescues PC12 cells from beta-amyloid-induced apoptotic death. *Free radical biology & medicine*, 36(3), 288–99. Retrieved from <http://www.ncbi.nlm.nih.gov/pubmed/15036348>
- James, P., Quadroni, M., Carafoli, E., & Gonnet, G. (1993). Protein identification by mass profile fingerprinting. *Biochemical and Biophysical Research Communications*, 195(1), 58–64. doi:10.1006/bbrc.1993.2009
- Jefferys, S. R., & Giddings, M. C. (2011). Baking a mass-spectrometry data PIE with McMC and simulated annealing: predicting protein post-translational modifications from integrated top-down and bottom-up data. *Bioinformatics (Oxford, England)*, 27(6), 844–52. doi:10.1093/bioinformatics/btr027
- Jeong, W., Park, S. J., Chang, T.-S., Lee, D.-Y., & Rhee, S. G. (2006). Molecular mechanism of the reduction of cysteine sulfinic acid of peroxiredoxin to cysteine by mammalian sulfiredoxin. *The Journal of Biological Chemistry*, 281(20), 14400–7. doi:10.1074/jbc.M511082200

- Jeppesen, J., Beniczky, S., Johansen, P., Sidenius, P., & Fuglsang-Frederiksen, A. (2015). Detection of epileptic seizures with a modified heart rate variability algorithm based on Lorenz plot. *Seizure*, *24*, 1–7. doi:10.1016/j.seizure.2014.11.004
- Kalim, S., Karumanchi, S. A., Thadhani, R. I., & Berg, A. H. (2014). Protein carbamylation in kidney disease: pathogenesis and clinical implications. *American Journal of Kidney Diseases : The Official Journal of the National Kidney Foundation*, *64*(5), 793–803. doi:10.1053/j.ajkd.2014.04.034
- Kang-Park, S., Lee, Y. I., & Lee, Y. I. (2003). PTEN modulates insulin-like growth factor II (IGF-II)-mediated signaling; the protein phosphatase activity of PTEN downregulates IGF-II expression in hepatoma cells. *FEBS letters*, *545*(2-3), 203–8. Retrieved from <http://www.ncbi.nlm.nih.gov/pubmed/12804776>
- Kanski, J., Behring, A., Pelling, J., & Schöneich, C. (2005). Proteomic identification of 3-nitrotyrosine-containing rat cardiac proteins: effects of biological aging. *American journal of physiology. Heart and circulatory physiology*, *288*(1), H371–81. doi:10.1152/ajpheart.01030.2003
- Kanski, J., Hong, S. J., & Schöneich, C. (2005). Proteomic analysis of protein nitration in aging skeletal muscle and identification of nitrotyrosine-containing sequences in vivo by nanoelectrospray ionization tandem mass spectrometry. *The Journal of biological chemistry*, *280*(25), 24261–6. doi:10.1074/jbc.M501773200
- Kendall, G., Cooper, H. J., Heptinstall, J., Derrick, P. J., Walton, D. J., & Peterson, I. R. (2001). Specific electrochemical nitration of horse heart myoglobin. *Archives of biochemistry and biophysics*, *392*(2), 169–79. doi:10.1006/abbi.2001.2451
- Kersten, S., Seydoux, J., Peters, J. M., Gonzalez, F. J., Desvergne, B., & Wahli, W. (1999). Peroxisome proliferator-activated receptor alpha mediates the adaptive response to fasting. *The Journal of Clinical Investigation*, *103*(11), 1489–98. doi:10.1172/JCI6223

- Khavinson, V. K., & Morozov, V. G. (n.d.). Peptides of pineal gland and thymus prolong human life. *Neuro Endocrinology Letters*, 24(3-4), 233–40. Retrieved from <http://www.ncbi.nlm.nih.gov/pubmed/14523363>
- Kim, J. H., Cho, H., Ryu, S. E., & Choi, M. U. (2000). Effects of metal ions on the activity of protein tyrosine phosphatase VHR: highly potent and reversible oxidative inactivation by Cu²⁺ ion. *Archives of biochemistry and biophysics*, 382(1), 72–80. Retrieved from <http://www.ncbi.nlm.nih.gov/pubmed/11051099>
- Kim, H. K., & Andreazza, A. C. (2012). The relationship between oxidative stress and post-translational modification of the dopamine transporter in bipolar disorder. *Expert Review of Neurotherapeutics*, 12(7), 849–59. doi:10.1586/ern.12.64
- Kirsch, M., Lomonosova, E. E., Korth, H. G., Sustmann, R., & de Groot, H. (1998). Hydrogen peroxide formation by reaction of peroxynitrite with HEPES and related tertiary amines. Implications for a general mechanism. *The Journal of Biological Chemistry*, 273(21), 12716–24. Retrieved from <http://www.ncbi.nlm.nih.gov/pubmed/9582295>
- Klaunig, J. E., Xu, Y., Isenberg, J. S., Bachowski, S., Kolaja, K. L., Jiang, J., Stevenson, D. E., & Walborg, Jr, E. F. The role of oxidative stress in chemical carcinogenesis (1998). *Environmental Health Perspectives*. 106(Suppl 1), 289-295.
- Koch, K. M. (1992). Dialysis-related amyloidosis. *Kidney International*, 41(5), 1416–29. Retrieved from <http://www.ncbi.nlm.nih.gov/pubmed/1614057>
- Kolmodin, K., & Aqvist, J. (2001). The catalytic mechanism of protein tyrosine phosphatases revisited. *FEBS Letters*, 498(2-3), 208–13. Retrieved from <http://www.ncbi.nlm.nih.gov/pubmed/11412859>

- Knebel, A., Rahmsdorf, H. J., Ullrich, A., & Herrlich, P. (1996). Dephosphorylation of receptor tyrosine kinases as target of regulation by radiation, oxidants or alkylating agents. *The EMBO journal*, *15*(19), 5314–25. Retrieved from <http://www.pubmedcentral.nih.gov/articlerender.fcgi?artid=452275&tool=pmcentrez&rendertype=abstract>
- Knowles, T. P. J., Vendruscolo, M., & Dobson, C. M. (2014). The amyloid state and its association with protein misfolding diseases. *Nature Reviews Molecular Cell Biology*, *15*(6), 384–396. doi:10.1038/nrm3810
- Kwon, J., Lee, S.-R., Yang, K.-S., Ahn, Y., Kim, Y. J., Stadtman, E. R., & Rhee, S. G. (2004). Reversible oxidation and inactivation of the tumor suppressor PTEN in cells stimulated with peptide growth factors. *Proceedings of the National Academy of Sciences of the United States of America*, *101*(47), 16419–24. doi:10.1073/pnas.0407396101
- Lai, Y.-J., Chen, C.-S., Lin, W.-C., & Lin, F.-T. (2005). c-Src-mediated phosphorylation of TRIP6 regulates its function in lysophosphatidic acid-induced cell migration. *Molecular and Cellular Biology*, *25*(14), 5859–68. doi:10.1128/MCB.25.14.5859-5868.2005
- Lai, Y., Song, M., Hakala, K., Weintraub, S. T., & Shiio, Y. (2011). Proteomic dissection of the von Hippel-Lindau (VHL) interactome. *Journal of Proteome Research*, *10*(11), 5175–82. doi:10.1021/pr200642c
- Landgraf, C., Panni, S., Montecchi-Palazzi, L., Castagnoli, L., Schneider-Mergener, J., Volkmer-Engert, R., Cesareni, G. (2004) Protein interaction networks by proteome peptide scanning. *PLoS Biol.* *2*(1):E14. doi:10.1371/journal.pbio.0020014
- Larsen, M. R., Trelle, M. B., Thingholm, T. E., & Jensen, O. N. (2006). Analysis of posttranslational modifications of proteins by tandem mass spectrometry. *BioTechniques*, *40*(6), 790–8. Retrieved from <http://www.ncbi.nlm.nih.gov/pubmed/16774123>

- Langhorne, P., Tong, B. L. P., Stott, D. J., & Indredavik, B. (2000). Association Between Physiological Homeostasis and Early Recovery After Stroke Response. *Stroke*, *31*(10), 2517–2527. doi:10.1161/01.STR.31.10.2517-f
- Lee, J. O., Yang, H., Georgescu, M. M., Di Cristofano, a, Maehama, T., Shi, Y., Dixon, J. E., et al. (1999). Crystal structure of the PTEN tumor suppressor: implications for its phosphoinositide phosphatase activity and membrane association. *Cell*, *99*(3), 323–34. Retrieved from <http://www.ncbi.nlm.nih.gov/pubmed/10555148>
- Lee, S.-R., Yang, K.-S., Kwon, J., Lee, C., Jeong, W., & Rhee, S. G. (2002). Reversible inactivation of the tumor suppressor PTEN by H₂O₂. *The Journal of biological chemistry*, *277*(23), 20336–42. doi:10.1074/jbc.M111899200
- Lehtinen, M. K., Zappaterra, M. W., Chen, X., Yang, Y. J., Hill, A., Lun, M., ... Walsh, C. A. (2011). The cerebrospinal fluid provides a proliferative niche for neural progenitor cells. *Neuron*, *69*(5), 893–905. doi:10.1016/j.neuron.2011.01.023
- Leuner, B., Glasper, E. R., & Gould, E. (2010). Sexual experience promotes adult neurogenesis in the hippocampus despite an initial elevation in stress hormones. *PloS One*, *5*(7), e11597. doi:10.1371/journal.pone.0011597
- Levine, R. L., Garland, D., Oliver, C. N., Amici, A., Climent, I., Lenz, A. G., ... Stadtman, E. R. (1990). Determination of carbonyl content in oxidatively modified proteins. *Methods in Enzymology*, *186*, 464–78. Retrieved from <http://www.ncbi.nlm.nih.gov/pubmed/1978225>
- Levine, R. L., Mosoni, L., Berlett, B. S., & Stadtman, E. R. (1996). Methionine residues as endogenous antioxidants in proteins. *Proceedings of the National Academy of Sciences of the United States of America*, *93*(26), 15036–40. Retrieved from <http://www.pubmedcentral.nih.gov/articlerender.fcgi?artid=26351&tool=pmcentrez&rendertype=abstract>

- Leslie, N R, Batty, I. H., Maccario, H., Davidson, L., & Downes, C. P. (2008). Understanding PTEN regulation: PIP2, polarity and protein stability. *Oncogene*, 27(41), 5464–76. doi:10.1038/onc.2008.243
- Leslie, Nick R, & Foti, M. (2011). Non-genomic loss of PTEN function in cancer: not in my genes. *Trends in pharmacological sciences*, 32(3), 131–40. doi:10.1016/j.tips.2010.12.005
- Leslie, Nick R, Maccario, H., Spinelli, L., & Davidson, L. (2009). The significance of PTEN's protein phosphatase activity. *Advances in enzyme regulation*, 49(1), 190–6. doi:10.1016/j.advenzreg.2008.12.002
- Li, J. (1997). PTEN, a Putative Protein Tyrosine Phosphatase Gene Mutated in Human Brain, Breast, and Prostate Cancer. *Science*, 275(5308), 1943–1947. doi:10.1126/science.275.5308.1943
- Li, L., Bin, L.-H., Li, F., Liu, Y., Chen, D., Zhai, Z., & Shu, H.-B. (2005). TRIP6 is a RIP2-associated common signaling component of multiple NF-kappaB activation pathways. *Journal of Cell Science*, 118(Pt 3), 555–63. doi:10.1242/jcs.01641
- Liu, Y.-Y., Schultz, J. J., & Brent, G. A. (2003). A Thyroid Hormone Receptor α Gene Mutation (P398H) Is Associated with Visceral Adiposity and Impaired Catecholamine-stimulated Lipolysis in Mice. *Journal of Biological Chemistry*, 278(40), 38913–38920. doi:10.1074/jbc.M306120200
- Liu, M., Zhang, L., Xu, Y., Yang, P., & Lu, H. (2013). Mass spectrometry signal amplification for ultrasensitive glycoprotein detection using gold nanoparticle as mass tag combined with boronic acid based isolation strategy. *Analytica Chimica Acta*, 788, 129–34. doi:10.1016/j.aca.2013.05.063

- Lin, H.-K., Hu, Y.-C., Lee, D. K., & Chang, C. (2004). Regulation of androgen receptor signaling by PTEN (phosphatase and tensin homolog deleted on chromosome 10) tumor suppressor through distinct mechanisms in prostate cancer cells. *Molecular endocrinology (Baltimore, Md.)*, 18(10), 2409–23. Retrieved from <http://www.ncbi.nlm.nih.gov/pubmed/15205473>
- Loboda, A., Krutchinsky, A., Bromirski, M., Ens, W., & Standing, K. (2000). A tandem quadrupole/time-of-flight mass spectrometer with a matrix-assisted laser desorption/ionization source: design and performance. *Rapid Communications in Mass Spectrometry: RCM*, 14(12), 1047–57. doi:10.1002/1097-0231(20000630)14:12<1047::AID-RCM990>3.0.CO;2-E
- Lou, Y.-W., Chen, Y.-Y., Hsu, S.-F., Chen, R.-K., Lee, C.-L., Khoo, K.-H., ... Meng, T.-C. (2008). Redox regulation of the protein tyrosine phosphatase PTP1B in cancer cells. *The FEBS Journal*, 275(1), 69–88. doi:10.1111/j.1742-4658.2007.06173.x
- Loughery, J., Cox, M., Smith, L. M., & Meek, D. W. (2014). Critical role for p53-serine 15 phosphorylation in stimulating transactivation at p53-responsive promoters. *Nucleic Acids Research*, 42(12), 7666–80. doi:10.1093/nar/gku501
- Louridas, G. E. and Lourida, K. G. (2012) Systems biology and biomechanical model of heart failure *Current Cardiology Review*, 8:(3): 220-230
doi:10.2174/157340312803217238
- Lotan, T., Gurel, B., Sutcliffe, S., Esopi, D., Liu, W., Xu, J., Hicks, J., et al. (2011). PTEN Protein Loss by Immunostaining: Analytic Validation and Prognostic Indicator for a High Risk Surgical Cohort of Prostate Cancer Patients. *Clinical cancer research: an official journal of the American Association for Cancer Research*, 17(20), 6563–6573. doi:10.1158/1078-0432.CCR-11-1244
- Lu, Y., Yu, Q., Liu, J. H., Zhang, J., Wang, H., Koul, D., McMurray, J. S., et al. (2003). Src family protein-tyrosine kinases alter the function of PTEN to regulate phosphatidylinositol 3-kinase/AKT cascades. *The Journal of biological chemistry*, 278(41), 40057–66. doi:10.1074/jbc.M303621200

- Maddika, S., Kavela, S., Rani, N., Palicharla, V. R., Pokorny, J. L., Sarkaria, J. N., & Chen, J. (2011). WWP2 is an E3 ubiquitin ligase for PTEN. *Nature cell biology*, 13(6), 728–33. Retrieved from <http://www.ncbi.nlm.nih.gov/pubmed/21532586>
- Maehama, T., & Dixon, J. E. (1999). PTEN: a tumour suppressor that functions as a phospholipid phosphatase. *Trends in cell biology*, 9(4), 125–8. Retrieved from <http://www.ncbi.nlm.nih.gov/pubmed/10203785>
- Mak, L. H., Vilar, R., & Woscholski, R. (2010). Characterisation of the PTEN inhibitor VO-OHpic. *Journal of chemical biology*, 3(4), 157–63. doi:10.1007/s12154-010-0041-7
- Mallozzi, C., Di Stasi, a M., & Minetti, M. (2001). Nitrotyrosine mimics phosphotyrosine binding to the SH2 domain of the src family tyrosine kinase lyn. *FEBS letters*, 503(2-3), 189–95. Retrieved from <http://www.ncbi.nlm.nih.gov/pubmed/11513880>
- Mann, M., Højrup, P., & Roepstorff, P. (1993). Use of mass spectrometric molecular weight information to identify proteins in sequence databases. *Biological Mass Spectrometry*, 22(6), 338–45. doi:10.1002/bms.1200220605
- Margreitter, C., Petrov, D., & Zagrovic, B. (2013). Vienna-PTM web server: a toolkit for MD simulations of protein post-translational modifications. *Nucleic Acids Research*, 41(Web Server issue), W422–6. doi:10.1093/nar/gkt41
- Martín, A., Batalla, P., Hernández-Ferrer, J., Martínez, M. T., & Escarpa, A. (2014). Graphene oxide nanoribbon-based sensors for the simultaneous bio-electrochemical enantiomeric resolution and analysis of amino acid biomarkers. *Biosensors & Bioelectronics*, 68C, 163–167. doi:10.1016/j.bios.2014.12.030
- Martinez, D. E. (1998) 'Mortality patterns suggest lack of senescence in hydra', *Experimental Gerontology*, 33, (3), pp. 217-225.

- Mayr, M., Zhang, J., Greene, A. S., Gutterman, D., Perloff, J., & Ping, P. (2006). Proteomics-based development of biomarkers in cardiovascular disease: mechanistic, clinical, and therapeutic insights. *Molecular & Cellular Proteomics : MCP*, 5(10), 1853–64. doi:10.1074/mcp.R600007-MCP200
- Miller, R. A., Harrison, D. E., Astle, C. M., Fernandez, E., Flurkey, K., Han, M., ... Strong, R. (2014). Rapamycin-mediated lifespan increase in mice is dose and sex dependent and metabolically distinct from dietary restriction. *Aging Cell*, 13(3), 468–77. doi:10.1111/accel.12194
- Min, K.-J., Lee, C.-K., & Park, H.-N. (2012). The lifespan of Korean eunuchs. *Current Biology : CB*, 22(18), R792–3. doi:10.1016/j.cub.2012.06.036
- Miura, Y., Sato, Y., Arai, Y., Abe, Y., Takayama, M., Toda, T., ... Endo, T. (2011). Proteomic analysis of plasma proteins in Japanese semisuper centenarians. *Experimental Gerontology*, 46(1), 81–5. doi:10.1016/j.exger.2010.10.002
- Moore, R. G., Jabre-Raughley, M., Brown, A. K., Robison, K. M., Miller, M. C., Allard, W. J., ... Skates, S. J. (2010). Comparison of a novel multiple marker assay vs the Risk of Malignancy Index for the prediction of epithelial ovarian cancer in patients with a pelvic mass. *American Journal of Obstetrics and Gynecology*, 203(3), 228.e1–6. doi:10.1016/j.ajog.2010.03.043
- Mori, M., Yoneda-Kato, N., Yoshida, A., & Kato, J. (2008). Stable form of JAB1 enhances proliferation and maintenance of hematopoietic progenitors. *The Journal of biological chemistry*, 283(43), 29011–21. doi:10.1074/jbc.M804539200
- Morris, H. R., Paxton, T., Dell, A., Langhorne, J., Berg, M., Bordoli, R. S., ... Bateman, R. H. (1996). High sensitivity collisionally-activated decomposition tandem mass spectrometry on a novel quadrupole/orthogonal-acceleration time-of-flight mass

- spectrometer. *Rapid Communications in Mass Spectrometry: RCM*, 10(8), 889–96.
doi:10.1002/(SICI)1097-0231(19960610)10:8<889::AID-RCM615>3.0.CO;2-F
- Mouls, L., Silajdzic, E., Haroune, N., Spickett, C. M., & Pitt, A. R. (2009). Development of novel mass spectrometric methods for identifying HOCl-induced modifications to proteins. *Proteomics*, 9(6), 1617–31. doi:10.1002/pmic.200800391
- Mueller, C., Liotta, L. A., & Espina, V. (2010). Reverse phase protein microarrays advance to use in clinical trials. *Molecular Oncology*, 4(6), 461–81.
doi:10.1016/j.molonc.2010.09.003
- Myers, J., Prakash, M., Froelicher, V., Do, D., Partington, S., & Atwood, J. E. (2009). Exercise Capacity and Mortality among Men Referred for Exercise Testing. <http://dx.doi.org/10.1056/NEJMoa011858>.
- Najarro, P., Traktman, P., & Lewis, J. A. (2001). Vaccinia virus blocks gamma interferon signal transduction: viral VH1 phosphatase reverses Stat1 activation. *Journal of virology*, 75(7), 3185–96. Retrieved from <http://www.pubmedcentral.nih.gov/articlerender.fcgi?artid=114112&tool=pmcentrez&endertype=abstract>
- Nakashima, N., Sharma, P. M., Imamura, T., Bookstein, R., & Olefsky, J. M. (2000). The tumor suppressor PTEN negatively regulates insulin signaling in 3T3-L1 adipocytes. *The Journal of biological chemistry*, 275(17), 12889–95. Retrieved from <http://www.ncbi.nlm.nih.gov/pubmed/10777587>
- Ng, C. J., Shih, D. M., Hama, S. Y., Villa, N., Navab, M., & Reddy, S. T. (2005). The paraoxonase gene family and atherosclerosis. *Free Radical Biology & Medicine*, 38(2), 153–63. doi:10.1016/j.freeradbiomed.2004.09.035
- Okahara, F., Ikawa, H., Kanaho, Y., & Maehama, T. (2004). Regulation of PTEN phosphorylation and stability by a tumor suppressor candidate protein. *The Journal of Biological Chemistry*, 279(44), 45300–3. doi:10.1074/jbc.C400377200
- Orlowski, R. Z. (1999). The role of the ubiquitin-proteasome pathway in apoptosis. *Cell Death and Differentiation*, 6(4), 303–13. doi:10.1038/sj.cdd.4400505

- Pacher, P., Beckman, J. S., & Liaudet, L. (2007). Nitric oxide and peroxynitrite in health and disease. *Physiological reviews*, 87(1), 315–424. Retrieved from <http://www.pubmedcentral.nih.gov/articlerender.fcgi?artid=2248324&tool=pmcentrez&rendertype=abstract>
- Paglia, D. E., & Valentine, W. N. (1967). Studies on the quantitative and qualitative characterization of erythrocyte glutathione peroxidase. *The Journal of Laboratory and Clinical Medicine*, 70(1), 158–69. Retrieved from <http://www.ncbi.nlm.nih.gov/pubmed/6066618>
- Pagliarini, D. J., Wiley, S. E., Kimple, M. E., Dixon, J. R., Kelly, P., Worby, C. A., Casey, P. J., et al. (2005). Involvement of a mitochondrial phosphatase in the regulation of ATP production and insulin secretion in pancreatic beta cells. *Molecular cell*, 19(2), 197–207. Retrieved from <http://www.ncbi.nlm.nih.gov/pubmed/16039589>
- Pagliarini, D. J., Worby, C. A., & Dixon, J. E. (2004). A PTEN-like phosphatase with a novel substrate specificity. *The Journal of biological chemistry*, 279(37), 38590–6. Retrieved from <http://www.ncbi.nlm.nih.gov/pubmed/15247229>
- Palmore, E, B (1982) Predictors of the Longevity Difference: A 25-Year Follow-Up *The Gerontologist* 22 (6): 513-518. doi: 10.1093/geront/22.6.513
- Pan, H., Chen, K., Chu, L., Kinderman, F., Apostol, I., & Huang, G. (2009). Methionine oxidation in human IgG2 Fc decreases binding affinities to protein A and FcRn. *Protein Science : A Publication of the Protein Society*, 18(2), 424–33. doi:10.1002/pro.45
- Pandey, K. B., Mishra, N., & Rizvi, S. I. (2010). Protein oxidation biomarkers in plasma of type 2 diabetic patients. *Clinical Biochemistry*, 43(4-5), 508–11. doi:10.1016/j.clinbiochem.2009.11.011

- Panizzi, P., Nahrendorf, M., Wildgruber, M., Waterman, P., Figueiredo, J.-L., Aikawa, E., McCarthy, J., et al. (2009). Oxazine conjugated nanoparticle detects in vivo hypochlorous acid and peroxynitrite generation. *Journal of the American Chemical Society*, *131*(43), 15739–44. Retrieved from <http://www.pubmedcentral.nih.gov/articlerender.fcgi?artid=2773134&tool=pmcentrez&rendertype=abstract>
- Pappin, D. J., Hojrup, P., & Bleasby, A. J. (1993). Rapid identification of proteins by peptide-mass fingerprinting. *Current Biology: CB*, *3*(6), 327–32. Retrieved from <http://www.ncbi.nlm.nih.gov/pubmed/15335725>
- Paradies, G., Petrosillo, G., Pistolese, M., & Ruggiero, F. M. (2000). The effect of reactive oxygen species generated from the mitochondrial electron transport chain on the cytochrome c oxidase activity and on the cardiolipin content in bovine heart submitochondrial particles. *FEBS letters*, *466*(2-3), 323–6. Retrieved from <http://www.ncbi.nlm.nih.gov/pubmed/10682852>
- Paradies, Giuseppe, Petrosillo, G., Pistolese, M., & Ruggiero, F. M. (2001). Reactive oxygen species generated by the mitochondrial respiratory chain affect the complex III activity via cardiolipin peroxidation in beef-heart submitochondrial particles. *Mitochondrion*, *1*(2), 151–159. Retrieved from [http://dx.doi.org/10.1016/S1567-7249\(01\)00011-3](http://dx.doi.org/10.1016/S1567-7249(01)00011-3)
- Paradies, Giuseppe, Ruggiero, F. M., Petrosillo, G., & Quagliariello, E. (1998). Peroxidative damage to cardiac mitochondria: cytochrome oxidase and cardiolipin alterations. *FEBS Letters*, *424*(3), 155–158. Retrieved from [http://dx.doi.org/10.1016/S0014-5793\(98\)00161-6](http://dx.doi.org/10.1016/S0014-5793(98)00161-6)
- Park, H., Kim, S. Y., Kyung, A., Yoon, T.-S., Ryu, S. E., & Jeong, D. G. (2012). Structure-based virtual screening approach to the discovery of novel PTPMT1 phosphatase

- inhibitors. *Bioorganic & medicinal chemistry letters*, 22(2), 1271–5. Retrieved from <http://www.ncbi.nlm.nih.gov/pubmed/22115589>
- Patterson, K. I., Brummer, T., O'Brien, P. M., & Daly, R. J. (2009). Dual-specificity phosphatases: critical regulators with diverse cellular targets. *The Biochemical journal*, 418(3), 475–89. Retrieved from <http://www.ncbi.nlm.nih.gov/pubmed/19228121>
- Pavic, K., Rios, P., Dzeyk, K., Koehler, C., Lemke, E. A., & Köhn, M. (2014). Unnatural Amino Acid Mutagenesis Reveals Dimerization As a Negative Regulatory Mechanism of VHR's Phosphatase Activity. *ACS Chemical Biology*, 9(7), 1451–1459. doi:10.1021/cb500240n
- Pawson, T. (2004). Specificity in signal transduction: from phosphotyrosine-SH2 domain interactions to complex cellular systems. *Cell*, 116(2), 191–203. Retrieved from <http://www.ncbi.nlm.nih.gov/pubmed/14744431>
- Perry, G., Cash, A. D., & Smith, M. A. (2002). Alzheimer Disease and Oxidative Stress. *Journal of Biomedicine & Biotechnology*, 2(3), 120–123. doi:10.1155/S1110724302203010
- Pettersen, E. F., Goddard, T. D., Huang, C. C., Couch, G. S., Greenblatt, D. M., Meng, E. C., & Ferrin, T. E. (2004). UCSF Chimera--a visualization system for exploratory research and analysis. *Journal of computational chemistry*, 25(13), 1605–12. Retrieved from <http://www.ncbi.nlm.nih.gov/pubmed/15264254>
- Pietrement, C., Gorisse, L., Jaisson, S., & Gillery, P. (2013). Chronic increase of urea leads to carbamylated proteins accumulation in tissues in a mouse model of CKD. *PloS One*, 8(12), e82506. doi:10.1371/journal.pone.0082506
- Poirier, P. (2014). Exercise, Heart Rate Variability, and Longevity: The Cocoon Mystery? *Circulation*, vol. 129 (21) p.2085-2087

- Porter, N. M., & Landfield, P. W. (1998). Stress hormones and brain aging: adding injury to insult? *Nature Neuroscience*, 1(1), 3–4. doi:10.1038/196
- Pramanik, M. K., Iijima, M., Iwadate, Y., & Yumura, S. (2009). PTEN is a mechanosensing signal transducer for myosin II localization in Dictyostelium cells. *Genes to cells: devoted to molecular & cellular mechanisms*, 14(7), 821–34. Retrieved from <http://www.ncbi.nlm.nih.gov/pubmed/19515202>
- Peptide fragmentation (2016 July 17) Retrieved from http://www.matrixscience.com/help/fragmentation_help.html
- Radi, Rafael. (2013). Protein tyrosine nitration: biochemical mechanisms and structural basis of functional effects. *Accounts of chemical research*, 46(2), 550–9. doi:10.1021/ar300234c
- Radi, R, Beckman, J. S., Bush, K. M., & Freeman, B. a. (1991). Peroxynitrite oxidation of sulfhydryls. The cytotoxic potential of superoxide and nitric oxide. *The Journal of biological chemistry*, 266(7), 4244–50. Retrieved from <http://www.ncbi.nlm.nih.gov/pubmed/11831852>
- Ragan, E. (2002). *Immune-related protein complexes and serpin-1 isoforms in manduca sexta plasma*. PhD thesis, University of California Berkeley. Ann Arbor: ProQuest/UMI (Publication No. AAT 3310814)
- Rahmouni, S., Cerignoli, F., Alonso, A., Tsutji, T., Henkens, R., Zhu, C., Louis-dit-Sully, C., et al. (2006). Loss of the VHR dual-specific phosphatase causes cell-cycle arrest and senescence. *Nature cell biology*, 8(5), 524–31. doi:10.1038/ncb1398
- Rao, R. S. P., Xu, D., Thelen, J. J., & Miernyk, J. A. (2013). Circles within circles: crosstalk between protein Ser/Thr/Tyr-phosphorylation and Met oxidation. *BMC Bioinformatics*, 14(Suppl 14), S14. <http://doi.org/10.1186/1471-2105-14-S14-S14>

- Rao, M. V, Campbell, J., Palaniappan, A., Kumar, A., & Nixon, R. A. (2016). Calpastatin inhibits motor neuron death and increases survival of hSOD1(G93A) mice. *Journal of Neurochemistry*, 137(2), 253–65. doi:10.1111/jnc.13536
- Rees, J. S., Lilley, K. S., & Jackson, A. P. (2015). The chicken B-cell line DT40 proteome, beadome and interactomes. *Data in Brief*, 3, 29–33. doi:10.1016/j.dib.2014.12.006
- Reiter, R. J. (1992). The ageing pineal gland and its physiological consequences. *BioEssays: News and Reviews in Molecular, Cellular and Developmental Biology*, 14(3), 169–75. doi:10.1002/bies.950140307
- Reuter, S., Gupta, S. C., Chaturvedi, M. M., & Aggarwal, B. B. (2010). Oxidative stress, inflammation, and cancer: how are they linked? *Free Radical Biology & Medicine*, 49(11), 1603–16. doi:10.1016/j.freeradbiomed.2010.09.006
- Richards, P. G., Coles, B., Heptinstall, J., & Walton, D. J. (1994). Electrochemical modification of lysozyme: Anodic reaction of tyrosine residues. *Enzyme and Microbial Technology*, 16(9), 795–801. doi:10.1016/0141-0229(94)90038-8
- Riordan, J.F., Vallee, B.L. (1972). Nitration with tetranitromethane. *Methods Enzymology*, 25:515-21. doi:10.1016/S0076-6879(72)25048-0.
- Roberts, J.D & Caserio, M.C. (1966). *Basic Principles of Organic Chemistry*. Benjamin, New York.
- Rodier, F., & Campisi, J. (2011). Four faces of cellular senescence. *Cell*, 192(4), 547–556. doi:10.1083/jcb.201009094
- Rodriguez, S., & Huynh-Do, U. (2012). The Role of PTEN in Tumor Angiogenesis. *Journal of oncology*, 141236. doi:10.1155/2012/141236
- Roepstorff, P., & Fohlman, J. (1984). Proposal for a common nomenclature for sequence ions in mass spectra of peptides. *Biomed Mass Spectrom*, 11(11):601. doi10.1002/bms.1200111109

- Rohan, P. J., Davis, P., Moskaluk, C. A., Kearns, M., Krutzsch, H., Siebenlist, U., & Kelly, K. (1993). PAC-1: a mitogen-induced nuclear protein tyrosine phosphatase. *Science (New York, N.Y.)*, *259*(5102), 1763–6. Retrieved from <http://www.ncbi.nlm.nih.gov/pubmed/7681221>
- Rosivatz, E., Matthews, J. G., McDonald, N. Q., Mulet, X., Ho, K. K., Lossi, N., ... Woscholski, R. (2006). A small molecule inhibitor for phosphatase and tensin homologue deleted on chromosome 10 (PTEN). *ACS Chemical Biology*, *1*(12), 780–90. doi:10.1021/cb600352f
- Rual, J.-F., Venkatesan, K., Hao, T., Hirozane-Kishikawa, T., Dricot, A., Li, N., Berriz, G. F., et al. (2005). Towards a proteome-scale map of the human protein-protein interaction network. *Nature*, *437*(7062), 1173–8. Retrieved from <http://www.ncbi.nlm.nih.gov/pubmed/16189514>
- Sagné, C., Isambert, M. F., Henry, J. P., & Gasnier, B. (1996). SDS-resistant aggregation of membrane proteins: application to the purification of the vesicular monoamine transporter. *Biochemical Journal*, *316*(Pt 3), 825–831.
- Salmena, L., Carracedo, A., & Pandolfi, P. P. (2008). Tenets of PTEN tumor suppression. *Cell*, *133*(3), 403–14. doi:10.1016/j.cell.2008.04.013
- Sauer, H., Wartenberg, M., & Hescheler, J. (2001). Reactive oxygen species as intracellular messengers during cell growth and differentiation. *Cellular Physiology and Biochemistry: International Journal of Experimental Cellular Physiology, Biochemistry, and Pharmacology*, *11*(4), 173–86. doi:47804
- Schraen-Maschke, S., Sergeant, N., Dhaenens, C.-M., Bombois, S., Deramecourt, V., Caillet-Boudin, M.-L., ... Buée, L. (2008). Tau as a biomarker of neurodegenerative diseases. *Biomarkers in Medicine*, *2*(4), 363–84. doi:10.2217/17520363.2.4.363

- Schulze, W. X., Deng, L., & Mann, M. (2005). Phosphotyrosine interactome of the ErbB-receptor kinase family. *Molecular Systems Biology*, *1*, 2005.0008.
doi:10.1038/msb4100012
- Schmid, A. C., Byrne, R. D., Vilar, R., & Woscholski, R. (2004). Bisperoxovanadium compounds are potent PTEN inhibitors. *FEBS Letters*, *566*(1-3), 35–8.
doi:10.1016/j.febslet.2004.03.102
- Schmidt, M. A., & Goodwin, T. J. (2013). Personalized medicine in human space flight: using Omics based analyses to develop individualized countermeasures that enhance astronaut safety and performance. *Metabolomics: Official Journal of the Metabolomic Society*, *9*(6), 1134–1156. doi:10.1007/s11306-013-0556-3
- Scortegagna, M., Ding, K., Oktay, Y., Gaur, A., Thurmond, F., Yan, L.-J., ... Garcia, J. A. (2003). Multiple organ pathology, metabolic abnormalities and impaired homeostasis of reactive oxygen species in *Epas1*^{-/-} mice. *Nature Genetics*, *35*(4), 331–40.
doi:10.1038/ng1266
- Sebolt-Leopold, J. S. (2008). Advances in the development of cancer therapeutics directed against the RAS-mitogen-activated protein kinase pathway. *Clinical cancer research: an official journal of the American Association for Cancer Research*, *14*(12), 3651–6.
Retrieved from <http://clincancerres.aacrjournals.org/cgi/content/abstract/14/12/3651>
- Selmeçi, L., Seres, L., Antal, M., Lukács, J., Regöly-Mérei, A., & Acsády, G. (2005). Advanced oxidation protein products (AOPP) for monitoring oxidative stress in critically ill patients: a simple, fast and inexpensive automated technique. *Clinical Chemical Laboratory Medicine*, *43*(3). doi:10.1515/CCLM.2005.050
- Shacter, E. (2000). Quantification and significance of protein oxidation in biological samples. *Drug Metabolism Reviews*, *32*(3-4), 307–26. doi:10.1081/DMR-100102336
- Sharpless, N. E., & Depinho, R. A. (2004). Telomeres , stem cells , senescence , and cancer. *Journal of Clinical Investigation*, *113*(2). doi:10.1172/JCI200420761. Every

- Sheehan, K. M., Calvert, V. S., Kay, E. W., Lu, Y., Fishman, D., Espina, V., ... Wulfkuhle, J. D. (2005). Use of reverse phase protein microarrays and reference standard development for molecular network analysis of metastatic ovarian carcinoma. *Molecular & Cellular Proteomics: MCP*, 4(4), 346–55. doi:10.1074/mcp.T500003-MCP200
- Shen, W. H., Balajee, A. S., Wang, J., Wu, H., Eng, C., & Pandolfi, P. P. (2007). Essential Role for Nuclear PTEN in Maintaining Chromosomal Integrity. *Cell*, 157–170. doi:10.1016/j.cell.2006.11.042
- Shewan, A., Eastburn, D. J., & Mostov, K. (2011). Phosphoinositides in cell architecture. *Cold Spring Harbor perspectives in biology*, 3(8), a004796. doi:10.1101/cshperspect.a004796
- Shu, C.-W., Sun, F.-C., Cho, J.-H., Lin, C.-C., Liu, P.-F., Chen, P.-Y., Chang, M. D.-T., et al. (2008). GRP78 and Raf-1 cooperatively confer resistance to endoplasmic reticulum stress-induced apoptosis. *Journal of cellular physiology*, 215(3), 627–35. doi:10.1002/jcp.21340
- Shu, L., Vivekanandan-Giri, A., Pennathur, S., Smid, B. E., Aerts, J. M. F., Hollak, C. E. M., & Shayman, J. A. (2014). Establishing 3-nitrotyrosine as a biomarker for the vasculopathy of Fabry disease. *Kidney International*, 86(1), 58–66. doi:10.1038/ki.2013.520
- Simard, J.-C., Girard, D., & Tessier, P. A. (2010). Induction of neutrophil degranulation by S100A9 via a MAPK-dependent mechanism. *Journal of Leukocyte Biology*, 87(5), 905–14. doi:10.1189/jlb.1009676

- Sin, O., & Nollen, E. A. A. (2015). Regulation of protein homeostasis in neurodegenerative diseases: the role of coding and non-coding genes. *Cellular and Molecular Life Sciences : CMLS*, 72(21), 4027–47. doi:10.1007/s00018-015-1985-0
- Singh, R. J., Hogg, N., Joseph, J., Konorev, E., Kalyanaraman, B. (1999). The peroxyxynitrite generator, SIN-1, becomes a nitric oxide donor in the presence of electron acceptors. *Arch Biochem Biophys*. 1999 Jan 15;361(2):331-9.
- Skarnes, W. C., Rosen, B., West, A. P., Koutsourakis, M., Bushell, W., Iyer, V., ... Bradley, A. (2011). A conditional knockout resource for the genome-wide study of mouse gene function. *Nature*, 474(7351), 337–42. doi:10.1038/nature10163
- Šlechtová, T., Gilar, M., Kalíková, K., & Tesařová, E. (2015). Insight into Trypsin Miscleavage: Comparison of Kinetic Constants of Problematic Peptide Sequences.
- Smith, M. A., Richey Harris, P. L., Sayre, L. M., Beckman, J. S., & Perry, G. (1997). Widespread peroxyxynitrite-mediated damage in Alzheimer's disease. *The Journal of Neuroscience : The Official Journal of the Society for Neuroscience*, 17(8), 2653–7. Retrieved from <http://www.ncbi.nlm.nih.gov/pubmed/9092586>
- Smith, M. A., Rottkamp, C. A., Nunomura, A., Raina, A. K., & Perry, G. (2000). Oxidative stress in Alzheimer's disease. *Biochimica et Biophysica Acta (BBA) - Molecular Basis of Disease*, 1502(1), 139–144. doi:10.1016/S0925-4439(00)00040-5
- Smyczynska, J., Hilczer, M., Stawerska, R., & Lewinski, A. (2010). Thyroid function in children with growth hormone (GH) deficiency during the initial phase of GH replacement therapy - clinical implications. *Thyroid Research*, 3(1), 2. doi:10.1186/1756-6614-3-2
- Soares-Miranda, L., Sattelmair, J., Chaves, P., Duncan, G. E., Siscovick, D. S., Stein, P. K., & Mozaffarian, D. (2014). Physical activity and heart rate variability in older adults: the Cardiovascular Health Study. *Circulation*, 129(21), 2100–10. doi:10.1161/CIRCULATIONAHA.113.005361

- Sokolovsky, M., Riordan, J. F., & Vallee, B. L. (1966). Tetranitromethane. A Reagent for the Nitration of Tyrosyl Residues in Proteins. *Biochemistry*, 5(11), 3582–3589.
doi:10.1021/bi00875a029
- Song, M. S., Carracedo, A., Salmena, L., Song, S. J., Egia, A., Malumbres, M., & Pandolfi, P. P. (2011). Nuclear PTEN regulates the APC-CDH1 tumor-suppressive complex in a phosphatase-independent manner. *Cell*, 144(2), 187–99.
doi:10.1016/j.cell.2010.12.020
- Song, M. S., Salmena, L., & Pandolfi, P. P. (2012). The functions and regulation of the PTEN tumour suppressor. *Nature Reviews. Molecular Cell Biology*, 13(5), 283–96.
doi:10.1038/nrm3330
- Spickett, C. M., & Pitt, A. R. (2010). Protein oxidation: role in signalling and detection by mass spectrometry. *Amino Acids*, 2010–2010. doi:10.1007/s00726-010-0585-4
- Spickett, C. M., Pitt, A. R., Morrice, N., & Kolch, W. (2006). Proteomic analysis of phosphorylation, oxidation and nitrosylation in signal transduction. *Biochimica et biophysica acta*, 1764(12), 1823–41. doi:10.1016/j.bbapap.2006.09.013
- Stadtman, E. R. (1990). Metal ion-catalyzed oxidation of proteins: biochemical mechanism and biological consequences. *Free Radical Biology & Medicine*, 9(4), 315–25.
Retrieved from <http://www.ncbi.nlm.nih.gov/pubmed/2283087>
- Stadtman, E. R. (2001). Protein oxidation in aging and age-related diseases. *Annals of the New York Academy of Sciences*, 928, 22–38. Retrieved from <http://www.ncbi.nlm.nih.gov/pubmed/11795513>
- Staruchova, M., Collins, A. R., Volkovova, K., Mislanová, C., Kovacikova, Z., Tulinska, J., ... Dusinska, M. (2008). Occupational exposure to mineral fibres. Biomarkers of oxidative damage and antioxidant defence and associations with DNA damage and repair. *Mutagenesis*, 23(4), 249–60. doi:10.1093/mutage/gen004
- Steck, P. A., Pershouse, M. A., Jasser, S. A., Yung, W. K., Lin, H., Ligon, A. H., Langford, L. A., et al. (1997). Identification of a candidate tumour suppressor gene, MMAC1, at

- chromosome 10q23.3 that is mutated in multiple advanced cancers. *Nature genetics*, 15(4), 356–62. Retrieved from <http://www.ncbi.nlm.nih.gov/pubmed/9090379>
- Stelzl, U., Worm, U., Lalowski, M., Haenig, C., Brembeck, F. H., Goehler, H., Stroedicke, M., et al. (2005). A human protein-protein interaction network: a resource for annotating the proteome. *Cell*, 122(6), 957–68. doi:10.1016/j.cell.2005.08.029
- Stewart, A. E., Dowd, S., Keyse, S. M., & McDonald, N. Q. (1999). Crystal structure of the MAPK phosphatase Pyst1 catalytic domain and implications for regulated activation. *Nature structural biology*, 6(2), 174–81. Retrieved from <http://www.ncbi.nlm.nih.gov/pubmed/10048930>
- Strobel, N. A., Fassett, R. G., Marsh, S. A., & Coombes, J. S. (2011). Oxidative stress biomarkers as predictors of cardiovascular disease. *International Journal of Cardiology*, 147(2), 191–201. doi:10.1016/j.ijcard.2010.08.008
- Su, W., Gao, X., Jiang, L., & Qin, J. (2015). Microfluidic platform towards point-of-care diagnostics in infectious diseases. *Journal of Chromatography. A*, 1377C, 13–26. doi:10.1016/j.chroma.2014.12.041
- Sullivan, S. G., Chiu, D. T., Errasfa, M., Wang, J. M., Qi, J. S., & Stern, A. (1994). Effects of H₂O₂ on protein tyrosine phosphatase activity in HER14 cells. *Free radical biology & medicine*, 16(3), 399–403. Retrieved from <http://www.ncbi.nlm.nih.gov/pubmed/8063203>
- Sultana, R., Perluigi, M., & Butterfield, D. A. (2006) Protein oxidation and lipid peroxidation in brain of subjects with Alzheimer's disease: insights into mechanism of neurodegeneration from redox proteomics. *Antioxidants & Redox Signaling*, 8(11-12), 2021–37. doi:10.1089/ars.2006.8.2021

- Sun, H., Charles, C. H., Lau, L. F., & Tonks, N. K. (1993). MKP-1 (3CH134), an immediate early gene product, is a dual specificity phosphatase that dephosphorylates MAP kinase in vivo. *Cell*, 75(3), 487–93. Retrieved from <http://www.ncbi.nlm.nih.gov/pubmed/8221888>
- Susin, S. A., Lorenzo, H. K., Zamzami, N., Marzo, I., Snow, B. E., Brothers, G. M., ... Kroemer, G. (1999). Molecular characterization of mitochondrial apoptosis-inducing factor. *Nature*, 397(6718), 441–6. doi:10.1038/17135
- Szabó, C., Ischiropoulos, H., & Radi, R. (2007). Peroxynitrite: biochemistry, pathophysiology and development of therapeutics. *Nature Reviews. Drug Discovery*, 6(8), 662–80. doi:10.1038/nrd2222
- Świderek, K., Tuñón, I., Martí, S., & Moliner, V. (2015). Protein Conformational Landscapes and Catalysis. Influence of Active Site Conformations in the Reaction Catalyzed by L-Lactate Dehydrogenase.
- Takahashi, Y., Morales, F. C., Kreimann, E. L., & Georgescu, M.-M. (2006). PTEN tumor suppressor associates with NHERF proteins to attenuate PDGF receptor signaling. *The EMBO journal*, 25(4), 910–20. Retrieved from <http://www.pubmedcentral.nih.gov/articlerender.fcgi?artid=1383560&tool=pmcentrez&rendertype=abstract>
- Tang, X., Powelka, A. M., Soriano, N. A., Czech, M. P., & Guilherme, A. (2005). PTEN, but not SHIP2, suppresses insulin signaling through the phosphatidylinositol 3-kinase/Akt pathway in 3T3-L1 adipocytes. *The Journal of biological chemistry*, 280(23), 22523–9. Retrieved from <http://www.ncbi.nlm.nih.gov/pubmed/15824124>
- Taylor, G. (1964). Disintegration of Water Drops in an Electric Field. *Proceedings of the Royal Society A: Mathematical, Physical and Engineering Sciences*, 280(1382), 383–397. doi:10.1098/rspa.1964.0151

- Terracciano, A., Löckenhoff, C. E., Zonderman, A. B., Ferrucci, L., & Costa, P. T. (2008). Personality predictors of longevity: activity, emotional stability, and conscientiousness. *Psychosomatic Medicine*, 70(6), 621–7. doi:10.1097/PSY.0b013e31817b9371
- Thamsen M, Jakob U (2011) The redoxome proteomic analysis of cellular redox networks. *Curr Opin Chem Biol* 15: 113–119.
- Theodoridis, G., Gika, H. G., & Wilson, I. D. (2011). Mass spectrometry-based holistic analytical approaches for metabolite profiling in systems biology studies. *Mass Spectrometry Reviews*, 30(5), 884–906. doi:10.1002/mas.20306
- Thomas, E. L. (1979). Myeloperoxidase, hydrogen peroxide, chloride antimicrobial system: nitrogen-chlorine derivatives of bacterial components in bactericidal action against *Escherichia coli*. *Infection and immunity*, 23(2), 522–31. Retrieved from <http://www.pubmedcentral.nih.gov/articlerender.fcgi?artid=414195&tool=pmcentrez&rendertype=abstract>
- Todd, J L, Tanner, K. G., & Denu, J. M. (1999). Extracellular regulated kinases (ERK) 1 and ERK2 are authentic substrates for the dual-specificity protein-tyrosine phosphatase VHR. A novel role in down-regulating the ERK pathway. *The Journal of biological chemistry*, 274(19), 13271–80. Retrieved from <http://www.ncbi.nlm.nih.gov/pubmed/10224087>
- Todd, Jacob L, Rigas, J. D., Rafty, L. A., & Denu, J. M. (2002). Dual-specificity protein tyrosine phosphatase VHR down-regulates c-Jun N-terminal kinase (JNK). *Oncogene*, 21(16), 2573–83. Retrieved from <http://www.ncbi.nlm.nih.gov/pubmed/11971192>
- Tong, Y., Ben-Shlomo, A., Zhou, C., Wawrowsky, K., & Melmed, S. (2008). Pituitary tumor transforming gene 1 regulates Aurora kinase A activity. *Oncogene*, 27(49), 6385–95. doi:10.1038/onc.2008.234

Tonks, N. K. (2006). Protein tyrosine phosphatases: from genes, to function, to disease.

Nature reviews. Molecular cell biology, 7(11), 833–46. Retrieved from

<http://www.ncbi.nlm.nih.gov/pubmed/17057753>

Torres, J., & Pulido, R. (2001) The tumour suppressor PTEN is phosphorylated by the protein kinase CK2 at its C terminus. Implications for PTEN stability to proteasome-mediated degradation. *J Biol Chem*, 276(2):993-8. doi:10.1074/jbc.M00913400

Tsutsui, H., Kinugawa, S., Matsushima, S., Abe, T., Ohga, Y., Tabayashi, N., ... Blatter, L. (2011). Oxidative stress and heart failure. *American Journal of Physiology. Heart and Circulatory Physiology*, 301(6), H2181–90. doi:10.1152/ajpheart.00554.2011

Valiente, M., Andrés-Pons, A., Gomar, B., Torres, J., Gil, A., Tapparel, C., Antonarakis, S. E., et al. (2005). Binding of PTEN to specific PDZ domains contributes to PTEN protein stability and phosphorylation by microtubule-associated serine/threonine kinases. *The Journal of biological chemistry*, 280(32), 28936–43. doi:10.1074/jbc.M504761200

Vandepoele, K., Van Roy, N., Staes, K., Speleman, F., & van Roy, F. (2005). A novel gene family NBPF: intricate structure generated by gene duplications during primate evolution. *Molecular Biology and Evolution*, 22(11), 2265–74. doi:10.1093/molbev/msi222

Van Ypersele de Strihou, C., Jadoul, M., Malghem, J., Maldague, B., & Jamart, J. (1991). Effect of dialysis membrane and patient's age on signs of dialysis-related amyloidosis. The Working Party on Dialysis Amyloidosis. *Kidney International*, 39(5), 1012–9. Retrieved from <http://www.ncbi.nlm.nih.gov/pubmed/2067196>

Vaupel, J. W., Baudisch, A., Dolling, M., Roach, D. A. and Gampe, J. (2004) 'The case for negative senescence', *Theoretical Population Biology*, 65, (4), pp. 339-351.

- Vazquez, F., Ramaswamy, S., Nakamura, N., & Sellers, W. R. (2000). Phosphorylation of the PTEN tail regulates protein stability and function. *Molecular and cellular biology*, 20(14), 5010–8. Retrieved from <http://www.pubmedcentral.nih.gov/articlerender.fcgi?artid=85951&tool=pmcentrez&rendertype=abstract>
- Verrastro, I., Tveen-Jensen, K., Woscholski, R., Spickett, C. M., & Pitt, A. R. (2016). Reversible oxidation of phosphatase and tensin homolog (PTEN) alters its interactions with signaling and regulatory proteins. *Free Radical Biology and Medicine*, 90, 24–34. doi:10.1016/j.freeradbiomed.2015.11.004
- Vinciguerra, M., & Foti, M. (2008a). PTEN and SHIP2 phosphoinositide phosphatases as negative regulators of insulin signalling. Retrieved from <http://informahealthcare.com/doi/abs/10.1080/13813450600711359>
- Vinciguerra, M., & Foti, M. (2008b). PTEN at the crossroad of metabolic diseases and cancer in. *Hepatology*, 7(June), 192–199.
- Vinciguerra, M., Sgroi, A., Veyrat-Durebex, C., Rubbia-Brandt, L., Buhler, L. H., & Foti, M. (2009). Unsaturated fatty acids inhibit the expression of tumor suppressor phosphatase and tensin homolog (PTEN) via microRNA-21 up-regulation in hepatocytes. *Hepatology (Baltimore, Md.)*, 49(4), 1176–84. doi:10.1002/hep.22737
- Vogelmann, R., Nguyen-Tat, M.-D., Giehl, K., Adler, G., Wedlich, D., & Menke, A. (2005). TGFbeta-induced downregulation of E-cadherin-based cell-cell adhesion depends on PI3-kinase and PTEN. *Journal of cell science*, 118(Pt 20), 4901–12. Retrieved from <http://www.ncbi.nlm.nih.gov/pubmed/16219695>
- Von Haller, P. D., Donohoe, S., Goodlett, D. R., Aebersold, R., & Watts, J. D. (2001). Mass spectrometric characterization of proteins extracted from Jurkat T cell detergent-

resistant membrane domains. *Proteomics*, 1(8), 1010–21. doi:10.1002/1615-9861(200108)1:8<1010::AID-PROT1010>3.0.CO;2-L

Wagner, W., Horn, P., Castoldi, M., Diehlmann, A., Bork, S., Saffrich, R., ... Ho, A. D. (2008). Replicative senescence of mesenchymal stem cells: a continuous and organized process. *PLoS One*, 3(5), e2213. doi:10.1371/journal.pone.0002213

Waldow, T., Alexiou, K., Witt, W., Wagner, F. M., Kappert, U., Knaut, M., & Matschke, K. (2004). Protection of lung tissue against ischemia/reperfusion injury by preconditioning with inhaled nitric oxide in an in situ pig model of normothermic pulmonary ischemia. *Nitric oxide : biology and chemistry / official journal of the Nitric Oxide Society*, 10(4), 195–201. doi:10.1016/j.niox.2004.04.006

Wallace, D. R., Dodson, S., Nath, A., & Booze, R. M. (2006). Estrogen attenuates gp120- and tat1-72-induced oxidative stress and prevents loss of dopamine transporter function. *Synapse (New York, N.Y.)*, 59(1), 51–60. doi:10.1002/syn.20214

Wan, X., Dennis, A. T., Obejero-Paz, C., Overholt, J. L., Heredia-Moya, J., Kirk, K. L., & Ficker, E. (2011). Oxidative inactivation of the lipid phosphatase phosphatase and tensin homolog on chromosome ten (PTEN) as a novel mechanism of acquired long QT syndrome. *The Journal of Biological Chemistry*, 286(4), 2843–52. doi:10.1074/jbc.M110.125526

Wang, J.-F., Shao, L., Sun, X., & Young, L. T. (2009). Increased oxidative stress in the anterior cingulate cortex of subjects with bipolar disorder and schizophrenia. *Bipolar Disorders*, 11(5), 523–9. doi:10.1111/j.1399-5618.2009.00717.x

Wang, Z., & Sun, Y. (2010). Targeting p53 for Novel Anticancer Therapy. *Translational Oncology*, 3(1), 1–12. Retrieved from <http://www.ncbi.nlm.nih.gov/pubmed/20165689>

Wang, J.-Y., Yeh, C.-L., Chou, H.-C., Yang, C.-H., Fu, Y.-N., Chen, Y.-T., Cheng, H.-W., et al. (2011). Vaccinia H1-related phosphatase is a phosphatase of ErbB receptors and

- is down-regulated in non-small cell lung cancer. *The Journal of biological chemistry*, 286(12), 10177–84. doi:10.1074/jbc.M110.163295
- Wang, L., Karpac, J., Jasper, H. (2014). Promoting longevity by maintaining metabolic and proliferative homeostasis. *The Journal of Experimental Biology*. 217, 109-118
doi:10.1242/jeb.089920
- Wang, Z., Nicholls, S. J., Rodriguez, E. R., Kummu, O., Hörkkö, S., Barnard, J., ... Hazen, S. L. (2007). Protein carbamylation links inflammation, smoking, uremia and atherogenesis. *Nature Medicine*, 13(10), 1176–84. doi:10.1038/nm1637
- Ward, Y., Gupta, S., Jensen, P., Wartmann, M., Davis, R. J., & Kelly, K. (1994). Control of MAP kinase activation by the mitogen-induced threonine/tyrosine phosphatase PAC1. *Nature*, 367(6464), 651–4. Retrieved from
<http://www.ncbi.nlm.nih.gov/pubmed/8107850f>
- Weiss, N., Miller, F., Cazaubon, S., & Couraud, P.-O. (2009). The blood-brain barrier in brain homeostasis and neurological diseases. *Biochimica et Biophysica Acta (BBA) - Biomembranes*, 1788(4), 842–857. doi:10.1016/j.bbamem.2008.10.022
- Witko-Sarsat, V., Friedlander, M., Capeillère-Blandin, C., Nguyen-Khoa, T., Nguyen, A. T., Zingraff, J., ... Descamps-Latscha, B. (1996). Advanced oxidation protein products as a novel marker of oxidative stress in uremia. *Kidney International*, 49(5), 1304–1313.
doi:10.1038/ki.1996.186
- Wong, K.-K., Maser, R. S., Bachoo, R. M., Menon, J., Carrasco, D. R., Gu, Y., ... DePinho, R. A. (2003). Telomere dysfunction and Atm deficiency compromises organ homeostasis and accelerates ageing. *Nature*, 421(6923), 643–8.
doi:10.1038/nature01385

- Wormall, A (1930). The immunological specificity of chemically altered proteins *JEM* vol. 51 no. 2 295-317.
- Wu, G., Feng, X., & Stein, L. (2010). A human functional protein interaction network and its application to cancer data analysis. *Genome biology*, 11(5), R53. Retrieved from <http://www.pubmedcentral.nih.gov/articlerender.fcgi?artid=2898064&tool=pmcentrez&rendertype=abstract>
- Xiao, J., Engel, J. L., Zhang, J., Chen, M. J., Manning, G., & Dixon, J. E. (2011). Structural and functional analysis of PTPMT1, a phosphatase required for cardiolipin synthesis. *Proceedings of the National Academy of Sciences of the United States of America*, 108(29), 11860–5. doi:10.1073/pnas.1109290108
- Yakovlev, V. A., Bayden, A. S., Graves, P. R., Kellogg, G. E., & Mikkelsen, R. B. (2010). Nitration of the tumor suppressor protein p53 at tyrosine 327 promotes p53 oligomerization and activation. *Biochemistry*, 49(25), 5331–9. doi:10.1021/bi100564w
- Yates, J. R., Speicher, S., Griffin, P. R., & Hunkapiller, T. (1993). Peptide mass maps: a highly informative approach to protein identification. *Analytical Biochemistry*, 214(2), 397–408. doi:10.1006/abio.1993.1514
- Yim, E.-K., Peng, G., Dai, H., Hu, R., Li, K., Lu, Y., Mills, G. B., et al. (2009). Rak functions as a tumor suppressor by regulating PTEN protein stability and function. *Cancer cell*, 15(4), 304–14. Retrieved from <http://www.pubmedcentral.nih.gov/articlerender.fcgi?artid=2673492&tool=pmcentrez&rendertype=abstract>
- Yin, Y., & Shen, W. H. (2008). PTEN: a new guardian of the genome. *Oncogene*, 27(41), 5443–53. doi:10.1038/onc.2008.241

- Yuvaniyama, J., Denu, J. M., Dixon, J. E., & Saper, M. A. (1996). Crystal structure of the dual specificity protein phosphatase VHR. *Science (New York, N.Y.)*, *272*(5266), 1328–31. Retrieved from <http://www.ncbi.nlm.nih.gov/pubmed/8650541>
- Zee, B. M., & Garcia, B. A. (2012). Discovery of lysine post-translational modifications through mass spectrometric detection. *Essays in Biochemistry*, *52*, 147–63. doi:10.1042/bse0520147
- Ziech, D., Franco, R., Georgakilas, A. G., Georgakila, S., Malamou-Mitsi, V., Schoneveld, O., ... Panayiotidis, M. I. (2010). The role of reactive oxygen species and oxidative stress in environmental carcinogenesis and biomarker development. *Chemico-Biological Interactions*, *188*(2), 334–9. doi:10.1016/j.cbi.2010.07.010
- Ziech, D., Franco, R., Pappa, A., & Panayiotidis, M. I. (2011). Reactive Oxygen Species (ROS)—Induced genetic and epigenetic alterations in human carcinogenesis. *Mutation Research/Fundamental and Molecular Mechanisms of Mutagenesis*, *711*(1), 167–173. doi:10.1016/j.mrfmmm.2011.02.015
- Zimmerli, L. U., Schiffer, E., Zürgbilg, P., Good, D. M., Kellmann, M., Moulis, L., ... Dominiczak, A. F. (2008). Urinary proteomic biomarkers in coronary artery disease. *Molecular & Cellular Proteomics: MCP*, *7*(2), 290–8. doi:10.1074/mcp.M700394-MCP200
- Zhan, X., Desiderio, D. M., (2004) The human pituitary nitroproteome: detection of nitrotyrosyl-proteins with two-dimensional Western blotting, and amino acid sequence determination with mass spectrometry. *Biochem Biophys Res Commun* *325*(4), 1180-6. doi:10.1016/j.bbrc.2004.10.169
- Zhang, J., Guan, Z., Murphy, A. N., Wiley, S. E., Perkins, G. A., Worby, C. A., Engel, J. L., et al. (2011). Mitochondrial phosphatase PTPMT1 is essential for cardiolipin biosynthesis. *Cell metabolism*, *13*(6), 690–700. Retrieved from <http://www.pubmedcentral.nih.gov/articlerender.fcgi?artid=3119201&tool=pmcentrez&rendertype=abstract>

Zheng, B., Fiumara, P., Li, Y. V., Georgakis, G., Snell, V., Younes, M., Vauthey, J. N., et al. (2003). MEK/ERK pathway is aberrantly active in Hodgkin disease: a signaling pathway shared by CD30, CD40, and RANK that regulates cell proliferation and survival. *Blood*, 102(3), 1019–27. Retrieved from <http://bloodjournal.hematologylibrary.org/cgi/content/abstract/102/3/1019>

Appendices

p53 (Biogrid, Salmena et al., 2008)
Myosin V (van Diepen et al., 2009)
Myosin based transport (van Diepen et al., 2009)
PAR-3 PDZ domain containing protein (Leslie et al., 2009)
NHERF PDZ domain containing protein (MINT, Leslie et al., 2009; Takahashi et al., 2006)
MAGI PDZ domain containing protein (Leslie et al. 2009)
MSP58 binding to phosphorylated Thr 366 (Leslie et al., 2009)
Myosin V C-terminal tail binding (Leslie et al., 2009)
Peroxiredoxin 1 (Prdx-1) c-terminal tail binding (Leslie et al., 2009)
P-Rex-2 c-terminal tail binding (Leslie et al., 2009)
Myosin V - Pict-1 – P-Rex-2 complex binding to c-terminal (Leslie et al., 2009)
Pict-1 c-terminal binding (Okahara et al, 2004; Leslie et al., 2009)
GSK3 c-terminal tail phosphorylation (Leslie et al., 2009)
CK2 c-terminal tail phosphorylation (Leslie et al., 2009)
XIAP (Van Themsche et al., 2009)
FAK (KEGG, Tamura et al., 1997; Leslie et al., 2009; Salmena et al., 2008)
MAST205 interaction via PDZ domain (Wu et al., 2000; Leslie et al., 2009)
DLG interaction via PDZ domain (Disks large homolog 1) (InterAct, APDI, Adey et al., 2000)
RAK (FRK) (InterAct, Leslie et al, 2009; Yim et al., 2009)
5-HT2C receptor (Ji et al., 2006)
Beta-catenin (Vogelmann et al., 2005)
PTEN (Vazquez et al, 2000; Shen et al., 2007)
PTEN auto-dephosphorylation (Vazquez et al., 2000)
PAR-3 - PIP2 – Apical membrane complex (Shewan et al., 2011)
NM-II (Pramanik et al., 2009)
WWP2 (Maddika et al., 2011)
Ubiquitin protein (Salmena et al., 2008)
PCAF (Salmena et al., 2008)
p300/CPB (Salmena et al., 2008)
MAGI 2 (IntAct, GST Pulldown, Beta-galactosidase, anti tag coip, yeast, simian, in vitro) (Valiente et al, 2005; Salmena et al, 2008)
CENP-C (Salmena et al., 2008)
MVP Major vault protein (BioGRID, APID, Salmena et al., 2008)
Ran nuclear membrane active transporter (Salmena et al., 2008)
MVP nuclear membrane active transporter (Salmena et al., 2008)
MAST1 mouse (IntACT, pull down, in vitro, yeast, beta-galactosidase, protein kinase assay, in vitro, Valiente et al, 2005)
SCG1 (Secretogranin1, CHGB) (InterAc, two hybrid screening, yeast, Stelz et al., 2005)
APC4(InterAct, Human prostate adenocarcinoma, anti tag coip, Song et al., 2011)
APC5 (InterAct, Human prostate adenocarcinoma, anti tag coip, Song et al., 2011)
APC7 (InterAct, Human prostate adenocarcinoma, anti tag coip, Song et al., 2011)
CDC27 (InterAct, Human prostate adenocarcinoma, anti tag coip, Song et al., 2011)
ANG (Ribonuclease 5, Angiogenin) (InterAct, two hybrid pooling, Stelzl et al., 2005)
Zn72D (InterAct, yeast two hybrid, Giot et al., 2003)
UTP14A (U3 small nucleolar RNA-associated protein 14 homolog A) (InterAct, two hybrid pooling, Stelzl et al., 2005)

MAGI 3 (Membrane-associated guanylate kinase inverted 3) (Pull down) (Valiente et al, 2005; InterAct)

Smurf2 (lumier) (InterAct, Narimatsu et al., 2009)

Cenpc1 (Centromere autoantigen C) (InterAct, anti bait coip, Shen et al., 2007)

Epac (Yeast two hybrid) (InterAct, Giot et al, 2003)

COPS6 (COP9 signalosome complex subunit 6) (InterAct,2 hybrid pooling, Stelzl et al., 2005)

PPP1CA (Serine/threonine-protein phosphatase PP1-alpha catalytic subunit) (antibody array) (Flores-Delgado G et al, 2007; InterAct)

alsD; GBAA_0867; BAS0824; BA_0867 (Bacterial protein) (Two hybrid pooling) (Dyer et al, 2010; InterAct)

HBA1; HBA2; Hemoglobin alpha chain (Two hybrid pooling, yeast) (Stelzl et al, 2005; IntAct)

Heat shock 70 kDa protein 5; HSPA5; GRP78; Endoplasmic reticulum lumenal Ca(2+)-binding protein grp78 (Co-sedimentation, H460 cells) (Shu et al, 2007, InterAct)

SLC9A3R2 (solute carrier family 9 (sodium/hydrogen exchanger) (STRING-db.org, association, Takahashi et al., 2006)

SLC9A3R1 ((solute carrier family 9 (sodium/hydrogen exchanger) (STRING-db.org)

PTK2; protein tyrosine kinase 2 (STRING-db.org)

STAT5A, STAT5: Signal transducer and activator of transcription 5A (PIPs prediction >12.5 score)

CRKL: Crk-like protein (PIPs prediction >12.5 score)

EEF1G, EF1G, PRO1608: Elongation factor 1-gamma (PIPs prediction >12.5 score)

STAT5B: Signal transducer and activator of transcription 5B (PIPs prediction >12.5 score)

NRHF2 (APID, MINT)

MAST2 (Mouse) (APID, IntAct)

MAST3 (APID, IntAct)

STK11 (Serine/threonine-protein kinase 11) (APID, HPRD)

(AR) Androgen receptor (BioGRID, APID)

Casein kinase II subunit alpha (APID, BioGRID)

Alpha 2 globin variant (MINT: APID)

PDGFR Beta (Beta-type platelet-derived growth factor receptor) (MINT)

Paxillin (PXN) (Zinc ion binding, ROS response, signalling complex assembly) (BioGRID, APID)

Estrogen receptor (ESR/ESR1) (BioGRID, APID)

Ubiquitin-conjugating enzyme E2 L3 (UB2L3) (BioGRID, APID)

SUMO-conjugating enzyme (UBC9) (BioGRID, APID)

Caveolin-1 (Cav1) (BioGRID, BIND, APID)

Membrane-associated guanylate kinase-related 3 (Q9HBC4) (BIND, APID)

ROCK1 (Rho-associated protein kinase 1) (BIND, APID)

Glioma tumor suppressor candidate region gene 2 protein (p60/GSCR2) (BIND, APID)

GLTSCR2 (APID; Okahara et al., 2004)

NIRF (UniProt, antibody array)

CHGB (SPIKE, direct interaction, Stelzl., 2005)

FRK (SPIKE, association, Yim., 2009)

SP1 (SPIKE, direct interaction, Kang-Park., 2003)

HSPA5 (SPIKE, association, Shu., 2008)

NEDD4 (SPIKE, direct interaction, Yim., 2009)

PREX2 (SPIKE, direct interaction, Fine., 2009)

AR (SPIKE, association, Lin., 2004)

RPS3A (Reactome, experimental knowledge based, Wu et al., 2010)

RB1CC1 (Reactome, experimental knowledge based, Wu et al., 2010)
PIP4K2B (Reactome, experimental knowledge based, Wu et al., 2010)
PIK3CB (Reactome, experimental knowledge based, Wu et al., 2010)
SYNJ1 (Reactome, experimental knowledge based, Wu et al., 2010)
CDIPT (Reactome, experimental knowledge based, Wu et al., 2010)
INPP5D (Reactome, experimental knowledge based, Wu et al., 2010)
ITGB1 (Reactome, experimental knowledge based, Wu et al., 2010)
INPP4B (Reactome, experimental knowledge based, Wu et al., 2010)
PLCB1 (Reactome, experimental knowledge based, Wu et al., 2010)
PREX1 (Reactome, experimental knowledge based, Wu et al., 2010)
GAB1 (Reactome, experimental knowledge based, Wu et al., 2010)
VAV1 (Reactome, experimental knowledge based, Wu et al., 2010)
RNF51 (MINT, anti tag coimmunoprecipitation, Fan et al., 2009)
PXN (irefindex, Haier and Nicolson., 2002)
AKT3 (Reactome, experimental knowledge based, Wu et al., 2010)
DKFZ (Reactome, experimental knowledge based, Wu et al., 2010)
INPP4A (Reactome, experimental knowledge based, Wu et al., 2010)
PI4KB (Reactome, experimental knowledge based, Wu et al., 2010)
PLCG2 (Reactome, experimental knowledge based, Wu et al., 2010)
PIK3CD (Reactome, experimental knowledge based, Wu et al., 2010)
CYTH2 (Reactome, experimental knowledge based, Wu et al., 2010)
PIK3C3 (Reactome, experimental knowledge based, Wu et al., 2010)
PDPK1 (Reactome, experimental knowledge based, Wu et al., 2010)
SHC1 (Reactome, experimental knowledge based, Wu et al., 2010)
AKT1 (Reactome, experimental knowledge based, Wu et al., 2010)
PTPMT1 (Reactome, experimental knowledge based, Wu et al., 2010)
CD79B (Reactome, experimental knowledge based, Wu et al., 2010)
PIP5K3 (Reactome, experimental knowledge based, Wu et al., 2010)
PI4KA (Reactome, experimental knowledge based, Wu et al., 2010)
BCR (Reactome, experimental knowledge based, Wu et al., 2010)
PLCB3 (Reactome, experimental knowledge based, Wu et al., 2010)
PDPK2 (Reactome, experimental knowledge based, Wu et al., 2010)
PIK3C2A (Reactome, experimental knowledge based, Wu et al., 2010)
PIK3C2G (Reactome, experimental knowledge based, Wu et al., 2010)
OCRL (Reactome, experimental knowledge based, Wu et al., 2010)
PIP5K1C (Reactome, experimental knowledge based, Wu et al., 2010)
PIK3C2B (Reactome, experimental knowledge based, Wu et al., 2010)
PIP5K1A (Reactome, experimental knowledge based, Wu et al., 2010)
HRAS (Reactome, experimental knowledge based, Wu et al., 2010)
PIP4K2A (Reactome, experimental knowledge based, Wu et al., 2010)
AKT2 (Reactome, experimental knowledge based, Wu et al., 2010)
PIK3CG (Reactome, experimental knowledge based, Wu et al., 2010)
GRB2 (Reactome, experimental knowledge based, Wu et al., 2010)
SYNJ2 (Reactome, experimental knowledge based, Wu et al., 2010)
PLCZ1 (Reactome, experimental knowledge based, Wu et al., 2010)
PIK3R3 (Reactome, experimental knowledge based, Wu et al., 2010)
PLCD4 (Reactome, experimental knowledge based, Wu et al., 2010)
PIK3R1 (Reactome, experimental knowledge based, Wu et al., 2010)
INPP5E (Reactome, experimental knowledge based, Wu et al., 2010)
PLCE1 (Reactome, experimental knowledge based, Wu et al., 2010)
PLCB4 (Reactome, experimental knowledge based, Wu et al., 2010)
PLCD3 (Reactome, experimental knowledge based, Wu et al., 2010)
PIP4K2C (Reactome, experimental knowledge based, Wu et al., 2010)
PIP5K1B (Reactome, experimental knowledge based, Wu et al., 2010)

EGR1 (Reactome, experimental knowledge based, Wu et al., 2010)

HDLG-1 (BIND)

Appendix 1. PTEN protein-protein interactors

Proteins annotated with database searched, technique to discover interactor, and corresponding publication.

MAPK1 (MINT database)

MAPK3 (MINT database, Todd et al., 1999)

CASK (IntAct database, two hybrid assay)

HLA-B (IntAct database, Spike, anti-bait coimmunoprecipitation, mass spectrometry, Ewing et al., 2007)

MCC (IntAct database, Ewing et al., 2007)

NEUROD1 (IntAct database, two hybrid assay)

BNIP3L (IntAct database, two hybrid assay)

FGF7 (Spike, coimmunoprecipitation, Rual et al., 2005; Ishibashi et al., 1992)

SYK (Spike, biochemical, Alonso et al., 2003)

ZAP70 (Spike, biochemical Alonso et al., 2003)

EGFR (APID, Ishibashi et al., 1992)

STAT1 (APID, in vivo, Najarro et al., 2001)

EGF (APID, Ishibashi et al., 1992)

PDGFA (APID, Ishibashi et al., 1992)

MAP2K2 (APID, Todd et al., 1999)

ERBB1 (Biogrid, Ishibashi et al., 1992)

ERK (Biogrid, Todd et al., 1999)

Appendix 2. VHR protein-protein interactors

Proteins annotated with database searched, technique to discover interactor, and corresponding publication.

>pGEX-6P-1 (NotI/BamHI)-pGEX-4T-1-PTEN (BamHI/NotI) (circular)

AATGAGCTGTTGACAATTAATCATCGGCTCGTATAATGTGTGGAATTGTGAGCGGATAACAATTTTAC
ACAGGAAACAGTATTCATGTCCCCTATACTAGGTTATTGGAAAATTAAGGGCCTTGTGCAACCCAC
TCGACTTCTTTTGGAAATATCTTGAAGAAAATATGAAGAGCATTGTATGAGCGCGATGAAGGTGA
TAAATGGCGAAACAAAAGTTTGAATTGGGTTTGGAGTTTCCCAATCTTCCTTATTATATTGATGGT
GATGTTAAATTAACACAGTCTATGGCCATCATACGTTATATAGCTGACAAGCACAACATGTTGGGT
GGTTGTCCAAAAGAGCGTGCAGAGATTTCAATGCTTGAAGGAGCGGTTTTGGATATTAGATACGG
GTTTTCGAGAATTGCATATAGTAAAGACTTTTGAAACTCTCAAAGTTGATTTTCTTAGCAAGCTACCT
GAAATGCTGAAAATGTTGCAAGATCGTTTATGTCATAAAACATATTTAAATGGTGATCATGTAACC
CATCCTGACTTCATGTTGTATGACGCTCTTGATGTTGTTTTATACATGGACCCAATGTGCCTGGATG
CGTTCCCAAATAGTTTGTGTTTTAAAAACGATTGAAGCTATCCACAAATTGATAAGTACTTGAA
ATCCAGCAAGTATATAGCATGGCCTTTCAGGGCTGGCAAGCCACGTTTGGTGGTGGCGACCATC
CTCCAAAATCGGATCTGGTTCCGCGTGGATCCCGGAATTCACAGCCATCATCAAAGAGATCGTTA
GCAGAAAACAAAAGGAGATATCAAGAGGATGGATTTCGACTTAGACTTGACCTATATTTATCCAAACAT
TATTGCTATGGGATTTCTGCAGAAAAGACTTGAAGGCGTATACAGGAACAATATTGATGATGTAGTA
AGGTTTTTGGATTCAAAGCATAAAAACCATTACAAGATATACAATCTTTGTGCTGAAAGACATTATGA
CACCGCCAAATTTAATTGCAGAGTTGCACAATATCCTTTTGAAGACCATAACCCACCACAGCTAGAA
CTTATCAAACCCTTTTGTGAAGATCTTGACCAATGGCTAAGTGAAGATGACAATCATGTTGCAGCAAT
TCACTGTAAAGCTGGAAAAGGACGAACCTGGTGTAAATGATATGTGCATATTTATTACATCGGGGCAA
TTTTTAAAGGCACAAGAGGCCCTAGATTTCTATGGGGAAGTAAGGACCAGAGACAAAAAGGGAGTA
ACTATCCCAGTCAGAGGCGCTATGTGTATTATTATAGCTACCTGTTAAAGAATCATCTGGATTATAG
ACCAGTGGCACTGTTGTTTCACAAGATGATGTTTGAAACTATTCCAATGTTTCAGTGGCGGAACCTTGC
AATCCTCAGTTTGTGGTCTGCCAGCTAAAGGTGAAGATATATTCTCCAATTCAGGACCCACACGCAC
GGGAAGACAAGTTCATGTACTTTGAGTTCCCTCAGCCGTTACCTGTGTGTGGTGATATCAAAGTAGA
GTTCTTCCACAACAGAACAAGATGCTAAAAAAGGACAAAATGTTTCACTTTTTGGGTAAATACATTCT
TCATACCAGGACCAGAGGAAACCTCAGAAAAAGTAGAAAAATGGAAGTCTATGTGATCAAGAAAATCGA
TAGCATTGTCAGTATAGAGCGTGCAGATAATGACAAGGAATATCTAGTACTTACTTTAACAAAAAATG
ATCTTGACAAAAGCAAATAAAGACAAAGCCAACCGATACTTTTCTCAAATTTTAAAGGTGAAGCTGTAC

TTCACAAAAACAGTAGAGGAGCCGTCAAATCCAGAGGCTAGCAGTTCAACTTCTGTAAACCAGATG
TTAGTGACAATGAACCTGATCATTATAGATATTCTGACACCCTGACTCTGATCCAGAGAATGAACCT
TTTGATGAAGATCAGCATAACAAAATTACAAAAGTCTGACTCGAGCGGCCGCATCGTGACTGACTGA
CGATCTGCCTCGCGCTTTTCGGTGATGACGGTGAAAACCTCTGACACATGCAGCTCCCGGAGACGG
TCACAGCTTGTCTGTAAGCGGATGCCGGGAGCAGACAAGCCCGTCAGGGCGCGTCAGCGGGTGT
GGCGGGTGTGCGGGGCGCAGCCATGACCCAGTCACGTAGCGATAGCGGAGTGTATAATTCTTGAAGA
CGAAAGGGCCTCGTATACGCCTATTTTTATAGTTAATGTCATGATAATAATGGTTTCTTAGACGTC
AGGTGGCACTTTTCGGGAAATGTGCGCGAAACCCCTATTTGTTTATTTTTCTAAATACATTCAAATA
TGTATCCGCTCATGAGACAATAACCTGATAAATGCTTCAATAATTTGAAAAAGGAAGAGTATGAGT
ATTCAACATTTCCGTGTGCGCCTTATTCCCTTTTTTGCGGCATTGCTTCCCTGTTTTTGTCAACCA
GAAACGCTGGTGAAAGTAAAAGATGCTGAAGATCAGTTGGGTGCACGAGTGGGTACATCGAACTG
GATCTCAACAGCGGTAAGATCCTTGAGAGTTTTTCGCCCGAAGAACGTTTTCCAATGATGAGCACTT
TTAAAGTTCTGCTATGTGGCGCGTATTATCCCGTGTGACGCGGGCAAGAGCAACTCGGTGCGC
GCATACACTATTCTCAGAATGACTTGGTTGAGTACTACCAGTCACAGAAAAGCATCTTACGGATGG
CATGACAGTAAGAGAATTATGCAGTGCTGCCATAACCATGAGTGATAAACTGCGGCCAACTTACTT
CTGACAACGATCGGAGGACCGAAGGAGCTAACCCTTTTTTGCACAACATGGGGGATCATGTAAC
CGCTTGTGCTGTTGGGAACCGGAGCTGAATGAAGCATAACCAACGACGAGCTGACACCAGATG
CCTGCAGCAATGGCAACAACGTTGCGCAAACCTTAACCTGGCGAACTACTACTGCTTCCCGGC
AACAAATTAATGACTGGATGGAGCGGATAAAGTTGACGAGCACTTCTGCGCTCGGCCCTTCCGG
CTGGCTGGTTTATTGCTGATAAATCTGGAGCCGGTGGAGCGTGGGTCTCGCGGTATCATTGCAGCAC
TGGGGCCAGATGGTAAGCCCTCCCGTATCGTAGTTATCTACACGACGGGGAGTCAGGCAACTATGG
ATGAACGAAATAGACAGATCGCTGAGATAGGTGCCTCACTGATTAAGCATTGGTAACTGTCAGACCA
AGTTTACTCATATATACTTTAGATTGATTTAAAACCTTCATTTTTAATTTAAAAGGATCTAGGTGAAGAT
CTTTTTGATAATCTCATGACCAAAATCCCTAACGTGAGTTTTCGTTCCACTGAGCGTCAGACCCCGT
AGAAAAGATCAAAGGATCTTCTTGAGATCCTTTTTTCTGCGCGTAATCTGCTGCTTGCAAACAAAA
AACCACCGCTACCAGCGGTGGTTTGTTCGGGATCAAGAGCTACCAACTTTTTTCCGAAGGTAAC
TGGCTTCCAGCAGCGCAGATACCAATACTGTCCTTCTAGTGTAGCCGAGTTAGGCCACCACTC
AAGAATCTGTAGCACCCGCTACATACCTGCTCTGCTAATCCTGTTACCAGTGGCTGCCAGTG
GCGATAAGTCTGTCTTACC GGTTGGACTCAAGACGATAGTTACCGGATAAGGCGCAGCGGTCCGG
GCTGAACGGGGGGTTCGTGCACACAGCCAGCTTGGAGCGAACGACCTACACCGAACTGAGATAC
CTACAGCGTGAGCTATGAGAAAGCGCCACGCTTCCCGAAGGGAGAAAGGCGGACAGGTATCCGGT
AAGCGGCAGGGTCCGAACAGGAGAGCGCAGGAGGAGCTTCCAGGGGAAACGCCTGGTATCTTT
ATAGTCCTGTGCGGTTTTCCGCCACCTCTGACTTGAGCGTCGATTTTTGTGATGCTCGTCAGGGGGC
GGAGCCTATGGAAAAACGCCAGCAACGCGGCCTTTTTACGGTTCCTGGCTTTTTGCTGGCCTTTTTGC
TCACATGTTCTTCTGCGTTATCCCCTGATTCTGTGGATAACCGTATTACCGCCTTTGAGTGAGCTG
ATACCGCTCGCCGACGCCAAGCAGCGAGCGCAGCGAGTCAGTGAGCGAGGAAGCGGAAGAGCG
CCTGATCGGTATTTTTCTCCTTACGCATCTGTGCGGTATTTACACCCGCATAAATCCGACACCTCG
AATGGTGCAAACCTTTTCGCGTATGGCATGATAGCGCCCGGAAGAGAGTCAATTCAGGGTGGTGA
ATGTGAAACCAGTAACGTTATACGATGTCGACAGATATGCCGGTGTCTTATCAGACCGTTTTCCCG
CGTGGTGAACCAGGCCAGCCACGTTTTCTGCGAAAACGCGGGAAAAAGTGGAAAGCGGCGATGGCGG
AGCTGAATTACATTTCCAACCGCGTGGCACAACAACCTGGCGGGCAAACAGTCGTTGCTGATTGGCG
TTGCCACCTCCAGTCTGGCCCTGCACGCGCCGTCGCAAATTTGTCGCGCGGATTAATCTCGCGCCG
ATCAACTGGGTGCCAGCGTGGTGGTGTGATGGTAGAACGAAGCGGCGTCAAGCCTGTAAAGCG
GCGGTGCACAATCTTCTGCGCAACGCGTCAGTGGGCTGATCATTAACTATCCGCTGGATGACCAG
GATGCCATTGCTGTGGAAGCTGCCTGCACTAATGTTCCGGCGTATTTCTTGTGATGCTCTGACCAGA
CACCCATCAACAGTATTATTTCTCCCATGAAGACGGTACGCGACTGGGCGTGGAGCATCTGGTCCG
ATTGGTCCACCAGCAAATCGCGCTGTTAGCGGCCCATTAAGTTCTGTCTCGGCGCTGCGCTG
GCTGGTGGCATAAATATCTCACTCGCAATCAAATTCAGCCGATAGCGGAACGGGAAGCGTACT
GAGTGCCATGTCCGGTTTTCAACAAACCATGCAAATGCTGAATGAGGGCATCGTTCCCACTGCGATG
CTGGTTGCCAACGATCAGATGGCGCTGGGCGCAATGCGCGCCATTACCGAGTCCGGGCTGCGCGT
TGGTGCAGATATCTCGGTAGTGGGATACGACGATACCGAAGACAGCTCATGTTATATCCCGCCGTTA
ACCACCATCAAACAGGATTTTCGCCTGCTGGGGCAAACAGCGTGGACCGCTTGTGCAACTCTCT
CAGGGCCAGCGGTGAAGGGCAATCAGCTGTTGCCCGTCTCACTGGTAAAAGAAAAACACCCTG
GCGCCCAATACGCAAACCGCCTCTCCCCGCGCGTTGGCCGATTCAATTAATGCAGCTGGCACGACAG
GTTTCCCGACTGGAAAGCGGGCAGTGAGCGCAACGCAATTAATGTGAGTTAGCTCACTCATTAGGC
ACCCAGGCTTTACACTTTATGCTTCCGGCTCGATGTTGTGTTGGAATTGTGACCGGATAACAATTT
ACACAGGAACAGCTATGACCATGATTACGGATTACTGCCCCTGTTTTACACGCTGCTGACTGGG
AAAACCTGGCGTTACCAACTTAATCGCCTTTCAGACACATCCCCCTTTCGCCAGCTGGCGTAATAG
CGAAGAGGCCCGCACCGATCGCCCTTCCAACAGTTGCGCAGCCTGAATGGCGAATGGCGCTTTGC
CTGGTTTCCGGCACCGAAGCGGTGCCGAAAGCTGGCTGGAGTGCAGTCTTCTGAGGGCCGATA
CTGTCGTGCTCCCTCAAACCTGGCAGATGCACGGTTACGATGCGCCCATCTACACCAACGTAACCTA
TCCATTACGGTCAATCCGCCGTTTGTCCACGGAGAATCCGACGGGTTGTTACTCGCTCACATTT
AATGTTGATGAAAGCTGGCTACAGGAAGGCCAGACGCGAATTTTTTGATGGCGTTGGAATTACGT
TATCGACTGCACGGTGCACCAATGCTTCTGGCGTCAGGCAGCCATCGGAAGCTGTGGTATGGCTGT
GCAGGTGTAATCACTGCATAATTCGTGTGCTCAAGGCGCACTCCCGTTCGGATAATGTTTTT
GCGCCGACATCATAACGGTTCGGCAAATATTCTGA

Appendix 3. pGEX-4T-1-PTEN plasmid construct

Contains PTEN as a GST fusion protein with a linker sequence that includes a thrombin cleavage sequence. The GST sequence (artificial sequence; Accession number ACF75943) is in bold. The PTEN sequence (mammalian; NP_001003192.1) is in italics. The linker sequences thrombin site is underlined.

>pGEX-4T-1 (Sall/BamHI)-VHR PCR product RS (BamHI/Sall) (circular)

```
CTCGAGCGGCCGCATCGTGACTGACTGACGATCTGCCTCGCGCTTTCGGTGATGACGGTGAAAAAC
CTCTGACACATGCAGCTCCCGGAGACGGTACAGCTTGTCTGTAAGCGGATGCCGGGAGCAGACAA
GCCCGTCAGGCGCGTACAGCGGGTGTGGCGGGTGTCCGGGCGCAGCCATGACCCAGTCAGTA
GCGATAGCGGAGTGTATAATCTTGAAGACGAAAGGGCCCTCGTGATACGCCTATTTTTATAGGTTAA
TGTCATGATAATAATGGTTTTCTTAGACGTCAAGGTGGCACTTTTCGGGGAAATGTGCGCGGAACCCCT
ATTTGTTTTATTTTTCTAAATACATTCAAATATGTATCCGCTCATGAGACAATAACCCTGATAAATGCTT
CAATAATATTGAAAAAGGAAGAGTATGAGTATTCAACATTTCCGTGTCGCCCTTATCCCTTTTTTGC
GGCATTGTCCTTCTGTTTTGCTCACCCAGAAACGCTGGTAAAAGTAAAAGATGCTGAAGATCAG
TTGGGTGCACGAGTGGGTTACATCGAAGTGGATCTCAACAGCGGTAAGATCCTTGAGAGTTTTCGCC
CCGAAGAACGTTTTCCAATGATGAGCACTTTTAAAGTTCTGCTATGTGGCGCGGTATTATCCCGTGT
GACGCCGGCAAGAGCAACTCGGTGCGCCGATACACTATTCTCAGAATGACTTGGTTGAGTACTCA
CCAGTCACAGAAAAGCATCTTACGGATGGCATGACAGTAAGAGAATTATGCAGTGTGCCATAACCA
TTGATAACACTGCGGCCAACTTACTTCTGACAACGATCGGAGGACCGAAGGAGCTAACCGCT
TTTTGCACAACATGGGGGATCATGTAACCTGCCTTGATCGTTGGGAACCGGAGCTGAATGAAGCCAT
ACCAAACGACGAGCGTGACACCACGATGCCTGCAGCAATGGCAACAACGTTGCGCAAACCTATTAAC
TGCGCAACTACTTACTCTAGCTTCCCGGCAACAATTAATAGACTGGATGGAGGCGGATAAAGTTGCA
GGACCACTTCTGCGCTCGGCCCTTCCGGCTGGCTGGTTATTGCTGATAAATCTGGAGCCGGTGAG
CGTGGGTCTCGCGGTATCATTGCAGCACTGGGGCCAGATGGTAAGCCCTCCCGTATCGTAGTTATC
TACACGACGGGAGTCAGGCAACTATGGATGAACGAAATAGACAGATCGCTGAGATAGGTGCCTCA
CTGATTAAGCATTGGTAAGTGTGACAGCAAGTTTACTCATAATACTTTAGATTGATTTAAAACCTTCAT
TTTTAATTTAAAAGGATCTAGGTGAAGATCCTTTTTGATAATCTCATGACCAAAATCCCTAACGTGAG
TTTTCGTTCCACTGAGCGTCAGACCCCGTAGAAAAGATCAAAGGATCTTCTTGAGATCCTTTTTTTCT
GCGCGTAATCTGTCTGCTTGCAAAACAAAAACCCAGCTACCAGCGGTGGTTTTGTTGCGGATCAA
GAGCTAACACTCTTTTTCCGAAGGTAACCTGGCTTACGACAGCGCAGATACCAATACTGTCTCTC
TAGTGTAGCCGTAGTTAGGCCACCACTTCAAGAAGTCTGTAGCACCGCCTACATACCTCGCTCTGCT
AATCCTGTTACCAGTGGCTGCTGCCAGTGGCGATAAGTCGTGTCTTACCGGGTTGGACTCAAGACG
ATAGTTACCGGATAAAGGCGCAGCGGTGCGGCTGAACGGGGGTTCTGTCACACAGCCCAGCTTGG
AGCGAACGACCTACACCGAACTGAGATACCTACAGCGTGAGCTATGAGAAAGCGCCACGCTTCCCG
AAGGGAGAAAGCGGACAGGTATCCGTAAGCGGCAGGGTCCGGAACAGGAGAGCGCACGAGGGA
GCTTCCAGGGGAAACGCCTGGTATCTTTATAGTCTGTGCGGTTTTCGCCACCTCTGACTTGAGCGT
CGATTTTTGTGATGCTCGTCAGGGGGCGGAGCCTATGGAAAACGCCAGCAACGCGGCCTTTTTTA
CGTTTCTGGCCTTTTGTGCTGACATGTTCTTCTGCGTTATCCCCTGATTCTGTGGA
TAACCGTATTACCGCCTTTGAGTGTGATACCGCTGACCGCTGCGCGCAGCCGAACGACCGCAGCA
TCAGTGTAGGAGGAAAGCGGAAGCGCCTGATGCGGTATTTTCTCCTTACGCATCTGTGCGGTAT
TTCACACCGCATAAATTCCGACACCATCGAATGGTGCAAAACCTTTTCGCGGTATGGCATGATAGCGC
CCGGAAGAGAGTCAATTCAGGGTGGTGAATGTGAAACCAGTAACGTTATACGATGTGCGCAGAGTAT
GCCGGTGTCTCTTATCAGACCGTTTCCCGCGTGGTGAACCAGGCCAGCCAGTTTCTGCGAAAACG
CGGGAAGAAAGTGAAGCGGCGATGGCGGAGCTGAATTACATTCCCAACCGCGTGGCACAACAACCTG
GCGGGCAAACAGTCGTTGCTGATTGGCGTTGCCACCTCCAGTCTGGCCCTGCACGCGCCGTCGCAA
ATTGTGCGCGGCGATTAAATCTCGCGCCGATCAACTGGGTGCCAGCGTGGTGGTGTGATGGTAGAA
CGAAGCGGCGTCAAGCCTGTAAGCGGCGGTGCACAATCTTCTCGCGCAACGCGTCAGTGGGCT
GATCATTAACTATCCGCTGGATGACCAGGATGCCATTGCTGTGGAAGCTGCCTGACTAATGTTCCG
GCGTTATTTCTTGATGTCTCTGACCAGACACCCATCAACAGTATTATTTTCTCCCATGAAGACGGTAC
CGGACTGGGCGTGGAGCATCTGGTCGCATTGGGTCAACCAGCAAATCGCGCTGTTAGCGGGCCCAT
AAGTTCTGTCTCGGCGCTCTGCGTCTGGCTGGCTGGCATAAATATCTCACTCGCAATCAAATTCAG
CCGATAGCGGAACGGGAAGGCGACTGGAGTGCCATGTCCGGTTTTCAACAAACCATGCAAATGCTG
AATGAGGGCATCGTTCCCACTGCGATGCTGGTTGCCAACGATCAGATGGCGCTGGGCGCAATGCGC
GCCATTACCGAGTCCGGGCTGCGCGTTGGTGGCGATATCTCGGTAGTGGGATACGACGATACCGAA
GACAGCTCATGTTATATCCCGCCGTTAACCACCATCAAACAGGATTTTCGCTGCTGGGGCAAACCA
GCGTGGACCGCTTGTGCAACTCTCTCAGGGCCAGGCGGTGAAGGGCAATCAGCTGTTGCCCGTCT
CACTGGTGAAGAAACCAACCTGGCGCCAATACGCAACCGCCTCTCCCCGCGCTTGGCCG
ATTCATTAATGCAGCTGGCAGACAGGTTTCCCGACTGAAAGCGGGCAGTGAAGCGCAACGCAATT
AATGTAGTTAGCTCACTCATTAGGCACCCAGGCTTTACACTTTATGCTTCCGCTCGTATGTTGTG
TGGAATTGTGAGCGGATAACAATTTACACACAGGAAACAGCTATGACCATGATTACGGATTCAGTGGC
CGTCTGTTTTACAACGTCGTGACTGGGAAAACCTGGCGTTACCCAACCTAATCGCCTTGCAGCACAT
CCCCCTTTCGCCAGCTGGCGTAATAGCGAAGAGGCCCGCACCGATCGCCCTTCCCAACAGTTGCGC
AGCCTGAATGGCGAATGGCGCTTTGCTGGTTTCCGGCACCAAGCGGTGCCGGAAGCTGGCT
```

GGAGTGGGATCTTCCTGAGGCCGATACTGTGTCGTCGCCCTCAAACCTGGCAGATGCACGGTTACGA
TGCGCCCATCTACACCAACGTAACCTATCCCATTACGGTCAATCCGCCGTTTGTCCACGGAGAAT
CCGACGGGTTGTTACTCGCTCACATTTAATGTTGATGAAAGCTGGCTACAGGAAGGCCAGACGCGA
ATTATTTTTGATGGCGTTGGAATTACGTTATCGACTGCACGGTGCACCAATGCTTCTGGCGTCAGGC
AGCCATCGGAAGCTGTGGTATGGCTGTGCAGGTCGTAATCACTGCATAATTCGTGTGCTCAAGG
CGCACTCCCGTTCTGGATAATGTTTTTTCGCCGACATCATAACGGTTCTGGCAAATATTCTGAAATG
AGCTGTTGACAATTAATCATCGGCTCGTATAATGTGTGGAATTGTGAGCGGATAACAATTTACACAG
GAAACAGTATTCATGTCCCCTATACTAGGTTATTGAAAAATTAAGGGCCTTGTGCAACCCACTCGAC
TCTTTTGAATATCTTGAAGAAAAATATGAAGAGCATTGTATGAGCGCGATGAAGGTGATAAATGGC
GAAACAAAAAGTTTGAATTGGGTTTGGAGTTTCCCAATCTTCCTTATTATATTGATGGTGATGTTAAAT
TAACACAGTCTATGGCCATCATACTGTTATATAGCTGACAAGCACAACATGTTGGGTGGTTGTCCAAA
AGAGCGTGCAGAGATTTCAATGCTTGAAGGAGCGGTTTTGGATATTAGATACGGTGTTCGAGAATT
GCATATAGTAAAGACTTTGAAACTCTCAAAGTTGATTTTCTTAGCAAGCTACCTGAAATGCTGAAAT
GTTGCAAGATCGTTTATGTCATAAAACATATTTAAATGGTGATCATGTAACCCATCCTGACTTCATGTT
GTATGACGCTCTTGATGTTGTTTTATACATGGACCAATGTGCCTGGATGCGTTCCCAAAATAGTTT
GTTTTAAAAACGTATTGAAGCTATCCCACAAATTGATAAGTACTTGAAATCCAGCAAGTATATAGCA
TGGCCTTTGCAGGGCTGGCAAGCCACGTTTGGTGGTGGCGACCATCCTCCAAAATCGGATCTGGTT
CCGCGTGGATCCATGTCGGGCTCGTTTCGAGCTCGTTGCGGATCTCAACGACATGCTCTCGGAC
GGCAGCGCTGCTACAGCCTCCCGAGCCAGCCCTGCAACGAGGTACCCCGCGGATCTACGTGGG
CAACGCGTCTGTGGCTCAGGACATCCCCAAGCTGCAGAACTAGGCATCACCCATGTGCTGAACGC
GGCTGAGGGCAGGTCCTTCATGCACGTCAACACCAATGCCAATTCTACAAGGACTCCGGCATCAC
ATACCTGGGCATCAAGGCCAACGACACACAGGAGTTCAACCTCAGCGCTTACTTTGAAAGGGCTGC
CGACTTCATTGACCAGGCTTTGGCTCAAAGAATGGCCGGGTGCTCGTCCACTGCCGGAAGGTTA
TAGCCGCTCCCAACGCTAGTTATCGCCTACCTCATGATGCGGCAGAAGATGGACGTCAGTCTGC
CCTGAGCATCGTGAGGCAGAACCCTGAGATCGGCCCAACGATGGCTTCTGGCCAGCTCTGCCA
GCTCAATGACAGACTAGCCAAGGAGG GAAGTTGAAACCCTAGGTCGA

Appendix 4. pGEX-4T-1-VHR plasmid construct

Contains VHR as a GST fusion protein with a linker sequence that includes a thrombin cleavage sequence.

>gil61358507|gb|AAX41578.1| phosphatase and tensin-like [synthetic construct]
MTAIIKEIVSRNKRRYQEDGFDLTYIYPNIIAMGFPAERLEGVYRNNIDDVVRFLDSKHRNHYKIYNLCA
ERHYDTAKFNCRVAQYPFEDHNPPQLELIKPFCELDQWLSDDNHVAAIHCKAGKGRGTGVMICAYLLH
RGKFLKAQEALDFYGEVTRDRKKGVTIPSQRRYVYSSYLLKNHLDYRVPVALLFHKMMFETIPMFSGGT
CNPQFVVCQLKVKIYSSNSGPTRRDKFMYFEFPQPLVCGDIKVEFFHKQNKMLKDKMFHFWVNTFF
IPGPEETSEKVENGLCDQEIDSICSIERADNDKEYLVLTLTKNLDKANKDKANRYFSPNFKVKLYFTKT
VEEPSNPEASSSTSVTPDVSNDNEPDHYRSDTTDSDPENEPFDEDQHTQITKV

Appendix 5. PTEN amino acid sequence

>gil194580258|gb|ACF75943.1| glutathione-S-transferase affinity tag [Cloning vector
pAW8_GST]MSPILGYWKIKGLVQPTRLLEYLEEKYEEHLYERDEGDKWRNKKFELGLEFPNLPYYIDGD
VKLTQSMIIRYIADKHNMLGGCPKERAEISMLEGAVLDIRYGVSRVIAYSKDFETLKVDFLSKLPPEMLKMF
DRLCHKTYLNGDHVTHPDFMLYDALDVVLYMDPMCLDAFPKLVCFKKRERIAIPQIDKYLKSSKYIAWPLQ
GWQATFGGGDHPKSDLVPR

Appendix 6. GST affinity tag amino acid sequence

GST protein sequence encoded in pGEX-4T-1-PTEN and VHR. Plasmid sequence analysed on NCBI BLAST (<http://blast.ncbi.nlm.nih.gov/Blast.cgi>), using Blastx. Displayed as FASTA formatted.

PGM commands:

;Initialize all Analyst synchronisation properties to 0.

ReadyToRun = 0

DoInject = 0

InjectResponse = 0
Sampler.TempCtrl = On
Sampler.Temperature.Nominal = 10.0 [°C]
Sampler.Temperature.LowerLimit = 4.0 [°C]
Sampler.Temperature.UpperLimit = 45.0 [°C]
Sampler.ReadyTempDelta = 10.0 [°C]
ColumnOven.TempCtrl = On
ColumnOven.Temperature.Nominal = 30.0 [°C]
ColumnOven.Temperature.LowerLimit = 5.0 [°C]
ColumnOven.Temperature.UpperLimit = 85.0 [°C]
ColumnOven.ReadyTempDelta = 5.0 [°C]
;Column_1.ActiveColumn = No
;Column_2.ActiveColumn = No
LoadingPump.Pressure.LowerLimit = 0 [bar]
LoadingPump.Pressure.UpperLimit = 350 [bar]
LoadingPump.MaximumFlowRampDown = 3 [µl/min²]
LoadingPump.MaximumFlowRampUp = 3 [µl/min²]
LoadingPump.%A.Equate = "%A"
LoadingPump.%B.Equate = "%B"
LoadingPump.%C.Equate = "%C"
MicroPump.Pressure.LowerLimit = 0 [bar]
MicroPump.Pressure.UpperLimit = 295 [bar]
; MasterPressure.LowerLimit = 0 [bar]
; MasterPressure.UpperLimit = 350 [bar]
MicroPump.MaximumFlowRampDown = 3 [µl/min²]
MicroPump.MaximumFlowRampUp = 3 [µl/min²]
MicroPump.%A.Equate = "%A"
MicroPump.%B.Equate = "%B"
MicroPump.%C.Equate = "%C"
AnalystMinVolume = 0.001 [µl]
AnalystDefaultVolume = 10.000 [µl]
AnalystMaxVolume = 25.000 [µl]
DrawSpeed = 300 [nl/s]
DrawDelay = 5000 [ms]
DispSpeed = 1000 [nl/s]
DispenseDelay = 2000 [ms]
WasteSpeed = 4000 [nl/s]
WashSpeed = 4000 [nl/s]
LoopWashFactor = 2.000
SampleHeight = 4.000 [mm]
PunctureDepth = 7.000 [mm]
WashVolume = 200.000 [µl]
; SyncWithPump = On

RinseBetweenReinjections = No
LowDispersionMode = Off
InjectMode = UserProg
ReagentAVial= R1
ReagentBVial= GA11
ReagentCVial= GB11
ReagentDVial= GC11
; UdpInjectValve Position=Load
LoadingPump_Pressure.Step = Auto
LoadingPump_Pressure.Average = On
; MicroPump_MasterPressure.Step = Auto
; MicroPump_MasterPressure.Average = On
ColumnOven_Temp.Step = Auto
ColumnOven_Temp.Average = On
; ColumnPressure.Step = Auto
; ColumnPressure.Average = On
ColumnOven_FC_BridgeFlow.Step = Auto
ColumnOven_FC_BridgeFlow.Average = On
ColumnOven_FC_Stepper.Step = Auto
ColumnOven_FC_Stepper.Average = On
LoadingPump.Flow = 30 [µl/min]
LoadingPump.%B = 0.0 [%]
LoadingPump.%C = 0.0 [%]
LoadingPump.Curve = 5
ValveLeft = 10_1
PrepVial= R1
UdpInjectValve Position=Load
UdpSyringeValve Position=Needle
UdpDraw From=ReagentAVial, Volume=5.000,
SyringeSpeed=GlobalSpeed, SampleHeight=GlobalHeight
UdpMixWait Duration=5
UdpDraw From=ReagentAVial, Volume=0.000,
SyringeSpeed=GlobalSpeed, SampleHeight=GlobalHeight
UdpDispense To=Waste, Volume=5.000, SyringeSpeed=GlobalSpeed,
SampleHeight=GlobalHeight
UdpDraw From=SampleVial, Volume=10.000,
SyringeSpeed=GlobalSpeed, SampleHeight=GlobalHeight
UdpMixWait Duration=5
UdpDraw From=SampleVial, Volume=0.000,
SyringeSpeed=GlobalSpeed, SampleHeight=GlobalHeight
UdpDraw From=ReagentAVial, Volume=1.400,
SyringeSpeed=GlobalSpeed, SampleHeight=GlobalHeight
UdpMixWait Duration=5
UdpDraw From=ReagentAVial, Volume=0.000,
SyringeSpeed=GlobalSpeed, SampleHeight=GlobalHeight

```

UdpInjectValve Position=Inject
UdpInjectMarker
UdpMixNeedleWash Volume=100.000
0.000 Wait ColumnOven.Ready and Sampler.Ready
;Chromeleon sets this property to signal to Analyst that it is ready to start
a run.
ReadyToRun = 1
;Analyst sets this property to start the injection.
Wait DoInject
MicroPump.Flow = 0.2 [µl/min]
MicroPump.%B = 2.0 [%]
MicroPump.%C = 0.0 [%]
Wait ColumnOven.Ready and Sampler.Ready
Inject
LoadingPump_Pressure.AcqOn
; MicroPump_MasterPressure.AcqOn
ColumnOven_Temp.AcqOn
; ColumnPressure.AcqOn
ColumnOven_FC_BridgeFlow.AcqOn
ColumnOven_FC_Stepper.AcqOn
;Chromeleon sets this property to signal the injection to Analyst.
InjectResponse = 1
;Depending on your system configuration it might be necessary to
manually insert
;a "Relay" command below in order to send the start signal to the MS.
;Typical syntaxes:
;Pump_Relay_1.Closed Duration = 2.00
;UM3PUMP_Relay1.On Duration = 2.00
MicroPump.Flow = 0.200 [µl/min]
MicroPump.%B = 2.0 [%]
MicroPump.%C = 0.0 [%]
0.100 MS_Start.State On
0.200 MS_Start.State Off
4.000 MicroPump.Flow = 0.2 [µl/min]
MicroPump.%B = 2.0 [%]
MicroPump.%C = 0.0 [%]
ValveLeft = 1_2
49.000 MicroPump.Flow = 0.2 [µl/min]
MicroPump.%B = 45.0 [%]
MicroPump.%C = 0.0 [%]
50.000 MicroPump.Flow = 0.2 [µl/min]
MicroPump.%B = 90.0 [%]
MicroPump.%C = 0.0 [%]

```

54.000 MicroPump.Flow = 0.2 [µl/min]
 MicroPump.%B = 90.0 [%]
 MicroPump.%C = 0.0 [%]
 55.000 MicroPump.Flow = 0.2 [µl/min]
 MicroPump.%B = 2.0 [%]
 MicroPump.%C = 0.0 [%]
 64.000 ValveLeft = 10_1
 65.000 LoadingPump_Pressure.AcqOff
 ; MicroPump_MasterPressure.AcqOff
 ColumnOven_Temp.AcqOff
 ; ColumnPressure.AcqOff
 ColumnOven_FC_BridgeFlow.AcqOff
 ColumnOven_FC_Stepper.AcqOff
 MicroPump.Flow = 0.2 [µl/min]
 MicroPump.%B = 2.0 [%]
 MicroPump.%C = 0.0 [%]
 InjectResponse = 0
 End

Appendix 7. Analyst MS chromatography method

Non-treated negative control PTEN, 1hr at 37°C						
Peptide	Peptide sequence	Observed ion (m/z)	Modification	Ion score	Retention Time (min)	Sequence coverage (%)
67-80	K.IYNL CAERH YDTAK. F	577.094 4	C5, Diox (C)	13	25,26	48
67-80	K.IYNL CAERH YDTAK. F	582.424 7	C5, Triox (C)	65	25.35	48
67-80	K.IYNL CAERH YDTAK. F	541.872 8	Y2, Nitro (Y)	19	25.67	48
67-80	K.IYNL CAERH YDTAK. F	542.392	Y2, Nitro (Y)	29	25.67	48
129-142	K.GRT GVMIC AYLLH R.G	564.419 2	Y10, Nitro (Y)	24	27.54	48

129-142	K.GRT GVMIC AYLLH R.G	564.419 6	Y10, Nitro (Y)	26	28.05	48
148-159	K.AQE ALDFY GEVR. T	721.519 7	Y8, Nitro (Y)	52	30.08	48
75:1 Sin-1:PTEN, 1hr at 37°C treated PTEN						
Peptide	Peptide sequence	Observed ion (m/z)	Modification	Ion score	Retention Time (min)	Sequence coverage (%)
42-55	R.LEGV YRNNI DDVVR .F	560.104 7	Y5, Ox (Y)	22	26.22	47
42-55	R.LEGV YRNNI DDVVR .F	560.105 4	Y5, Ox (Y)	32	26.91	47
67-74	K.YINL CAER. H	515.372 2	C5, Triox (C)	47	27.4	47
67-80	K.IYNL CAERH YDTAK. F	582.424 2	C5, Triox (C)	49	25.17	47
129-142	K.GRT GVMIC AYLLH R.G	564.418 4	Y10, Nitro (Y)	19	27.35	47
129-142	K.GRT GVMIC AYLLH R.G	564.420 3	Y10, Nitro (Y)	25	27.9	47
131-142	R.TGV MICAY LLHR.G	725.567 4	M4, Ox (M)	29	29.91	47
148-159	K.AQE ALDFY GEVR. T	707.529 8	Y8, Ox (Y)	52	28.7	47
148-159	K.AQE ALDFY GEVR. T	707.530 1	Y8, Ox (Y)	51	28.12	47
148-159	K.AQE ALDFY GEVR. T	707.533 5	Y8, Ox (Y)	49	29.24	47

148-159	K.AQE ALDFY GEVR. T	722.030 6	Y8, Nitro (Y)	38	32.29	47
222-233	K.VKIY SSNSG PTR.R	442.344	Y4, Ox (Y)	47	21.74	47
150:1 Sin-1:PTEN, 1hr at 37°C treated PTEN						
Peptide	Peptide sequence	Observed ion (m/z)	Modification	Ion score	Retention Time (mins)	Sequence coverage (%)
42-55	R.LEGV YRNNI DDVVR .F	560.103 9	Y5, Ox (Y)	34	26.21	55
67-80	K.IYNL CAERH YDTAK. F	582.493	C5, Triox (C)	36	25.21	56
67-80	K.IYNL CAERH YDTAK. F	596.425 2	C5, Diox (C)	13	25.37	56
75-84	R.HYD TAKFN CR.V	452.975 1	Y2, Nitro (Y)	25	22.66	55
129-142	K.GRT GVMIC AYLLH R.G	564.419 1	Y10, Nitro (Y)	30	27.35	55
129-142	K.GRT GVMIC AYLLH R.G	564.421	Y10, Nitro (Y)	18	27.87	55
131-142	R.TGV MICAY LLHR.G	725.573 6	M4, Ox (M)	32	29.9	55
131-142	R.TGV MICAY LLHRG K.F	545.764 3	M4, Ox (M)	24	27.92	55
148-159	K.AQE ALDFY GEVR. T	707.529 3	Y8, Ox (Y)	68	28.66	55
148-159	K.AQE ALDFY GEVR. T	707.530 5	Y8, Ox (Y)	64	28.11	55

148-159	K.AQE ALDFY GEVR. T	722.033	Y8, Nitro (Y)	57	32.3	55
222-233	K.VKIY SSNSG PTR.R	442.342 9	Y4, Ox (Y)	43	21.77	55
224-233	K.IYSS NSGPT R.R	563.907 1	Y2, Nitro (Y)	24	22.18	55
224-234	K.IYSS NSGPT RR.E	418.302 3	Y2, Ox (Y)	18	34.68	55
235-254	R.EDKF MYFEF PQPLP VCDIK. V	826.287 4	M5, Ox (M)	27	33.85	55
333-342	K.ANR YFSPN FK.V	420.648 9	Y4, Ox (Y)	18	24.61	55
336-342	R.YFSP NFK.V	474.336 7	Y1, Nitro (Y)	32	28.64	55

Appendix 8. Oxidative modifications observed in tryptic peptides of PTEN by MS/MS with collisionally-induced decomposition after validity sequencing of b and y series ions from 75:1 and 150:1 SIN-1 oxidation and incubation at 37°C for 1 hour Mascot search for Nitro (Y), Ox (Y), Ox (M), Ox (H), Ox (W). The letter designation followed by a number denotes the one letter amino acid code and the sequence of the predicted modified residue within the peptide fragment. Ox = oxidation, Nitro = nitration, Diox = Dioxidation, Triox = Trioxidation.

30:1 HOCl:PTEN, 1hr at RT treated PTEN						
Peptide	Peptide sequence	Observed ion (m/z)	Modification	Ion score	Retention Time (mins)	Sequence coverage (%)
67-74	K.IYNL CAER. H	507.369 1	C5, Diox (C)	16	27.29	70
67-80	K.IYNL CAERH YDTAK. F	577.090 3	C5, Triox (C)	20	25.29	70
67-80	K.IYNC AERHY DTAK.F	582.423 5	C5, Triox (C)	58	25.37	70
131-142	R.TGV MICAY LLHR.G	489.369 3	M4, Ox (M); Y8 Ox (Y)	22	31.71	69
198-	K.MMF	947.026	M8, Ox (M)	40	35.05	69

221	ETIPMF SGGTC NPQFV VCQLK .V	9				
314- 327	K.EYLV LTLTK NDLDK. A	567.444 6	Y2, Chloro (Y)	16	30.2	69
300:1 HOCl:PTEN, 1hr at RT treated PTEN						
Peptide	Peptide sequence	Observed ion (m/z)	Modification	Ion score	Retention Time (mins)	Sequence coverage (%)
67-74	K.IYNL CAER. H	515.372 3	C5, Triox (C)	38	27.54	54
67-74	K.IYNL CAER. H	515.372 3	C5, Triox (C)	14	28.13	54
67-80	K.IYNC AERHY DTAK.F	577.088 5	C5, Triox (C)	12	25.30	54
129- 142	K.GRT GVMIC AYLLH R.G	555.100 9	M6, Ox (M)	63	28.18	63
131- 144	R.TGV MICAY LLHRG K.F	545.765 2	M4, Ox (M)	54	28.1	63
174- 183	R.YVYY YSYLL K.N	481.335 8	Y4, Chloro (Y), Y5, Ox (Y), Y6, Ox (Y)	17	0.08	63
224- 234	K.IYSS NSGPT RR.E	418.634 8	Y2, Ox (Y)	6	35.4	63
235- 254	R.EDKF MYFEF PQPLP VCDIK. V	826.287 9	M5, Ox (M)	26	34.04	63
270- 289	K.MFH FWVNT FFIPGP EETSE K.V	820.610 5	M1, Ox (M)	31	35.4	63

Appendix 9. Oxidative modifications observed in tryptic peptides of PTEN by MS/MS with collisionally-induced decomposition after validity sequencing of b and y series ions from 1:30 and 1:300 molar ratio HOCl oxidation and incubation at room temperature for 1 hour

Mascot search for Chloro (Y), Dichloro (Y), Ox (Y), Ox (M), Ox (H) Ox (W). The letter designation followed by a number denotes the one letter amino acid code and the sequence of the predicted modified residue within the peptide fragment. Ox = oxidation, Chloro = chlorination.

Non-treated negative control VHR, 1hr at 37⁰C						
Peptide	Peptide sequence	Observed ion (m/z)	Modification	Ion score	Retention Time (mins)	Sequence coverage (%)
37-50	R.IYVGNA SVAQDIP K.L	746.0486	Ox(Y) Y2	25	30.65 to 31.34	74
37-50	R.IYVGNA SVAQDIP K.L	746.0486	Ox(P) P13	33	30.65	68
37-50	R.IYVGNA SVAQDIP K.L	753.5638	DiOx(Y) Y 2	20	30.78 to 31.47	68
67-79	R.SFMHV NTNANFY K.D	530.3302	Ox(M) M3	20	27.88 to 28.58	67-79
67-79	R.SFMHV NTNANFY K.D	794.8926	Oxidation (M3)	55	21.44	61
67-79	R.SFMHV NTNANFY K.D	794.8926	Ox H (H4)	46	21.4	59
67-79	R.SFMHV NTNANFY K.D	530.3302	Ox(H) H4	19	27.88 to 28.58	68
67-79	R.SFMHV NTNANFY K.D	803.037	DiOx(M) M3	37	27.16 to 28.14	68
67-79	R.SFMHV NTNANFY K.D	811.0351	DiOx(M) M3, Ox(H) H4	36	33.68	68
67-89	R.SFMHV NTNANFY KDSGItYL GIK.A	879.6446	Ox(H) H4	79	33.39	68
67-89	R.SFMHV NTNANFY KDSGItYL GIK.A	879.6446	Ox(M) M3	84	33.39	74
90-104	K.ANDTQ EFNLSAY FER.A	617.3846	Nitro(Y) Y12	37	43.27	74
90-104	K.ANDTQ EFNLSAY FER.A	925.63	Nitro(Y) Y12	70	42.39 to 44.03	74
120-125	R.VLVHCR .E	379.732	DiOx (C) C5	22	19.88 to 21.53	74
126-142	R.EGYSR SPTLVIA LMMR.Q	668.4649	Ox(M) M15	36	40.55	74
131-142	R.SPTLVIA YLMMR.Q	470.9315	Oxidation (M11)	50	35.95	61

131-142	R.SPTLVIA YLMMR.Q	470.9796	Ox (M) M10	72	42.22	74
131-142	R.SPTLVIA YLMMR.Q	476.2651	Oxidation (M10, M11)	55	32.28	61
131-142	R.SPTLVIA YLMMR.Q	713.9027	Oxidation (M10, M11)	68	32.19	61
131-142	R.SPTLVIA YLMMR.Q	476.2651	Dioxidation (M11)	47	32.41	61
131-142	R.SPTLVIA YLMMR.Q	713.9027	Dioxidation (M11)	43	32.19	59
131-142	R.SPTLVI AYLMMR. Q	476.3109	2 Ox (M) M10, M11	34	38.44 to 39.11	74
131-142	R.SPTLVI AYLMMR. Q	476.3109	DiOx(M) M11	32	38.44 to 39.11	68
131-142	R.SPTLVI AYLMMRQ K.M	561.8775	DiOx(M) M11	21	51.05 to 51.76	68
159-176	R.EIGPND GFLAQLC QLNDR.L	679.1241	DiOx (C) C13	8	43.78	74
159-176	R.EIGPND GFLAQLC QLNDR.L	1018.2431	DiOx (C) C13	36	41.54 to 44.51	74
10:1 Sin-1:VHR, 1hr at 37°C treated VHR						
Peptide	Peptide sequence	Observed ion (m/z)	Modification	Ion score	Retention Time (mins)	Sequence coverage (%)
37-50	R.IYVGNA SVAQDIP K.L	745.9217	OxY (Y2)	43	26.03	65
37-50	R.IYVGNA SVAQDIP K.L	497.8427	Nitro(Y) Y2	10	31.94	67
37-50	R.IYVGNA SVAQDIP K.L	745.9217	Ox (P) P13	48	25.15	59
54-66	K.LGITHV LNAEGR. S	683.8897	Ox(H) H5	89	29.71	59
54-66	K.LGITHV LNAEGR. S	456.2868	Ox(H) H5	28	28.69	65
67-79	R.SFMHV NTNANFY K.D	530.289	Ox (M) M3	78	24.67 to 26.8	67
67-79	R.SFMHV NTNANFY K.D	794.9396	Ox (M) M3	88	25.09 to 26.13	67
67-79	R.SFMHV NTNANFY K.D	535.313	Ox (M) M3, Ox(Y) Y12	10	23.84	67
67-79	R.SFMHV NTNANFY K.D	530.289	Ox(H) H4	71	24.67 to 26.80	65
67-79	R.SFMHV NTNANFY K.D	794.9396	Ox(H) H4	58	25.09 to 26.13	65

67-79	R.SFMHV NTNANFY K.D	535.313	DiOx(M) M3	7	23.84	65
67-79	R.SFMHV NTNANFY K.D	802.938	DiOx(M) M3	57	33.34	65
80-89	K.DSGITY LGIK.A	541.3064	Ox (Y) Y6	44	29.68 to 30.50	67
90-104	K.ANDTQ EFNLSAY FER.A	911.0036	Ox(Y) Y12	26	38.09	67
105-116	R.AADFID QALAGK. N	653.8918	OX(K) K12	39	29.72	65
131-142	R.SPTLVI AYLMMR. Q	470.9605	Ox (M) M11	55	42.14 to 42.48	67
131-142	R.SPTLVI AYLMMR. Q	705.9457	Ox (M) M10	75	40.29 to 40.99	67
131-142	R.SPTLVI AYLMMR. Q	470.9664	Ox (M) M10	71	40.41 to 40.74	67
131-142	R.SPTLVI AYLMMR. Q	705.9479	Ox (M) M11	88	42.06 to 43.44	67
131-142	R.SPTLVI AYLMMR. Q	476.2901	2 Ox (M) M10, M11	41	38.05	67
131-142	R.SPTLVI AYLMMR. Q	713.945	2 Ox (M) M10, M11	63	38.43 to 38.72	67
131-142	R.SPTLVI AYLMMR. Q	476.2901	DiOx(M) M11	29	38.05	65
159-176	R.EIGPND GFLAQLC QLNDR.L	679.0529	DiOx (C) C13	24	42.64 to 43.44	67
159-176	R.EIGPND GFLAQLC QLNDR.L	1018.0963	DiOx (C) C13	50	42.68 to 43.69	67
159-176	R.EIGPND GFLAQLC QLNDR.L	1026.0189	TriOx(C) (C13)	81	37.1	65
75:1 Sin-1:VHR, 1hr at 37°C treated VHR						
Peptide	Peptide sequence	Observed ion (m/z)	Modification	Ion score	Retention Time (mins)	Sequence coverage (%)
37-50	R.IYVGNA SVAQDIP K.L	746.0488	Ox(Y) Y2	58	28.52 to 31.38	75
37-50	R.IYVGNA SVAQDIP K.L	497.8705	Ox(Y) Y2	12	30.75	75
37-50	R.IYVGNA SVAQDIP K.L	754.0565	Ox(P) P13, Ox(K) K14	55	30.87	68
37-50	R.IYVGNA SVAQDIP	745.9633	Ox(P) P13	42	29.26 to 30.77	63

	K.L					
51-66	K.LQKLGIT THVLNAA EGR.S	579.4155	Ox(K) K3	23	29.46	68
54-66	K.LGITHV LNAAEGR. S	456.2855	Ox(H) H5	23	29.3	63
54-66	K.LGITHV LNAAEGR. S	684.013	Ox(H) H5	34	27.68 to 29.38	68
67-79	R.SFMHV NTNANFY K.D	794.5534	Ox (M) M3	31	32.75 to 33.73	75
67-79	R.SFMHV NTNANFY K.D	530.328	Ox (M) M3	66	26.73 to 28.81	75
67-79	R.SFMHV NTNANFY K.D	794.5534	Ox(H) H4	40	32.75 to 33.73	68
67-79	R.SFMHV NTNANFY K.D	530.3284	Ox(H) H4	56	26.73 to 28.81	68
67-79	R.SFMHV NTNANFY K.D	795.038	DiOx(M) M3	46	27.55	68
67-79	R.SFMHV NTNANFY K.D	535.3365	DiOx(M) M3	53	27.59 to 29.46	68
67-79	R.SFMHV NTNANFY K.D	810.5724	DiOx(M) M3, Ox(H) H4	31	29.38	68
67-89	R.SFMHV NTNANFY KDSGItYL GIK.A	879.6483	Ox (M) M3	100	33.77	75
67-89	R.SFMHV NTNANFY KDSGItYL GIK.A	889.3165	Nitro(Y) Y12	21	39.06	75
67-89	R.SFMHV NTNANFY KDSGItYL GIK.A	879.6483	Ox(H) H4	93	33.77	68
80-89	K.DSGITY LGIK.A	541.8832	Ox (Y) Y6	52	28.47	75
80-89	K.DSGITY LGIK.A	541.8832	Ox (K) K10	24	28.47	68
80-89	K.DSGITY LGIK.A	555.833	Nitro (Y) Y6	33	34.51 to 38	67
105-116	R.AADFID QALAGK. N	653.8914	Ox(K) K12	48	34.26	63
90-104	K.ANDTQ EFNLSAY FER.A	607.2947	Ox(Y) Y12	9	35.76	67
90-104	K.ANDTQ EFNLSAY FER.A	911.0033	Ox(Y) Y12	105	34.13	67
90-104	K.ANDTQ	617.3297	Nitro(Y) Y12	59	42.14 to 42.27	67

	EFNLSAY FER.A					
90-104	K.ANDTQ EFNLSAY FER.A	925.5024	Nitro(Y) Y12	114	42.1	67
105-116	R.AADFID QALAQK. N	653.8914	Ox(K) K12	48	34.26	63
120-125	R.VLVHCR .E	379.7307	DiOx (C) C5	16	20.87 to 21.59	75
126-142	R.EGYSR SPTLVIA LMMR.Q	673.8308	2 Ox(M) M15, M16	9	41.75	75
131-142	R.SPTLVIA YLMMR.Q	470.9797	Ox (M) M10	63	42.58	72
131-142	R.SPTLVIA YLMMR.Q	470.9831	Ox (M) M11	75	44.41 to 45.17	72
131-142	R.SPTLVIA YLMMR.Q	760.019	Ox (M) M11	56	43.45 to 48.88	72
131-142	R.SPTLVIA YLMMR.Q	760.0218	Ox (M) M10	63	41.38 to 42.75	72
131-142	R.SPTLVIA YLMMR.Q	476.3145	2 Ox (M) M10, M11	57	40.2	72
131-142	R.SPTLVIA YLMMR.Q	714.0106	Ox (M) M10, Ox(Y) Y8	22	43.9	72
131-142	R.SPTLVIA YLMMR.Q	714.0234	2 Ox (M) M10, M11	63	40.45 to 41.8	72
131-142	R.SPTLVIA YLMMR.Q	721.5072	2 Ox (M) M10, M11, Ox(Y) Y8	19	35.43	72
131-142	R.SPTLVIA YLMMR.Q	476.3145	DiOx(M) M11	39	40.2	72
131-142	R.SPTLVIA YLMMR.Q	714.0106	DiOx(Y) Y8	9	43.9	72
159-176	R.EIGPND GFLAQLC QLNDR.L	1018.2469	DiOx (C) C13	39	42.34 to 44.39	75
159-176	R.EIGPND GFLAQLC QLNDR.L	1026.2541	TriOx (C) C13	52	41.84 to 42.72	75
159-176	R.EIGPND GFLAQLC QLNDR.L	783.2153	TriOx (C) C13	17	35.87	75
159-176	R.EIGPND GFLAQLC QLNDR.L	1038.7724	Ox(P) P4	47	38.97	68
150:1 Sin-1:VHR, 1hr at 37°C treated VHR						
Peptide	Peptide sequence	Observed ion (m/z)	Modification	Ion score	Retention Time (mins)	Sequence coverage (%)
37-50	R.IYVGNA SVAQDIP K.L	745.9069	HydroxyY (Y2)	70	25.76	61
37-50	R.IYVGNA SVAQDIP K.L	497.8123	HydroxyY (Y2)	20	24.98	61
37-50	R.IYVGNA SVAQDIP K.L	507.2714	NitroY (Y2)	63	27.57	61

37-50	R.IYVGNA SVAQDIP K.L	760.4047	NitroY (Y2)	20	27.53	61
37-50	R.IYVGNA SVAQDIP K.L	745.966	Ox(P) P13	48	29.15 to 31.91	64
37-50	R.IYVGNA SVAQDIP K.L	502.7737	DiOx(Y)	10	30.07 to 30.74	64
54-66	K.LGITHV LNAAEGR. S	684.007	Ox(H) H5	74	36.22 to 37.02	67
67-79	R.SFMHV NTNANFY K.D	794.8835	Oxidation (M3)	46	21.61	61
67-79	R.SFMHV NTNANFY K.D	794.8835	Ox (H) H4	40	21.57	57
67-79	R.SFMHV NTNANFY K.D	803.0463	Ox (M) M3, Ox(Y) Y12	16	25.94	68
67-79	R.SFMHV NTNANFY K.D	817.5461	Ox (M) M3, Nitro(Y) Y12	81	30.44	68
67-79	R.SFMHV NTNANFY K.D	802.5747	DiOx(M) M3	19	27.55 to 28.22	67
67-79	R.SFMHV NTNANFY K.D	535.6619	DiOx(M) M3	17	26.66 to 28.18	67
80-89	K.DSGITY LGIK.A	541.7987	HydroxyY (Y6)	56	26.43	61
80-89	K.DSGITY LGIK.A	556.295	NitroY (Y6)	69	31.77	61
80-89	K.DSGITY LGIK.A	541.7987	Ox(K) K 10	27	26.43	57
105-116	R.AARIDQ LAQK.N	653.4587	Ox(K) K12	13	34.58 to 36.68	67
90-104	K.ANDTQ EFNLSAY FER.A	911.0023	Ox(Y) Y12	86	33.77	64
90-104	K.ANDTQ EFNLSAY FER.A	608.0025	Ox(Y) Y12	46	39.05	64
90-104	K.ANDTQ EFNLSAY FER.A	617.3273	Nitro(Y) Y12	67	41.9 to 41.98	64
90-104	K.ANDTQ EFNLSAY FER.A	925.5	Nitro(Y) Y12	82	41.85	64
105-116	R.AADFID QALAQK.k	653.8991	Ox (K) K12	28	29.65	64
105-119	R.AADFID QALAQKN GR.V	817.5784	Ox(K) K12	74	36.51	67
131-142	R.SPTLVIA YLMMR.Q	470.9269	HydroxyY (Y8)	20	36.33	61
131-142	R.SPTLVIA YLMMR.Q	705.8895	HydroxyY (Y8)	28	36.03	61

131-142	R.SPTLVIA YLMMR.Q	470.9269	Oxidation (M11)	68	36.33	61
131-142	R.SPTLVIA YLMMR.Q	705.8895	Oxidation (M11)	70	36.03	61
131-142	R.SPTLVIA YLMMR.Q	476.2597	2 Oxidations (M10, M11)	39	32.23	61
131-142	R.SPTLVIA YLMMR.Q	713.8904	2 Oxidations (M10, M11)	59	32.44	61
131-142	R.SPTLVIA YLMMR.Q	470.9281	Oxidation (M10)	23	34.51	61
131-142	R.SPTLVIA YLMMR.Q	705.8895	Oxidation (M10)	38	34.42	61
131-142	R.SPTLVIA YLMMR.Q	476.2597	DiOx(M) M11	36	32.23	57
131-142	R.SPTLVIA YLMMR.Q	713.8893	DiOx(M) M11	44	32.44	57
131-142	R.SPTLVIA YLMMR.Q	714.0191	Ox (M) M10, Ox(Y) Y8	27	37.66	68
131-142	R.SPTLVIA YLMMR.Q	714.0201	Ox (M) M10, Ox(Y) Y8	30	40.21 to 41.57	68
131-142	R.SPTLVIA YLMMR.Q	728.5211	Ox (M) M11, Nitro(Y) Y8	20	45.23 to 45.90	68
131-142	R.SPTLVIA YLMMR.Q	491.3152	2 Ox (M) M10, M11, Nitro (Y) Y8	21	42.41	68
131-142	R.SPTLVIA YLMMR.Q	722.4588	Ox(Y), Y8, 2 Ox (M) M10, M11	20	38.24	64
159-176	R.EIGPND GFLAQLC QLNDR.L	684.3761	TriOx (C) C13	13	42.68	64
159-176	R.EIGPND GFLAQLC QLNDR.L	1026.0884	TriOx (C) C13	71	41.73	64
300:1 Sin-1:VHR, 1hr at 37°C treated VHR						
Peptide	Peptide sequence	Observed ion (m/z)	Modification	Ion score	Retention Time (mins)	Sequence coverage (%)
37-50	R.IYVGNA SVAQDIP K.L	745.9035	HydroxyY (Y2)	80	26.17	61
497.3117	Ox(Y) Y2	18	30.34	68	497.3117	Ox(Y) Y2
37-50	R.IYVGNA SVAQDIP K.L	745.9035	Ox(P) P13	20	26.17	57
37-50	R.IYVGNA SVAQDIP K.L	761.7457	Ox(P) P13, DiOx (Y2)	17	31.6	57
37-50	R.IYVGNA SVAQDIP K.L	507.2703	NitroY (Y2)	71	27.7	61
37-50	R.IYVGNA SVAQDIP K.L	760.4011	NitroY (Y2)	100	27.58	61
54-66	K.LGITHV LNAAEGR. S	456.286	Ox(H) H5	28	25.54	67
54-66	K.LGITHV	683.9368	Ox(H) H5	94	35.44	67

	LNAEGR. S					
67-79	R.SFMHV NTNANFY K.D	794.9394	Ox (M) M3	88	26.05 to 28.52	68
67-79	R.SFMHV NTNANFY K.D	530.6166	Ox (M) M3	64	25.75 to 30.96	68
67-79	R.SFMHV NTNANFY K.D	817.4315	Nitro(Y), Y12, Ox (M) M3	61	29.23	68
67-79	R.SFMHV NTNANFY K.D	794.9394	Ox(H) H4	57	26.05 to 28.52	67
67-79	R.SFMHV NTNANFY K.D	535.6244	DiOx(M)M3	40	27.08	67
67-79	R.SFMHV NTNANFY K.D	802.9344	DiOx(M)M3	45	27.13 to 27.21	67
67-89	R.SFMHV NTNANFY KDSGItYL GIK.A	879.5208	Ox (M) M3	80	33.41	68
67-89	R.SFMHV NTNANFY KDSGItYL GIK.A	888.5208	Nitro(Y), Y12	36	37.01	68
67-89	R.SFMHV NTNANFY KDSGItYL GIK.A	879.5208	Ox(H) H4	72	33.41	67
80-89	K.DSGITY LGIK.A	541.7947	Ox(K) K10	21	26.38	57
80-89	K.DSGITY LGIK.A	541.834	Ox (Y) Y6	45	32.03	68
80-89	K.DSGITY LGIK.A	556.3305	Nitro (Y) Y6	41	35.65 to 38.52	68
90-104	K.ANDTQ EFNLSAY FER.A	911.0033	Ox(Y) Y12	88	35.56	68
90-104	K.ANDTQ EFNLSAY FER.A	617.3277	Nitro(Y) Y12	76	42.22 to 42.51	68
90-104	K.ANDTQ EFNLSAY FER.A	925.5013	Nitro(Y) Y12	91	42.18 to 43.13	68
105-116	R.AADFID QALAQK. N	653.8947	Ox(K) K12	6	35.1 to 35.77	67
131-142	R.SPTLVIA YLMMR.Q	470.9577	Ox (M) M11	65	43.38 to 44.49	68
131-142	R.SPTLVIA YLMMR.Q	470.9613	Ox (M) M10	72	40.98 to 44.06	68
131-142	R.SPTLVIA YLMMR.Q	750.9458	Ox (M) M11	73	40.86 to 45.2	68
131-142	R.SPTLVIA YLMMR.Q	476.2904	2 Ox (M) M10, M11	56	38.43 to 39.48	68
131-142	R.SPTLVIA	713.9408	2 Ox (M) M10,	56	42.39	68

	YLMMR.Q		M11			
131-142	R.SPTLVIA YLMMR.Q	721.9343	Ox(Y), Y8, 2 Ox (M) M10, M11	25	39.73	68
131-142	R.SPTLVIA YLMMR.Q	728.4381	Nitro(Y), Y8, Ox (M) M11	57	44.23	68
131-142	R.SPTLVIA YLMMR.Q	491.2885	Nitro(Y), Y8, 2 Ox (M) M10, M11	40	41.35 to 41.43	68
131-142	R.SPTLVIA YLMMR.Q	736.4376	Nitro(Y), Y8, 2 Ox (M) M10, M11	20	41.19	68
131-142	R.SPTLVIA YLMMR.Q	476.2904	DiOx(M) M11	42	38.43 to 39.48	67
131-142	R.SPTLVIA YLMMR.Q	713.94	DiOx(M) M11	57	42.39	67
145-155	K.MDVKS ALSIVR.Q	618.3947	Ox(M) M1	29	33.94	68
159-176	R.EIGPND GFLAQLC QLNDR.L	679.0528	DiOx (C) C13	16	43.22 to 43.34	68
159-176	R.EIGPND GFLAQLC QLNDR.L	1026.0914	TriOx (C) C13	51	42.1 to 43.01	68

Appendices 10. Oxidative modifications observed in tryptic peptides of VHR by MS/MS with collisionally-induced decomposition after validity sequencing of b and y series ions from 10:1, 75:1, 150:1 and 300:1 molar ratio sin-1 oxidation and incubation at 37°C for 1 hour

Mascot search for Ox (Y), Ox (M), Ox (H) Ox (W), Nitro (Y), DiOx (C), TriOx (C), Ox (K), Ox (P). The letter designation followed by a number denotes the one letter amino acid code and the sequence of the predicted modified residue within the peptide fragment. Ox = oxidation, Nitro = nitration, Diox = Dioxidation, Triox = Trioxidation.

30:1 HOCl:VHR, 1hr at RT treated VHR						
Peptide	Peptide sequence	Observed ion (m/z)	Modification	Ion score	Retention Time (mins)	Sequence coverage (%)
37-50	R.IYVGN ASVAQDI PK.L	503.5933	ChloroY (Y2)	47	27.26	62
37-50	R.IYVGN ASVAQDI PK.L	745.4635	Ox(Y) Y2	82	30.1 to 31.48	70
37-50	R.IYVGN ASVAQDI PK.L	755.3817	ChloroY (Y2)	59	29.47	62
67-79	R.SFMHV NTNANF YK.D	794.8718	Oxidation (M3)	68	21.69	67
67-79	R.SFMHV NTNANF YK.D	802.874	Oxidation (M3)	56	22.04	67

67-79	R.SFMHV NTNANF YK.D	812.4242	Ox (M) M3, Chloro(Y) Y12	21	29.06	70
80-89	K.DSGIT YLGIK.A	541.8361	Ox (Y) Y6	16	33.73	70
80-89	K.DSGIT YLGIK.A	550.8214	Chloro (Y) Y6	12	36.39	70
90-104	K.ANDTQ EFNLSAY FER.A	613.6055	ChloroY (Y12)	48	35.52	62
90-104	K.ANDTQ EFNLSAY FER.A	608.0064	Ox(Y) Y12	51	39.62	70
90-104	K.ANDTQ EFNLSAY FER.A	919.9903	Chloro(Y) Y12	28	41.51	70
120-130	R.VLVHC REGYSR. S	467.5794	TriOx (C) C5, Chloro(Y) Y9	14	22.48	120-130
131-142	R.SPTLVI AYLMMR. Q	705.8883	Oxidation (M11)	70	34.7	67
131-142	R.SPTLVI AYLMMR. Q	705.8883	Oxidation (M10)	75	34.74	67
131-142	R.SPTLVI AYLMMR. Q	470.9262	Oxidation (M11)	70	36.32	67
131-142	R.SPTLVI AYLMMR. Q	470.9252	Oxidation (M10)	23	34.6	67
131-142	R.SPTLVI AYLMMR. Q	3	Oxidation (M10, M11)	476.255 6	33.08	67
131-142	R.SPTLVI AYLMMR. Q	2	Oxidation (M10 or M11)	713.883	32.1	67
131-142	R.SPTLVI AYLMMR. Q	3	Oxidation (M10, M11)	713.886 2	33.45	67
131-142	R.SPTLVI AYLMMR. Q	3	Oxidation and Dioxidation (M10 oxidation, M11 Dioxidation)	481.587 3	33.41	67
131-142	R.SPTLVI AYLMMR. Q	3	Oxidation and Dioxidation (M10 or M11 yet not identified)	721.882 9	33.16	67

			which residue dioxidised)			
159-176	R.EIGPN DGFLAQ LCQLND R.L	679.0555	DiOx (C) C13	27	43.07	70
159-176	R.EIGPN DGFLAQ LCQLND R.L	1017.997	DioxC (C13)	26	37.69	62
159-176	R.EIGPN DGFLAQ LCQLND R.L	684.3314	TriOxC (C13)	69	34.4	62
159-176	R.EIGPN DGFLAQ LCQLND R.L	1025.996 9	TriOxC (C13)	95	95	62
150:1 HOCl:VHR, 1hr at RT treated VHR						
Peptide	Peptide sequence	Observed ion (m/z)	Modification	Ion score	Retention Time (mins)	Sequence coverage (%)
37-50	R.IYVGN ASVAQDI PK.L	754.8874	ChloroY (Y2)	105	27.25	52
67-79	R.SFMHV NTNANF YK.D	794.8718	Oxidation (M3)	59	21.28	59
67-79	R.SFMHV NTNANF YK.D	535.5827	Dioxidation (M3)	48	21.96	59
131-142	R.SPTLVI AYLMMR. Q	470.9237	Oxidation (M11)	56	35.96	59
131-142	R.SPTLVI AYLMMR. Q	705.885	Oxidation (M10)	76	34.36	59
131-142	R.SPTLVI AYLMMR. Q	476.2517	Oxidation (M10, M11)	49	32.55	59
131-142	R.SPTLVI AYLMMR. Q	713.884	Oxidation (M10, M11)	57	32.03	59
131-142	R.SPTLVI AYLMMR. Q	476.2591	Dioxidation (M11)	44	32.46	59
159-176	R.EIGPN DGFLAQ LCQLND R.L	684.3306	TriOxC (C13)	66	36.66	52
300:1 HOCl:VHR, 1hr at RT treated VHR						
Peptide	Peptide sequence	Observed ion (m/z)	Modification	Ion score	Retention Time (mins)	Sequence coverage (%)
67-79	R.SFMHV	530.2463	Oxidation	62	21.14	57

	NTNANF YK.D		(M3)			
67-79	R.SFMHV NTNANF YK.D	795.4354	Ox (M) M3	31	27.33 to 27.49	63
131-142	R.SPTLVI AYLMMR. Q	470.9563	Ox (M) M10	75	41.27 to 41.57	63
131-142	R.SPTLVI AYLMMR. Q	705.9454	Ox (M) M11	78	41.23	63
131-142	R.SPTLVI AYLMMR. Q	476.2535	2 Oxidation (M10, M11)	46	32.31	57
131-142	R.SPTLVI AYLMMR. Q	713.8787	2 Oxidation (M10, M11)	53	32.46	57

Appendices 11. Oxidative modifications observed in tryptic peptides of VHR by MS/MS with collisionally-induced decomposition after validating sequencing of b and y series ions from 30:1, 150:1 and 300:1 molar ratio HOCl oxidation and incubation at room temperature for 1 hour

Mascot search for Chloro (Y), Ox (Y), Ox (M), DiOx (M) Ox (H) Ox (W). The letter designation followed by a number denotes the one letter amino acid code and the sequence of the predicted modified residue within the peptide fragment. Ox = oxidation, Chloro = chlorination, Diox = Dioxidation, Triox = Trioxidation.

10:1 Tetranitromethane:VHR, 1hr at 37⁰C treated VHR						
Peptide	Peptide sequence	Observed ion (m/z)	Modification	Ion score	Retention Time (mins)	Sequence coverage (%)
37-50	R.IYVGNA SVAQDIP K.L	497.3394	Ox(Y) Y2	35	31.32 to 32.74	76
37-50	R.IYVGNA SVAQDIP K.L	745.5139	Ox(Y) Y2	36	34.05 to 34.78	76
37-50	R.IYVGNA SVAQDIP K.L	497.3394	Ox (K) K14	15	31.32 to 32.74	71
37-53	R.IYVGNA SVAQDIP KLQK.L	944.7171	Nitro(Y) Y2	14	34.65 to 38.43	76
37-53	R.IYVGNA SVAQDIP KLQK.L	930.1933	Ox (K) K14	26	36.6	71
54-66	K.LGITHV LNAAEGR. S	683.487	Ox (H) H5	22	30.59	71
54-66	K.LGITHV LNAAEGR. S	456.3033	Ox (H) H5	32	28.69	71
67-79	R.SFMHV NTNANFY K.D	795.0195	Ox(M) M3	82	27.25 to 29.42	76
67-79	R.SFMHV	795.0195	Ox (H) H4	52	27.25 to	71

	NTNANFY K.D				29.42	
67-79	R.SFMHV NTNANFY K.D	535.3181	DiOx (M) M3	54	28.53	71
67-79	R.SFMHV NTNANFY K.D	803.0222	DiOx (M) M3	61	28.57	71
67-89	R.SFMHV NTNANFY KDSGiTYL GIK.A	879.6212	Ox(M) M3	101	34.9 to 36.97	76
67-89	R.SFMHV NTNANFY KDSGiTYL GIK.A	879.6212	Ox (H) H4	81	34.9 to 36.97	71
80-89	K.DSGITY LGIK.A	542.1587	Nitro(Y) Y6	19	34.57	76
90-104	K.ANDTQ EFNLSAY FER.A	617.3711	Nitro(Y) Y12	44	43.81	76
90-104	K.ANDTQ EFNLSAY FER.A	925.6143	Nitro(Y) Y12	78	43.6	76
105-119	R.AADFID QALAQKN GR.V	545.2466	Ox (K) K12	5	32.91	71
120-125	R.VLVHCR .E	379.7315	DiOx© C5	20	17.81	76
120-125	R.VLVHCR EGGYSR. SE	699 (mod + 70.9663)	Phospho (C) C5	48	24.31	76
126-142	R.EGYSR SPTLVIA LMMR.Q	668.466	Ox(M) M16	11	40.56	76
131-142	R.SPTLVIA YLMMR.Q	705.5268	Ox (M) M10	53	45.92 to 49.99	76
131-142	R.SPTLVIA YLMMR.Q	470.9776	Ox (M) M10	68	43.14	76
131-142	R.SPTLVIA YLMMR.Q	470.9803	Ox (M) M11	66	44.44 to 46.46	76
131-142	R.SPTLVIA YLMMR.Q	706.0075	Ox (M) M11	80	41.1 to 45.24	76
131-142	R.SPTLVIA YLMMR.Q	714.0071	2 Ox (M) M10, M11	45	40.75 to 41.43	76
131-142	R.SPTLVIA YLMMR.Q	721.5211	2 Ox (M) M10, M11, Ox(Y) Y8	8	41.35 to 42.02	76
131-142	R.SPTLVIA YLMMR.Q	705.5268	Ox (P) P2	6	45.92 to 49.99	71
131-142	R.SPTLVIA YLMMR.Q	470.9802	Ox (P) P2	36	47.86	71
131-142	R.SPTLVIA YLMMR.Q	714.0071	DiOx (M) M11	34	40.75 to 41.43	71
156-176	R.QNREIG PNDGFLA WLCQLND R.L	1216.866 5	DiOx (C)C16	11	41.8	76

156-176	R.QNREIG PNDGFLA WLCQLND R.L	811.8874	DiOx (C) C16	29	40.22 to 42.47	76
156-176	R.QNREIG PNDGFLA WLCQLND R.L	1224.855 3	TriOx (C) C16	48	39.30 to 40.01	76
156-176	R.QNREIG PNDGFLA WLCQLND R.L	817.2292	TriOx (C) C16	76	38.97 to 39.67	76
159-176	R.EIGPND GFLAQLC QLNDR.L	679.1109	DiOx (C) C13	16	44.19 to 45.54	76
159-176	R.EIGPND GFLAQLC QLNDR.L	1018.214 9	DiOx (C) C13	35	43.77 to 45.79	76
159-179	R.EIGPND GFLAQLC QLNDR.L K.E	1174.363 4	DiOx (C) C13	9	43.81	76
159-179	R.EIGPND GFLAQLC QLNDR.L K.E	788.5582	TriOx (C) C13	12	42.85	76
75:1 Tetronitromethane:VHR, 1hr at 37°C treated VHR						
Peptide	Peptide sequence	Observe d ion (m/z)	Modification	Ion score	Retention Time (mins)	Sequence coverage (%)
37-50	R.IYVGNA SVAQDIP K.L	745.503	Ox(Y) Y2	22	29.34	37-50
37-50	R.IYVGNA SVAQDIP K.L	497.6695	Ox(Y) Y2	33	30.79 to 32.13	37-50
37-50	R.IYVGNA SVAQDIP K.L	760.5409	Nitro(Y) Y2	66	31.5	37-50
37-50	R.IYVGNA SVAQDIP K.L	507.661	Nitro(Y) Y2	39	33.65 to 34.52	37-50
37-53	R.IYVGNA SVAQDIP KLQK.L	630.4659	Nitro(Y) Y2	15	34.15	37-53
37-53	R.IYVGNA SVAQDIP KLQK.L	930.2122	Ox (K) K14	16	35.62 to 36.33	37-53
54-66	K.LGITHV LNAAEGR. S	456.3028	Ox (H) H5	38	27.95 to 28.67	54-66
54-66	K.LGITHV LNAAEGR. S	684.0011	Ox (H) H5	19	28.71	54-66
67-79	R.SFMHV NTNANFY K.D	530.3206	Ox(M) M3	24	30.22	67-79
67-79	R.SFMHV NTNANFY	795.0254	Ox(M) M3	75	26.5 o 28.63	67-79

	K.D					
67-79	R.SFMHV NTNANFY K.D	535.3966	Ox(M) M3 Ox(Y) Y12	14	26.46	67-79
67-79	R.SFMHV NTNANFY K.D	530.3206	Ox (H) H4	22	26.5 to 28.63	67-79
67-79	R.SFMHV NTNANFY K.D	795.0254	Ox (H) H4	49	26.50 to 28.63	67-79
67-79	R.SFMHV NTNANFY K.D	535.3418	DiOx (M) M3	28	27.62	67-79
67-79	R.SFMHV NTNANFY K.D	803.0302	DiOx (M) M3	47	31.5	67-79
67-79	R.SFMHV NTNANFY K.D	811.0243	DiOx (M) M3, Ox (H) H4	39	28.75	67-79
67-89	R.SFMHV NTNANFY KDSGiTYL GIK.A	879.6251	Ox(M) M3	83	33.98 to 36.2	67-89
67-89	R.SFMHV NTNANFY KDSGiTYL GIK.A	879.6251	Ox (H) H4	65	28.75	67-89
80-89	K.DSGITY LGIK.A	541.867	Ox(Y) Y6	22	31.87	80-89
80-89	K.DSGITY LGIK.A	556.3704	Nitro(Y) Y6	53	36.41 to 38.43	80-89
90-104	K.ANDTQ EFNLSAY FER.A	617.3766	Nitro(Y) Y12	59	42.89 to 44.31	90-104
90-104	K.ANDTQ EFNLSAY FER.A	925.6042	Nitro(Y) Y12	74	47.02	90-104
120-130	R.VLVHCR EGYSR.S	706.4477	TriOx© C5, Nitro(Y) Y5	57	23.37	120-130
131-142	R.SPTLVIA YLMMR.Q	470.9802	Ox (M) M11	31	46.64 to 47.48	131-142
131-142	R.SPTLVIA YLMMR.Q	470.9802	Ox (M) M10	72	41.71 to 42.39	131-142
131-142	R.SPTLVIA YLMMR.Q	706.0089	Ox (M) M11	64	41.79 to 50.6	131-142
131-142	R.SPTLVIA YLMMR.Q	706.0089	Ox (M) M10	61	59.59	131-142
131-142	R.SPTLVIA YLMMR.Q	476.3124	2 Ox (M) M10, M11	35	39.31 to 39.48	131-142
131-142	R.SPTLVIA YLMMR.Q	714.0082	Ox(Y) Y8, Ox(M) M11	22	44.02	131-142
131-142	R.SPTLVIA YLMMR.Q	714.0104	2 Ox (M) M10, M11	62	39.81 to 41.16	131-142
131-142	R.SPTLVIA YLMMR.Q	720.5111	Nitro(Y) Y8	58	48.83 to 49.52	131-142
131-142	R.SPTLVIA YLMMR.Q	728.5089	Nitro(Y) Y8, Ox(M) M11	40	45.5 to 46.19	131-142
131-142	R.SPTLVIA	470.9802	Ox (P) P2	56	46.64 to	131-142

	YLMMR.Q				47.48	
131-142	R.SPTLVIA YLMMR.Q	476.3124	Di(Ox) M11	23	39.31 to 39.48	131-142
131-142	R.SPTLVIA YLMMR.Q	714.0082	Di(Ox) M10	54	45.5	131-142
131-142	R.SPTLVIA YLMMR.Q	714.0104	Di(Ox) M11	46	39.81 to 41.16	131-142
156-176	R.QNREIG PNDGFLA WLCQLND R.L	1225.391	TriOx (C) C16	57	37.72	156-176
159-176	R.EIGPND GFLAQLC QLNDR.L	678.782	DiOx (C) C13	30	44.07	159-176
159-176	R.EIGPND GFLAQLC QLNDR.L	1018.223 8	DiOx (C) C13	40	42.85 to 44.19	159-176
159-176	R.EIGPND GFLAQLC QLNDR.L	1026.227 4	TriOx (C) C13	56	49.13 to 49.8	159-176
159-179	R.EIGPND GFLAQLC QLNDR.L K.E	788.2349	TriOx (C) C13	78	42.31 to 43.01	159-179
150:1 Tetronitromethane:VHR, 1hr at 37°C treated VHR						
Peptide	Peptide sequence	Observed ion (m/z)	Modification	Ion score	Retention Time (mins)	Sequence coverage (%)
37-50	R.IYVGNA SVAQDIP K.L	745.5458	Ox(Y) Y2	66	30.33	76
37-50	R.IYVGNA SVAQDIP K.L	760.5461	Nitro(Y) Y2	100	34.17 to 34.87	76
37-53	R.IYVGNA SVAQDIP KLQK.L	620.4367	Ox(Y) Y2	8	33.47	76
37-53	R.IYVGNA SVAQDIP KLQK.L	620.4367	Ox (P) P13	41	33.47	68
37-53	R.IYVGNA SVAQDIP KLQK.L	620.447	Ox (K) K14	23	36.37 to 37.07	68
37-53	R.IYVGNA SVAQDIP KLQK.L	930.7104	Ox (P) P13	23	36.2 to 37.03	68
54-66	K.LGITHV LNAAEGR. S	456.3046	Ox (H) H5	43	29.71	68
54-66	K.LGITHV LNAAEGR. S	684.0027	Ox (H) H5	27	29.75	68
67-79	R.SFMHV NTNANFY K.D	530.3252	Ox(M) M3	36	29.22	76
67-79	R.SFMHV NTNANFY K.D	795.0267	Ox(M) M3	55	27.25 to 28.6	76

67-79	R.SFMHV NTNANFY K.D	530.3252	Ox (H) H4	35	29.22	68
67-79	R.SFMHV NTNANFY K.D	795.0267	Ox (H) H4	38	27.25 to 28.6	68
67-79	R.SFMHV NTNANFY K.D	535.6535	DiOx (M) M3	53	28.64	68
67-79	R.SFMHV NTNANFY K.D	803.0278	DiOx (M) M3	65	34.42 to 35.26	68
67-79	R.SFMHV NTNANFY K.D	811.0261	DiOx (M) M3, Ox (H) H4	48	35.13	68
67-89	R.SFMHV NTNANFY KDSGiTYL GIK.A	884.9601	Ox(M) M3 Ox(Y) Y12	8	39.45 to 40.13	76
67-89	R.SFMHV NTNANFY KDSGiTYL GIK.A	889.2998	Nitro(Y) Y12	105	38.91	76
67-89	R.SFMHV NTNANFY KDSGiTYL GIK.A	884.9601	DiOx (M) M3	31	39.45 to 40.13	68
67-79	R.SFMHV NTNANFY K.D	811.0328	Diox(M) M3 + Ox(F) F2	60	35.13	76
80-89	K.DSGITY LGIK.A	541.8686	Ox(Y) Y6	46	35.08	76
80-89	K.DSGITY LGIK.A	541.8686	Ox (K) K10	25	35.08	68
90-104	K.ANDTQ EFNLSAY FER.A	911.1135	Ox(Y) Y12	53	37.97	76
90-104	K.ANDTQ EFNLSAY FER.A	617.3798	Nitro(Y) Y12	68	43.34	76
90-104	K.ANDTQ EFNLSAY FER.A	925.6198	Nitro(Y) Y12	86	47.45	76
120-125	R.VLVHCR .E	387.7313	TriOx (C) C5	43	18.36	76
120-130	R.VLVHCR EGYSR.S	461.6081	TriOx (C) C5, Ox(Y) Y5	25	18.74 to 20.89	76
120-130	R.VLVHCR EGYSR.S	691.9548	TriOx (C) C5, Ox(Y) Y5	72	20.63	76
120-130	R.VLVHCR EGYSR.S	698.4565	DiOx(C) C5, Nitro(Y) Y5	21	23.82	76
120-130	R.VLVHCR EGYSR.S	471.2775	TriOx(C) C5,Nitro(Y) Y5	41	23.39 to 24.07	76
126-142	R.EGYSR SPtLVIAYL MMR.Q	1002.259 5	Ox(M) M16	8	41.95	76
131-142	R.SPTLVIA YLMMR.Q	470.9821	Ox (M) M10	75	42.17 to 42.84	76

131-142	R.SPTLVIA YLMMR.Q	470.9839	Ox (M) M11	49	44.26 to 46.31	76
131-142	R.SPTLVIA YLMMR.Q	706.0135	Ox (M) M10	78	41.61 to 48.49	76
131-142	R.SPTLVIA YLMMR.Q	706.0158	Ox (M) M11	58	40.3	76
131-142	R.SPTLVIA YLMMR.Q	476.3182	2 Ox (M) M10, M11	46	40.04	76
131-142	R.SPTLVIA YLMMR.Q	714.0152	2 Ox (M) M10, M11	58	40.3	76
131-142	R.SPTLVIA YLMMR.Q	720.5154	Nitro(Y) Y8	43	49 to 49.84	76
131-142	R.SPTLVIA YLMMR.Q	728.5173	Nitro(Y) Y8, Ox(M) M11	29	45.92 to 46.61	76
131-142	R.SPTLVIA YLMMR.Q	476.3182	DiOx(M) M11	33	40.04	68
131-142	R.SPTLVIA YLMMR.Q	714.0152	DiOx(M) M11	46	40.3	68
156-176	R.QNREIG PNDGFLA WLCQLND R.L	1216.888 6	DiOx (C) C16	20	41.44	76
156-176	R.QNREIG PNDGFLA WLCQLND R.L	811.8887	DiOx (C) C16	61	39.92	76
156-176	R.QNREIG PNDGFLA WLCQLND R.L	816.9085	TriOx (C) C16	35	41.44	76
156-176	R.QNREIG PNDGFLA WLCQLND R.L	1225.404 7	TriOx (C) C16	96	39.35 to 39.04	76
159-176	R.EIGPND GFLAQLC QLNDR.L	679.1176	DiOx (C) C13	23	49.21	76
159-176	R.EIGPND GFLAQLC QLNDR.L	1018.224	DiOx (C) C13	30	43.8 to 45.28	76
159-176	R.EIGPND GFLAQLC QLNDR.L	684.4545	TriOx (C) C13	71	47.28	76
159-176	R.EIGPND GFLAQLC QLNDR.L	1025.228 5	TriOx (C) C13	64	42.88 to 50.72	76
159-179	R.EIGPND GFLAQLC QLNDR.L K.E	1182.396 1	TriOx (C) C13	96	41.87 to 42.59	76
159-179	R.EIGPND GFLAQLC QLNDR.L K.E	788.7406	TriOx (C) C13	8	43.09 to 43.76	76
300:1 Tetronitromethane:VHR, 1hr at 37⁰C treated VHR						
Peptide	Peptide sequence	Observed ion (m/z)	Modification	Ion score	Retention Time (mins)	Sequence coverage (%)

37-50	R.IYVGNA SVAQDIP K.L	745.4805	Ox(Y) Y2	107	31.93 to 33.31	74
37-50	R.IYVGNA SVAQDIP K.L	497.339	Ox(Y) Y2	70	30.46 to 33.22	74
37-50	R.IYVGNA SVAQDIP K.L	507.3298	Nitro (Y) Y2	48	35.52	74
37-50	R.IYVGNA SVAQDIP K.L	760.549	Nitro (Y) Y2	24	38.75	74
37-53	R.IYVGNA SVAQDIP KLQK.L	930.7202	Ox (K) K14	9	37.31	67
54-66	K.LGITHV LNAAEGR. S	456.3141	Ox (H) H5	39	29.69	67
54-66	K.LGITHV LNAAEGR. S	684.005	Ox (H) H5	40	31.32	67
67-79	R.SFMHV NTNANFY K.D	794.5256	Ox(Y)12	50	30.63	74
67-79	R.SFMHV NTNANFY K.D	539.9919	Nitro (Y)12	13	35.81	74
67-79	R.SFMHV NTNANFY K.D	809.5334	Nitro (Y)12	64	33.35 to 35.4	74
67-79	R.SFMHV NTNANFY K.D	545.3334	Nitro (Y)12, Ox(M) M3	39	31.79	74
67-79	R.SFMHV NTNANFY K.D	817.5354	Nitro (Y)12, Ox(M) M3	80	31.24	74
67-79	R.SFMHV NTNANFY K.D	794.5256	Ox (K) K13	38	30.63	67
67-79	R.SFMHV NTNANFY K.D	803.0336	DiOx(M) M3	64	28.99	67
67-79	R.SFMHV NTNANFY K.D	811.0369	DiOx(M) M3 + Ox (H) H4	36	29.61 to 31.16	67
67-89	R.SFMHV NTNANFY KDSGiTYL GIK.A	879.6364	Nitro (Y)12	58	35.07 to 35.77	74
67-89	R.SFMHV NTNANFY KDSGiTYL GIK.A	889.1187	Nitro (Y)12	47	37.98 to 40.07	74
80-89	K.DSGITY LGIK.A	555.873	Nitro(Y) Y6	8	35.15 to 42.99	74
90-104	K.ANDTQ EFNLSAY FER.A	911.1316	Ox(Y) Y12	104	35.85	74
90-104	K.ANDTQ	617.3768	Nitro(Y) Y12	73	43.48	74

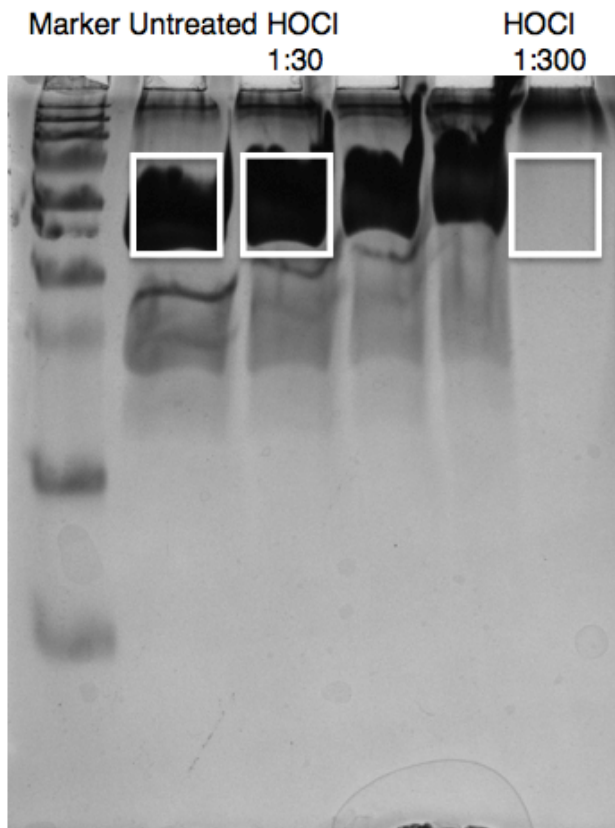
	EFNLSAY FER.A					
90-104	K.ANDTQ EFNLSAY FER.A	925.6223	Nitro(Y) Y12	49	45.52 to 47.59	74
120-125	R.VLVHCR .E	387.7308	TriOx(C) C5	33	18.67	74
120-130	R.VLVHCR EGYSR.S	461.6106	TriOx(C) C5, Ox(Y) Y5	32	19.76 to 21.79	74
120-130	R.VLVHCR EGYSR.S	691.9613	TriOx(C) C5, Ox(Y) Y5	50	21.75	74
120-130	R.VLVHCR EGYSR.S	706.4587	TriOx(C) C5, Nitro(Y) Y5	65	24.38 to 25.09	74
131-142	R.SPTLVIA YLMMR.Q	470.9812	Ox (M) M10	68	42.7	74
131-142	R.SPTLVIA YLMMR.Q	470.9823	Ox (M) M11	30	45.82	74
131-142	R.SPTLVIA YLMMR.Q	706.0144	Ox (M) M11	60	41.45 to 47.63	74
131-142	R.SPTLVIA YLMMR.Q	476.3144	2 Ox (M) M10, M11	58	40.75	74
131-142	R.SPTLVIA YLMMR.Q	714.0161	2 Ox (M) M10, M11	52	40.58	74
131-142	R.SPTLVIA YLMMR.Q	480.6482	Nitro (Y) Y8	52	49.02	74
131-142	R.SPTLVIA YLMMR.Q	720.5199	Nitro (Y) Y8	47	49.2 to 49.91	74
131-142	R.SPTLVIA YLMMR.Q	728.5207	Nitro (Y) Y8, Ox(M) M11	53	46.2 to 46.87	74
131-142	R.SPTLVIA YLMMR.Q	491.3153	Nitro (Y) Y8, Ox (M) M11, Ox(M) M10	38	42.99	74
131-142	R.SPTLVIA YLMMR.Q	736.5229	Nitro (Y) Y8, Ox (M) M11, Ox(M) M10	20	42.9	74
156-176	R.QNREIG PNDGFLA WLCQLND R.L	1216.893 4	DiOx (C) C16	15	42.04	74
156-176	R.QNREIG PNDGFLA WLCQLND R.L	817.2357	TriOx (C) C16	11	41.79 to 42.46	74
156-176	R.QNREIG PNDGFLA WLCQLND R.L	1225.454 7	TriOx (C) C16	68	39.04 to 39.74	74
1000:1 Tetronitromethane:VHR, 1hr at 37°C treated VHR						
Peptide	Peptide sequence	Observe d ion (m/z)	Modification	Ion score	Retention Time (mins)	Sequence coverage (%)
37-50	R.IYVGNA SVAQDIP K.L	497.3403	Ox(Y) Y2	56	30.67 to 32.8	75
37-50	R.IYVGNA SVAQDIP K.L	745.5213	Ox(Y) Y2	73	45.1 to 45.99	75
37-50	R.IYVGNA	507.3396	Nitro (Y) Y2	70	34.16 to	75

	SVAQDIP K.L				35.57	
37-50	R.IYVGNA SVAQDIP K.L	760.5537	Nitro (Y) Y2	53	42.1	75
37-53	R.IYVGNA SVAQDIP KLQK.L	944.7182	Nitro (Y) Y2	26	36.07 to 38.26	75
54-66	K.LGITHV LNAAEGR. S	683.4822	Ox (H) H5	52	37.29	68
54-66	K.LGITHV LNAAEGR. S	456.3094	Ox (H) H5	28	29.88	68
67-79	R.SFMHV NTNANFY K.D	530.3266	Ox(M) M3	55	27.65	75
67-79	R.SFMHV NTNANFY K.D	795.0319	Ox(Y)Y12	21	30.71 to 32.3	75
67-79	R.SFMHV NTNANFY K.D	539.9928	Nitro (Y) Y12	50	35.3 to 35.9	75
67-79	R.SFMHV NTNANFY K.D	545.3298	Nitro (Y) Y12, Ox(M) M3	70	31.38 to 33.7	75
67-79	R.SFMHV NTNANFY K.D	817.5486	Nitro (Y) Y12, Ox(M) M3	61	31.34	75
67-79	R.SFMHV NTNANFY K.D	530.3266	Ox (H) H4	58	27.65 to 29.68	68
67-79	R.SFMHV NTNANFY K.D	795.0319	Ox (K) K13	5	30.71 to 32.30	68
67-79	R.SFMHV NTNANFY K.D	803.0388	DiOx (M) M3	67	35.62	68
67-89	R.SFMHV NTNANFY KDSGiTYL GIK.A	879.6492	Ox(M) M3	62	35.15 to 35.82	75
67-89	R.SFMHV NTNANFY KDSGiTYL GIK.A	889.3151	Nitro (Y)12	56	38.9 to 40.25	75
80-89	K.DSGITY LGIK.A	361.2293	Ox(Y) Y6	22	33.83	75
80-89	K.DSGITY LGIK.A	541.8816	Ox(Y) Y6	20	30.71 to 31.38	75
80-89	K.DSGITY LGIK.A	556.3677	Nitro (Y) Y6	65	39.07	75
	R.AADFID QALAQKN GR.V	825.5633 (mod + 31.9357)	DiOx(K) K12	61	36.11	75
90-104	K.ANDTQ EFNLSAY FER.A	911.1196	Ox(Y) Y12	64	41.22 to 41.93	75
90-104	K.ANDTQ	617.3918	Nitro(Y) Y12	77	43.96 to	75

	EFNLSAY FER.A				47.61	
90-104	K.ANDTQ EFNLSAY FER.A	925.6301	Nitro(Y) Y12	72	41.76	75
120-125	R.VLVHCR .E	387.7319	TriOx(C) C5	43	18.97	75
120-130	R.VLVHCR EGYSR.S	461.6114	TriOx(C) C5, Ox(Y) Y5	24	20.79 to 21.64	75
120-130	R.VLVHCR EGYSR.S	691.9611	TriOx(C) C5, Ox(Y) Y5	62	21.9	75
120-130	R.VLVHCR EGYSR.S	706.506	TriOx(C) C5, Nitro(Y) Y5	39	24.49 to 25.88	75
120-130	R.VLVHCR EGYSR.S	722.4612 (mod +31.9898)	DiOx (R) R6 TriOx(C) C5, Nitro(Y) Y5	52	29.88	75
131-142	R.SPTLVIA YLMMR.Q	470.6315	Ox (M) M10	37	43.63	75
131-142	R.SPTLVIA YLMMR.Q	470.9828	Ox (M) M11	47	45.27 to 45.95	75
131-142	R.SPTLVIA YLMMR.Q	706.0182	Ox (M) M11	56	46.52 to 47.22	75
131-142	R.SPTLVIA YLMMR.Q	706.0237	Ox (M) M10	65	41.63 to 43.03	75
131-142	R.SPTLVIA YLMMR.Q	476.3161	2 Ox (M) M10, M11	52	40.76	75
131-142	R.SPTLVIA YLMMR.Q	714.0056	Ox(Y) Y8, Ox (M) M11	23	37.62	75
131-142	R.SPTLVIA YLMMR.Q	714.0247	2 Ox (M) M10, M11	53	40.68	75
131-142	R.SPTLVIA YLMMR.Q	480.6517	Nitro(Y) Y8	62	49.01 to 49.86	75
131-142	R.SPTLVIA YLMMR.Q	720.5133	Nitro(Y) Y8	48	49.27 to 50.63	75
131-142	R.SPTLVIA YLMMR.Q	485.9838	Nitro(Y) Y8, Ox(M) M11	60	46.03 to 46.73	75
131-142	R.SPTLVIA YLMMR.Q	728.5238	Nitro(Y) Y8, Ox(M) M11	56	45.99 to 47.47	75
131-142	R.SPTLVIA YLMMR.Q	491.3158	Ox(Y) Y8, 2 Ox (M) M10, M11	63	43.12	75
131-142	R.SPTLVIA YLMMR.Q	736.5164	Ox(Y) Y8, 2 Ox (M) M10, M11	19	44.05	75
131-144	R.SPTLVIA YLMMRQK .M	576.9005	Ox(Y) Y8, 2 Ox (M) M10, M11	29	52.55	75
131-142	R.SPTLVIA YLMMR.Q	706.0182	Ox (P) P2	18	46.52 to 47.22	68
131-142	R.SPTLVIA YLMMR.Q	476.3161	DiOx(M) M11	31	45.9	68
131-142	R.SPTLVIA YLMMR.Q	714.0056	DiOx(M) M11	20	37.62	68
131-144	R.SPTLVIA YLMMRQK .M	745.5213	DiOx (M) M11, DiOx (M) M10, DiOx (Y) Y8	10	45.10 to 45.99	68
159-176	R.EIGPND	1017.732	DiOx (C) C13	10	41.43 to	75

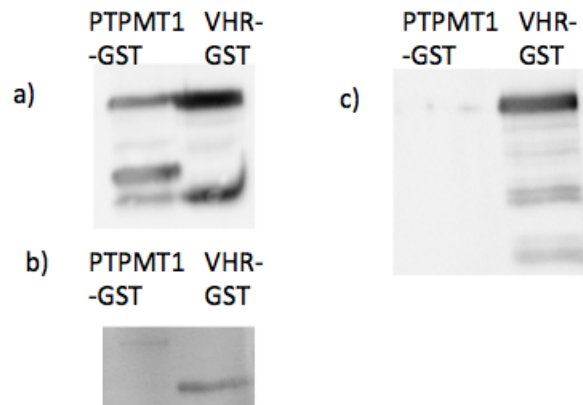
	GFLAQLC QLNDR.L	5			44.43	
159-176	R.EIGPND GFLAQLC QLNDR.L	1025.755 3	TriOx (C) C13	79	47.65	75

Appendices 12. Oxidative modifications observed in tryptic peptides of VHR by MS/MS with collisionally-induced decomposition after validatory sequencing of b and y series ions from 10:1, 75:1, 150:1, 300:1 and 1000:1 molar ratio tetranitromethane oxidation and incubation at 37°C temperature for 1 hour
Mascot search for TriOx(C), DiOx(C), Ox(Y), DiOx(Y), Ox (M), DiOx(M), Nitro(W), Nitro(Y), Ox(K), Ox(P), Ox (H), Ox (W), DiOx (W) and Error Tolerant Search. The letter designation followed by a number denotes the one letter amino acid code and the sequence of the predicted modified residue within the peptide fragment. Ox = oxidation, Nitro = nitration, DiOx = Dioxidation, Triox = Trioxidation.

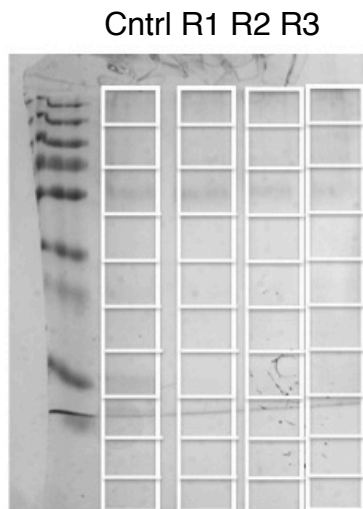


Appendices 13. Excision of protein from SDS PAGE post Coomassie staining from HOCl treated VHR

White boxes denote method for excision parameters for scalpel excision and boxes for calculating densitometry. Exemplar shown.



Appendices 14. Western blot tests of anti-GST, anti-PTPMT1 and anti-VHR primary and secondary antibodies conjugated to horseradish peroxidase vs. PTPMT1-GST and VHR-GST purified samples. 2ug of sample PTPMT1-GST and VHR-GST purified with glutathione column. Samples in A, B and C are from same purification and from same sample preparation a) PTPMT1-GST and VHR-GST probed with anti-GST primary antibody and anti-rabbit horseradish peroxidase conjugated secondary b) PTPMT1-GST and VHR-GST probed with anti-PTPMT1 primary antibody and anti-mouse horseradish peroxidase conjugated secondary c) PTPMT1-GST and VHR-GST probed with anti-VHR primary antibody and anti-mouse horseradish peroxidase conjugated secondary.



Appendices 15. Excision of protein from SDS PAGE post Coomassie staining from HCT116 cells transfected with pcDNA3.1-VHR-Flag for LC-MS, Mascot and Progenesis analysis

White boxes denote method for excision parameters for scalpel excision. R1-3 = Transfection replicates of pcDNA3.1-VHR-Flag. Cntrl = pcDNA3.1 empty vector control. n = 6